$$-\frac{\mathrm{d}c}{\mathrm{d}t} = k_n c^n$$

CHEMICAL KINETICS

V. I. Dybkov

$$\frac{\mathrm{d}x}{\mathrm{d}t} = k_0 /[1 + (k_0 x / k_1)]$$

IPMS Publications
Київ 2013 Kyiv

НАЦІОНАЛЬНА АКАДЕМІЯ НАУК УКРАЇНИ

ІНСТИТУТ ПРОБЛЕМ МАТЕРІАЛОЗНАВСТВА

ім. І.М. Францевича

Chemical Kinetics

V.I. Dybkov

Department of Physical Chemistry of Inorganic Materials
Institute of Problems of Materials Science
National Academy of Sciences of Ukraine
Kyiv 03142, Ukraine

vdybkov@ukr.net, vdybkov@ipms.kiev.ua

www.dybkov.kiev.ua

IPMS Publications
Київ – 2013 – Kyiv

UDC 544.42
“Chemical kinetics” - V.I. Dybkov.
National Academy of Sciences of Ukraine. I.M. Frantsevich Institute of Problems of Materials Science.- 286 p. (in English).
Basic concepts and laws of chemical kinetics are provided. Main attention is paid to solid-state heterogeneous reactions. Addressed to researchers, engineers, post-graduates and students of chemical, physical, metallurgical and other specialties.
Illustr. - 103. Tables - 27. Refs.- 173.

УДК 544.42
“Хімічна кінетика” - В.І. Дибков.
Національна академія наук України. Інститут проблем матеріалознавства ім. І.М. Францевича.- 286 с. (Англійскою мовою).
Наведено базові поняття і закони хімічної кінетики. Основну увагу приділено твердофазним гетерогенним реакціям. Адресовано науковцям, інженерам, аспірантам і студентам хімічних, фізичних, металургійних та інших спеціальностей.
Ілюстр.- 103. Табл.- 27. Бібліогр.- 173 назви.

УДК 544.42
“Химическая кинетика” - В.И. Дыбков.
Национальная академия наук Украины. Институт проблем материаловедения им. И.Н. Францевича.- 286 с. (На английском языке).
Приведено базовые понятия и законы химической кинетики. Основное внимание уделено твердофазным гетерогенным реакциям. Адресовано научным работникам, инженерам, аспирантам и студентам химических, физических, металлургических и других специальностей.
Иллюстр.- 103. Табл.- 27. Библиогр.- 173 назв.

First published: November 20, 2013

Print version
ISBN: 978-966-02-7029-9

Electronic (on-line) version
ISBN: 978-966-02-7030-5

All rights reserved

Copyright © V.I. Dybkov, 2013

Contents

Preface

This edition is actually my previous book "Solid State Reaction Kinetics" (IPMS Publications, Kyiv, 2013) less the vast majority of experimental data. To the best of my knowledge, it and other books "Kinetics of Solid State Chemical Reactions" (Naukova Dumka, Kiev, 1992, in Russian), "Growth Kinetics of Chemical Compound Layers" (Cambridge International Science Publishing, Cambridge, 1998) and "Reaction Diffusion and Solid State Chemical Kinetics" (First edition, IPMS Publications, 2002, in Ukrainian and English; Second edition, Trans Tech Publications, 2010) are used by most curious students, post-graduates and lecturers as textbooks.

For this category of readers, it appears to be most essential to understand the theoretical basis of chemical kinetics, whereas numerous available experimental data are of little interest, if at all. Therefore, the results of experimental work are only invoked in those cases in which they are needed for (*i*) deeper understanding the theory of reaction kinetics and (*ii*) its practical application. Restriction on their amount and accordingly on the number of references made this book much less voluminous than the previous one and, I hope, more convenient for reading.

First chapter provides an overview of basic concepts, assumptions and laws of the kinetics of homogeneous chemical reactions. As long as I myself was unable to make any contribution to the theory of homogeneous reaction kinetics, its content is based entirely on the results of work of our prominent predecessors. Their contributions to the subject are presented in much more detail, for example, in Refs [1-15]. Only the data on the kinetics of main types of homogeneous reactions, sufficient for understanding the distinction between the kinetics of homogeneous and heterogeneous reactions, are considered in this chapter. Specific reactions (catalytic, photochemical, *etc*.) are not considered at all.

Second to sixth chapters based largely on my own theoretical results are devoted to the kinetics of heterogeneous chemical reactions. Considered in the second chapter is the interfacial formation of a single compound layer between two solids. Attempt is made to explain in word, as far as possible, the physico-chemical background behind the mathematical relations, so that it would be understandable to the beginners. Even though the subject of diffusion in solids relates more to physics than to chemistry, it is nonetheless considered in this chapter, the main aim being to show the misleading character of some existing theoretical views assumed to be conventional. In particular, this concerns the interrelation between the reaction- and self-diffusion coefficients of the components of a chemical compound and the influence of native structure defects on the growth rate of a solid compound layer between reacting phases.

Third chapter provides the main kinetic relationships typical of solid-state growth of two compound layers at the interface of elementary substances. It is explained why the occurrence of the layers in most reaction couples is likely to be sequential rather than simultaneous. Also, difference between the reaction and diffusion regimes of their growth is elucidated.

Fourth chapter is intended to indicate the reasons of formation of multiple compound layers (three or more). It is shown that these can occur and grow only under conditions of reaction (chemical) control. Under conditions of diffusion control, only two of them will grow, whereas the others, even if available initially in an intentionally prepared reaction couple, will shrink and eventually must disappear. This kinetic instability of chemical compounds in the layered structures is by no means connected with their thermodynamic stability under given temperature-pressure conditions.

Comparative analysis of the growth kinetics of the same compound layer in various reaction couples of a multiphase binary system is presented in the fifth chapter. Mathematical expressions relating the growth rate of the layer in one of the couples to that in the others are provided. Possible formation of duplex structures in these couples is discussed, with the emphasis on the determination of the ratio of the sub-layers of a layer of the same compound, which look like the layers of two quite different chemical compounds.

Sixth chapter elucidates the peculiarities of reaction kinetics at the interface of a solid with a liquid and a solid with a gas. The dissolution in the solid-liquid systems as well as the evaporation in the solid-gas systems is shown to exert a significant effect on the rate of solid-state growth of any chemical compound layer. These effects are taken into account in mathematical equations describing the rate of its formation under conditions of simultaneous dissolution in the liquid phase or evaporation into the gaseous phase. Also, mechanism of partial oxidation of chemical compounds is briefly considered.

The book is addressed to researchers, engineers, lecturers, post-graduates and students of chemical, physical, metallurgical and other specialties, who wish to know the basic principles and laws of chemical kinetics. It may equally be used by theoreticians, experimentalists and technologists.

V.I. Dybkov, November 2013

1: Homogeneous chemical reactions

1.1: Distinction between homogeneous and heterogeneous reactions

From the point of view of their kinetics and mechanism, chemical reactions are conventionally divided into two broad groups. The first group is homogeneous chemical reactions taking place entirely within one phase which in most cases is gaseous or liquid. The second is heterogeneous chemical reactions involving two or more phases.

In the course of any homogeneous chemical reaction, its reactants and products are intermixed within the three-dimensional reaction volume (bulk) by convection, mechanical agitation or diffusion at the microscopic (atomic, ionic or molecular) level, as illustrated schematically (two-dimensionally) in Fig. 1.1a for a reaction of the type

$$A + B = AB. \tag{1.1}$$

The reactants and products are therefore in close proximity to each other, the distance between them normally being of the order of typical sizes of interacting particles. All the particles involved into the interaction are able to move more or less freely in any direction within a reaction volume, the size of which in three dimensions far exceeds their sizes.

By contrast, the reactants and products of any heterogeneous chemical reaction exist as macroscopic individual phases (layers) separated from each other by interfaces (Fig. 1.1b). Interface is regarded as a transition region between the interacting phases, the width of which is not very different from the interatomic distances in those phases. In the case of heterogeneous chemical reactions, no three-dimensional reaction volume is available, where the reactants and products could intermix.

Here, consideration of heterogeneous kinetics is restricted to reactions resulting in the formation of solid layers of chemical compounds. Under constant temperature-pressure conditions of occurrence of any heterogeneous chemical reaction, its product will therefore be assumed to be solid and to form a continuous compact layer adherent to initial phases.

Note that in heterogeneous systems under consideration no reactions can proceed within the bulk of any product phase (layer). The layer bulk only serves as a medium for transport of reacting atoms, ions, molecules (rarely) or radicals (still more rarely, if at all) from one layer interface to another by means of diffusion.

I. Homogeneous chemical reaction *A* + *B* = *AB*

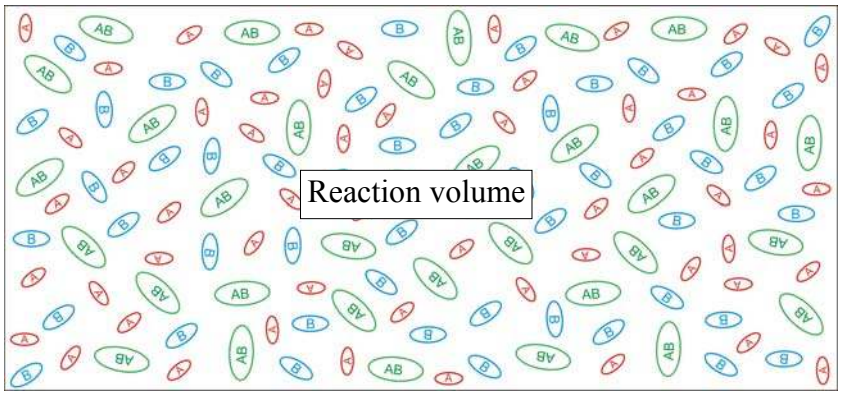

(a)

II. Heterogeneous chemical reaction *A* + *B* = *AB*

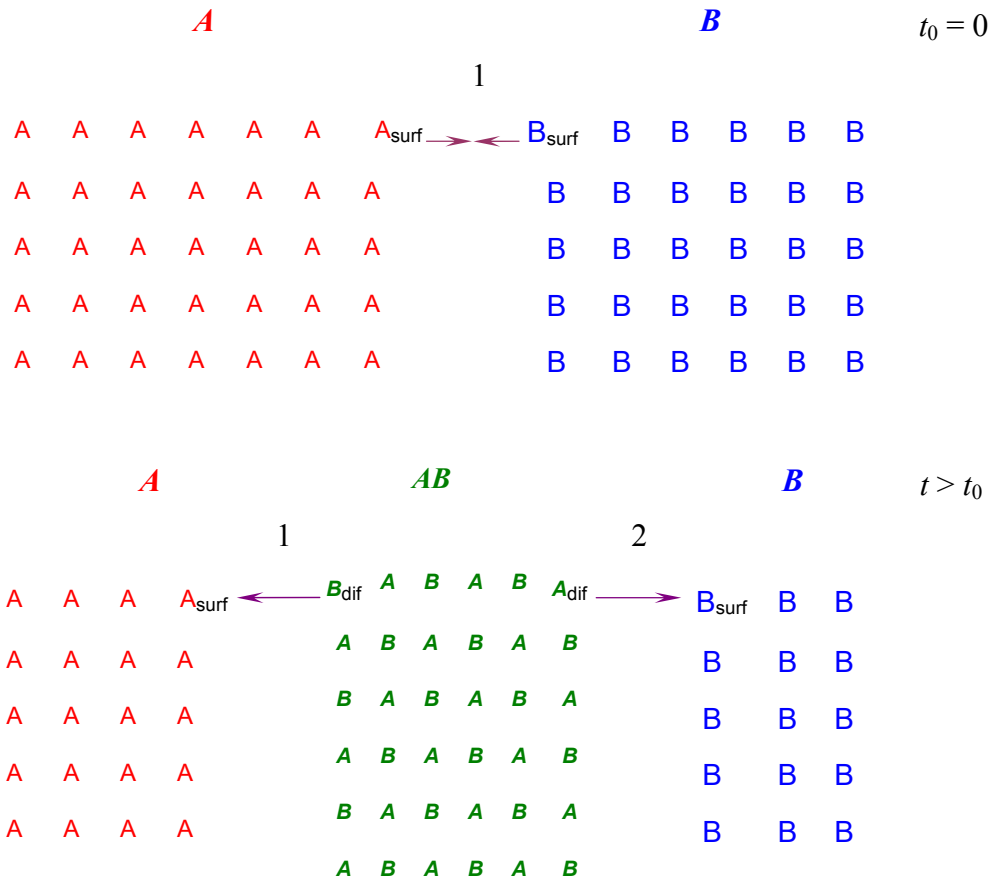

(b)

Fig. 1.1. Schematic illustration of the main distinction between (a) homogeneous and (b) heterogeneous reactions. The reactants and products of the former are intermixed at the microscopic (molecular) level, while those of the latter exist as macroscopic phases (layers) separated from each other by interfaces.

Diffusion is followed by further chemical transformations between the diffusing atoms of one of reacting substances and the surface atoms of the other (see Section 2.2). In heterogeneous reactions, any chemical transformations always take place exclusively at the interfaces of those substances.

When the A and B phases capable of forming a chemical compound AB are brought into intimate contact with each other at $t_0 = 0$, immediate reaction between the surface A and B atoms

$$A_{\text{surface}} + B_{\text{surface}} = AB \tag{1.2}$$

starts to proceed (see Fig. 1.1b).

As long as the reacting A and B phases prove to be separated from one another by a continuous layer of the AB compound, immediate chemical reaction between those atoms taking place initially at the common A–B interface 1 becomes impossible. Therefore, at $t > t_0$ it splits into two (kinetically different) partial chemical reactions between the diffusing and surface atoms, namely,

$$B_{\text{dif}} + A_{\text{surf}} = AB \tag{1.3}$$

at the A–AB interface (interface 1 in Fig. 1.1b) and

$$A_{\text{dif}} + B_{\text{surf}} = AB \tag{1.4}$$

at the AB–B interface (interface 2). Clearly, this happens soon after the AB compound layer, a few (theoretically, even one) crystal-lattice units thick, has formed.

1.2: Basic concepts and laws of the kinetics of homogeneous reactions

To show more clearly the similarity and distinctions of the homogeneous and heterogeneous kinetics, it appears relevant first to remind the main concepts, laws and relationships of the kinetics of homogeneous chemical reactions. As these are considered in detail in numerous texts on physical chemistry, chemical kinetics and metallurgy (see, for example, Refs [1-15]), only their short consideration is provided in this chapter, sufficient for further comparison with those typical of the kinetics of heterogeneous chemical reactions that are considered in the remaining chapters.

When considering the kinetics of homogeneous chemical reactions, it is always explicitly or tacitly assumed that, if a few reactions are taking place simultaneously in a given system, their elementary acts are independent of each other. Hence, the rate of each of those reactions can mathematically be described by an individual differential equation. These rates are then combined algebraically to yield a general differential equation for the overall reaction rate.

The principle of independency of elementary chemical processes is one of the fundamental assumptions on which the consideration of reaction kinetics rests. Its validity can only be verified by the extent of agreement between theoretical predictions obtained with its use and available experimental data. Wherever applied properly, it is known to yield reasonable final results.

The *rate* of a *homogeneous chemical reaction* is characterised by the *change* in *concentration* of its reagents per *unit time*. The concentration c is defined as the *amount* of a *reactant* or a *product* of the reaction in *unit volume*. It is expressed in the *number of particles*, *moles* or *kilograms* per *cubic metre* (m^{-3}, mol m^{-3} or kg m^{-3}, respectively).

Application of other concentration units such as mass or atomic percent, mole or volume fraction, molality, *etc*., must be substantiated in each particular case to avoid errors in calculation of numerical values of reaction rates and some other chemical and physical quantities (for example, diffusion coefficients) because generally different concentration units are not proportional to each other.

The rate of a homogeneous reaction of the type $A + B = AB$ can be expressed in terms of molar concentrations of its reactants A and B or its product AB as follows

$$-\frac{\mathrm{d}c_A}{\mathrm{d}t} = -\frac{\mathrm{d}c_B}{\mathrm{d}t} = +\frac{\mathrm{d}c_{AB}}{\mathrm{d}t}. \qquad (1.5)$$

The negative or positive sign indicates that the concentrations of the reactants A and B are decreasing, while the concentration of the product AB is increasing with time as the reaction proceeds. The reaction rate is always considered to be a positive quantity. In the case of more complicated reactions of the type $pA + qB = A_pB_q$, the rate of the reaction can alternatively be written as

$$-\frac{1}{p}\frac{\mathrm{d}c_A}{\mathrm{d}t} = -\frac{1}{q}\frac{\mathrm{d}c_B}{\mathrm{d}t} = +\frac{\mathrm{d}c_{A_pB_q}}{\mathrm{d}t}. \qquad (1.6)$$

Note that the use of the term *concentration* necessarily implies the availability of a macroscopic reaction volume. The reactants and products are supposed to be distributed uniformly within this volume.

According to the *law* of *mass action* formulated by C.M. Guldberg and P. Waage in its final form in 1867, the *rate* of any *homogeneous chemical reaction* involving i reactants is proportional to the product of their *concentrations* c_i, with each reactant concentration raised to a *numerical power* n_i. The value of n_i defines the *order* of a reaction with regard to a given reactant. The sum of these values for all the reactants is the total order of the reaction.

If any reaction proceeded exactly according to the stoichiometric chemical equation, then the *order* of this reaction would coincide with its *molecularity* determined from the balancing coefficients in the chemical equation. The *molecularity* of an elementary reaction involving no *intermediate steps* (*stages*) in its mechanism is defined by the minimum number of atoms, molecules or other species taking part in that reaction. According to the classification first proposed by J. H. van't Hoff in 1884 in his work entitled "*Études de dynamique chimique*", reactions of the type $A = Products$ ($H_2 = 2H$) are monomolecular (or unimolecular), those of the type $A + B = Products$ and $2A = Products$ ($2HJ = H_2 + J_2$) are bimolecular, those of the type $A + B + C = Products$, $2A + B = Products$ ($2NO + O_2 = 2NO_2$) and $3A = Products$ are trimolecular. In fact, however, the order of a reaction coincides with its molecularity only for the limited number of simple chemical reactions proceeding exclusively in one step (stage) that is a relatively rare exception rather than the rule.

Note that, unlike the molecularity which is always an integer varying from 1 to 3 (probability of many-particle collisions involving four or more atoms, molecules or other reacting species is quite negligible) and can never be zero, the order of a reaction can be, as established experimentally, zero, an integer, a fraction or a changing and even a negative number, indicative of a complicated reaction mechanism including a few intermediate steps (stages) with the formation of the *intermediate products* (*intermediates* or *intermediaries*), either detectable or, in most cases, only postulated. The slowest of those steps is the *rate-determining* step for the overall reaction.

From a kinetic viewpoint, forward, reversible (opposing, opposed), parallel (competitive), consecutive, chain and other types of homogeneous chemical reactions are distinguished. Forward reactions are those that proceed only in one direction, from reactants to products. Reversible reactions can proceed in opposite directions, from reactants to products and *vise versa*. In parallel reactions, one reactant yields a few products simultaneously. Consecutive reactions yield their products sequentially, the product of any of preceding ones being a reactant of the next. Chain reactions give rise to a progressive increase in the amount of products.

1.3: Forward chemical reactions

1.3.1: First-order reactions

Reaction $A = B$ is first-order ($n = 1$) and its rate is proportional to the instantaneous concentration c_A of A at a time t

$$-\frac{\mathrm{d}c_A}{\mathrm{d}t} = k_\mathrm{I} c_A, \tag{1.7}$$

where k_I is a rate constant numerically equal to the reaction rate at $c_A = 1$. Its dimension is the reciprocal of the time, t^{-1}. In SI units, it is measured in s^{-1}.

After integration with the initial condition $c_A = c_{A0}$ at $t = 0$, equation (1.7) yields

$$c_A = c_{A0} \exp(-k_\mathrm{I} t). \tag{1.8}$$

Hence, concentration of *A* decreases, while that of *B* increases exponentially with passing time, as shown schematically in Fig. 1.2a and b for two values of k_I: (a) 1.00 and (b) 0.25 s^{-1}.

This kind of kinetic dependence was first established experimentally when studying the conversion of a sucrose solution into a mixture of fructose and glucose, and then treated theoretically using differential equations by L.F. Wilhelmy in 1850. Though not estimated properly by the contemporaries, his pioneer work gave rise to an exponential increase in the number of investigations devoted to reaction kinetics.

As seen in Fig. 1.2, the greater the rate constant k_I, the quicker the reaction is completed. At $k_\mathrm{I} = 1.0\ \mathrm{s}^{-1}$, it is practically completed in around 7 seconds ($c_A \approx 0.0009 c_{A0}$ at $t = 7$ s). If $k_\mathrm{I} = 0.25\ \mathrm{s}^{-1}$, the greater time (> 50 s) is required for its completion.

In first-order reactions, the *half-life period* or simply *half-life*, $\tau_{1/2}$, *i.e.* the time taken for the reactant concentration to decrease from c_{A0} to $c_{A0}/2$, is seen from equation (1.8) to be independent of c_{A0}. It is inversely proportional to k_I:

$$\tau_{1/2} = \frac{\ln 2}{k_\mathrm{I}} \approx \frac{0.69}{k_\mathrm{I}}. \tag{1.9}$$

The reciprocal of k_I is often called the *lifetime*, τ_life. It is the time necessary for the reactant concentration to decrease from c_{A0} to c_{A0}/e ($c_{A0}/e \approx 0.37\ c_{A0}$), with *e* being the natural logarithm base ($e \approx 2.72$),

$$\tau_\mathrm{life} = \frac{1}{k_\mathrm{I}} \ln \frac{c_{A0} e}{c_{A0}} = \frac{1}{k_\mathrm{I}} \tag{1.10}$$

In the case of first-order chemical reactions, a plot of either $\ln c_A$ or $\ln (c_A/c_{A0})$ or $\ln (c_{A0}/c_A)$ against *t* is a straight line, as shown schematically in Fig. 1.3a and b for a value of $k_\mathrm{I} = 1.0\ \mathrm{s}^{-1}$. Plots of Fig. 1.3a and b only differ by their ordinates.

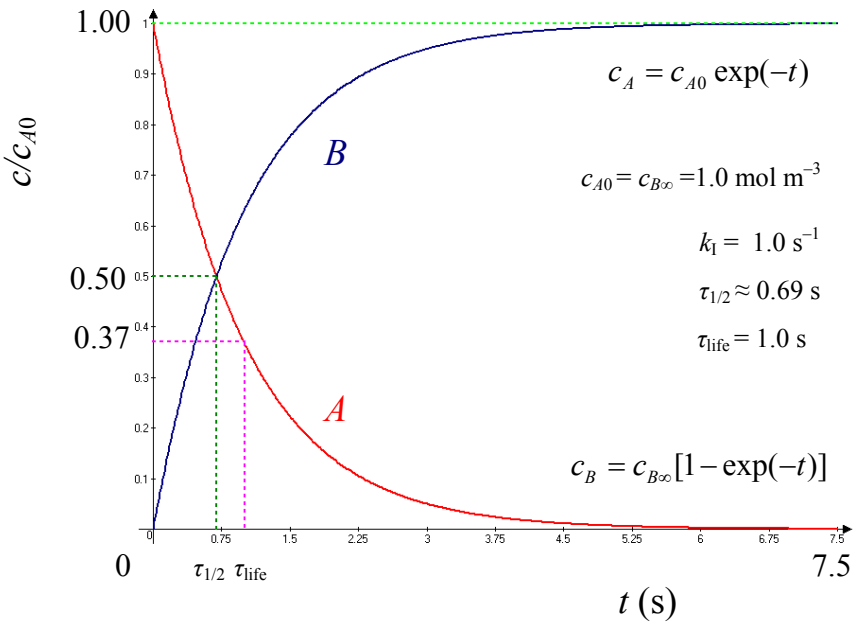

(a)

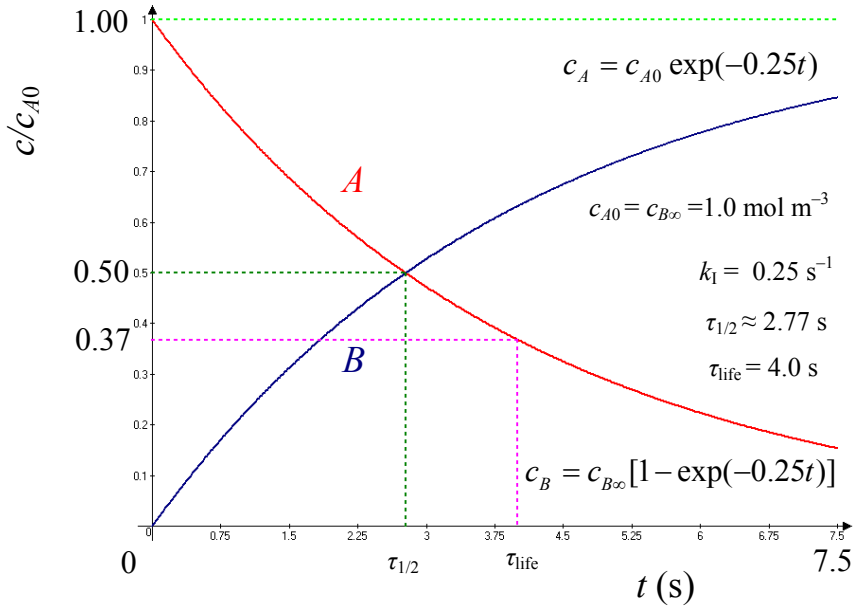

(b)

Fig. 1.2. Typical plots of the concentration c of the reagents A and B against time t in the first-order reaction $A = B$ for two values of k_I: (a) 1.0 and (b) 0.25 s^{-1}.

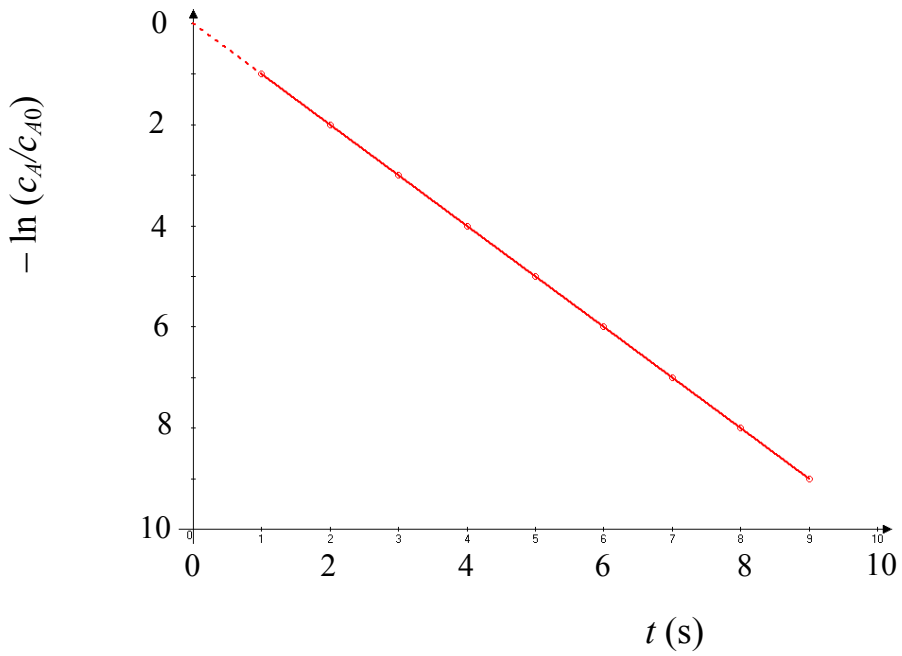

(a)

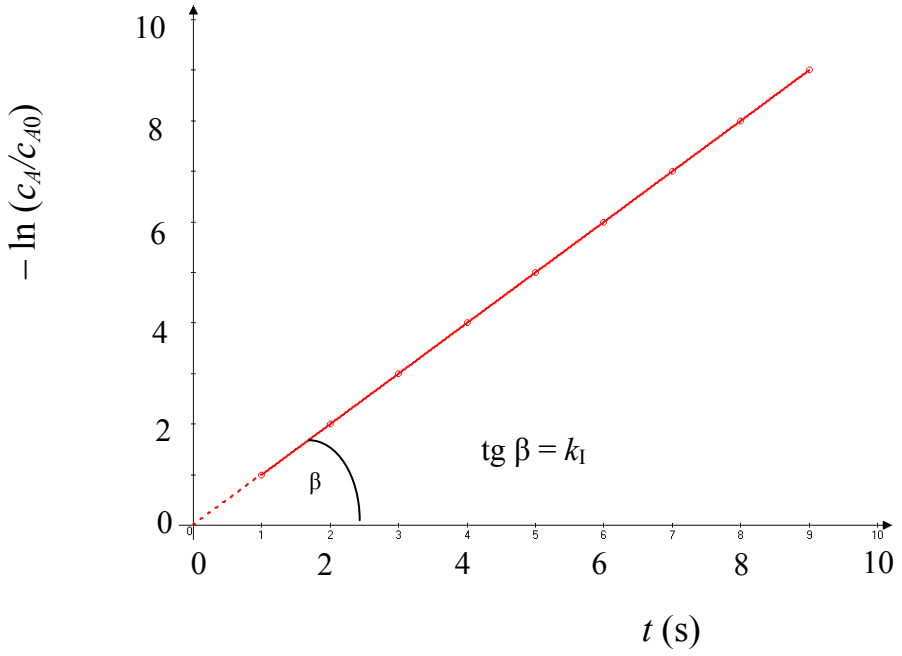

(b)

Fig. 1.3. Two kinds of representation of ln (c_A/c_{A0}) – t relationship in the first-order reaction $A = B$ for a value of k_I = 1.0 s^{-1}. These only differ by the sequence of numbers on the ordinate axis.

The slope of the straight line to the abscissa axis is conventionally used to find out a numerical value of the reaction constant k_I from the experimental data obtained. Their statistical treatment using standard analytical functions, exponential in particular, available in computer programs allows the quick and easy determination of the reaction constant k_I together with a regression coefficient and confidence limits at any given level of probability.

1.3.2: Second-order reactions

Second-order reactions are those in which the rate is proportional either to the product of molar concentrations of two reactants as in the general case of reactions $A + B = Products$ or to the square of the concentration of one of the reactants, if initially both concentrations are equal or if only one reactant is involved into the reaction ($2A = Products$). In the former case,

$$-\frac{dc_A}{dt} = k_{II} c_A c_B . \qquad (1.11)$$

The total order of the reaction is second, while its order with regard to either A or B is first.

In the latter case ($c = c_A = c_B$),

$$-\frac{dc}{dt} = k_{II} c^2 . \qquad (1.12)$$

The integrated form of this equation ($c = c_0$ at $t = 0$) gives

$$\frac{1}{c} - \frac{1}{c_0} = k_{II} t . \qquad (1.13)$$

A plot of c against t is shown in Fig. 1.4a ($c_0 = 1.0$ mol m^{-3}, $k_{II} = 1.0$ mol^{-1} m^3 s^{-1}).

If any reaction is second-order, a plot of $1/c$ against t must yield a straight line (Fig. 1.4b). The slope of this line is equal to the reaction-rate constant, k_{II}. The half-life is

$$\tau_{1/2} = \frac{1}{k_{II} c_0} . \qquad (1.14)$$

For second-order reactions, it is seen to be dependent on both k_{II} and c_0.

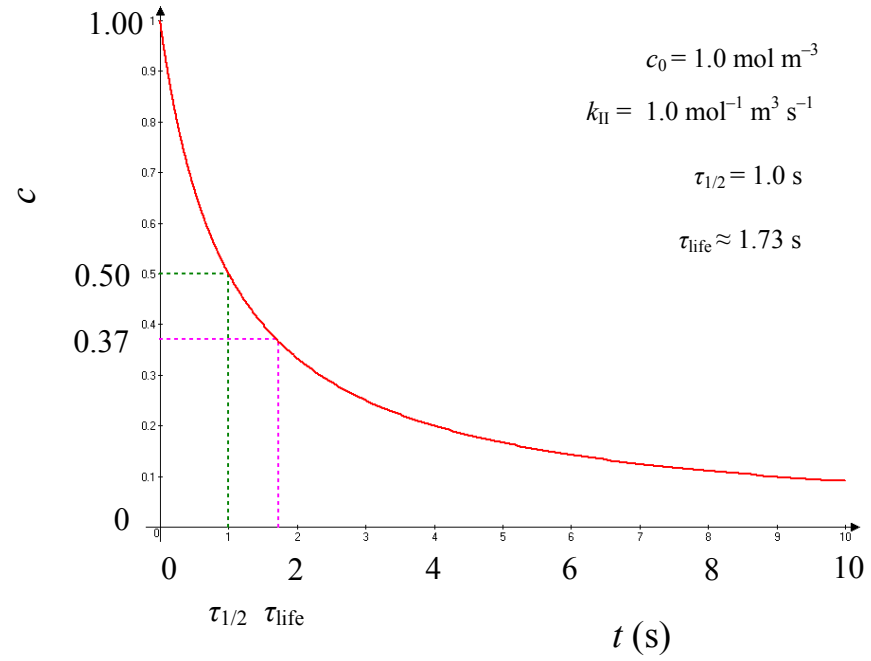

(a)

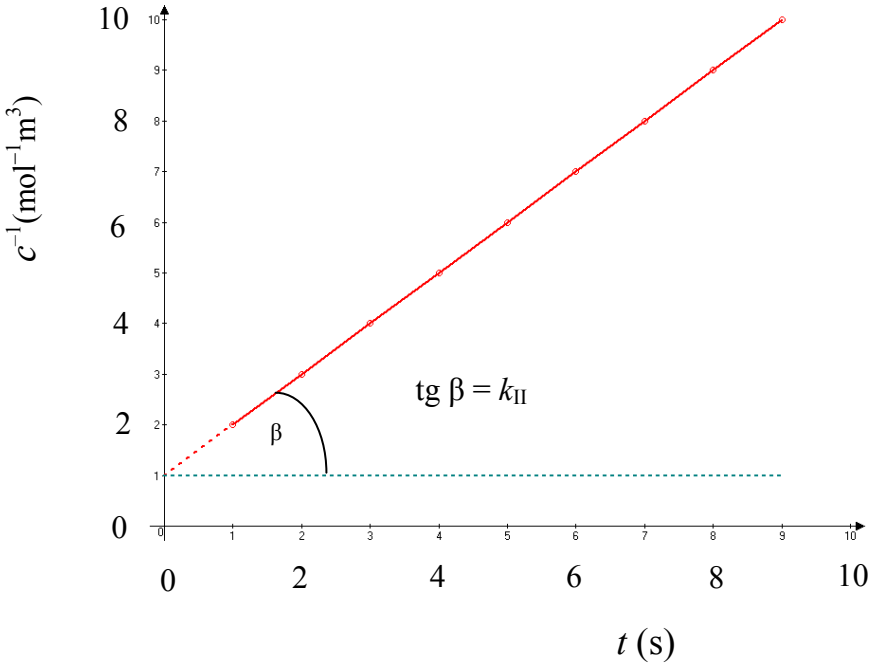

(b)

Fig. 1.4. Plots of (a) the concentration c of the reagents A and B and (b) $1/c$ against time t in the second-order reaction $A + B = Products$ at equal initial concentrations $c_{A0} = c_{B0} = c_0 = 1.0$ mol m^{-3} and a value of $k_{II} = 1.0$ mol^{-1} m^3 s^{-1}.

Accordingly, the lifetime

$$\tau_{\text{life}} = \frac{e-1}{k_{\text{II}} c_0} \approx \frac{1.72}{k_{\text{II}} c_0} \tag{1.15}$$

also depends on both k_{II} and c_0.

As any chemical reaction, even the simplest like isomerisation or dissociation, involves at least one molecule, zero-order reactions are clearly impossible from the point of view of their molecularity. However, if a given reactant, for example *B*, in any reaction of the type *A* + *B* = *Products*, is taken in large excess, its concentration remains almost unchanged during the time of observation and does not influence the overall reaction rate. Then, the reaction can formally be considered to be zero-order with regard to this reactant: $n = 0$, $c_B^0 = 1$. Hence, its rate is (see equation (1.11))

$$-\frac{\mathrm{d}c_A}{\mathrm{d}t} = k_{\text{II}} c_A c_B^0 = k_{\text{II}} c_A . \tag{1.16}$$

The bimolecular second-order reaction thus becomes first-order.

The total order of any other reaction involving a few reactants can similarly be lowered, but obviously not to zero, because all the reactants cannot simultaneously be taken in large excess. Therefore, if a reaction is found experimentally to be zero-order with regard to all the reactants, it simply means that this reaction, though otherwise homogeneous, proceeds by a different mechanism under particular conditions of its occurrence. Such are, for example, chemical reactions taking place on solid catalysts.

In this case, the reaction proceeds in the diffusion boundary layer at the solid-gas or solid-liquid interface, saturated by all the reagents. Its rate-determining step is independent of their instantaneous concentrations in the bulk of the gaseous or liquid phase. Formally, the total order of the reaction becomes zero and the rate is constant. The reactants are consumed, while the products are accumulated linearly with passing time until the reaction has completed, which case is not typical of homogenous reactions, as seen from the rate equations of this section. In this and similar cases, it appears better not to apply at all the concept *order of reaction* to the overall reaction.

1.3.3: Third-order reactions

In the particular case of third-order reaction *A* + *B* + *C* = *Products*, where the initial molar concentrations of all the reactants are equal, the kinetic equation is of the form

$$-\frac{\mathrm{d}c}{\mathrm{d}t} = k_{\mathrm{III}} c^3 . \tag{1.17}$$

After integration ($c = c_0$ at $t = 0$), it becomes

$$\frac{1}{2}\left(\frac{1}{c^2} - \frac{1}{c_0^2}\right) = k_{\mathrm{III}} t . \tag{1.18}$$

A plot of c against t is shown in Fig. 1.5a ($c_0 = 1.0$ mol m^{-3}, $k_{\mathrm{III}} = 1.0$ mol^{-2} m^6 s^{-1}). The rate constant k_{III} is determined from the slope of a plot of $1/c^2$ against t (Fig. 1.5b).

By putting $c = c_0/2$ in equation (1.18), the half-life is obtained

$$\tau_{1/2} = \frac{3}{2k_{\mathrm{III}} c_0^2} . \tag{1.19}$$

Like the case of $n = 2$, it depends on both the rate constant k_{III} and the initial concentration c_0 of the reactants.

The lifetime

$$\tau_{\mathrm{life}} = \frac{e^2 - 1}{2k_{\mathrm{III}} c_0^2} \approx \frac{6.39}{2k_{\mathrm{III}} c_0^2} \tag{1.20}$$

is also dependent on both k_{III} and c_0.

1.3.4: Reactions of order n

For any reaction of order n, whose rate is dependent on the concentration of only one reactant ($nA = Products$ or $A + A_1 + \ldots + A_n = Products$, with the initial molar concentrations of all the reactants being equal), the rate equation is

$$-\frac{\mathrm{d}c}{\mathrm{d}t} = k_n c^n \quad . \tag{1.21}$$

Its integrated form ($c = c_0$ at $t = 0$) yields a dependence of c upon t

$$c^{-(n-1)} = c_0^{-(n-1)} + (n-1) k_n t . \tag{1.22}$$

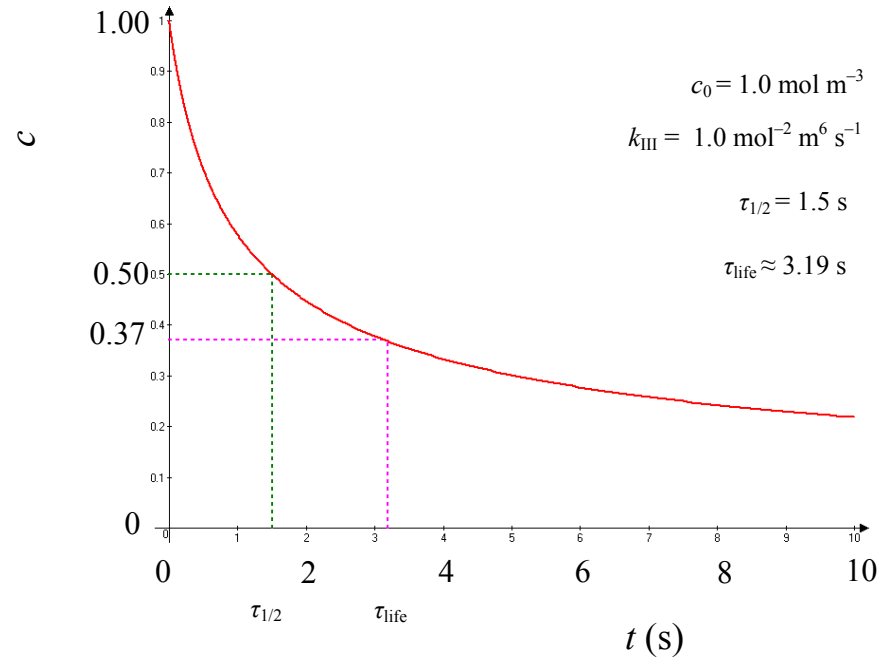

(a)

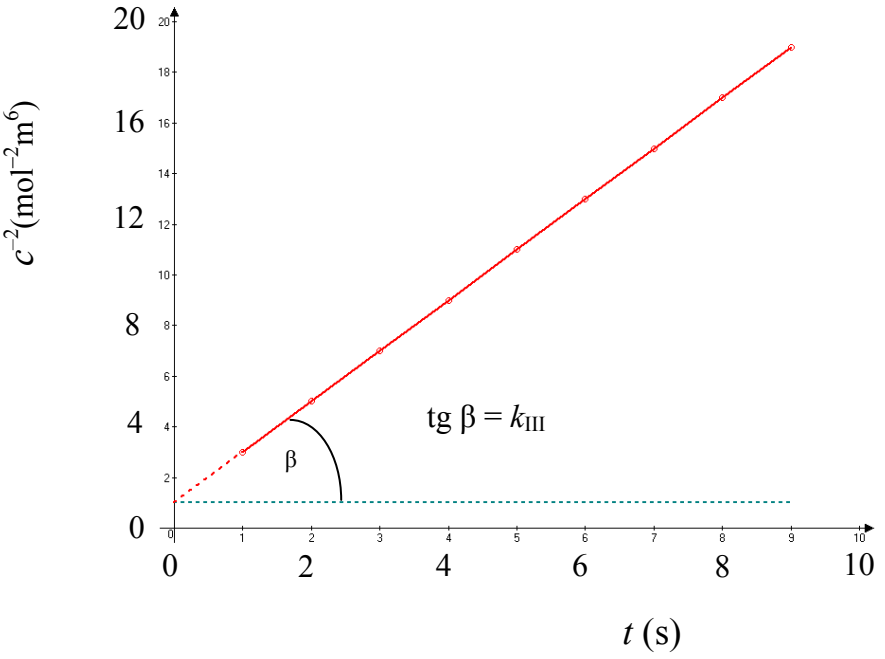

(b)

Fig. 1.5. Plots of (a) the concentration c of the reagents and (b) $1/c^2$ against time t in the third-order reaction $A + B + C = Products$ at equal initial concentrations of A, B and C $c_0 =$ 1.0 mol m^{-3} and a value of $k_{III} = 1.0$ mol^{-2} m^6 s^{-1}.

By plotting $c^{-(n-1)}$ against t, a straight line is obtained. Its slope is equal to $(n-1)\,k_n$, with n being any number (positive, negative, whole or fractional). In the case of $n = 1$, application of l'Hôpital's rule converts an indeterminate form of this equation to the determinate one $\ln c_0 - \ln c = k_1 t$ (see equation (1.8)).

The half-life and lifetime for reactions of order n ($n \neq 1$) are

$$\tau_{1/2} = \frac{2^{n-1} - 1}{(n-1)k_n c_0^{n-1}}. \tag{1.23}$$

and

$$\tau_{\text{life}} = \frac{e^{n-1} - 1}{(n-1)k_n c_0^{n-1}}, \tag{1.24}$$

respectively.

1.3.5: Determination of the order of chemical reactions

First of all, concentrations of reactants or products are to be measured at various times in the course of a chemical reaction. Its progress can be followed by suitable chemical or physical means. As a result, a dependence of the concentration upon time is established. The methods of calculating the order of a reaction are based either on differential mathematical equations or on their integrated forms.

The *differential method* is based on equation (1.21) which for two different concentrations c_1 and c_2 yields

$$-\frac{\mathrm{d}c_1}{\mathrm{d}t} = k_n c_1^n \text{ and } -\frac{\mathrm{d}c_2}{\mathrm{d}t} = k_n c_2^n. \tag{1.25}$$

By taking logarithms and term-by–term subtracting the two expressions, one obtains

$$\ln\left(-\frac{\mathrm{d}c_1}{\mathrm{d}t}\right) - \ln\left(-\frac{\mathrm{d}c_2}{\mathrm{d}t}\right) = n(\ln c_1 - \ln c_2). \tag{1.26}$$

Hence,

$$n = \frac{\ln\left(-\frac{\mathrm{d}c_1}{\mathrm{d}t}\right) - \ln\left(-\frac{\mathrm{d}c_2}{\mathrm{d}t}\right)}{\ln c_1 - \ln c_2}. \tag{1.27}$$

The value of n can therefore be estimated by taking two values of concentration and measuring appropriate rates of a chemical reaction.

Consider the procedure of calculations using the first-order reaction as an example. Initial data are presented in Table 1.1. The concentrations c_{ideal} (circles in Fig. 1.6) were found according to the equation $c = 1.00 \exp(-0.25t)$. In reality, experimental points (squares in Fig. 1.6) are more or less scattered (almost always more than less), as shown in columns 3 and 4 of the table.

For further comparisons, let us first carry out calculations for the ideal case by taking two points $c_2 = 0.6065$ mol m^{-3} at $t_2 = 2$ s and $c_4 = 0.3679$ mol m^{-3} at $t_4 = 4$ s of the equation $c = 1.00 \exp(-0.25t)$. The subscripts at c and t correspond to appropriate values of time. Thus,

$$n = \frac{\ln(-\frac{dc_2}{dt}) - \ln(-\frac{dc_4}{dt})}{\ln c_2 - \ln c_4} = \frac{\ln(0.1516) - \ln(0.09197)}{\ln(0.6065) - \ln(0.3679)} = \frac{-1.8865 + 2.3863}{-0.5001 + 0.9999} = 1.00.$$

In the real case, however, only a set of experimental points c_i at t_i is available. Neither the exact $c - t$ relationship, nor the derivatives for appropriate points are clearly known *a priori*. The derivatives should therefore be found by one of graphical or numerical methods. Their values can readily be calculated from the experimental $c - t$ relationship, for example, by the numerical three-point method using a conventional computer program (linear approximation).

To find the derivative for a given experimental point c_i at t_i by this method, data for its two neighbouring points c_{i-1} at t_{i-1} and c_{i+1} at t_{i+1} are used. Left-hand and right-hand derivatives $(c_i - c_{i-1})/(t_i - t_{i-1})$ and $(c_{i+1} - c_i)/(t_{i+1} - t_i)$ are first found for this point. Then, the average value is calculated. The derivatives can thus be found for all experimental points, excepting clearly the first and last ones for which one of the neighbouring points is lacking.

By taking the neighbouring points $c_1 = 0.76$ mol m^{-3} at $t_1 = 1$ s and $c_3 = 0.44$ mol m^{-3} at $t_3 = 3$ s, one obtains a value of the derivative $(-dc_2/dt) = [(0.76 - 0.63) + (0.63 - 0.44)]/2 = 0.16$ mol m^{-3} s^{-1} for the point $c_2 = 0.63$ mol m^{-3} at $t_2 = 2$ s. Similarly, for the point $c_4 = 0.35$ mol m^{-3} at $t_4 = 4$ s with the neighbouring points $c_3 = 0.44$ mol m^{-3} at $t_3 = 3$ s and $c_5 = 0.28$ mol m^{-3} at $t_5 = 5$ s a value of the derivative $(-dc_4/dt)$ is $[(0.44 - 0.35) + (0.35 - 0.28)]/2 = 0.08$ mol m^{-3} s^{-1}. Hence,

$$n = \frac{\ln(-\frac{dc_2}{dt}) - \ln(-\frac{dc_4}{dt})}{\ln c_2 - \ln c_4} = \frac{\ln(0.16) - \ln(0.08)}{\ln(0.63) - \ln(0.35)} = \frac{-1.8326 + 2.5257}{-0.4620 + 1.0498} = 1.18.$$

Table 1.1. Initial data for calculating the order of a chemical reaction

t (s)	c_{ideal} (mol m^{-3}) $c = 1.00 \exp(-0.25t)$	c_{real} (mol m^{-3}) $c = 1.03 \exp(-0.27t)$	$c_{ideal} - c_{real}$ (mol m^{-3})
1	0.7788	0.76	+0.0188
2	0.6065	0.63	–0.0235
3	0.4724	0.44	+0.0324
4	0.3679	0.35	+0.0179
5	0.2865	0.28	+0.0065
6	0.2231	0.21	+0.0131
7	0.1738	0.19	–0.0162
8	0.1353	0.12	+0.0153
9	0.1054	0.08	+0.0254
10	0.0821	0.07	+0.0121

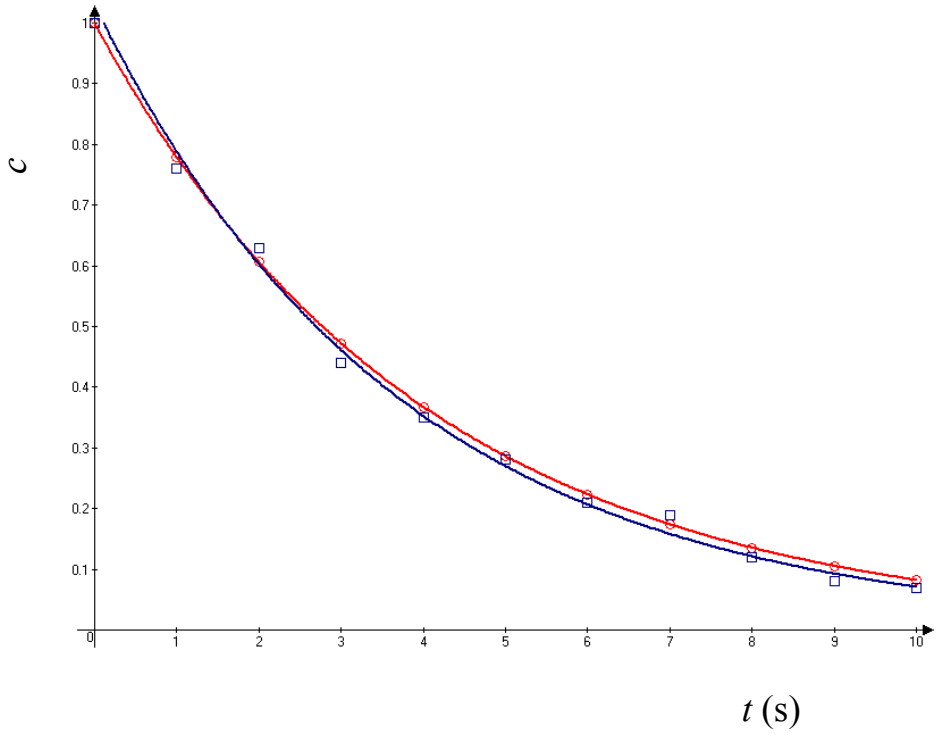

Fig. 1.6. Ideal (circles) and real (squares) plots of the concentration c against time t. For the sake of illustration, the first-order reaction $A = B$ with a value of $k_I = 0.25$ s^{-1} was arbitrarily chosen (see also Fig. 1.2b).

The accuracy of calculations is seen to be not very high. However, it can be improved substantially by approximating the experimental $c - t$ relationship by one of suitable mathematical functions.

In the *integral method*, the integrated equations such as (1.8), (1.13) and (1.18) are employed to decide which of them yields a best fit to the experimental data, with the rate constant remaining unchanged over the whole time range investigated. This trial-and-error method is not very sensitive in distinguishing between the orders. Clearly, changing, fractional or negative orders tend to be missed. The obvious modification of this method is to draw plots in the coordinates $\ln c - t$, $1/c - t$ and $1/c^2 - t$ that should yield straight lines for reactions of first, second and third order, respectively.

In the *half-life method*, values of the half-life $\tau_{1/2}$ are used. Expressions for $\tau_{1/2}$ at equal molar concentrations of the reactants are summarised in Table 1.2. Also presented in the table are dimensions of rate constants and τ_{life} for chemical reactions of different orders.

Table 1.2. Dimension of the rate constant k, $\tau_{1/2}$ and τ_{life} for chemical reactions of different orders

Kinetic order	Dimension of k	$\tau_{1/2}$	τ_{life}
1	t^{-1}	$\frac{\ln 2}{k_I}$	$\frac{1}{k_I}$
2	$c^{-1}t^{-1}$	$\frac{1}{k_{II}c_0}$	$\frac{e-1}{k_{II}c_0} \approx \frac{1.72}{k_{II}c_0}$
3	$c^{-2}t^{-1}$	$\frac{3}{2k_{III}c_0^2}$	$\frac{e^2-1}{2k_{III}c_0^2} \approx \frac{6.39}{2k_{III}c_0^2}$
n	$c^{-(n-1)}t^{-1}$	$\frac{2^{n-1}-1}{(n-1)k_n c_0^{n-1}}$	$\frac{e^{n-1}-1}{(n-1)k_n c_0^{n-1}}$

A distinguishable characteristic of first-order reactions is the independency of the half-life of the initial concentrations of the reactants, whereas for reactions of other orders

$$\tau_{1/2} \propto \frac{1}{c_0^{n-1}}.$$

Hence, by using two initial concentrations c_{01} and c_{02} in separate experiments, the ratio is obtained

$$\frac{(\tau_{1/2})_1}{(\tau_{1/2})_2} = \frac{c_{02}^{n-1}}{c_{01}^{n-1}}.$$

Taking logarithms and subsequent rearranging terms yields an equation of the form

$$n = 1 + \frac{\ln[(\tau_{1/2})_1 / (\tau_{1/2})_2]}{\ln(c_2 / c_1)}. \tag{1.28}$$

This equation can readily be employed to determine the order of a reaction. Clearly, it is applicable to any other convenient fraction of the total reaction time than half-life.

If two or more reactants are involved in a reaction, experiments are carried out in such a way that only one reactant concentration varies. The order of the reaction with regard to this reactant is determined. The orders with regard to other reactants are determined similarly and then summed up to give the total order of that reaction.

1.4: Reversible chemical reactions

Reversible (opposing, opposed) reactions proceed simultaneously in both directions. For a reversible first-order reaction $A \leftrightarrow B$, the rate of the forward reaction $A \rightarrow B$ with the constant k_f is

$$\left(\frac{dx}{dt}\right)_{\text{forward}} = k_f (a - x), \tag{1.29}$$

while that of the reverse reaction $B \rightarrow A$ with the constant k_r is

$$\left(\frac{dx}{dt}\right)_{\text{reverse}} = -k_r (b + x), \tag{1.30}$$

where a and b are initial molar concentrations of A and B, respectively, and x is the amount of A in unit volume that has reacted to form B (the decrease in concentration of A or, alternatively, the increase in concentration of B) at time t.

The overall reaction rate is

$$\frac{\mathrm{d}x}{\mathrm{d}t} = k_\mathrm{f}(a-x) - k_\mathrm{r}(b+x)\,. \tag{1.31}$$

At (dynamic) equilibrium, the rate of the forward reaction $A \rightarrow B$ becomes equal to that of the reverse reaction $B \rightarrow A$. Hence, the overall rate is zero ($\mathrm{d}x/\mathrm{d}t = 0$), and

$$k_\mathrm{f}(a-x_\infty) = k_\mathrm{r}(b+x_\infty)\,, \tag{1.32}$$

where x_∞ is the decrease in concentration of A or the increase in concentration of B at the position of equilibrium.

Rearrangement gives

$$\frac{b+x_\infty}{a-x_\infty} = \frac{k_\mathrm{f}}{k_\mathrm{r}} = K_\mathrm{equil}\,, \tag{1.33}$$

where K_equil is the equilibrium constant of the reaction, a thermodynamic quantity.

Equation (1.31) can be re-written as follows

$$\frac{\mathrm{d}x}{\mathrm{d}t} = k_\mathrm{f}a - k_\mathrm{f}x - k_\mathrm{r}b + k_\mathrm{r}x = (k_\mathrm{f}+k_\mathrm{r})\left(\frac{k_\mathrm{f}a - k_\mathrm{r}b}{k_\mathrm{f}+k_\mathrm{r}} - x\right). \tag{1.34}$$

From equation (1.33),

$$\frac{k_\mathrm{f}a - k_\mathrm{r}b}{k_\mathrm{f}+k_\mathrm{r}} = x_\infty\,. \tag{1.35}$$

By inserting this relation into equation (1.34), one obtains

$$\frac{\mathrm{d}x}{\mathrm{d}t} = (k_\mathrm{f}+k_\mathrm{r})(x_\infty - x) \tag{1.36}$$

or, after integration from 0 to t and from 0 to x,

$$\ln \frac{x_\infty}{x_\infty - x} = (k_\mathrm{f} + k_\mathrm{r})t\,. \tag{1.37}$$

By plotting ln [x_∞/($x_\infty - x$) against t, the sum of k_f and k_r is obtained. Their ratio and then separate values are found, using equation (1.33) and an experimental value of x_∞.

1.5: Parallel chemical reactions

Parallel (competitive) reactions are those in which a reactant or a few reactants yield two or more different sets of products. For reactions $A \rightarrow B$ and $A \rightarrow C$ taking place simultaneously, the rate equations are

$$-\frac{\mathrm{d}c_A}{\mathrm{d}t} = k_A c_A\,, \quad \frac{\mathrm{d}c_B}{\mathrm{d}t} = k_B c_A\,, \quad \frac{\mathrm{d}c_C}{\mathrm{d}t} = k_C c_A\,, \tag{1.38}$$

where $k_A = k_B + k_C$.

If the products B and C are missing initially,

$$c_A = c_{A0} \exp(-k_A t) = c_{A0} \exp[-(k_B + k_C)t]\,, \tag{1.39}$$

$$c_B = c_{A0} \frac{k_B}{k_B + k_C} \{1 - \exp[-(k_B + k_C)t]\}\,, \tag{1.40}$$

$$c_C = c_{A0} \frac{k_C}{k_B + k_C} \{1 - \exp[-(k_B + k_C)t]\}\,. \tag{1.41}$$

The concentration of the reactant A decreases with time from its initial value, $c_{A0,}$ to zero, while the concentrations of the products B and C increase exponentially until A has consumed completely, the ratio of the concentration of B to that of C being constant during the whole course of the reaction,

$$\frac{c_B}{c_C} = \frac{k_B}{k_C}\,. \tag{1.42}$$

Equation (1.39) is similar to (1.8). The sum of k_B and k_C is determined from the slope of a plot of ln c_A against t. Then, by using the ratio of these constants found from the

experimental values of the concentrations of B and C at any fixed time, the values of k_B and k_C can be calculated separately.

1.6: Consecutive chemical reactions

Consecutive reactions involve a sequence of a few reactions following one another. In the case of consecutive reactions of the type $A \rightarrow B \rightarrow C$, if initially ($t = 0$) the concentration of A is a and the substances B and C are missing, while at any moment of time, t, the concentrations are $a - x$ for A, $x - y$ for B and y for C, the rate equations are

$$\frac{dx}{dt} = k_A(a - x) \tag{1.43}$$

for the transformation of A into B with the rate constant k_A and

$$\frac{dy}{dt} = k_B(x - y) \tag{1.44}$$

for the subsequent transformation of B into C with the rate constant k_B.

The integrated equations are

$$x = a[1 - \exp-(k_A t)] \tag{1.45}$$

for A and

$$y = a\{1 + [\frac{k_A}{k_B - k_A}\exp-(k_B t)] - [\frac{k_B}{k_B - k_A}\exp-(k_A t)]\} \tag{1.46}$$

for C.

By subtracting equation (1.46) from (1.45), an expression for the intermediate product B is obtained

$$x - y = a\frac{k_A}{k_B - k_A}\{[\exp-(k_A t)] - [\exp-(k_B t)]\}. \tag{1.47}$$

The determinate forms

$$x - y = akt[\exp-(kt)] \tag{1.48}$$

and

$$y = a\{1-[\exp-(kt)]-[kt\exp-(kt)]\} \tag{1.49}$$

of equations (1.46) and (1.47) in the case of equal values, $k_A = k_B = k$, of both constants are found, using l'Hôpital's rule.

As seen from equation (1.48), the function $(x - y)$ describing the time dependence of the concentration of B must have a maximum because initially ($t = 0$) it is zero, then increases almost linearly {$\exp–(kt)$ is close to unity at small t} and finally again tends to zero {[t $\exp–(kt)$] → 0, as $t \to \infty$}. The time when the maximum is reached can readily be found by differentiating equation (1.48) with respect to time and further equating the first derivative to zero, giving

$$t_{\max} = \frac{1}{k}. \tag{1.50}$$

In this particular case of equal rate constants, the maximum value of the concentration of B is

$$(x-y)_{\max} = a/e, \tag{1.51}$$

where e is the natural logarithm base.

The kinetic dependences for A, B and C in the general case of commensurate values of both constants k_A and k_B are shown schematically in Fig. 1.7. As equations (1.45)-(1.47) contain a on their right-hand parts, the reduced concentrations of the reagents are provided on the ordinate (in fractions relative to the initial concentration of A).

The concentration of A is seen to decrease exponentially from unity to zero with passing time (ordinary first-order reaction). The concentration-time relationship for B again goes through a maximum that is attained at the time

$$t_{\max} = \frac{\ln(k_B / k_A)}{k_B - k_A}. \tag{1.52}$$

Its height is found by inserting $t_{\max}$ into equation (1.47). Hence,

$$(x-y)_{\max} = \frac{a}{r-1}[r^{-1/(r-1)} - r^{-r/(r-1)}], \qquad (1.53)$$

where $r = k_B / k_A$. The maximum value, $(x - y)_{\max}$, of the concentration of B is seen to depend only on the ratio of the rate constants and not on their absolute values.

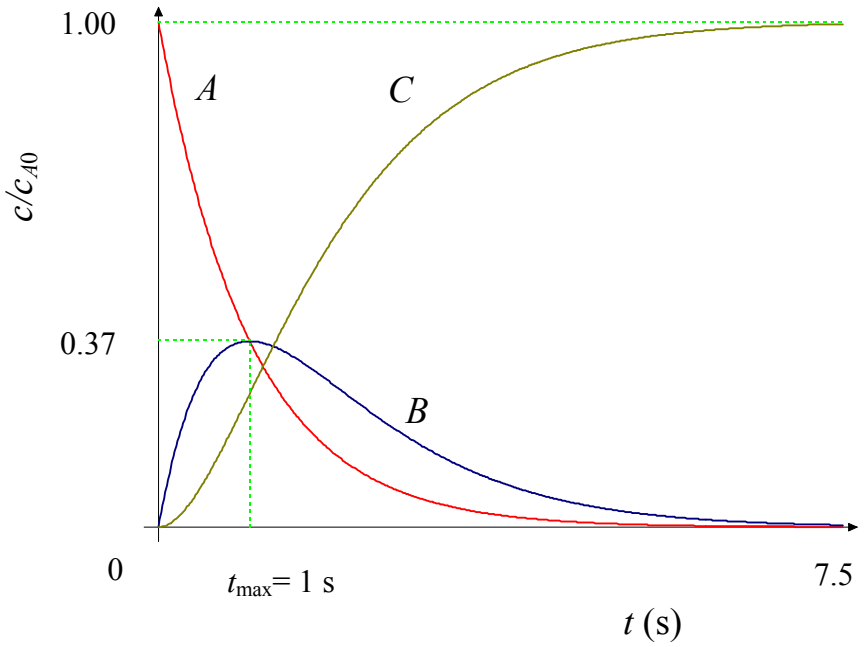

Fig. 1.7. Typical plots of the concentrations c of the reagents A, B and C against time t in the consecutive reaction $A \rightarrow B \rightarrow C$ in the case of equal values of both constants k_A and k_B ($k_A = k_B = 1\ s^{-1}$).

The concentration-time relationship for C is sigmoid in shape and exhibits a point of inflection, whose position coincides with $t_{\max}$. Initially, the rate of formation of the final product C is very low. The initial stage when the product C is hardly detectable is often called the *induction* period of the consecutive reaction. Then, the reaction $A \rightarrow C$ accelerates and after the inflection point has reached it again becomes progressively slow. Finally, the concentration of C attains the initial concentration of A, whereas the latter drops to zero.

Consider two extreme cases. If $k_A >> k_B$ and hence r is very small, then its value can be neglected in comparison with unity, and equation (1.53) yields

$$(x-y)_{\max} \approx \frac{a}{-1}(r^{+1} - r^{-r}) \approx a\,. \qquad (1.54)$$

The concentration-time relationships for this case are shown schematically in Fig. 1.8. The concentration of A drops very rapidly from its initial value a (or unity in relative fractions) to almost zero, so that the concentration curve for A practically coincides with the plot axes and is readily distinguishable only if drawn in colour.

At the same time, the concentration of B increases from zero to values close to a (unity). In other words, A rapidly transforms into B. Accordingly, the maximum on the concentration curve for B becomes higher (0.95 in Fig. 1.8 instead of 0.37 in Fig. 1.7) and displaces towards the origin (t_{max}= 0.05 s). Further reaction actually consists in the consumption of the accumulated substance B in the subsequent slow transformation $B \rightarrow C$. The reaction $B \rightarrow C$ thus becomes *rate-determining* for the whole series of consecutive transformations $A \rightarrow B \rightarrow C$.

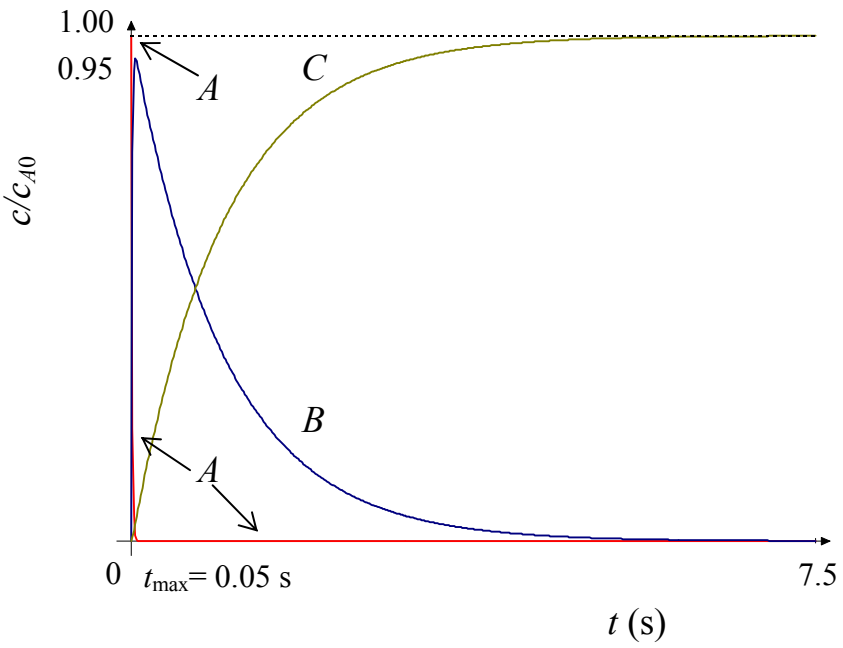

Fig. 1.8. Typical plots of the concentrations c of the reagents A, B and C against time t in the consecutive reaction $A \rightarrow B \rightarrow C$ in the case where $k_A >> k_B$ (k_A = 100 s^{-1}, k_B = 1 s^{-1}).

If $k_A << k_B$ and hence r is very large, then in equation (1.42) unity can be neglected in comparison with its value. Therefore,

$$(x-y)_{max} \approx \frac{a}{r}(r^{-1/r} - r^{-1}) \approx \frac{a}{r} \quad . \qquad (1.55)$$

In this case, the first transformation $A \rightarrow B$ is very slow and therefore is rate-determining for the overall reaction $A \rightarrow B \rightarrow C$. The height of the maximum for B is extremely small.

It should be noted that in both extreme cases none of the reactions ceases entirely. They all are continuing, though at very different rates, until A is consumed completely.

The case in which $k_B > k_A$ and the ratio, k_B/k_A, of the rate constants remains unchanged, while the difference $k_B - k_A$ varies appreciably, deserves further consideration. If k_B / k_A = const, the height of the maximum for B determined from equation (1.53) is the same, whatever the difference $k_B - k_A$, as illustrated schematically in Fig. 1.9 for the hypothetical reaction with $k_B/k_A = 10$ and four values of the difference $k_B - k_A$.

However, as evidenced from equation (1.52), the position of this maximum is dependent upon the difference $k_B - k_A$, so that the smaller the difference $k_B - k_A$, the greater is t_{max}. Also, as seen from Fig. 1.9, the maximum broadens significantly, as the value of $k_B - k_A$ decreases.

It means that at $t > t_{max}$ the rate of formation of B remains close to zero during a rather long period of time. Hence, the *quasi-stationary* regime is established when the rate of formation of B in the first reaction $A \rightarrow B$ of their series $A \rightarrow B \rightarrow C$ is almost equal to the rate of its consumption in the second $B \rightarrow C$.

It is also worth mentioning that, if $k_B > k_A$, the term exp $(-k_B t)$ of equation (1.47) becomes negligibly small at sufficiently long times in comparison with the term exp $(-k_A t)$, and this equation takes the simpler form

$$x - y = a \frac{k_A}{k_B - k_A} \exp -(k_A t). \tag{1.56}$$

Dividing this expression by $a - x = a$ exp $(-k_A t)$ determined from equation (1.45) yields

$$\frac{c_B}{c_A} = \frac{x - y}{a - x} = \frac{k_A}{k_B - k_A}. \tag{1.57}$$

Hence, the *quasi-stationary* state (sometimes also called the *transition equilibrium*) is established when the ratio of the concentration of the intermediate product B to that of the reactant A remains constant.

If $k_B >> k_A$, then $(k_B - k_A) \approx k_B$ and equation (1.46) becomes

$$\frac{c_B}{c_A} = \frac{k_A}{k_B} = \frac{(\tau_{1/2})_B}{(\tau_{1/2})_A} = \frac{(\tau_{life})_B}{(\tau_{life})_A}. \tag{1.58}$$

In this particular case, the reactant *A* and the intermediate product *B* are said to be in *secular equilibrium* with each other, even though it is only the quasi-stationary state and by no means a real equilibrium.

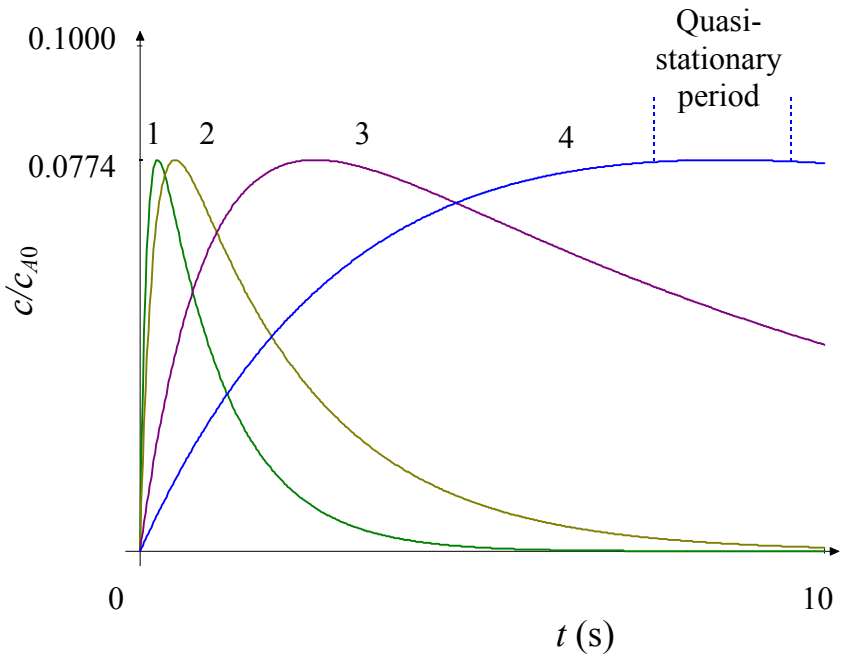

Fig. 1.9. Plots of the concentration c of the intermediate product B formed in the consecutive reaction $A \rightarrow B \rightarrow C$ against time t in the case where $k_B/k_A = 10$ and $k_B = 10.0\ s^{-1}$, $k_A = 1.0\ s^{-1}$ (line 1); $k_B = 5.0\ s^{-1}$, $k_A = 0.5\ s^{-1}$ (line 2); $k_B = 1.0\ s^{-1}$, $k_A = 0.1\ s^{-1}$ (line 3) and $k_B = 0.3\ s^{-1}$, $k_A = 0.03\ s^{-1}$ (line 4).

1.7: Chain chemical reactions

Chain chemical reactions proceed by a series of self-propagating steps. The concept *chain reaction* appears to have been introduced first by M. Bodenstein in 1913. In the course of any chain chemical reaction, not only the molecules of the final products are formed but also the valency-unsaturated atoms or radicals which are able to subsequently react with the parent molecules even more easily than the initial reactants. If in any link of the reaction chain, two or more such atoms or radicals are produced, the reaction chain is likely to grow and branch. In similar subsequent reactions, the valency-unsaturated atoms or radicals are thus multiplied at an increasing rate, giving rise to an exponential increase in the amount of the products.

Consider the main steps of chain reactions using a classical example of the reaction of hydrogen H_2 with chlorine Cl_2 to yield hydrogen chloride HCl: $H_2 + Cl_2 = 2HCl$.

1. Initiation. Unlike ordinary chemical reactions taking place immediately after the reactants are mixed together, any chain reaction only starts after it has been initiated by physical or chemical means. In the example under consideration, the mixture of hydrogen and chlorine does not reveal any tendency to react for a long time, if kept in the dark in a clean vessel. In the light of appropriate frequency v and energy of a quantum hv (with h being Planck's constant) or when a small amount of sodium atoms are admitted, the hydrogen-chlorine reaction begin to proceed appreciably. This chain-initiating step yields chlorine atoms either by

$$Cl_2 + hv = 2Cl^{\bullet}$$

or by

$$Cl_2 + Na = NaCl + Cl^{\bullet}.$$

At this step, chemically active chlorine atoms $Cl^{\bullet}$ are produced. The symbol $^{\bullet}$ designates an unpaired electron.

2. Propagation. The reaction then proceeds by steps

$$Cl_2 + H_2 = HCl + H^{\bullet},$$

$$H^{\bullet} + Cl_2 = HCl + Cl^{\bullet} \text{ and so on.}$$

Each of these elementary steps is seen to give an active atom ($H^{\bullet}$ or $Cl^{\bullet}$) which continue the reaction chain. Two particular cases are

(*i*) chain transfer when one active particle produces a molecule of the product and another active particle which further interact with one of the reactants, and so on (Fig. 1.10a). The chain formed thus becomes progressively longer with passing time, as in the reaction of formation of HCl.

(*ii*) chain branching when one active particle produces, besides a molecule of the product, two or more active particles, thus giving rise not only to the continuation of the existing chain but also to the initiation of new ones (Fig. 1.10b).

An example of branching chain reactions is the oxidation of hydrogen by oxygen $2H_2 + O_2 = 2H_2O$ when each active hydrogen atom is able to produce three new active species by reactions

$H^{\bullet} + O_2 = O^{\bullet}H + O^{\bullet\bullet}$,

$O^{\bullet\bullet} + H_2 = O^{\bullet}H + H^{\bullet}$.

As a result, two new chains may be initiated in addition to the existing one.

In the case (*i*), the chain reaction is called *non-branching*, while in the case (*ii*) *branching* (partly or entirely).

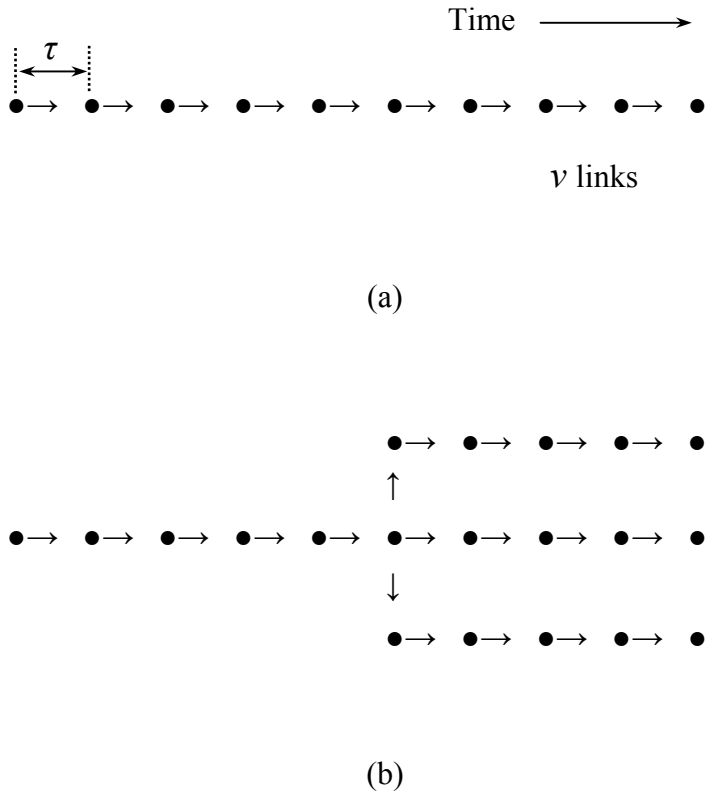

Fig. 1.10. Schematic illustration of (a) non-branching and (b) branching chain chemical reactions. The symbol ● designates an active particle (atom or radical).

3. Termination. This is a step in which an active particle loses its activity without transferring the chain. It may happen as a result of

(*i*) recombination of active atoms into the molecules of either the reactants ($H^{\bullet} + H^{\bullet} = H_2$, $Cl^{\bullet} + Cl^{\bullet} = Cl_2$) or the product ($H^{\bullet} + Cl^{\bullet} = HCl$),

(*ii*) interaction of active atoms with a third body which is able to take away at least some part of the energy liberated when those atoms combine. The walls of a vessel or an inert diluter can serve as this third body. Therefore, the rate of chain chemical reactions is to a significant extent dependent on the size of a vessel (its surface area-to-volume ratio) that is not characteristic of ordinary reactions.

Termination of the chains in the reaction of formation of HCl may be due to reactions of the type (W designates a wall)

$$H^{\bullet} + H^{\bullet} + W = H_2 + W,$$

$$Cl^{\bullet} + Cl^{\bullet} + W = Cl_2 + W.$$

(*iii*) interaction of an active atom with a chemical compound of a polyvalence metal which is able either to provide an electron to that atom or to assume an electron from it.

In chain reactions, as many as 10^6 molecules of the product can be formed per one initiating particle. Their rate is therefore strongly dependent on the presence of impurities which are able to combine such particles into low-active ones, thereby causing the termination of the chain. The effect of impurities (inhibitors) may be comparable to that of initiators.

A quantitative theory of the kinetics of chain chemical reactions has been put forward by N.N. Semyonov and C.N. Hinshelwood in the 1930s. Strict theoretical considerations are based on the solution of a system of differential equations. Presented is a less sophisticated and easily tractable variant of the theory that follows from a probability analysis (see, for example, Ref. [11]).

Consider a chain consisting of ν links, each of which is formed during a time τ. This chain is initiated by a single active particle and thus ν characterises its average length. The product $\nu\tau$ is clearly the average time of propagation of the chain.

Let the number of active particles occurred in unit volume per unit time be n_0. Obviously, this quantity is a measure of the rate of initiation of the chains.

If the termination of a given chain happens after its ν links has formed, the probability of termination β is $1/(\nu - 1)$ or $\beta = 1/\nu$ since $\nu >> 1$. Let us assume that the concentration of active particles, *i.e.* their number per unit volume, is n. Then, the rate of change in concentration of these particles will be $n/(\nu\tau) = \beta n/\tau$.

Branching the chains exerts an effect opposite to that of termination by diminishing the probability of termination to $\beta - \delta$, where δ is the probability of branching. Hence, the rate of change in concentration of active particles can finally be written as

$$\frac{\mathrm{d}n}{\mathrm{dt}} = n_0 - (\beta - \delta)\frac{n}{\tau}. \qquad (1.59)$$

Separating the variables and integration with the initial condition $n = 0$ at $t = 0$ yields

$$n = \frac{n_0\tau}{\beta - \delta}[1 - \exp(-\frac{\beta - \delta}{\tau}t)]. \qquad (1.60)$$

Since the total number of particles occurred in unit volume per unit time is n/τ, the rate of the chain reaction is expressed by an equation of the form

$$\upsilon = \frac{n_0}{\beta - \delta}[1 - \exp(-\frac{\beta - \delta}{\tau}t)]. \qquad (1.61)$$

Three typical cases following from this equation are worth further analysis.

1. If the branching of chains is lacking ($\delta = 0$), equation (1.61) becomes

$$\upsilon = \frac{n_0}{\beta}[1 - \exp(-\frac{\beta}{\tau}t)]. \qquad (1.62)$$

Hence, the rate of the chain reaction increases with passing time and eventually reaches its maximal value of $n_0/\beta = \nu n_0$ (Fig. 1.11, line 1). It means that a stationary state of constant reaction rate must be established. Because of the presence of chains, this stationary rate is ν times greater than the rate of their initiation n_0. In other words, the rate of the chain reaction proves ν times greater than that which would be observed in the absence of any chains when $\nu = 1$.

2. If the branching of chains takes place but the probability of branching is less than the probability of termination ($0 < \delta < \beta$), a stationary state of constant reaction rate $n_0/(\beta - \delta)$ is again established. The reaction rate (line 2 in Fig. 1.11) is seen to be greater than that in the former case.

3. If the probability of branching is greater than the probability of termination ($\delta > \beta$), equation (1.61) assumes the form

$$\upsilon = \frac{n_0}{\delta - \beta}[\exp(\frac{\delta - \beta}{\tau}t) - 1] \approx \frac{n_0}{\delta - \beta}\exp(\frac{\delta - \beta}{\tau}t). \qquad (1.63)$$

Unlike the first two cases, in this case the reaction rate increases very abruptly after a relatively long induction (or acceleratory) period, as illustrated schematically in Fig. 1.11

(line 3). The formation of a huge amount of reaction products in a short time may eventually result in inflammation or explosion of a mixture of reacting substances.

General numerical estimations indicate that in a chain reaction lasting around six seconds only 0.1 % of the total amount of the reagents reacts in the first three seconds (see, for example, Ref. [11]. Then, the amount reacted is 14 % in four seconds and 80 % in five seconds. Thus, the induction period of this reaction constitutes around half the total reaction time. The reaction actually commences and ends between third and sixth seconds.

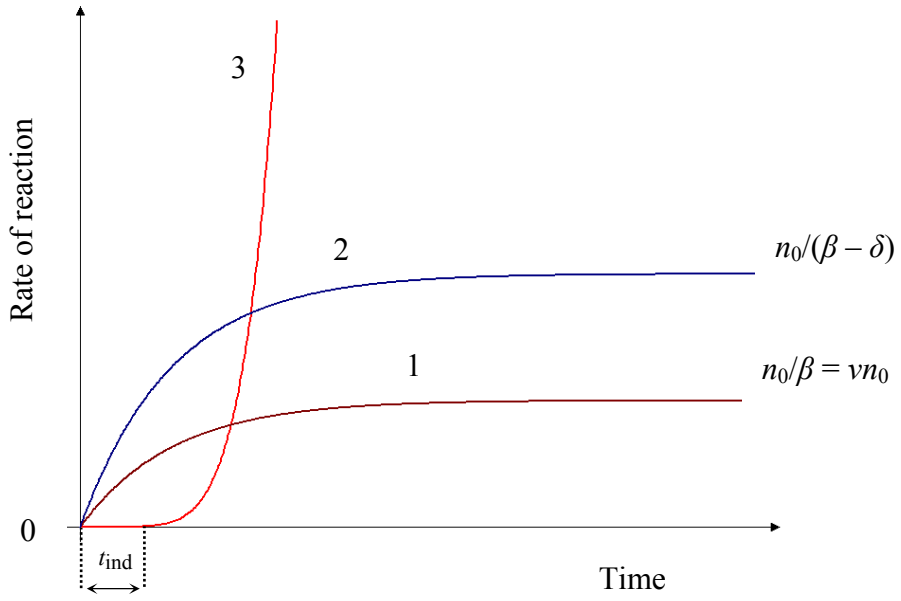

Fig. 1.11. Typical plots of the rate of reaction against time for chain reactions. 1, no branching; 2, the probability of branching is less than the probability of termination ($0 < \delta < \beta$); 3, the probability of branching is greater than the probability of termination ($\delta > \beta$).

It should be noted that the analytical considerations presented in this section are based on the assumption that the concentrations of the reagents are maintained constant, while the products are taken away from the reaction zone. These conditions are rarely fulfilled in practice because the amount of initial substances in any reaction is finite, while the products remain in the reaction zone. Therefore, any reaction eventually ceases in view of the full consumption of at least one of the reagents. It may also happen that the reagents are consumed completely before the stationary state is established.

1.8: Homogeneous chemical reactions: short conclusions

1. Any homogeneous chemical reaction takes place within one phase. Its reagents are (or at least can be) intermixed at the microscopic (atomic, ionic or molecular) level (Fig. 1.12).

2. If a variety of reactions proceed simultaneously in a given system, their elementary acts are considered to be independent of each other. Accordingly, the rate of each of those reactions is expressed by an individual mathematical equation. These equations are summarised algebraically to give a general equation for the total rate of the reaction.

3. Kinetics of homogeneous chemical reactions are largely described by equations of the exponential type.

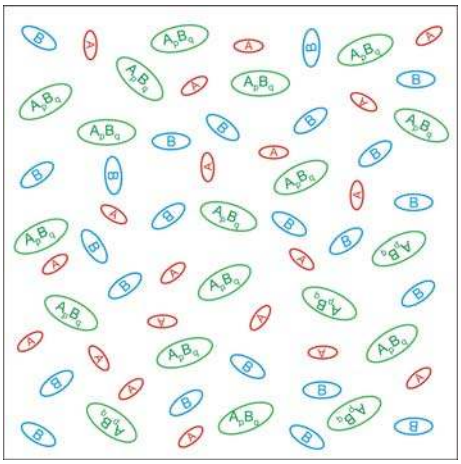

Fig. 1.12. Schematic illustration of a homogeneous chemical reaction of the type $pA + qB = A_pB_q$. Three reacting species A, B and A_pB_q are intermixed at the molecular level. The size of the reaction volume far exceeds the size of the particles involved into the reaction.

2: Interfacial formation of a chemical compound layer between elementary substances

2.1: Description of the kinetics of solid-state heterogeneous reactions

Let us begin an analysis of the process of formation of chemical compounds in heterogeneous systems with the simplest case of growth of a solid layer between elementary substances A and B which form, according to the equilibrium phase diagram of the A–B binary system, only one chemical compound A_pB_q, p and q being positive numbers (Fig. 2.1). The substances A and B are considered to be solid at reaction temperature T_1 and mutually insoluble.

An example of interfacial formation of a single compound layer is provided in Fig. 2.2 where the microstructure of the Ni-Bi transition zone is shown. The $NiBi_3$ intermetallic layer is formed at the interface between nickel and bismuth (solid or liquid) [16].

It is easy to notice that the basic concepts and laws of the kinetics of homogeneous chemical reactions surveyed in the preceding section can hardly be used in considering the examined *heterogeneous* process. Indeed, difficulties already arise when employing the main concepts of chemical kinetics, namely, the *concentration* of a reactant or a product in the system and the *rate* of a chemical reaction.

In the case of any homogeneous system in which all reacting substances are mixed at the atomic or molecular level, the definition of the concentration as the amount of a substance in unit volume is applicable to the entire system consisting of initial substances and reaction products as a whole. By contrast, in the case of any heterogeneous system, it is only rational for components A and B within each of its homogeneous parts (phases).

In the examined case of the A–A_pB_q–B system, it is clearly possible to define the concentration (content) of component, for example A, in initial phases A and B or in a growing layer of the compound A_pB_q. However, it is quite irrational to consider the concentration of substance A, A_pB_q or B in the entire heterogeneous system consisting of non-mixing phases A, A_pB_q and B. In contrast to any homogeneous system in which the concentration of a given substance at any moment of time is the same at all points of the reaction volume or at least changes smoothly from point to point, in any heterogeneous system this is so only within each of the phases involved into the interaction. At the phase interfaces its value changes abruptly (see Figs. 2.1 and 2.2). Therefore, in heterogeneous systems the distribution of the concentrations of components A and B with distance becomes important. In reaction couples without any mutual solubility of the components, it resembles a waterfall with a flat step between its top and bottom.

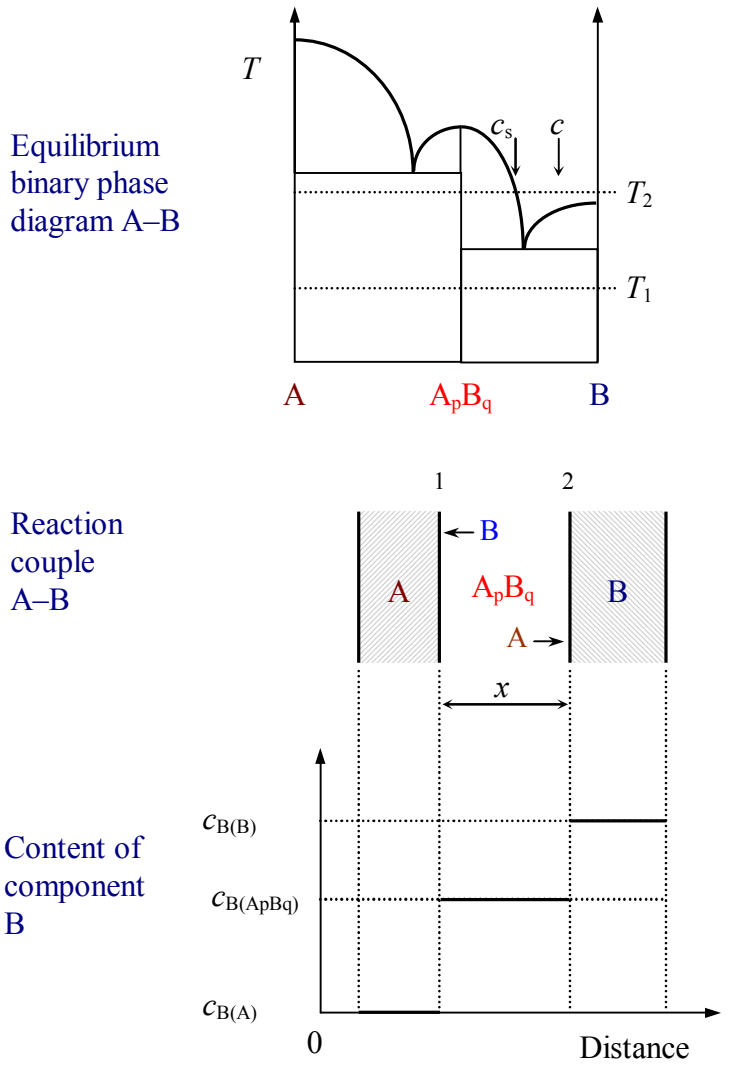

Fig. 2.1. Schematic diagram to illustrate the heterogeneous process of growth of the A_pB_q chemical compound layer at the interface between mutually insoluble elementary substances A and B.

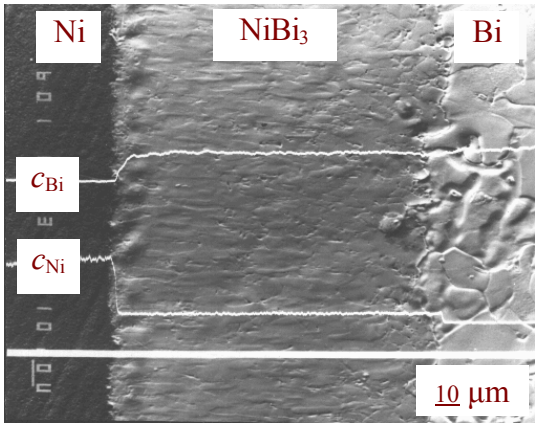

Fig.2.2. Microstructure (secondary electron image) of the Ni–Bi transition zone and the concentration profiles of both components within the phases involved into the interaction. Reaction conditions: temperature 250 °C, holding time 9×10^4 s (25 h). The $NiBi_3$ intermetallic compound is seen to form a continuous compact layer between nickel and bismuth.

In application to heterogeneous systems under consideration, the chemical compound may defined as an ordered phase of constant composition. Ordering means that in the crystal lattice of any compound each component forms its own sublattice in which all the sites are only occupied by atoms or ions of this component.

The constancy of composition is a consequence of the valency rule as, for example, in the case of oxides (Al_2O_3, CuO, TiO_2, Fe_3O_4), or of much more complicated and still poorly understood laws as in the case of intermetallics where compounds of somewhat surprising and hardly tractable composition ($NiBi_3$, Fe_2Al_5, $CoSn_2$, IrMo) are formed. Though the solids definitely contain no molecules, for example, of Al_2O_3 or $NiBi_3$ as such, the composition of the Al_2O_3 or $NiBi_3$ phases is on average described by these chemical formulae.

Stoichiometry resulting from the chemist's laws of definite (J.L. Proust, 1794) and multiple (J. Dalton, 1804) proportions is a characteristic feature of chemical compounds that distinguishes them from solid solutions, *i.e.* disordered phases of varying composition. As will be clear from further considerations, it is just the *stoichiometry* of a chemical compound and not the presence of *inherent structure defects*, as usually assumed, that determines the growth kinetics of the solid layer of that compound at the interface of initial substances.

Obviously, such a measure of the rate of a chemical reaction taking place in any homogeneous system as the change in *concentration* of reacting substances or its products per unit time at constant reaction volume (see Section 1.2) can by no means be applied to heterogeneous systems. In any heterogeneous system, the concentration (content) of components A and B both in initial phases and in a growing layer of the A_pB_q compound

having no homogeneity range always remains constant, in spite of the occurrence of any chemical reaction.

Therefore, a quantitative characteristic of the rate of a chemical reaction in any heterogeneous system is the change of the *thickness* or *mass* of a solid compound layer per unit time. Choice of the method of following the growth process of any compound layer (either by its thickness or by mass) depends entirely upon the efficiency of experimental techniques available for the investigation of interaction of initial substances in a particular heterogeneous system.

In this book, attention will only be paid to the parallel-plane layers whose thickness is the same over the entire surface of contact of the reactants. In addition, the length of the layer in the direction normal to the direction of diffusion of components *A* and *B* (see Fig. 2.1) is assumed to be considerably greater than its thickness. In this case, the edge effects on the process of layer growth can be neglected.

2.2: Reaction-diffusion process in a heterogeneous system

As its name indicates, the reaction-diffusion process includes two alternate steps (reaction and diffusion) and results in the occurrence of a continuous solid compound layer between initial substances. Unlike homogeneous reactions, in this case the reaction product necessarily stays in place at the interface and is not carried away from the reaction site, thus separating the reacting phases from each other (see Figs 1.1b and 2.1).

The term *reaction diffusion* reflects the most important feature of the layer-formation mechanism. Namely, the layer growth is due to a continuous alternation of two consecutive steps:

(1) *diffusion* of atoms (ions) of the reactants across its bulk in the opposite directions;

(2) *subsequent chemical transformations* taking place at the layer interfaces with the participation of diffusing atoms of one of the components and the surface atoms of another component (*chemical reaction* as such).

In the present case, reaction-diffusion process may thus be defined concisely as chemical transformations after diffusion or *vice versa*, both steps being inseparably linked to one another. It should be emphasised that the term *diffusional* (or *diffusion-controlled*) *growth* (*formation*) of chemical compound layers, used largely by physicists and metallurgists, only reflects one of the two aspects of the layer-growth mechanism, namely, atomic diffusion.

The inadequacy of terminology is not so unimportant as it may seem at first sight. If employed solely to mask the attempt to tacitly neglect the step of *chemical transformations* inherent in the reaction-diffusion process, it results, as will be seen later, in a chain of misleading consequences and views, even though the treatment of the kinetics of solid-state formation of *chemical compounds* can formally be declared.

In the case under consideration, the concept *chemical transformations* (synonyms: *chemical reaction*, *chemical interaction*) unites the following processes.

(1) Transition of the atoms (ions) of a given kind through the interface from one phase into the other. This is *external* diffusion, different from *internal* diffusion taking place inside any growing compound layer.

(2) Redistribution of the electronic density of atomic orbitals resulting in the formation of molecules, ions, radicals or other stable groupings of atoms included in a growing compound layer.

(3) Rearrangement of the crystal lattices of parent phases into the crystal lattice of a chemical compound formed.

It should be noted that something like the elementary act of external diffusion also occurs in homogeneous reactions taking place in solutions or gases. Indeed, in order to be combined into a molecule, the reacting particles must move (diffuse) towards each other. The second of these processes in a liquid-phase or a gas homogeneous system results in the formation of an individual molecule that is able to travel relatively freely within the reaction volume.

In the solid-state heterogeneous system under consideration, however, the "molecule" formed is rigidly fixed in the crystal lattice of a chemical compound together with a number of other similar "molecules", thus lost their individuality. What is only possible in this case is the substitution of atoms of any of the "molecules" comprising the layer for equivalent atoms, not violating the stoichiometry of a compound and the total balance of atoms in the entire system.

In the general case of comparable mobility of components A and B within the A_pB_q crystal lattice, the A_pB_q compound layer grows at the expense of diffusion of the B atoms to interface 1 (see Fig. 2.1) where a *partial* chemical reaction then takes place in accordance with the equation

$$qB_{\text{dif}} + pA_{\text{surf}} = A_pB_q \qquad (2.1)$$

and also at the expense of diffusion of the A atoms to interface 2 followed by another *partial* chemical reaction

$$pA_{\text{dif}} + qB_{\text{surf}} = A_pB_q. \qquad (2.2)$$

Clearly, the rates of these reactions are different. Indeed, before entering reaction (2.1), the B atoms must lose any contact with the main body of substance B and be transferred across the A_pB_q layer from interface 2 to interface 1. On the contrary, component A enters this reaction in the form of particles (atoms or ions) located onto the surface of phase A and therefore bonded chemically with the bulk of substance A. The A atoms diffusing across the

A_pB_q layer from interface 1 to interface 2 and the surface B atoms enter reaction (2.2). In addition, reactions (2.1) and (2.2) take place at different interfaces of the A_pB_q layer and are therefore separated in space. Hence, the equality of their rates is a rare exception rather than the rule. Kinetically, these are actually two different parallel chemical reactions.

Note that parallel reactions (2.1) and (2.2) have nothing in common with parallel homogeneous chemical reactions treated in Section 1.5, except for the word *parallel*. In the former case, two parallel reactions proceeding at two layer interfaces yield a single compound layer. In the latter, one reactant produces two or a few products. Their kinetics are described by quite different mathematical equations.

It should be emphasised that in any heterogeneous system that attained constant temperature-pressure conditions from below (from smaller to higher values), no reaction ever proceeds within the bulk of the A_pB_q layer. Inside the A_pB_q layer, the A and B atoms (or ions) can and do exchange of their positions but these acts of natural diffusion by no means represent any chemical reaction.

It is also worth mentioning that some relatively short initial period of interaction of elementary substances when there is still no compound layer and consequently there is only one common interface at which substances A and B are able to react immediately is outside the scope of the proposed macroscopic consideration. This period of formation of a chemical compound layer between reacting phases is to be the subject of examination within the framework of a microscopic theory that would indicate, amongst other parameters of the process, a minimal value of the layer thickness sufficient to identify the reaction product accumulated at the A–B interface as the chemical compound A_pB_q possessing its typical physical and chemical properties.

It should be noted, however, that available experimental data provide evidence that this minimal value appears to be very small in comparison with really measured thicknesses of compound layers. Compound layers around 5 nm thick are known to be readily identifiable by refined experimental techniques such as electron microscopy, X-ray diffraction, Rutherford backscattering of light ions, electron probe microanalysis, ion mass spectrometry, *etc*.

As the values of lattice spacing of chemical compounds are usually of the order of 0.5 nm or more, it follows that any compound layer 5 nm thick contains at most 10 crystal-lattice units. Nonetheless, such thin layers in vast majority of cases reveal the stoichiometry and the crystal structure of bulk phases. Hence, the neglect of the initial immediate reaction between substances A and B does no appear to exert any noticeable influence on the kinetic layer thickness-time dependences observed in practice.

2.3: Growth of the A_pB_q layer at the expense of diffusion of component B

Let us assume that reaction (2.1) is the only one in the A–A_pB_q–B system, *i.e*. the diffusivity of component A in the crystal lattice of the A_pB_q compound is negligible in comparison with that of component B. The kinetic equation expressing the growth rate of the

A_pB_q layer as a result of diffusion of the B atoms and subsequent reaction (2.1) can readily be found using the following three assumptions (postulates).

(1) The time dt required for increasing the thickness of the A_pB_q layer by dx_{B1} (from x to x + dx_{B1}, Fig. 2.3) is the sum of the time $\mathrm{d}t_{\mathrm{dif}}^{(B)}$ of diffusion of the B atoms across its bulk to the reaction site (interface 1) and the time $\mathrm{d}t_{\mathrm{chem}}^{(B)}$ of their subsequent chemical interaction with the surface A atoms at interface 1

$$\mathrm{d}t = \mathrm{d}t_{\mathrm{dif}}^{(B)} + \mathrm{d}t_{\mathrm{chem}}^{(B)}. \tag{2.3}$$

(2) The time $\mathrm{d}t_{\mathrm{dif}}^{(B)}$ of diffusion of the B atoms is directly proportional to both the increase dx_{B1} of the thickness of the A_pB_q layer and its total thickness x

$$\mathrm{d}t_{\mathrm{dif}}^{(B)} = \frac{x}{k_{1B1}}\mathrm{d}x_{B1}, \tag{2.4}$$

where k_{1B1} is a physical (diffusional) constant (m^2 s^{-1}).

(3) The time $\mathrm{d}t_{\mathrm{chem}}^{(B)}$ of chemical transformations at interface 1 with the participation of diffusing B atoms (chemical reaction as such) is directly proportional to the increase dx_{B1} of the thickness of the A_pB_q layer and is independent of its total thickness x

$$\mathrm{d}t_{\mathrm{chem}}^{(B)} = \frac{1}{k_{0B1}}\mathrm{d}x_{B1}, \tag{2.5}$$

where k_{0B1} is a chemical constant (m s^{-1}).

The subscript Bl at dx indicates that the increase in thickness the A_pB_q layer is a result of diffusion of the B atoms and takes place at interface 1. In the subscripts 0B1 at the chemical constant k_{0B1} and 1B1 at the physical (diffusional) constant k_{1B1}, the first digit shows that $\mathrm{d}t_{\mathrm{chem}}^{(B)}$ is proportional to x^0, while $\mathrm{d}t_{\mathrm{dif}}^{(B)}$ is proportional to x^1; the letter B and the last digit 1 have the former meaning.

Basic assumptions 1 to 3 were put forward [16] as a result of analysis (*i*) of the reaction-diffusion mechanism described in detail by V.I. Arkharov [17] and (*ii*) of a linear-parabolic equation derived for the first time by U.R. Evans from somewhat different considerations [18].

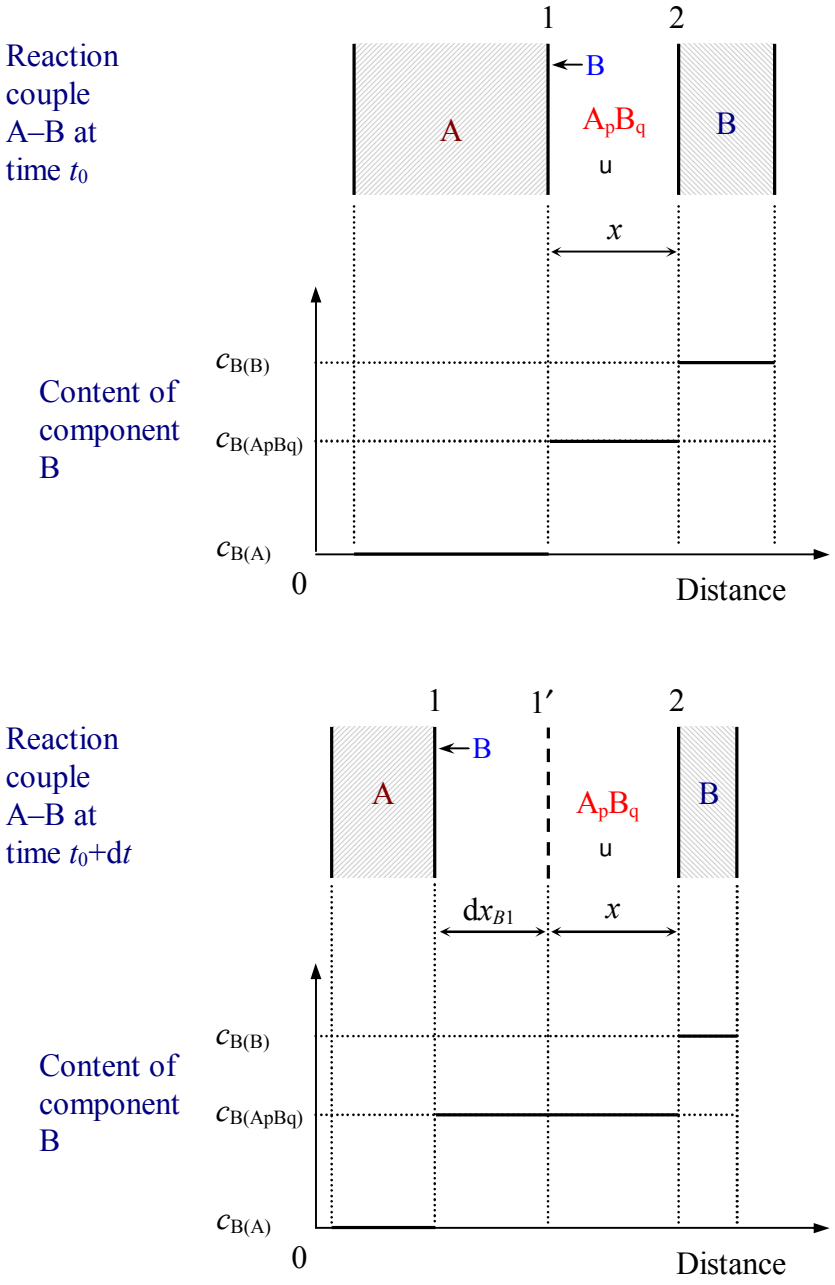

Fig. 2.3. Schematic diagram to illustrate the growth process of the A_pB_q layer between elementary substances A and B at the expense of diffusion of the B atoms and their subsequent chemical interaction with the surface A atoms. The symbol u designates an inert marker inside the A_pB_q layer. An increase in layer thickness takes place only at the A–A_pB_q interface. Not to scale; in fact, $dx_{B1} << x$.

It should be noted that similar assumptions were also used earlier by B.Ya. Pines [19], who, when deriving differential forms of kinetic equations, summed up the duration of external and internal diffusion. Physicist B.Ya. Pines appears to be unaware of chemical studies of U.R. Evans. He never referred to his works and in all probability rediscovered independently the kinetic equation that had already been known for decades, at least to chemists.

Substituting the expressions for $\mathrm{d}t_{\mathrm{dif}}^{(B)}$ and $\mathrm{d}t_{\mathrm{chem}}^{(B)}$ from equations (2.4) and (2.5) into equation (2.3) yields a differential form of the required kinetic equation describing the growth rate of the A_pB_q compound layer due to partial chemical reaction (2.1)

$$\mathrm{d}t = \left(\frac{x}{k_{1B1}} + \frac{1}{k_{0B1}} \right) \mathrm{d}x_{B1} \tag{2.6}$$

or

$$\frac{\mathrm{d}x_{B1}}{\mathrm{d}t} = \frac{k_{0B1}}{1 + \dfrac{k_{0B1}x}{k_{1B1}}}. \tag{2.7}$$

Integration of equation (2.6) with initial condition $x = 0$ at $t = 0$ gives an expression relating the time of growth of the A_pB_q layer to its total thickness

$$t = \frac{x^2}{2k_{1B1}} + \frac{x}{k_{0B1}}. \tag{2.8}$$

These equations represent differential (equations (2.6) and (2.7)) and integrated (equation (2.8)) forms of Evans' equation. In fact, their distinction from the original Evans equation only consists in the lesser amount of constants. After eliminating excessive constants, it is easy to appreciate the significance and importance of Evans' equation that is not merely one of a number of known kinetic dependences.

Obviously, in an initial period of interaction of substances A and B when the A_pB_q layer is still very thin, the number of the B atoms which could have diffused to interface 1 per unit time is considerably greater than the number of those atoms which could be combined in the A_pB_q compound by the surface A atoms. It should be noted that, in spite of the displacement of interface 1 in the course of reaction (2.1), the number of the A atoms per unit area of the surface of substance A adjacent to the A_pB_q layer remains constant. As seen in Fig. 2.4, the number of the A atoms is the same in all sections of phase A by the vertical plane passing through the atomic sites.

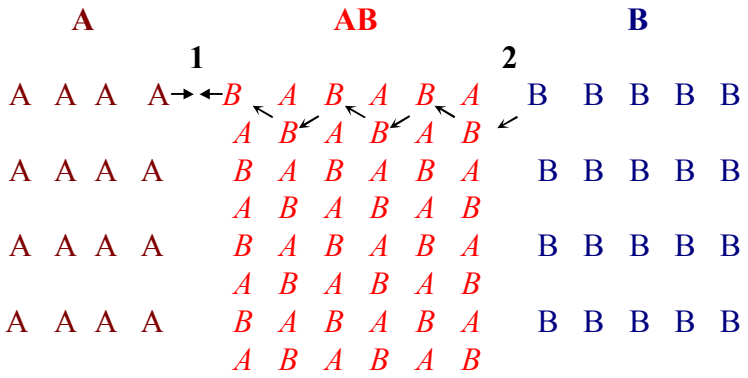

Fig. 2.4. Schematic diagram to illustrate the mechanism of growth of the *AB* compound layer between elementary substances *A* and *B* at the expense of diffusion of component *B*. Arrows indicate only one of the four shortest paths of supply of the *B* atoms from substance *B* to interface 1 where subsequent chemical transformations with their participation take place.

For real crystalline substances, this only holds with the accuracy to the lattice spacing. Since the lattice spacing is much less than the layer thickness, initial substances can be considered as macroscopically isotropic, at least in the direction of layer growth.

Each surface *A* atom is able to chemically bond a certain number of diffusing *B* atoms. For the *AB* compound (see Fig. 2.4), this number is equal to unity, while for the A_pB_q compound to q/p. Since the number of the *A* atoms onto the surface of phase *A*, which are ready to immediately react with the diffusing *B* atoms, is finite, it is obvious that the reactivity of the *A* surface towards these atoms is also finite.

The *reactivity* (or *combining ability*) of the *surface* of substance *A towards the B atoms* is equal to the largest number of diffusing *B* atoms that can be combined per unit time by the surface *A* atoms into a compound of certain composition. For example, if each of the four surface *A* atoms shown in Fig. 2.4 combines per second one diffusing *B* atom into the *AB* compound at interface 1, the reactivity of the *A* surface towards the *B* atoms is four *B* atoms per second.

Initially, when the A_pB_q layer is very thin, the reactivity of the *A* surface is realised to the full extent because the supply of the *B* atoms is almost instantaneous due to the negligibly short diffusion path. In such a case, the condition $k_{0B1} << k_{1B1}/x$ is satisfied. Therefore, if the surface area of contact of reacting phases *A* and A_pB_q remains constant, chemical reaction (2.1) takes place at an almost constant rate. In practice, this regime of layer growth is usually referred to as *reaction controlled*. Though much less suited, the terms *interface controlled regime* and *kinetic regime* are also used.

In the reaction controlled regime, the overall rate of layer formation is only limited by the rate of chemical transformations (chemical reaction as such). Therefore, the A_pB_q layer grows at the highest rate possible under given temperature-pressure conditions:

$$\left(\frac{dx_{B1}}{dt}\right)_{\text{reaction controlled regime}} = k_{0B1}. \qquad (2.9)$$

Equation (2.9) results from equations (2.6) and (2.7) if $k_{0B1} << k_{1B1}/x$. In this case, the first term on the right-hand side of equation (2.8) is negligibly small compared to the second one. Hence, initial growth of the A_pB_q layer is linear:

$$x = k_{0B1}t. \qquad (2.10)$$

The chemical constant k_{0B1} can readily be determined from the experimental dependence of the A_pB_q layer thickness upon time plotted in coordinates $x - t$ (Fig. 2.5a). The slope of its initial linear portion gives a value of k_{0B1}.

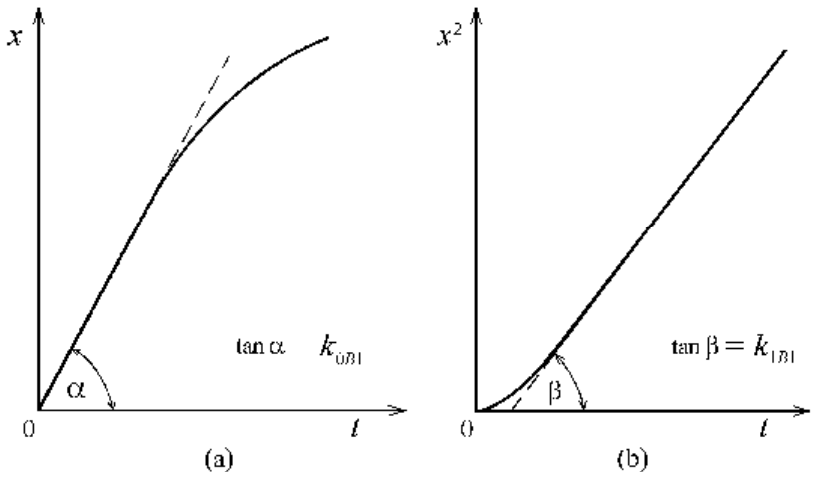

Fig. 2.5. Experimental determination of reaction-diffusion constants from a linear-parabolic dependence between the layer thickness, x, and time, t, of interaction of initial substances: $\tan \alpha = k_{0B1}$ (a), $\tan \beta = k_{1B1}$ (b). Not to scale. In fact, linear region of Fig. 2.5a corresponds to the beginning of non-linear region of Fig. 2.5b.

It is easy to understand that the reaction controlled regime of growth of the A_pB_q layer is one of the two extremes. Another is its growth in the *diffusion controlled* (or simply *diffusional*) regime. Indeed, as long as the A_pB_q layer steadily thickens, the transport of the B atoms across its bulk from interface 2 to interface 1 (see Fig. 2.3) becomes increasingly slow. Therefore, with passing time the overall rate of layer formation becomes more and more dependent on the rate of diffusion of the B atoms, whereas the effect of the rate of chemical transformations gradually decreases and eventually becomes negligible by comparison.

During growth of the A_pB_q layer in the diffusion controlled regime, the condition $k_{0B1} >> k_{1B1}/x$ is satisfied in equations (2.6) to (2.8). In this case, the rate of growth of the layer is inversely proportional to its total thickness x existing at a time t

$$\left(\frac{\mathrm{d}x_{B1}}{\mathrm{d}t}\right)_{\text{diffusion controlled regime}} = \frac{k_{0B1}}{x}. \qquad (2.11)$$

The time dependence of the A_pB_q layer thickness is therefore described by a parabolic equation of the form

$$x^2 = 2k_{1B1}t. \qquad (2.12)$$

The physical (diffusional) constant k_{1B1} can readily be found from a long-time portion of the same A_pB_q layer thickness-time dependence but now plotted in coordinates $x^2 - t$ (Fig. 2.5b). The slope of a plot of the squared thickness of the A_pB_q layer against time yields a value of k_{1B1}. If reaction times and accordingly layer thicknesses are insufficiently large to neglect a linear portion of the A_pB_q layer thickness-time dependence without any noticeable error, equation (2.11) must be integrated with the use of initial condition $x = x_0$ at $t = 0$ or $x = x_0$ at $t = t_0$, giving

$$x^2 - x_0^2 = 2k_{1B1}t \qquad (2.13)$$

or

$$x^2 - x_0^2 = 2k_{1B1}(t - t_0). \qquad (2.14)$$

Thus, both constants (chemical and physical) are determined from different portions of one and the same kinetic dependence of the Evans type.

It should be noted that if one reaction (2.5) takes place in the A–A_pB_q–B system, not only the differential time dt is the sum of two terms $\mathrm{d}t_{\mathrm{dif}}^{(B)}$ and $\mathrm{d}t_{\mathrm{chem}}^{(B)}$, but the integral time t required for the A_pB_q layer to grow from 0 to x also consists of two terms, namely, the time $t_{\mathrm{dif}}^{(B)}$ of diffusion of the B atoms from interface 2 to interface 1

$$t_{\mathrm{dif}}^{(B)} = \frac{x^2}{2k_{1B1}} \tag{2.15}$$

and the time $t_{\mathrm{chem}}^{(B)}$ of chemical transformations with their participation at interface 1

$$t_{\mathrm{chem}}^{(B)} = \frac{x}{k_{0B1}}. \tag{2.16}$$

As the steps of diffusion and chemical transformations are consecutive and alternate, this result appears to be quite obvious.

The idea about the summation of the times of consecutive steps of the examined solid-state process is of primary importance for understanding the peculiarities of multiple formation of compound layers in heterogeneous systems. Moreover, even in the case of growth of a single compound layer, this idea makes it possible to reveal a few aspects of the reaction-diffusion process, which remained overlooked until the year 1982 [16].

2.3.1: Critical thickness of the A_pB_q layer with regard to component B

While the reactivity of the A surface towards the B atoms remains constant, the flux of the B atoms across the A_pB_q layer gradually decreases from infinitely high to infinitely small values, as the layer thickness increases with passing time from zero to infinitely high values. Hence, there is a single *critical* thickness of the A_pB_q layer [16]

$$x_{1/2}^{(B)} = \frac{k_{1B1}}{k_{0B1}} \tag{2.17}$$

at which these quantities are equal. Equation (2.17) is obtained from equations (2.3)-(2.6) by putting $\mathrm{d}t_{\mathrm{dif}}^{(B)} = \mathrm{d}t_{\mathrm{chem}}^{(B)}$.

The equality $\mathrm{d}t_{\mathrm{dif}}^{(B)} = \mathrm{d}t_{\mathrm{chem}}^{(B)}$ means that half the differential time dt is spent on the transport of the B atoms to the reaction site, while another half is spent on further chemical transformations in which those atoms take part. This is denoted by the index 1/2 at x.

At $x < x_{1/2}^{(B)}$, the reactivity of the A surface towards the B atoms is less than the flux of these atoms across the A_pB_q layer. Therefore, there are “excessive” B atoms which may be used in the formation of either other chemical compounds (enriched in component A in

comparison with the A_pB_q compound) of a multiphase binary system or a solid solution of B in A.

On the contrary, at $x > x_{1/2}^{(B)}$, there is a deficit of the B atoms because the reactivity of the A surface exceeds the flux of these atoms across the A_pB_q layer. Therefore, on reaching interface 1, each B atom is combined at this interface into the A_pB_q compound. In this case, there are no "excessive" B atoms for the formation of other compounds enriched in component A. Thus, none of compound layers located between A and A_pB_q can grow at the expense of diffusion of component B. This almost obvious result following in a natural way from the proposed physico-chemical considerations is crucial for understanding the mechanism of formation of multiple compound layers. Perhaps, just its evident character is the main reason, firstly, why it was overlooked by other investigators and, secondly, why it was met with prejudice by many university professors and members of different academies, but fortunately not by students and active researchers whose minds are flexible enough to readily accept obvious facts.

It should be emphasised that in the examined case of growth of a single layer of the A_pB_q compound, there is only the *possibility* of occurrence of an "excess" of the B atoms at $x < x_{1/2}^{(B)}$, but not this excess as such in the form of a build-up of those atoms at interface 1. In the solid-state reactions, there is simply no free space for this to take place. Therefore, the word *excess* was inserted in the commas, in contrast to the word *deficit*. At $x > x_{1/2}^{(B)}$, a relative deficit of the B atoms is the severe reality even for the A_pB_q layer itself, which could otherwise have grown at a much higher rate.

The thickness $x_{1/2}^{(B)}$ of the A_pB_q layer is referred to as *critical* because the growth conditions for the layers of other compounds of a given multiphase system become indeed critical if $x > x_{1/2}^{(B)}$. At this thickness, all other compound layers lose a source of the B atoms (only substance B is actually such a source) and their growth at the expense of diffusion of the B atoms proves impossible. This problem will be examined in more detail when analysing the process of formation of two or more chemical compound layers.

The existence of a critical thickness of any growing layer can easily be understood without any complicated mathematical equations from a schematic diagram shown in Fig. 1.10. This diagram explains the mechanism of physico-chemical processes taking place in the *A–AB–B* system. Only one of the diffusion paths, along which the B atoms can move (see Fig. 2.4), is shown in Fig. 2.6. To simplify the diagram, the number of "molecular" *AB* units was halved in comparison with their number in Fig. 2.4.

Let us assume that the chemical transformations resulting in the formation of an additional "molecule" *AB* require six seconds, of which the diffusion of a B atom through interface 1 to phase A takes one second, whereas the redistribution of electrons and the rearrangement of the A lattice into the *AB* lattice take five seconds in total. It is also assumed that the transition of each B atom to the adjacent vacant site of the *AB* lattice takes place within one second. The time of external diffusion of a B atom from phase B through interface 2 into the *AB* lattice is considered to be one second as well.

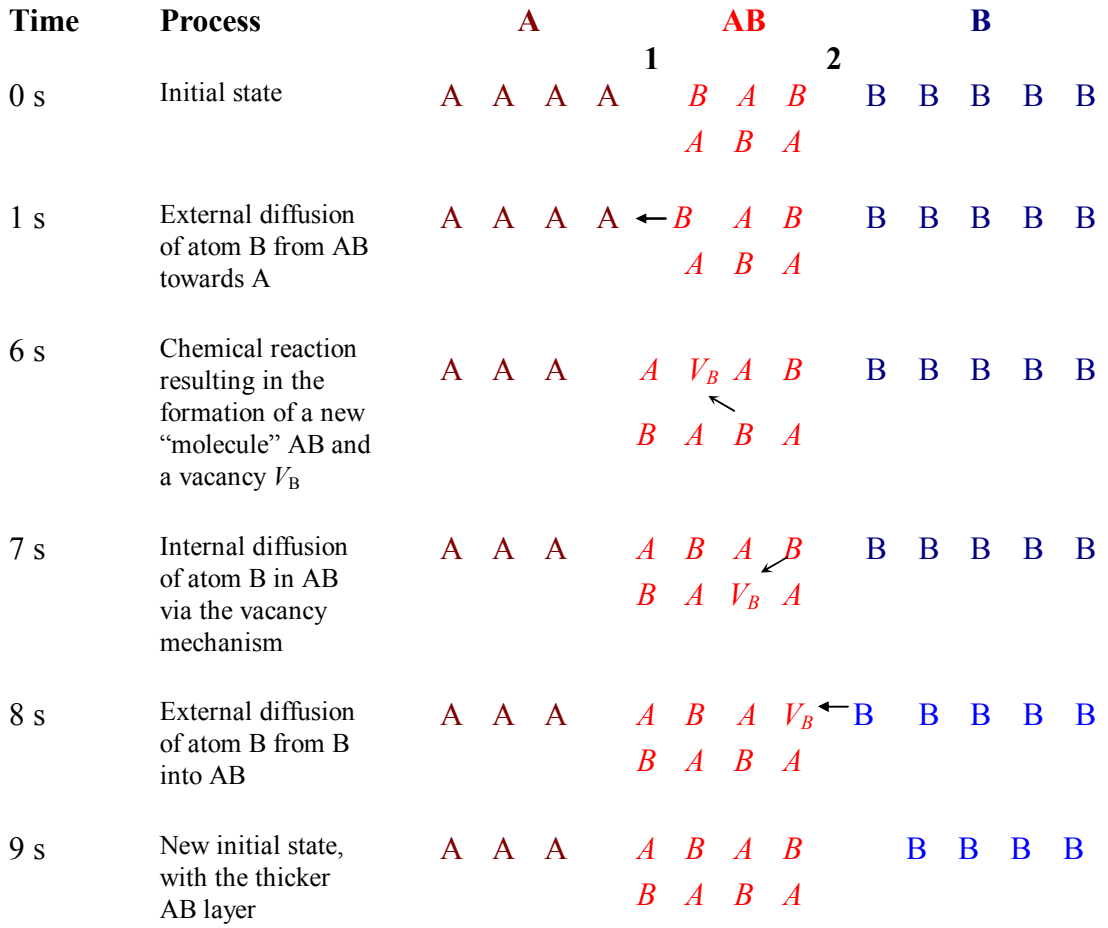

Fig. 2.6. Physico-chemical processes taking place in the *A–AB–B* system during growth of the *AB* layer at the expense of diffusion of component *B* (see also Fig. 2.4).

It is obvious that a new *AB* plane will form at the end of the sixth second. This plane corresponds to an additional "molecule" *AB*, while a vacancy occurs in the previous plane instead of the *B* atom that has reacted with the surface *A* atom. This vacancy is step-by-step filled with adjacent *B* atoms, and at the end of the eighth second it will be located onto the surface of phase *AB* from the side of interface 2. Finally, it is filled with another *B* atom from substance *B*.

Thus, at the end of ninth second the system *A–AB–B* returns to a new initial state which differs from the previous one only by the lesser number of atoms (atomic planes in two dimensions) in initial phases *A* and *B* and the greater number of "molecular" *AB* units in the growing *AB* layer. The reaction-diffusion process is repeated again and again, with the diffusion path of the *B* atoms from interface 2 to interface 1 becoming progressively longer, until either *A* or *B* is consumed completely.

It is easy to notice that during the same nine seconds three B atoms could have displaced from substance B across the AB layer to interface 1, if the chemical transformations at interface 1 (including also external diffusion of the B atoms to phase A through interface 1) would occur instantaneously or if the "excessive" B atoms (there are two such atoms in the case under consideration) would be used in the formation of the layers of other compounds of the same binary system. In the examined case of a single compound, this possibility of diffusion of "excessive" B atoms from interface 2 to interface 1 is not realised because the diffusion path is closed up until chemical transformations at interface 1 have completed. However, the existence of such a possibility must be borne in mind when considering the multiple layer growth.

Obviously, the critical thickness of the AB layer at which all the B atoms, capable of reaching interface 1 by a given moment of time, will be combined into the AB compound is six atomic planes corresponding to AB "molecules" (see Fig. 2.4). Indeed, in this case the reactivity of the A surface towards the B atoms is equal to one-sixth of B atom per second (one B atom per six seconds). The flux of the B atoms across the bulk of the AB layer is also equal to the same value (six consecutive displacements of the B atoms to adjacent sites within the AB lattice plus the transition of one of them through interface 2 last 6 seconds, so that one B atom crosses interface 1 as a result of these movements). At a greater thickness of the AB layer the rate of diffusion of the B atoms across its bulk is already insufficient to satisfy to the full extent the reactivity (combining ability) of the surface of phase A towards these atoms.

2.3.2: Growth regime of the A_pB_q layer with regard to component B: theoretical definition

The existence of the critical thickness $x_{1/2}^{(B)}$ of the A_pB_q layer makes it possible to give a strict *theoretical* definition of its growth regime. Namely, the regime of growth of the A_pB_q layer is *reaction controlled with regard to component B* at

$$x < x_{1/2}^{(B)}$$

and is *diffusion controlled with regard to this component* at

$$x > x_{1/2}^{(B)}.$$

If the A_pB_q layer grows in the reaction controlled regime with regard to component B, then

$$\mathrm{d}t_{\mathrm{chem}}^{(B)} > \mathrm{d}t_{\mathrm{dif}}^{(B)}.$$

If growth of the A_pB_q layer is diffusion controlled with regard to component B, then

$$\mathrm{d}t_{\mathrm{chem}}^{(B)} < \mathrm{d}t_{\mathrm{dif}}^{(B)}.$$

From a theoretical viewpoint, the layer thickness-time dependence can therefore be divided into two distinct regions: reaction controlled at $0 < x < x_{1/2}^{(B)}$ and diffusion controlled at $x > x_{1/2}^{(B)}$ (Fig. 2.7a).

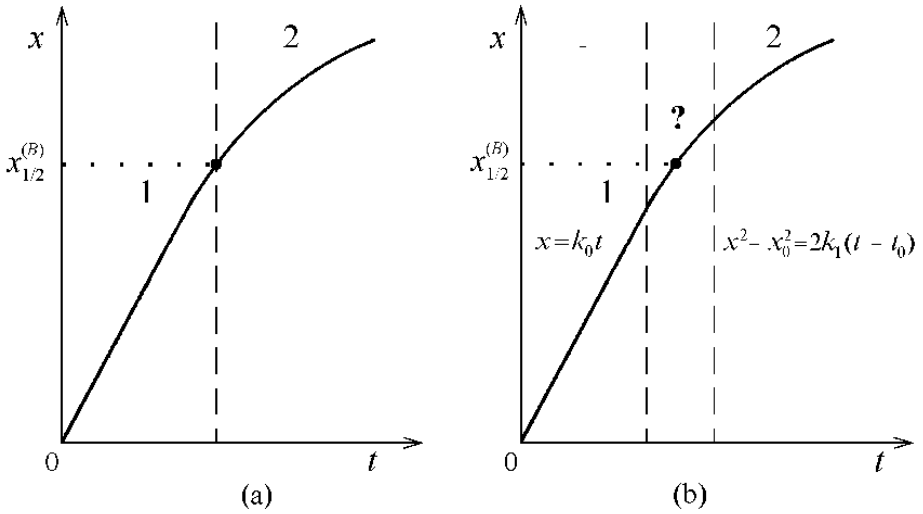

Fig. 2.7. Schematic diagram explaining (a) the theoretical definition of the concept of the growth regime of the A_pB_q layer and (b) the "practical" one. 1, region of reaction control; 2, region of diffusion control.

It is easy to notice a principal difference between the proposed theoretical definition of the concept of the growth regime of any compound layer and the previous "practical" one. In practice, the reaction controlled regime is in fact associated with the linear stage of layer growth ($k_{0B1} << k_{1B1}/x$), while the diffusion controlled regime with the parabolic stage ($k_{0B1} >> k_{1B1}/x$). Hence, the first stage corresponds to layer thicknesses much less than $x_{1/2}^{(B)}$

$$x << x_{1/2}^{(B)},$$

whereas the second stage corresponds to layer thicknesses much greater than $x_{1/2}^{(B)}$

$$x >> x_{1/2}^{(B)}.$$

Therefore, instead of the definite point $x_{1/2}^{(B)}$ of change of the growth regime of the A_pB_q layer, there occurs a transition region of uncertain width. In Fig. 2.7b, this region is designated by the question mark to indicate its uncertainty.

2.3.3: Stationary point

Although the validity of equation (2.8) as one of basic kinetic dependences has been verified by numerous experiments and is now beyond any doubt, its derivation given originally by U.R. Evans and then repeated in many papers, monographs and textbooks is unfortunately misleading. Firstly, it is quite inapplicable to chemical compounds without any range of homogeneity. Secondly, it is based on the separate description of the rates of the reaction and diffusion controlled stages of any solid-state chemical reaction by some functions $(dx/dt)_{\text{reaction stage}} = f_1$ and $(dx/dt)_{\text{diffusion stage}} = f_2$ which are assumed to be equal in some "stationary" or "equilibrium" state (for more detail, see Ref. [18]).

It is obvious, however, that neither the diffusion of atoms nor their chemical transformations, even if they would happen to take place in isolation from each other, can result in increase of the layer thickness by dx. Therefore, both the rate of diffusional supply of atoms and the rate of chemical transformations cannot in general be expressed in the form of any derivative dx/dt, with x being the thickness of the A_pB_q layer at time t.

This misunderstanding is likely to arise from the unjustified application of the concept of stationary or steady state, which proved to be helpful in analysing the kinetics of *consecutive chemical reactions* in a homogeneous system, to the case of a single solid-state process taking place in a heterogeneous system in a few *consecutive steps* which are often also referred to as *stages*. It is probably the last word that leads to confusion. In fact, kinetics of consecutive homogeneous chemical reactions briefly considered in Section 1.6 have nothing in common with the examined reaction-diffusion process resulting in the solid-state growth of a chemical compound layer.

Indeed, in the former case it is possible to indicate for each reacting substance the appropriate mass m and accordinally the concentration c and to characterise the rate of their formation by the derivatives dm/dt or dc/dt, whereas in the latter case it is only possible to indicate that part dt_i of the differential time dt, which is necessary for the i-th step of the process to complete. In general, each dt_i is a function of both x and dx. The sum of dt_i is equal to the time, dt, during which the thickness of a growing layer increases by dx (or its mass by dm) since, of a chain of successive steps in a solid-state heterogeneous system, any next step can only start after the preceding step has completed.

It should be emphasised that, although there are several such steps, they can readily be divided into two groups on the basis of their dependence on dx and x.

(1) The steps that depend on dx but are independent of x. These were united under the term *chemical transformations* (see Section 2.2).

(2) The steps that depend on both dx and x, with the only representative being the diffusion of atoms (ions or other paricles) across a growing chemical compound layer.

Therefore, equations (2.3) and (2.5) contain only two terms on their right-hand sides. In regards to the stationary state of the reaction-diffusion process, it should be noted that the number of the B atoms diffusing across the A_pB_q layer is always equal to their number combined by the A surface into the A_pB_q compound at interface 1, provided that the growth of this layer is not accompanied by the formation of other compounds or solid solutions. This is a *forced stationary state* due to (*i*) the impossibility of any build-up of atoms at interfaces between the solids, (*ii*) the limited number of diffusion paths in the A_pB_q layer for the B atoms to travel from interface 2 to interface 1 and (*iii*) the finite value of the reactivity of the A surface towards the B atoms. It is clear that the real stationary state would only be observed at $x = x_{1/2}^{(B)}$.

Actually, in the case under consideration there is a single stationary point and not the steady state. If it were possible to maintain the thickness of the A_pB_q layer equal to $x_{1/2}^{(B)}$ by

continuous removing the product of reaction (2.1), which is accumulating above this value, such growth conditions would indeed correspond to the stationary state in which the number of the B atoms diffusing to interface 1 per unit time is equal to their number which the A surface is able to combine into the A_pB_q compound. The time at which the A_pB_q layer reaches the thickness $x_{1/2}^{(B)}$ is the only moment of full harmony between reaction and diffusion. At smaller times reaction predominates, whereas at greater times diffusion becomes dominant. In any heterogeneous A–A_pB_q–B system given to itself, no steady state is clearly possible.

In the general case of varying thickness of the A_pB_q layer, the summation of $\mathrm{d}t_{\mathrm{dif}}^{(B)}$ and $\mathrm{d}t_{\mathrm{chem}}^{(B)}$ makes it possible to match the diffusional flux of the atoms across its bulk with the flux of the same atoms combined at the corresponding interface into the chemical compound. Actually, it is employed instead of any kind of the continuity equation that can hardly be applied directly in the case under consideration.

2.4: Growth of the A_pB_q layer at the expense of diffusion of components A and B

If components A and B have comparable mobilities in the A_pB_q lattice, then reactions (2.1) and (2.2) proceed simultaneously. In fact, these are two parallel reactions each of which takes place in two consecutive steps.

Note that, in application to any A–A_pB_q–B system, the word *reaction* may be and is used in the following three senses. Most broadly, it merely means that A and B react forming A_pB_q. In the less broad sense, it is used to designate partial reactions (2.1) and (2.2) resulting in the formation of A_pB_q at interfaces 1 and 2. Actually, this word unites reaction as such and diffusion supplying atoms for it to proceed. Also, it is employed as a synonym of the terms *chemical interaction* and *chemical transformations* (see Section 2.2).

During the time $\mathrm{d}t$, the thickness of the A_pB_q layer increases from x to $x + \mathrm{d}x_{B1}$ at interface 1 due to reaction (2.1) and from x to $x + \mathrm{d}x_{A2}$ at interface 2 due to reaction (2.2), as shown in Fig. 2.8. Using the results of Section 2.3, it is easy to find an equation relating $\mathrm{d}t$ to $\mathrm{d}x_{A2}$. Again, the following three assumptions are employed.

(1) The differential time $\mathrm{d}t$ necessary to increase the thickness of the A_pB_q layer by $\mathrm{d}x_{A2}$ (from x to $x + \mathrm{d}x_{A2}$) is the sum of the time $\mathrm{d}t_{\mathrm{dif}}^{(A)}$ of diffusion of the A atoms across its bulk to interface 2 where reaction (2.2) takes place and the time $\mathrm{d}t_{\mathrm{chem}}^{(A)}$ of their subsequent chemical interaction with the surface B atoms at this interface

$$\mathrm{d}t = \mathrm{d}t_{\mathrm{dif}}^{(A)} + \mathrm{d}t_{\mathrm{chem}}^{(A)}. \qquad (2.18)$$

This equation differs from equation (2.3) only by the numerical values of the terms on the right-hand side.

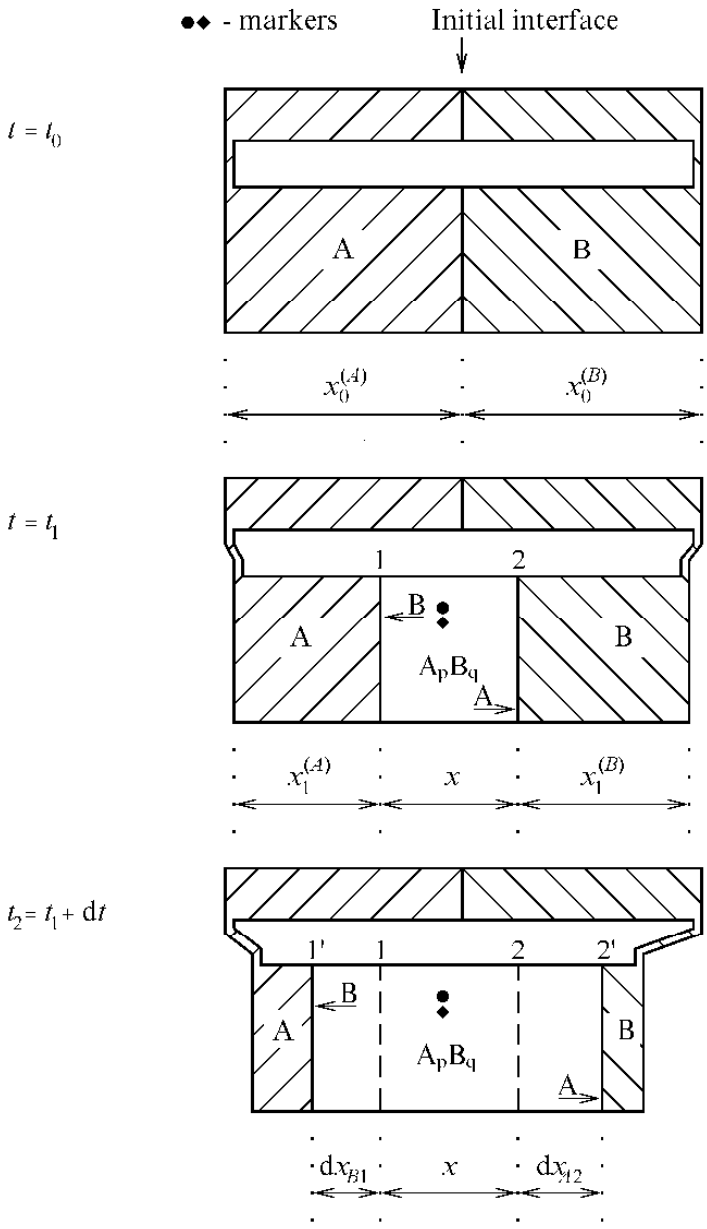

Fig. 2.8. Schematic representation of the growth process of the A_pB_q layer between elementary substances A and B due to the simultaneous diffusion of both components. Formation of the A_pB_q compound is accompanied by a decrease in volume of that part of the couple where the components A and B are able to react with each other (negative volume effect). Positive volume effect (an increase in volume of the couple) can also be observed.

(2) The time $dt_{dif}^{(A)}$ of diffusion of the A atoms is directly proportional to both the increase dx_{A2} of the thickness of the A_pB_q layer and its total thickness x

$$dt_{dif}^{(A)} = \frac{x}{k_{1A2}} dx_{A2}, \tag{2.19}$$

where k_{1A2} is another physical (diffusional) constant. The values of the constants k_{1B1} and k_{1A2} are in general different.

(3) The time $dt_{chem}^{(A)}$ of their chemical interaction with the surface B atoms is directly proportional to the increase dx_{A2} of the thickness of the A_pB_q layer and is independent of its total thickness x

$$dt_{chem}^{(A)} = \frac{1}{k_{0A2}} dx_{A2}, \tag{2.20}$$

where k_{0A2} is another chemical constant different from k_{0B1}.

Substituting the expressions for $dt_{dif}^{(A)}$ and $dt_{chem}^{(A)}$ from equations (2.19) and (2.20) into equation (2.18) yields the required differential equation

$$dt = \left(\frac{x}{k_{1A2}} + \frac{1}{k_{0A2}} \right) dx_{A2}. \tag{2.21}$$

It is analogous to equation (2.6).

2.4.1: Critical thickness and growth regime of the A_pB_q layer with regard to component A

It seems obvious that, in addition to $x_{1/2}^{(B)}$, there is another critical value $x_{1/2}^{(A)}$ of the thickness of the A_pB_q layer, at which all the A atoms capable of reaching interface 2 (see Figs 2.4 and 2.8) by a given moment of time are combined at this interface by the surface B atoms into the A_pB_q compound. To find out this value, it is sufficient to put $dt_{dif}^{(A)} = dt_{chem}^{(A)}$ in equations (2.18)-(2.21). Hence,

$$x_{1/2}^{(A)} = \frac{k_{1A2}}{k_{0A2}}. \tag{2.22}$$

At $x < x_{1/2}^{(A)}$, there is an "excess" of diffusing A atoms since the reactivity of the B surface towards these atoms is less than their flux across the A_pB_q layer. The "excessive" A atoms can

be consumed in the formation of the layers of other chemical compounds of a given binary system enriched in component B in comparison with A_pB_q, if present on the equilibrium phase diagram.

On the contrary, if $x > x_{1/2}^{(A)}$, there is a deficit of the A atoms even for the growth of the A_pB_q layer itself because the reactivity of the B surface towards the A atoms is greater than the flux of these atoms across its bulk. On reaching interface 2, each A atom is combined at this interface into the A_pB_q compound. Therefore, there are no "excessive" A atoms for the growth of other compounds enriched in component B in comparison with A_pB_q.

Like the case of component B, it is possible to theoretically define the concept of the regime of growth of the A_pB_q layer with regard to component A as well. The growth regime of the A_pB_q layer is *reaction controlled with regard to component A* at

$$x < x_{1/2}^{(A)}$$

and *diffusion controlled with regard to this component* at

$$x > x_{1/2}^{(A)}.$$

If the layer of the A_pB_q chemical compound grows in the reaction controlled regime with regard to component A, then

$$\mathrm{d}t_{\mathrm{chem}}^{(A)} > \mathrm{d}t_{\mathrm{dif}}^{(A)}.$$

During its growth in the diffusion controlled regime with regard to component A,

$$\mathrm{d}t_{\mathrm{chem}}^{(A)} < \mathrm{d}t_{\mathrm{dif}}^{(A)}.$$

Critical thicknesses $x_{1/2}^{(B)}$ and $x_{1/2}^{(A)}$ of the A_pB_q layer are in general different. Therefore, from a theoretical viewpoint, the layer thickness-time dependence (see Fig. 2.7a) can once again be divided into the following two regions: reaction controlled with regard to component A at $0 < x < x_{1/2}^{(A)}$ and diffusion controlled with regard to this component at $x > x_{1/2}^{(A)}$. In most reaction couples, such a division with regard to components A and B does not coincide (Fig. 2.9). Hence, during some period of time (at $x_{1/2}^{(B)} < x < x_{1/2}^{(A)}$) the A_pB_q layer grows in the reaction controlled regime with regard to component A and in the diffusion controlled regime with regard to component B.

Since the "practical" definition of the concept of the layer growth regime is based on the conditions $k_{0B1} << k_{1B1}/x$ and $k_{0A2} << k_{1A2}/x$ for the reaction controlled regime and $k_{0B1} >> k_{1B1}/x$ and $k_{0A2} >> k_{1A2}/x$ for the diffusion controlled regime (see Section 2.3.2), it is clear that in this case there is no need to indicate the component with regard to which the growth regime is defined. Indeed, according to the "practical" definition of this concept, $x << x_{1/2}^{(B)}$ and $x << x_{1/2}^{(A)}$ during growth of the A_pB_q layer in the reaction controlled regime and $x >> x_{1/2}^{(B)}$ and $x >> x_{1/2}^{(A)}$ during its growth in the diffusion controlled regime.

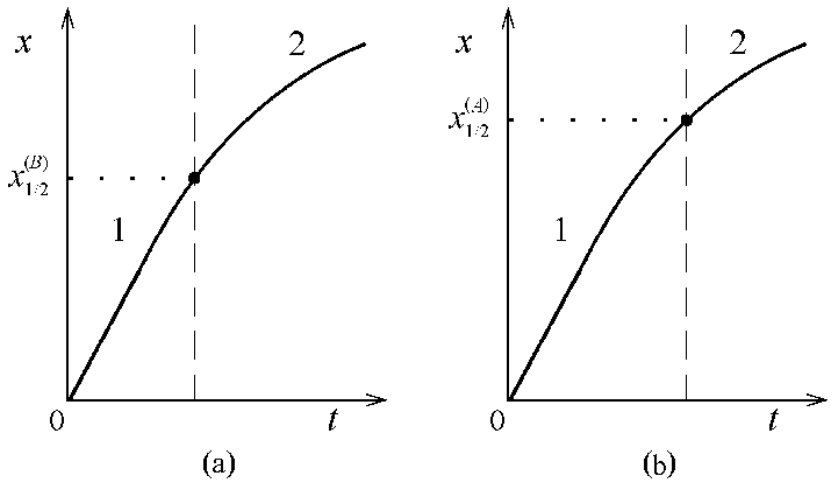

Fig. 2.9. Schematic diagram to explain the theoretical definition of the concept of the growth regime of the A_pB_q layer with regard to components A and B. (a): 1, region of *reaction* (or, more precisely, *chemical*) control with regard to component B; 2, region of *diffusion* control with regard to component B. (b): 1, region of *reaction* (*chemical*) control with regard to component A; 2, region of *diffusion* control with regard to component A.

Thus, the width of the transition region between the two "practical" growth regimes of the layer becomes even more uncertain than in the case of diffusion of only one component B. In contrast, the theoretical definition gives two definite points of change of the growth regime of the A_pB_q layer, namely, $x_{1/2}^{(A)}$ with regard to component A and $x_{1/2}^{(B)}$ with regard to component B [16].

Note that, to be most precise and to avoid any confusion with the terminology, it would be more relevant to use the term *chemical control* instead of *reaction control*. Then, the A_pB_q layer formation could be specified as its growth under conditions of either *chemical control* or *diffusion control*.

It should be noted that in the absence of stress the position of the A_pB_q layer as a whole relative to the initial interface between the phases A and B (see Fig. 2.8) only depends on the stoichiometry of the A_pB_q chemical compound but by no means on the speed of movement of diffusing species in the crystal lattice of this compound. The initial interface cannot therefore serve as a marker to identify the faster diffusing component of the compound.

Most chemical reactions are in fact accompanied by the occurrence of stress due to (*i*) the difference in the coefficients of thermal expansion of the phases involved into the interaction and (*ii*) the volume effect associated with the formation of a chemical compound, the volume of the reactants consumed being in general not equal to the volume of the product(s) formed. As the stresses arisen at both layer interfaces are different, the layer displacement relative to the initial interface may also depend on their magnitudes.

2.4.2: Single compound layer: general kinetic equation

Equations (2.6) and (2.21) relating the time dt to the increases dx_{B1} and dx_{A2} of the thickness of the A_pB_q layer are assumed to be independent of each other. Here, the principle of independency of the rates of elementary chemical processes taking place in a given system is used. This principle was successfully employed as a basis for examining the kinetics of homogeneous reactions (see Section 1.2). Also, in the case of solid-state heterogeneous reactions, the results obtained using this principle are, as will become clear later, in good agreement with the available experimental data, indicative of the fundamental nature of this postulate of chemical kinetics.

The counter-fluxes j_A and j_B of the A and B atoms across the bulk of the growing A_pB_q layer are assumed to be independent of each other as well. Indeed, in the ordered lattice of any chemical compound the atoms of each of its components can readily move on the sites of their own sublattice, thus not hindering the movement of the atoms of another component.

Regrouping the terms of equation (2.21) gives an expression for the growth rate of the A_pB_q layer at interface 2 at the expense of diffusion of the A atoms and subsequent partial chemical reaction (2.2)

$$\frac{\mathrm{d}x_{A2}}{\mathrm{d}t} = \frac{k_{0A2}}{1+\dfrac{k_{0A2}x}{k_{1A2}}}. \qquad (2.23)$$

Summation of the right-hand parts of equations (2.7) and (2.23) yields a general kinetic equation describing the rate of growth of the A_pB_q layer between initial substances A and B due to the simultaneous occurrence of partial chemical reactions (2.1) and (2.2)

$$\frac{\mathrm{d}x}{\mathrm{d}t} = \frac{k_{0B1}}{1+\dfrac{k_{0B1}x}{k_{1B1}}} + \frac{k_{0A2}}{1+\dfrac{k_{0A2}x}{k_{1A2}}}. \qquad (2.24)$$

This type of equation appears to have been proposed first to treat the experimental data on solid-state kinetics by B.Ya. Pines in 1959 [19]. The solution to equation (2.24) with the initial condition $x = 0$ at $t = 0$ is

$$\mathrm{R}_1x^2 + \mathrm{R}_2x - \mathrm{R}_3\ln(1 + \mathrm{R}_4x) = t, \qquad (2.25)$$

where

$$R_1 = \frac{1}{2(k_{1B1} + k_{1A2})},$$

$$R_2 = \frac{k_{1B1}^2 k_{0A2} + k_{0B1} k_{1A2}^2}{k_{0B1} k_{0A2} (k_{1B1} + k_{1A2})},$$

$$R_3 = \frac{k_{1B1} k_{1A2} \left| k_{0B1} k_{1A2} - k_{1B1} k_{0A2} \right|^2}{k_{0B1}^2 k_{0A2}^2 (k_{1B1} + k_{1A2})^3},$$

$$R_4 = \frac{k_{0B1} k_{0A2} (k_{1B1} + k_{1A2})}{k_{1B1} k_{1A2} (k_{0B1} + k_{0A2})}.$$

Equation (2.25) is much more complicated than equation (2.8) because in general the values of the chemical constants k_{0B1} and k_{0A2} as well as those of the diffusional constants k_{1B1} and k_{1A2} are not equal. Even the proportionality of the diffusional and chemical constants, so that $x_{1/2}^{(A)} = x_{1/2}^{(B)}$, is probably a rare occasion. In the particular case where $k_{0B1} = k_{0A2} = k_0$ and $k_{1B1} = k_{1A2} = k_1$, equations (2.24) and (2.25) are simplified to

$$\frac{dx}{dt} = \frac{2k_0}{1 + \frac{k_0 x}{k_1}} \qquad (2.26)$$

and

$$t = \frac{x^2}{4k_1} + \frac{x}{2k_0}, \qquad (2.27)$$

respectively.

Equation (2.27) produces a layer thickness-time dependence that at low values of x is close to the straight line $x = 2k_0 t$, while at high values of x it tends to the parabola $x^2 = 4k_1 t$. In this case, the increases of the thickness of the A_pB_q layer at both interfaces with initial phases A and B are equal. Again, the duration of the steps of chemical transformations at interface 1 with the participation of diffusing B atoms is equal to the duration of the steps of chemical transformations at interface 2 with the participation of diffusing A atoms. The durations of diffusion of the A and B atoms across the bulk of the A_pB_q layer are also equal. Therefore, equation (2.27) assumes the same simple form as equation (2.8). Its right-hand side consists of the time of diffusion of the A and B atoms respectively to interfaces 2 and 1 during growth of the A_pB_q layer from 0 to x:

$$t_{\text{dif}} = \frac{x^2}{4k_{1B1}} \tag{2.28}$$

and the time of chemical transformations with the participation of these atoms

$$t_{\text{chem}} = \frac{x}{2k_{0B1}}. \tag{2.29}$$

It can be seen that, if the contributions of diffusing A and B atoms to the process of formation of the A_pB_q layer are equal, the time necessary for the layer to reach any given thickness x is two times less compared to the case where only one component is diffusing (compare equations (2.8), (2.16) and (2.17) on the one hand with equations (2.27)-(2.29) on the other).

In the general case where these contributions are different, some initial portion of the dependence of the layer thickness upon time is also linear. Indeed, if $k_{0B1} << k_{1B1}/x$ and $k_{0A2} << k_{1A2}/x$ ($x << x_{1/2}^{(B)}$ and $x << x_{1/2}^{(A)}$), then

$$\frac{\mathrm{d}x}{\mathrm{d}t} = k_{0B1} + k_{0A2} \tag{2.30}$$

and therefore

$$x = (k_{0B1} + k_{0A2})t. \tag{2.31}$$

At sufficiently high x, the conditions $k_{0B1} >> k_{1B1}/x$ and $k_{0A2} >> k_{1A2}/x$ ($x >> x_{1/2}^{(B)}$ and $x >> x_{1/2}^{(A)}$) are satisfied. Hence,

$$\frac{\mathrm{d}x}{\mathrm{d}t} = \frac{k_{1B1} + k_{1A2}}{x}. \tag{2.32}$$

Thus, at long times the layer thickness-time dependence is almost parabolic

$$x^2 = 2(k_{1B1} + k_{1A2})t. \tag{2.33}$$

If the integration of equation (2.32) with the initial condition $x = 0$ at $t = 0$ produces unsatisfactory results, it must be carried out using the initial condition $x = x_0$ at $t = 0$ or $x = x_0$ at $t = t_0$ (see equations (2.13) and (2.14)).

The temperature dependence of the chemical and physical (diffusional) constants is in most cases described by an equation of the Arrhenius type (see Refs [1-6])

$$K = K_0 \exp\left(-\frac{E}{RT}\right), \tag{2.34}$$

where K stands for any of the two constants, K_0 is the pre-exponential factor, E is the activation energy, R is the gas constant and T is the absolute temperature.

Since the activation energy E_{chem} of chemical transformations is known to be a few times higher than the activation energy E_{dif} of diffusion , from equation (2.34) it follows that the rate of chemical transformations decreases with decreasing temperature far more rapidly than the rate of atomic diffusion. Therefore, just at low temperatures the rate of chemical transformations at phase interfaces limits the observed rate of layer formation.

Clearly, in this case the growth rate of the layer of any chemical compound is low but the linear region of its growth becomes wider in time and therefore can more easily be studied experimentally. On the contrary, at high temperatures the time of linear growth may even be shorter than the time of heating of the examined reaction couple up to the required temperature.

Note that within the framework of phenomenological considerations it is impossible to predict the shape of the layer thickness-time dependence for any particular binary system, since the values of the chemical and physical (diffusional) constants are not known *a priori* and must be found from experimental studies. For different systems, these can vary over a wide range. For this reason, under close experimental conditions in one binary system the layer growth can proceed in the reaction controlled regime, in the second in the diffusion controlled regime, and in the third in the transition (mixed) regime (see Section 2.3.2 and Fig. 2.7b).

2.4.3: Separate determination of reaction-diffusion constants

It is obvious that from any experimental dependence of the total layer thickness upon time it is only possible to determine the sum of the chemical constants as well as the sum of physical (diffusional) constants. The former sum is to be found from an initial portion of this dependence plotted in coordinates $x - t$, while the latter from its long-time portion plotted in coordinates $x^2 - t$ or $x - t^{1/2}$. For their separate determination, it is necessary to measure the increases in thickness of the A_pB_q layer at its both interfaces with initial substances A and B.

The specimen, most suitable for such measurements, is shown schematically in Fig. 2.8. The upper part of the specimen is used as reference. To prevent the interaction of components A and B in this part, a thin barrier layer of some substance which does not react with both A and B under chosen experimental conditions is deposited. The position of the layer interfaces is measured at certain moments of time relative to the inert markers located at the initial interface between substances A and B and inside the A_pB_q layer. Microhardness indentations onto the specimen cross-section surface, thin wires or strips of chemically inert materials, bubbles of inert gases, *etc*., can serve as the markers.

As already pointed out earlier, in most cases the formation of chemical compounds is accompanied by considerable changes of the volume of reaction couples. Figure 2.8 represents the case where the layer occurrence reduces the total volume of the A–A_pB_q–B reaction system. This causes the displacement of that part of the specimen, where initial substances interact, relative to the other where they do not react with each other. A thin cut made throughout the entire depth of the specimen almost up to its ends makes it possible to reduce the mechanical stresses between the reference and measurement parts.

Separate determination of the chemical constants k_{0B1} and k_{0A2} can be carried out in practice using the following procedure. First, it is necessary to reveal a temperature-time range in which the time dependence of the total thickness of the A_pB_q layer is linear. Then, by measuring the position of its interfaces 1 and 2 relative to the markers at some moments of time t_1 and $t_2 = t_1+\Delta t$, the increases, Δx_{B1} and Δx_{A2}, in thickness of the A_pB_q layer during the time Δt must be determined (see Fig. 2.8 in which dt should be replaced by Δt, dx_{B1} by Δx_{B1}, and dx_{A2} by Δx_{A2}). The chemical constants k_{0B1} and k_{0A2} are found from the equations

$$k_{0B1} = \frac{\Delta x_{B1}}{\Delta t} \tag{2.35}$$

and

$$k_{0A2} = \frac{\Delta x_{A2}}{\Delta t}\ , \tag{2.36}$$

respectively.

To determine the physical (diffusional) constants k_{1B1} and k_{1A2}, it is necessary to establish the conditions under which the total thickness of the A_pB_q layer increases with time parabolically. Then, like the previous case, the increases, Δx_{B1} and Δx_{A2}, in thickness of the layer at its interfaces 1 and 2 are to be measured. The values of the physical (diffusional) constants k_{1B1} and k_{1A2} are calculated from the equations

$$k_{1B1} = x_{\text{mean}} \frac{\Delta x_{B1}}{\Delta t} \tag{2.37}$$

and

$$k_{1A2} = x_{\text{mean}} \frac{\Delta x_{A2}}{\Delta t} \tag{2.38}$$

where x_{mean} is the mean value of the total thickness of the A_pB_q layer in the time range Δt.

It should be emphasised that in determining the chemical constants k_{0B1} and k_{0A2} the time range Δt can be chosen arbitrarily. It is only important to remain within the linear region of layer growth. When determining the physical (diffusional) constants, however, the increases, Δx_{B1} and Δx_{A2}, should be sufficiently small, so that during the time Δt there were no large change of the total thickness of the A_pB_q layer. If this condition is not satisfied, the constants k_{1B1} and k_{1A2} obtained will clearly be time-dependent.

It is evident that the separate determination of the chemical and physical (diffusional) constants is much more difficult in comparison with conventional experiments where only the total thickness of the growing A_pB_q layer is measured, with the further search for its growth law by means of mathematical treatment of the results using linear, parabolic, logarithmic and other dependences (see, for example, Ref. [18]). However, the former procedure ultimately gives a more complete and adequate description of the interaction in the examined reaction couple A–B compared to the latter.

It should be noted that the value of each of the chemical constants k_{0B1} and k_{0A2} depends on the physical and chemical properties of two reacting phases. The value of k_{0B1} depends on the nature of substance A and the compound A_pB_q, while the value of k_{0A2} depends on the nature of substance B and the compound A_pB_q. Both physical (diffusional) constants depend only on the nature of the chemical compound A_pB_q and are therefore characteristic of this compound layer wherever it grows. However, as will be demonstrated in the next chapters, the stoichiometry of adjacent phases must also be taken into account when estimating the growth rate of the A_pB_q layer in various reaction couples of the A–B binary system.

The sum of the chemical constants k_{0B1} and k_{0A2} as well as the sum of the physical (diffusional) constants k_{1B1} and k_{1A2} can also be determined from the decrease in thickness of the layers of initial substances A and B. Indeed, using equations (2.1) and (2.2), it can readily be shown that the decrease $\Delta x^{(A)}$ in thickness of the layer of substance A and that $\Delta x^{(B)}$ of the layer of substance B during the time Δt is related to the increases Δx_{B1} and Δx_{A2} in thickness of the A_pB_q layer during this time through the relationships

$$\Delta x^{(A)} = \frac{pV_A}{V_{A_pB_q}} (\Delta x_{B1} + \Delta x_{A2}) \tag{2.39}$$

and

$$\Delta x^{(B)} = \frac{qV_B}{V_{A_pB_q}}(\Delta x_{B1} + \Delta x_{A2}) \tag{2.40}$$

where V is the molar volume of appropriate substances.

Therefore, in the region of linear growth of the A_pB_q layer

$$\Delta x^{(A)} = \frac{pV_A}{V_{A_pB_q}}(k_{0B1} + k_{0A2})\Delta t \tag{2.41}$$

and

$$\Delta x^{(B)} = \frac{qV_B}{V_{A_pB_q}}(k_{0B1} + k_{0A2})\Delta t, \tag{2.42}$$

while in the parabolic region

$$\Delta x^{(A)} = \frac{pV_A}{V_{A_pB_q}}\left(\frac{k_{1B1} + k_{1A2}}{x_{\text{mean}}}\right)\Delta t \tag{2.43}$$

and

$$\Delta x^{(B)} = \frac{qV_B}{V_{A_pB_q}}\left(\frac{k_{1B1} + k_{1A2}}{x_{\text{mean}}}\right)\Delta t. \tag{2.44}$$

It can easily be seen that this method has practically no advantages in comparison with direct measuring the thickness of the growing A_pB_q layer. Its disadvantages are obvious. Firstly, the diffusional constants are calculated using the differential forms of kinetic equations. This usually produces a larger computational error than the calculations with the use of the integrated equations. Secondly, the amount of initial substances A and B consumed in the reaction of compound formation is in most cases much less than their total amount present. Therefore, the decrease $\Delta x^{(A)}$ or $\Delta x^{(B)}$ is the difference of two large magnitudes, each of which is determined at some error. The procedure where a small magnitude is determined as the difference of two large figures is known to yield insufficiently accurate results.

2.5: Formation of the $NiBi_3$ layer in the nickel-bismuth reaction couple

The Ni–Bi reaction couple is suitable to illustrate the mechanism of formation of a single compound layer (for more detail, see Ref. [16]). Though two intermetallic compounds NiBi and $NiBi_3$ are known to exist in the nickel-bismuth binary system, only the $NiBi_3$ intermetallic compound is formed as a compact layer between solid nickel and solid or liquid bismuth at reaction times up to 300 h (see Fig. 2.2).

No indication of the presence of the NiBi intermetallic compound was found. The reasons for its absence from the Ni–Bi couple will be discussed in the next chapters. Here, it suffices to underline that those are of kinetic rather than thermodynamic nature. Consider characteristic features of formation of the $NiBi_3$ compound layer at the Ni–Bi interface, with particular emphasis on the determination of (*i*) the main diffusing species in the growth process and (*ii*) the values of the reaction-diffusion constants.

2.5.1: Main diffusing species in the growth process of the $NiBi_3$ layer

Generally, growth of the $NiBi_3$ compound layer (except at the very beginning of the Ni–Bi interaction) is due to two partial chemical reactions. Firstly, the Bi atoms may diffuse across the layer bulk from interface 2 to interface 1 (Fig. 2.10) and then react with the surface Ni atoms to form $NiBi_3$ at the Ni–$NiBi_3$ interface:

$$3Bi_{dif} + Ni_{surf} = NiBi_3. \qquad (2.45)$$

Secondly, the Ni atoms may diffuse across the layer bulk in the opposite direction and then react with the surface Bi atoms to form more $NiBi_3$ at the $NiBi_3$–Bi interface:

$$Ni_{dif} + 3Bi_{surf} = NiBi_3. \qquad (2.46)$$

In view of the different size of the Ni and Bi atoms and the great difference in melting points of the components, the contributions of these reactions to the layer growth process can hardly be expected to be equal. On the one hand, the atomic radius of nickel (0.124 nm) is much less than that of bismuth (0.182 nm). Smaller atoms may reasonably be expected to diffuse faster.

On the other hand, however, bismuth has the much lower melting point 271 °C compared to that (1451 °C) of nickel. From this viewpoint, bismuth may be expected to diffuse predominantly in the $NiBi_3$ layer as its atoms are evidently more mobile at 150-250 °C than the nickel atoms. Microhardness indentation markers allow these contributions to be visualised unambiguously.

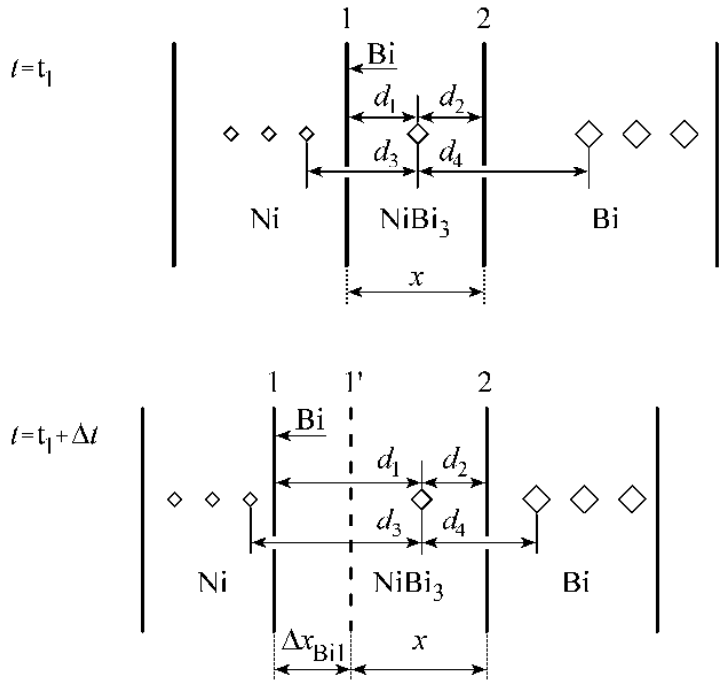

Fig. 2.10. Schematic illustration of the $NiBi_3$ growth process at the nickel-bismuth interface.

The distances between the markers at the same place of the Ni–Bi interface were measured three times:

(1) before each successive anneal, except the first one of an as-received Ni–Bi specimen;

(2) after each anneal, without any polishing of the cross-section surface;

(3) after the electrolytic re-polishing of the cross-section to remove some amount of the cross-section material from its surface, so that the craters of the microhardness indentations remained visible under optical microscope.

In the latter two cases, no noticeable differences were observed in measured values of the distance between the appropriate markers (compare the numbers in the last two rows of Table 2.1), indicative of the lack of any surface effect.

Additional proof for the absence of any significant surface effect was obtained by comparing the layer thickness existing, say, after the second anneal and before the third one. Namely, before the third anneal the Ni–Bi specimen was ground to remove 0.3 to 0.5 mm of its surface material and again polished electrolytically. Comparison of the layer thickness in both cases did not reveal any perceptible difference.

Table 2.1. Typical changes in distance between the microhardness indentation markers onto the surface of a Ni–Bi cross-section. Temperature 250 °C. Time of the first anneal is 18×10^4 s (50 h), while that of the second is 9×10^4 s (25 h); 27×10^4 s or 75 h in total

Measurements made	Distance (μm)											
	Between five markers in the Ni phase				d_1	d_2	d_3	d_4	Between five markers in the Bi phase			
(1) before second anneal	80	79	77	80	88	104	142	158	76	76	77	78
(2) after second anneal, without polishing	81	79	78	79	122	104	174	121	77	75	78	77
(3) after second anneal, with slight electrolytic polishing	80	78	77	79	121	105	174	120	76	75	77	78

The distance d_2 between a marker located initially in the middle part of the $NiBi_3$ layer and interface 2 did not change during annealing. Hence, no appreciable diffusion of the Ni atoms across the growing $NiBi_3$ layer took place. In contrast, the distance d_1 between this marker and interface 1 was found to increase with increasing annealing time. Therefore, at temperatures of 150-250 °C the $NiBi_3$ layer growth is due to partial chemical reaction (2.46), the contribution of partial chemical reaction (2.45) being quite negligible, if any. The newly-grown $NiBi_3$ phase occurs entirely at the Ni–$NiBi_3$ interface (see Figs 2.11 and 2.12). Hence, the Bi atoms appear to be the only diffusing species in the course of layer formation.

It is worth noting that the sum of the distances d_3 and d_4 slightly diminished during annealing. This is due to a decrease in volume of any Ni–$NiBi_3$–Bi specimen, connected with the formation of the $NiBi_3$ intermetallic compound. The ratio of the decrease in $(d_3 + d_4)$ value to the corresponding increase in thickness of the $NiBi_3$ layer was experimentally found to be 0.20 ± 0.05.

Note that the distances between the markers located in the Ni phase did not change in the course of annealing, indicative of no formation of a solid solution of bismuth in nickel. The distances between the markers located in the Bi phase remained unchanged as well. Also, no changes in size or configuration of the microhardness indentations were observed in either phase. Hence, the components are indeed mutually insoluble in the temperature range of 150-250 °C.

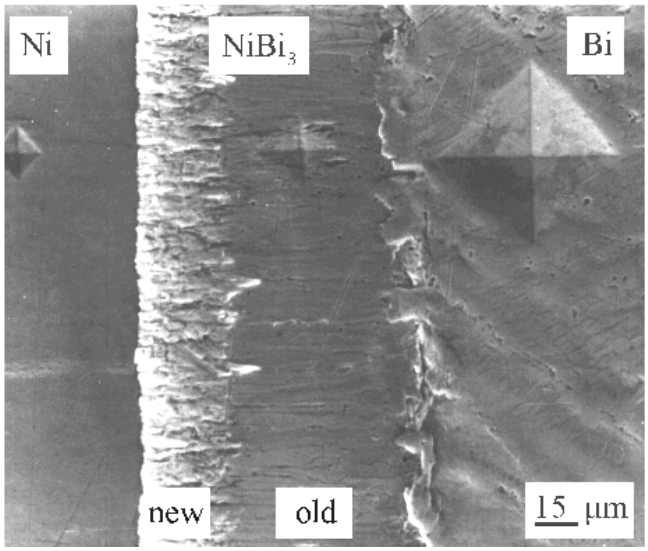

Fig. 2.11. Secondary electron image of the Ni–Bi transition zone after the second anneal in the as-received condition. Temperature 250 °C. Time of the first anneal is 14400 s (4 h), while that of the second is 12600 s (3.5 h); 27000 s or 7.5 h in total. Microhardness indentations were put onto the electropolished surface of the cross-section after the first anneal at a load of 0.196 N (20 g).

Microstructures of Fig. 2.12 deserve a more detailed discussion. Shown in Fig. 2.12a is the microstructure of the Ni–Bi transition zone after the second anneal at 200 °C for 100 h in two steps of 50 h. As this cross-section was polished electrolytically after annealing, the $NiBi_3$ layer is quite homogeneous in appearance. Then, the specimen was annealed for the third time at 200 °C for 100 h (200 h in total). Figure 2.12b shows its microstructure in the as-received condition (without any polishing). The newly-grown $NiBi_3$ phase is much darker than the old one and therefore is easily distinguishable.

Before the third anneal, microhardness indentation markers were put onto the electropolished cross-section surface in the Ni phase (five markers, about 50 μm from each other), in the middle of the $NiBi_3$ layer (one marker) and in the Bi phase (five markers, about 75 μm from each other). Only part of them are shown in Fig. 2.12.

After the third anneal, the distance d_1 between the marker 3 and the Ni–$NiBi_3$ interface increased from 76 to 137 μm, whereas the distance d_2 between this marker and the $NiBi_3$–Bi interface remained unchanged (70 μm). Marker 4 almost disappeared as a result of consumption of the Bi phase. Distance between the markers 3 and 5 decreased by 61 μm (from 202 to 141 μm). In terms of thickness, the consumption of nickel (around 6 μm) is seen to be much less than that of bismuth (61 μm). These values agree with the stoichiometry of the $NiBi_3$ intermetallic compound, as it must be from a chemical viewpoint.

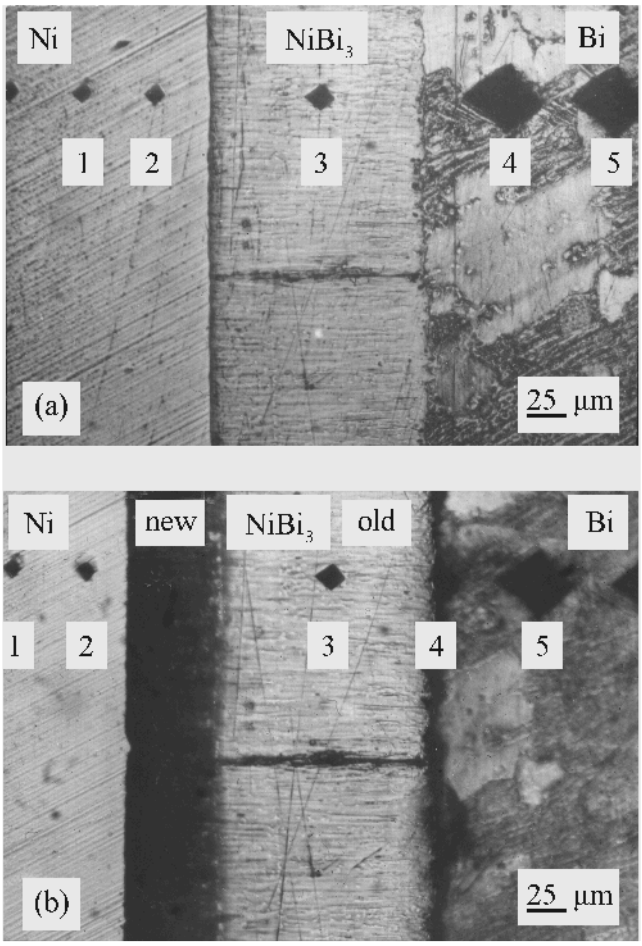

Fig. 2.12. Optical micrographs of the Ni–Bi transition zone (a) before and (b) after the third anneal. Temperature 200 °C, (a) annealed two times 18×10^4 s + 18×10^4 s (50 h + 50 h), (b) the same place after the third anneal for 36×10^4 s (100 h) in the as-received condition. Microhardness indentations were put onto the electropolished surface of the Ni–Bi cross-section after the second anneal at a load of 0.196 N (20 g).

Indeed,

$$\frac{x_{\mathrm{Ni}}}{x_{\mathrm{Bi}}} = \frac{c_{\mathrm{Ni}}\rho_{\mathrm{Bi}}}{c_{\mathrm{Bi}}\rho_{\mathrm{Ni}}} \qquad (2.47)$$

where x, c and ρ are respectively the thickness consumed, the content in $NiBi_3$ and the density of nickel or bismuth. As $c_{\mathrm{Ni}} = 8.55$ mass %, $c_{\mathrm{Bi}} = 91.45$ mass %, $\rho_{\mathrm{Ni}} = 8.9 \times 10^3$ kg m^{-3} and $\rho_{\mathrm{Bi}} = 9.8 \times 10^3$ kg m^{-3}, equation (2.47) yields $x_{\mathrm{Ni}} = 0.1\, x_{\mathrm{Bi}}$.

Hence, the thickness of the consumed bismuth phase is ten times greater than that of the consumed nickel phase. Therefore, relative to the initial Ni–Bi interface, the growing $NiBi_3$ layer mostly displaces as a whole into the side of bismuth, though its increase takes place entirely at the opposite side (near nickel).

2.5.2: $NiBi_3$ layer growth kinetics

As only the Bi atoms are diffusing and experimental values of the $NiBi_3$ layer thickness are large enough, its growth kinetics at the Ni–Bi interface is described by simplified equations of the type (2.32) and (2.33):

$$\frac{dx}{dt} = \frac{k_{1Bi1}}{x} \tag{2.48}$$

and

$$x^2 = 2k_{1Bi1}t \tag{2.49}$$

where x is the total layer thickness at time t and k_{1Bi1} is a physical (diffusional) constant.

The latter equation can also be rewritten as follows:

$$x = (2k_{1Bi1}t)^{1/2}. \tag{2.50}$$

If the layer thickness-time dependence is described by these equations, then the growth process is undoubtedly diffusion controlled. A plot of the layer thickness against the square root of the annealing time is shown in Fig. 2.13. The experimental points are seen to yield three straight lines. Thus, the $NiBi_3$ layer growth is indeed diffusion controlled.

The value of the physical (diffusional) constant $k_{1Bi1}^{(integral)}$ can be calculated using integrated equations (2.49) or (2.50). The superscript *integral* is used to distinguish between the value of the constant calculated from the integrated equation and that found from the differential equation. The latter is denoted $k_{1Bi1}^{(differential)}$.

The experimental values of $k_{1Bi1}^{(integral)}$ at 150, 200 and 250 °C are listed in Table 2.2 together with their 0.95 confidence limits. These values represent the volume diffusivities of the Bi atoms in the $NiBi_3$ lattice in the course of the reaction-diffusion process or, in other words, the *reaction-diffusion coefficients* of bismuth. The interconnection between the reaction- and self-diffusion coefficients of any component of a chemical compound will be discussed later.

The diffusional constant can also be calculated from a differential equation similar to equation (2.37). The values of $k_{1Bi1}^{(differential)}$ obtained are also provided in Table 2.2. If the $NiBi_3$ layer growth is indeed diffusion controlled and follows the parabolic law, then $k_{1Bi1}^{(integral)}$ and

$k_{1Bi1}^{(differential)}$ must clearly coincide at each annealing temperature. As seen in Table 2.2, this is in fact the case.

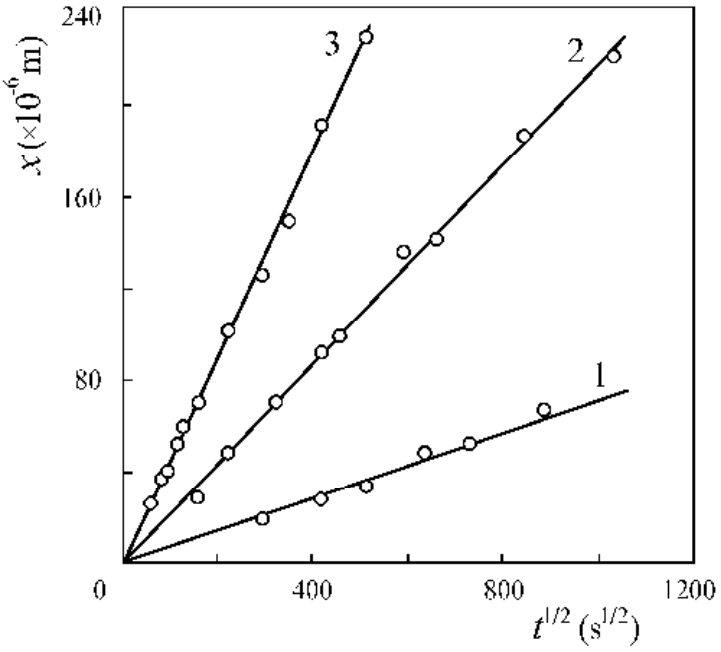

Fig. 2.13. Thickness of the $NiBi_3$ intermetallic layer plotted against the square root of the annealing time. Temperature: 1, 150 °C; 2, 200 °C; 3, 250 °C.

Table 2.2. Experimental values of the diffusional constants for the $NiBi_3$ layer growing between nickel and bismuth

Temperature (°C)	$k_{1Bi1}^{(integral)}$ ($m^2\ s^{-1}$)	0.95 confidence limits for $k_{1Bi1}^{(integral)}$ ($m^2\ s^{-1}$)	$k_{1Bi1}^{(differential)}$ ($m^2\ s^{-1}$)	0.95 confidence limits for $k_{1Bi1}^{(differential)}$ ($m^2\ s^{-1}$)
150	2.4×10^{-15}	$\pm0.4\times10^{-15}$	2.6×10^{-15}	$\pm0.3\times10^{-15}$
200	2.2×10^{-14}	$\pm0.2\times10^{-14}$	2.1×10^{-14}	$\pm0.2\times10^{-14}$
250	9.5×10^{-14}	$\pm0.3\times10^{-14}$	9.5×10^{-14}	$\pm0.5\times10^{-14}$

Note that $k_{1Bi1}^{(integral)}$ is identical to $k_{1Bi1}^{(differential)}$ only in this particular case where one component (bismuth) is diffusing across the growing layer. In the general case, where two components *A* and *B* are diffusing at comparable rates, $k_{1Bi1}^{(integral)}$ is equal to the sum of

$k_{1Bi1}^{(differential)}$ for A and $k_{1Bi1}^{(differential)}$ for B. The latter quantities should be determined from the partial increases in layer thickness at its both interfaces with initial phases (see Section 1.4.3).

The temperature dependence of the reaction-diffusion coefficient (diffusional constant) of bismuth atoms in (or, rather, across) the growing $NiBi_3$ layer is described by the Arrhenius relation (see equation (2.34)). As seen in Fig. 2.14, a graph of the logarithm of the diffusional constant $\ln k_1$ plotted against the reciprocal temperature $1/T$ yields a straight line.

Using the average values of the reaction-diffusion coefficient presented in Table 2.3, the equation

$$\ln k_1 = (0.49 \pm 0.05) \times 10^{-6} \exp\,[-(67.1 \pm 0.7)\ \text{kJ mol}^{-1}/\text{R}T]\ \text{m}^2\ \text{s}^{-1}$$

was obtained by the least-squares fit method. The value, $E = 67.1$ kJ mol^{-1} of the energy of activation falls within a range typical of diffusion controlled processes.

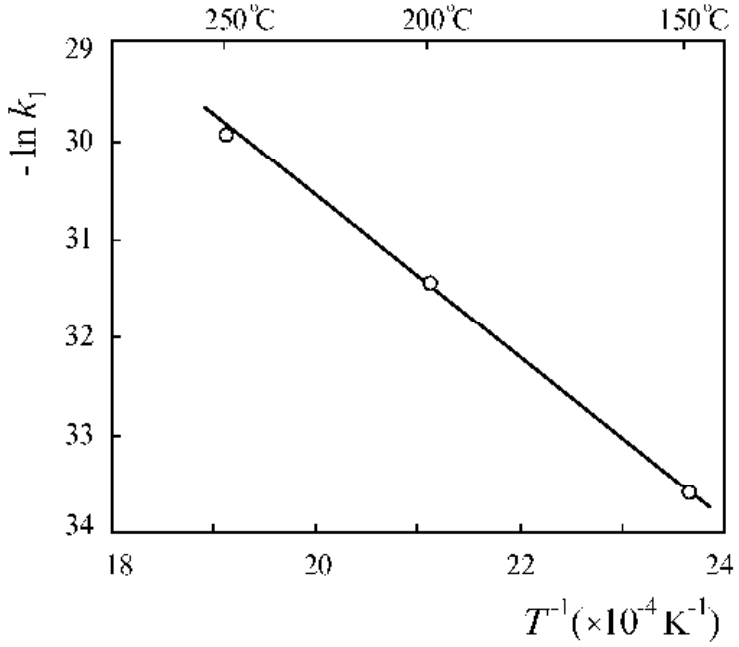

Fig. 2.14. Temperature dependence of the reaction-diffusion coefficient of the bismuth atoms in the growing $NiBi_3$ layer.

Table 2.3. Temperature dependence of the reaction-diffusion coefficient of the bismuth atoms in the growing $NiBi_3$ layer (see equation (2.34))

Temperature		T^{-1} ($\times 10^{-3}$ K^{-1})	k_1 (m^2 s^{-1})	ln k_1	Pre-exponential factor ($\times 10^{-6}$ m^2 s^{-1})	Activation energy (kJ mol^{-1})
(°C)	(K)					
150	423	2.364	2.5×10^{-15}	–33.622	0.49 ± 0.05	67.1 ± 0.7
200	473	2.114	2.1×10^{-14}	–31.494		
250	523	1.912	9.5×10^{-14}	–29.985		

2.6: Interrelation between the reaction-diffusion coefficients of the components of a chemical compound and their self-diffusion coefficients

Experimental data available in the literature show large, if not to say huge, differences between the values of diffusion coefficients of the elements A and B in the A_pB_q chemical compound layer growing at the A–B interface and the values of diffusion coefficients of the same elements in a separate specimen of the same chemical compound. In other words, for the same component of the same compound the value of the reaction-diffusion coefficient is quite different from the value of the self-diffusion coefficient, with the difference amounting to a few orders of magnitude. Note that the reaction-diffusion coefficient is always greater than the appropriate self-diffusion coefficient. Examples can readily be found in Ref. [16].

2.6.1: Reasons for the difference in reaction- and self-diffusion coefficients

In the case of the reaction-diffusion process, of all conceivable diffusion mechanisms [18-36], the most probable ones are vacancy, interstitial and grain-boundary. What is diffusing (molecule, atom or ion) depends on the structure of a chemical compound and the physical and chemical properties of its components, in particular of the radius of their atoms or ions.

Diffusion of a reacting substance across the bulk of a growing compound layer in the form of molecules appears to be a very rare phenomenon, typical of loosely packed lattices. Such a structure is characteristic, for example of silicon oxide SiO_2. Its lattice contains channels along which the oxygen molecules can readily travel [29].

The difference in values of the diffusion coefficient of a constituent in the growing and non-growing layers of a chemical compound is often explained by the influence of grain-boundary diffusion. Such an explanation seems too “universal” in order to be valid in all cases. Firstly, the “width” of any grain boundary is small in comparison with the size of adjacent grains except, perhaps, for very fine ones. Therefore, in spite of high values of grain-

boundary diffusion coefficients of reacting atoms, their fluxes along grain boundaries across a growing chemical compound layer can hardly be large, at least in coarse-grained structures. Secondly, if grain-boundary diffusion predominates, a growing compound layer should be thicker in the vicinity of the boundaries of any grain in comparison with the central part of that grain. This is quite opposite to what has been observed experimentally, for example, in the case of growing Fe_2Al_5 layers [16].

In fact, the main reason for the difference in reaction- and self-diffusion coefficients appears to lie in the peculiarities of the reaction-diffusion mechanism itself. Indeed, the description of diffusion processes in both growing and non-growing compound layers is conventionally based upon Fick's laws that are too fundamental for their validity and applicability to be doubted in such simple cases. Of all quantities entering into Fick's equations, only the concentration c of a diffusing species can be treated ambiguously. Diffusion coefficient D of any component, being a characteristic of the squared atomic displacement per unit time, can hardly be expected to be dependent on whether this compound is growing or non-growing, if the diffusion mechanism is the same in both cases.

Most chemical compounds are characterised by diffusion of the components across the bulks of their growing layers in the form of atoms or ions and not in the form of molecules or radicals, just because the former are of smaller size than the latter. The process of bulk diffusion is described by Fick's laws. The first Fick law relates the flux of atoms of a given component to its diffusion coefficient and concentration gradient in the direction of diffusion at constant surface area of contacting phases:

$$j_A = -D_A \frac{\partial c_A}{\partial x} \qquad (2.51)$$

where j_A is the flux of A atoms across the bulk of a growing layer (mol m^{-2} s^{-1} or kg m^{-2} s^{-1}), D_A is the diffusion coefficient of the A atoms in the lattice of a compound (m^2 s^{-1}), c_A is the concentration (content) of component A in a compound (mol m^{-3} or kg m^{-3}).

The second Fick law describes a change in concentration of diffusing particles at a given point of space with passing time:

$$\frac{\partial c_A}{\partial t} = D_A \frac{\partial^2 c_A}{\partial x^2} \quad . \qquad (2.52)$$

Note that the use in Fick's equations of the concentration units other than the number of particles or their mass per unit volume (molar, mass or volume fraction, mass or atomic percent, *etc*.) must be substantiated in each particular case. Otherwise, the numerical values of the diffusion coefficients obtained with the use of different units will generally be different. Though widespread, employment of these other units in theoretical treatments does not appear reasonable.

In the case of chemical compounds of constant composition, application of Fick's equations is, on the one hand, facilitated by the obvious fact that it is not necessary to take into account the concentration dependence of the diffusion coefficient. On the other hand, however, there arise serious, if not insurmountable, difficulties with the direct use of those equations because no concentration gradient can evidently exist in any growing layer, if a compound has no homogeneity range. It is therefore not surprising that most authors give preference to analysing the process of formation of the layers of chemical compounds having a narrow range of homogeneity (in comparison with the average content of a given component). This is one of ideal cases for theoreticians to treat.

Firstly, the concentration dependence of the diffusion coefficient can be neglected. Secondly, the concentration of components at the interfaces of any growing layer can be assumed to be equal to the limits of the homogeneity range of a compound according to the equilibrium phase diagram of the *A–B* binary system. Thirdly, the concentration distribution of the components across a compound layer at any instant can reasonably be assumed to be close to linear (Fig. 2.15a), so that

$$\frac{\partial c_A}{\partial t} \approx 0 \,. \qquad (2.53)$$

Equation (2.53) expresses the condition of the quasi-stationary concentration distribution when the concentrations of components *A* and *B* in the growing layer *AB* or A_pB_q are functions of only coordinate *x* and do not depend on time *t*. Simply speaking, on a time scale of the diffusion of atoms across the layer, the redistribution of concentration of the components along the layer takes place at a relatively high rate. For compounds of constant composition, this condition is clearly always satisfied. The distribution of concentration of the components in each particular case can readily be established, for example, by means of electron probe microanalysis.

Indeed, if for the layers of a given compound of different thickness obtained on the same *A–B* specimen by interrupting the chemical reaction at certain moments of time, the distribution of contents of the components across the width of the layer proves close to linear as shown in Fig. 2.15a, then the quasi-stationary condition is fulfilled quite satisfactorily. Of course, one may object that, firstly, the accuracy of measurements is not always sufficiently high and, secondly, the content of the components in any compound layer can be measured only at some distance from the interfaces.

The latter difficulty is easily overcome by extrapolation. Furthermore, it is clear that if the mean content of a component in a compound is equal to 40-60%, while the range of homogeneity is 1-2% or less, then possible deviations from the quasi-stationary concentration distribution can hardly be expected to have any noticeable effect on the results of analytical description of layer-growth kinetics. This is especially so in the case of the reaction-diffusion process.

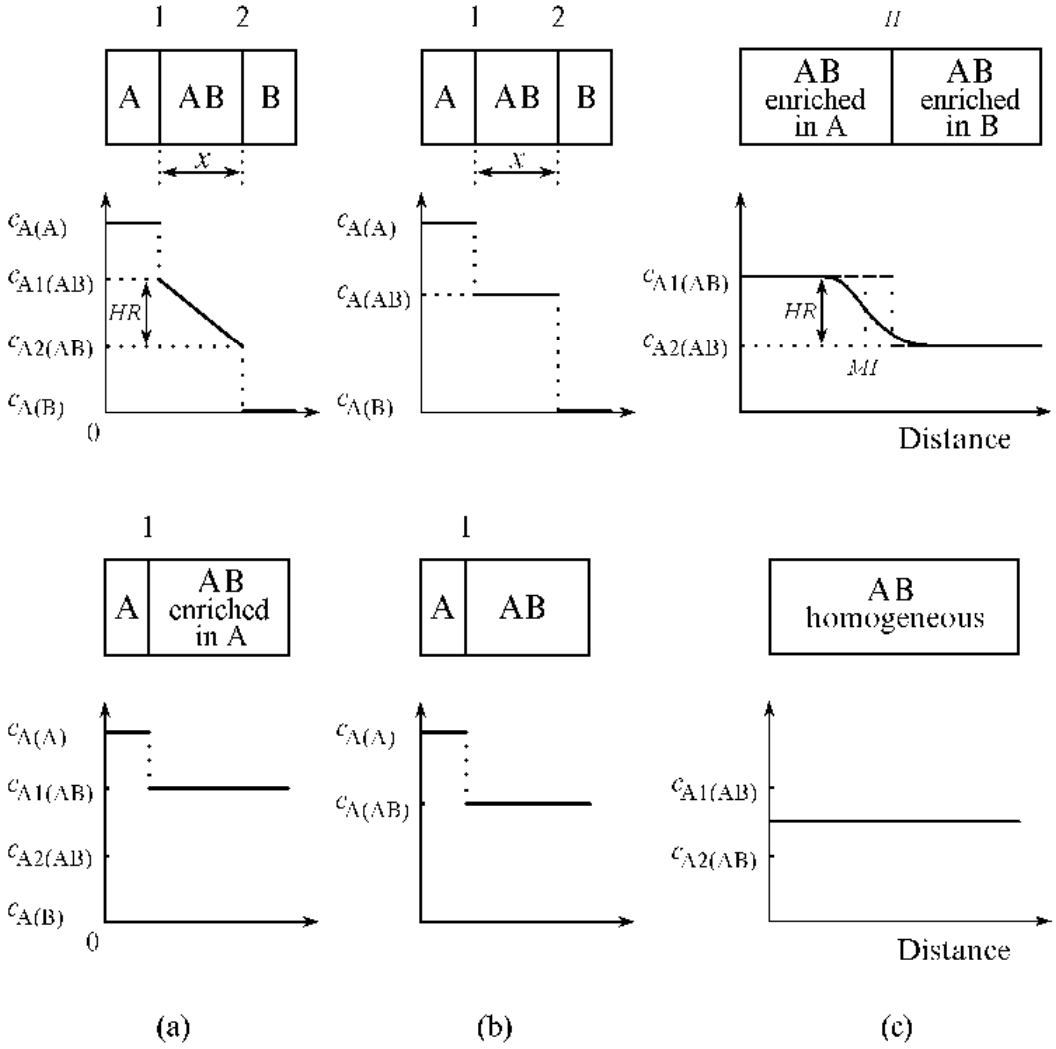

Fig. 2.15. Evolution of reaction couples up to the establishment of equilibrium. (a) Growth process of a layer of the compound *AB* having a (narrow) range of homogeneity. Phase *A* and the compound *AB* with the content of component *A* equal to the upper limit of the range of homogeneity remain under equilibrium. (b) Growth process of a layer of the compound *AB* without any range of homogeneity. (c) Homogenising a diffusion couple consisting of the compound *AB* with different contents of component *A*. *HR* is the range of homogeneity of the compound *AB*, *II* is the initial interface, *MI* is Matano's plane.

The layer of any chemical compound grows at the expense of *stoichiometry* of that compound and not at the expense of its range of homogeneity. Therefore, from the point of view of formal kinetics, it does not matter whether the compound has any range of homogeneity or not. To explain why this conclusion (quite opposite to the views of most, if not all, investigators in the field) was drawn in the 1980s (see Ref. [16]), consider a conventional treatment of diffusional processes.

If the concentration distribution of component A in the AB layer is linear (see Fig. 2.15a), then its concentration gradient can be expressed through the boundary values c_{A1} and c_{A2} and the thickness x of the growing layer:

$$-\frac{\partial c_A}{\partial x} = \frac{c_{A1} - c_{A2}}{x} . \qquad (2.54)$$

Hence, the flux of component A across the bulk of the AB layer from interface 1 to interface 2 is

$$j_A = D_A \frac{(c_{A1} - c_{A2})}{x}. \qquad (2.55)$$

This flux is entirely consumed in the formation of the AB chemical compound at interface 2. Therefore, assuming that the chemical transformations with participation of the diffusing A atoms and the surface B atoms take place instantaneously, its value can also be expressed as follows

$$j_A = \frac{c_{A1} + c_{A2}}{2}\left(\frac{\mathrm{d}x}{\mathrm{d}t}\right)_{\text{diffusional regime}} . \qquad (2.56)$$

Equating the right-hand sides of equations (2.55) and (2.56) yields

$$\left(\frac{\mathrm{d}x}{\mathrm{d}t}\right)_{\text{diffusional regime}} = \frac{2D_A(c_{A1} - c_{A2})}{(c_{A1} + c_{A2})x}. \qquad (2.57)$$

As, on the other hand (see equation (2.11)),

$$\left(\frac{\mathrm{d}x}{\mathrm{d}t}\right)_{\text{diffusional regime}} = \frac{k_{1A2}}{x}, \qquad (2.58)$$

a relation between the diffusion coefficient of the A atoms across the bulk of any growing compound layer and the diffusional constant is

$$D_A = \frac{(c_{A1} + c_{A2})}{2(c_{A1} - c_{A2})} k_{1A2}. \qquad (2.59)$$

Note that this equation holds for chemical compounds of any composition A_pB_q, not only for AB. The quantity $(c_{A1} + c_{A2})/2 = c_{\text{average}}$ is the average content of component A in a chemical compound. The difference of its contents at the layer interfaces $\Delta c_A = c_{A1} - c_{A2} = HR$ represents the range of homogeneity of the compound under given temperature-pressure conditions.

It is usually assumed that Δc_A is the driving force for the process of formation of a chemical compound layer, *i.e.* $j_A \sim \Delta c_A$. If it were the case, however, the layers of chemical compounds without any homogeneity ranges like Al_2O_3 or $NiBi_3$ would not grow at all that contradicts experimental observations. This is the first inconsistency of the conventional diffusional approach. Again, at any finite value of k_{1A2} equation (2.59) produces unrealistically high values of the diffusion coefficient because $D_A \to \infty$, as $\Delta c_A \to 0$ (second inconsistency). In the limit, it actually means dividing by zero. From a physical viewpoint, such values of D_A are hardly possible.

Generally, wide ranges of homogeneity are not characteristic of chemical compounds. Therefore, equation (2.59) either yields too high values of diffusion coefficients of the components in growing layers of chemical compounds having narrow ranges of homogeneity (Fe_2Al_5, $CoSn_2$, $Fe_{3-\delta}O_4$) or cannot be employed at all in the case of compounds without any homogeneity range ($NiBi_3$, FeB, Al_2O_3). By assuming that the driving force for the reaction-diffusion process of the A atoms across the bulk of the growing AB layer is the difference in *concentration* of *vacancies* of component A at the A–AB and AB–B interfaces of this layer, both inconsistencies of the diffusional approach are readily eliminated.

It is necessary, however, to distinguish between the newly-formed and native (equilibrium) vacancies. The newly-formed vacancies arise in the course of partial chemical reactions proceeding at the layer interfaces. These are thus reaction-induced vacancies which do not normally exist in a given equilibrated compound. The native (inherent), mainly thermal, vacancies are present in the compound initially (in the equilibrium state), their number being quite negligible by comparison, except perhaps at temperatures close to its melting point. Both the newly-formed and native vacancies are clearly supposed to be of the same character.

Equation (2.59) can be re-written as

$$k_{1A2} = \frac{2D_A(c_{A1} - c_{A2})}{(c_{A1} + c_{A2})} = \frac{D_A(c_{A1} - c_{A2})}{c_{\text{average}}}. \qquad (2.60)$$

If the concentration of newly-formed vacancies of component A in the AB layer at the reacting interface 2 (see Fig. 2.15a) where these vacancies are continuously created as a result of partial chemical reaction $A_{dif} + B_{surf} = AB$, like (2.2), is assumed to be *numerically* equal to the content of this component in the AB compound with the opposite sign

$$-c_{\text{vacancies } A} = c_A,$$

while that at another (non-reacting) interface 1 zero (ideal case in which no native vacancies are available in the compound), then from equation (2.60) it follows

$$k_{1A2} = \frac{D_A(0 + c_{A2})}{c_{\text{average}}}. \qquad (2.61)$$

If $HR = 0$ (see Fig. 2.15b), then $c_{A1} = c_{A2} = c_{\text{average}}$. Hence, $k_{1A2} = D_A\,(0 + c_{A2})/c_{\text{average}} = D_A$. Thus, the physical (diffusional) constant k_{1A2} is identified with the reaction-diffusion coefficient D_A of component A in the lattice of any chemical compound.

If $HR \neq 0$,

$$k_{1A2} = \frac{D_A(0 + c_{A2})}{c_{\text{average}}} \approx D_A, \qquad (2.62)$$

with the difference between k_{1A2} and D_A decreasing, as HR tends to zero. In other words, the closer the compound to its stoichiometric composition, the more nearly k_{1A2} approaches D_A.

From equations (2.60)-(2.62), it must be clear that the role of native point defects such as vacancies of component A in the reaction-diffusion process of formation of any chemical compound is *opposite* to their role in the process of self-diffusion of that component in the compound taken as a separate phase.

In the absence of complicating factors, the *higher* the amount of native A vacancies in AB, the *higher* is the rate of self-diffusion of component A in the separate AB phase. Contrary to this, the *higher* the amount of native A vacancies in AB, the *less* is the rate of growth of the AB layer in the A–B couple at the expense of diffusion of component A, *i.e.* the *less* is a value of the physical (diffusional) constant k_{1A2}.

From a chemical viewpoint, this conclusion appears to be quite obvious and understandable because unoccupied (empty) sites (vacancies) can hardly take part in chemical reactions yielding material products. It is just available atoms, ions, molecules or radicals and not native vacancies that are responsible for the progress of any interfacial chemical reaction. The formation of a reaction product is a result of their joint efforts.

In the case of the reaction-diffusion process, it does not seem substantiated to make a relatively small amount of missing atoms, say one atom in every hundred atoms, responsible

for its course and to consider a much greater amount of available atoms (99) as an inert mass. The actual role of this single missing atom can roughly be estimated as 100% with the plus sign in the self-diffusion process and as 1% with the minus sign in the reaction-diffusion one.

The influence of deviations from the stoichiometry of any chemical compound on the growth rate of its solid layer can be illustrated by the following numerical example. If at some fixed temperature the *AB* homogeneity range is 5% (say, 35 to 40% *A*), then a relation between the physical (diffusional) constant k_{1A2} of the *AB* layer and the reaction-diffusion coefficient D_A of component *A* in the *AB* lattice is (see equations (2.61)-(2.62))

$$k_{1A2} = \frac{D_A(0+35)}{(40+35)/2} = 0.93D_A.$$

If at the same temperature the *AB* homogeneity range is reduced (by change of pressure or any other means) to 2% (38 to 40% *A*), then this relation is

$$k_{1A2} = \frac{D_A(0+38)}{(40+38)/2} = 0.97D_A.$$

The effect is seen to be rather perceptible. Its magnitude is in general agreement with the values observed for oxides of deficient structure [27, 28]. Similar effect must also be observed, though not so easily experimentally, with intermetallics and other chemical compounds.

Clearly, similar consideration also applies to component *B*. A row (a plane in two dimensions) of *B* vacancies is formed in the *AB* layer at interface 1 as a result of chemical interaction between the diffusing *B* atoms and the surface *A* atoms (Fig. 2.16, $t_1 > t_0$). From Fig. 2.16, it can easily be understood that, on the one hand, the concentration of newly-formed *B* vacancies, continuously created at the *A–AB* interface (interface 1) in the course of partial chemical reaction $B_{dif} + A_{surf} = AB$, is *numerically* equal to the content of component *B* in the *AB* compound.

On the other hand, there are almost no *B* vacancies at the *AB–B* interface (interface 2) since those are mainly thermal, their amount at not too high temperatures being negligibly small. Therefore, due to this difference in vacancy concentrations, during $t_2 > t_1$ the row of *B* vacancies moves as a whole across the bulk of the *AB* layer until it reaches interface 2 at $t_3 > t_2$. At $t_4 > t_3$, this basic act of the reaction-diffusion process is completed by the formation of an additional row of "molecules" *AB* and then is repeated with the *AB* layer thicker by one plane of "molecules" *AB*, and so on.

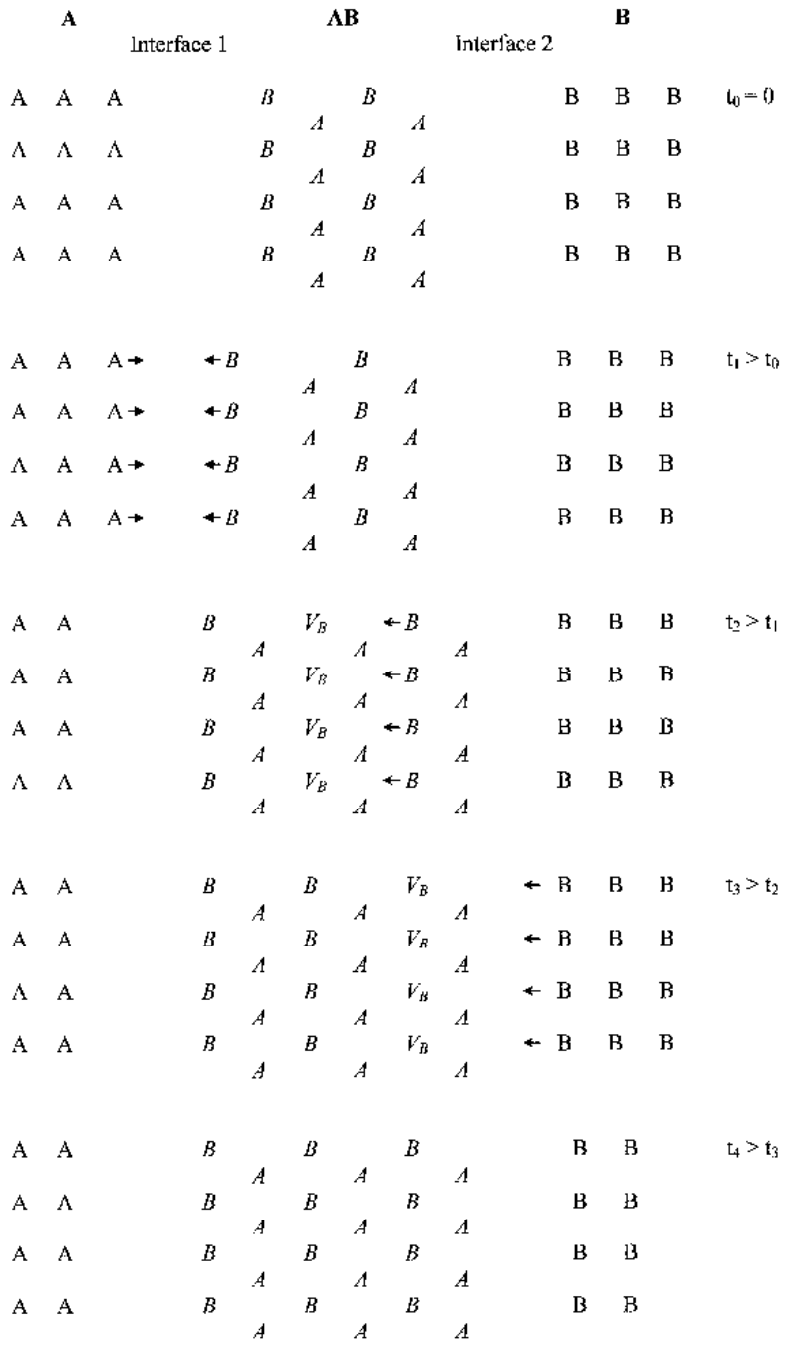

Fig. 2.16. Formation and displacement of a row (a plane in two dimensions) of vacancies of component *B* in the bulk of the growing *AB* layer in the course of the reaction-diffusion process. Component *A* is considered to be immobile in the *AB* lattice. At t_1, the diffusing *B* atoms start to interact chemically with the surface *A* atoms to form the *AB* "molecules" at interface 1. As a result, a row (a plane) of *B* vacancies occurs in the *AB* layer at t_2. These vacancies are filled with neighbouring *B* atoms, so that a row (a plane) of *B* vacancies moves as a whole towards interface 2. At t_3, this row (plane) of *B* vacancies is filled with *B* atoms from phase *B*. At t_4, the system returns to a new initial state and all the processes described are repeated again and again with the increasingly thicker *AB* layer.

Its driving force is the difference in values of the chemical potential of component B in initial phases A and B. This constant difference exists until at least one of initial substances A or B is entirely exhausted.

In the general case where both components A and B are sufficiently mobile in the AB lattice, two rows (planes) of vacancies are formed, namely, one row of A vacancies and one row of B vacancies, as shown in Fig. 2.17. Measurement of partial increases in thickness of the layer at its interfaces makes it possible to calculate

$$k_{1A2} = D_A \text{ and } k_{1B1} = D_B$$

for the compound without any homogeneity range, $HR = 0$, or

$$k_{1A2} \approx D_A \text{ and } k_{1B1} \approx D_B$$

for the compound with a homogeneity range, $HR > 0$.

Generally, during growth of any chemical compound layer, the rows of A and B vacancies move across its bulk in opposite directions. These vacancies appear as a result of the occurrence of chemical reactions at the interfaces of this layer with initial phases. It should be stressed that the vacancies formed cannot be distributed uniformly within the bulk of a chemical compound layer. Their amount exceeds all permissible equilibrium limits under given temperature-pressure conditions. Existence of such vacancies is only possible in growing compound layers.

If the reaction is arrested at some moment of time when a moving row of vacancies is far away from the interfaces, component A or B must form a separate phase within the bulk of a grown layer of the compound AB or A_pB_q. In thin films, the amount of this phase may be relatively large. It must therefore be detectable by sufficiently sensitive experimental methods.

In real reaction couples, the interaction rarely starts simultaneously over the whole interface between initial substances A and B. The reasons may be different, from local contaminations of the surface of reacting phases to inherent structure imperfections. In such cases, a few shorter rows of vacancies are formed and move with some shift in space across a compound layer.

Note that the concentration gradient of components A and B in the growing layer of any chemical compound is established only in the case of existence of a considerable homogeneity range of that compound (see Fig. 2.15b). Establishment of this gradient is in fact a *consequence* of the *reaction-diffusion process* and not the *reason* for this process to proceed, as is often erroneously assumed.

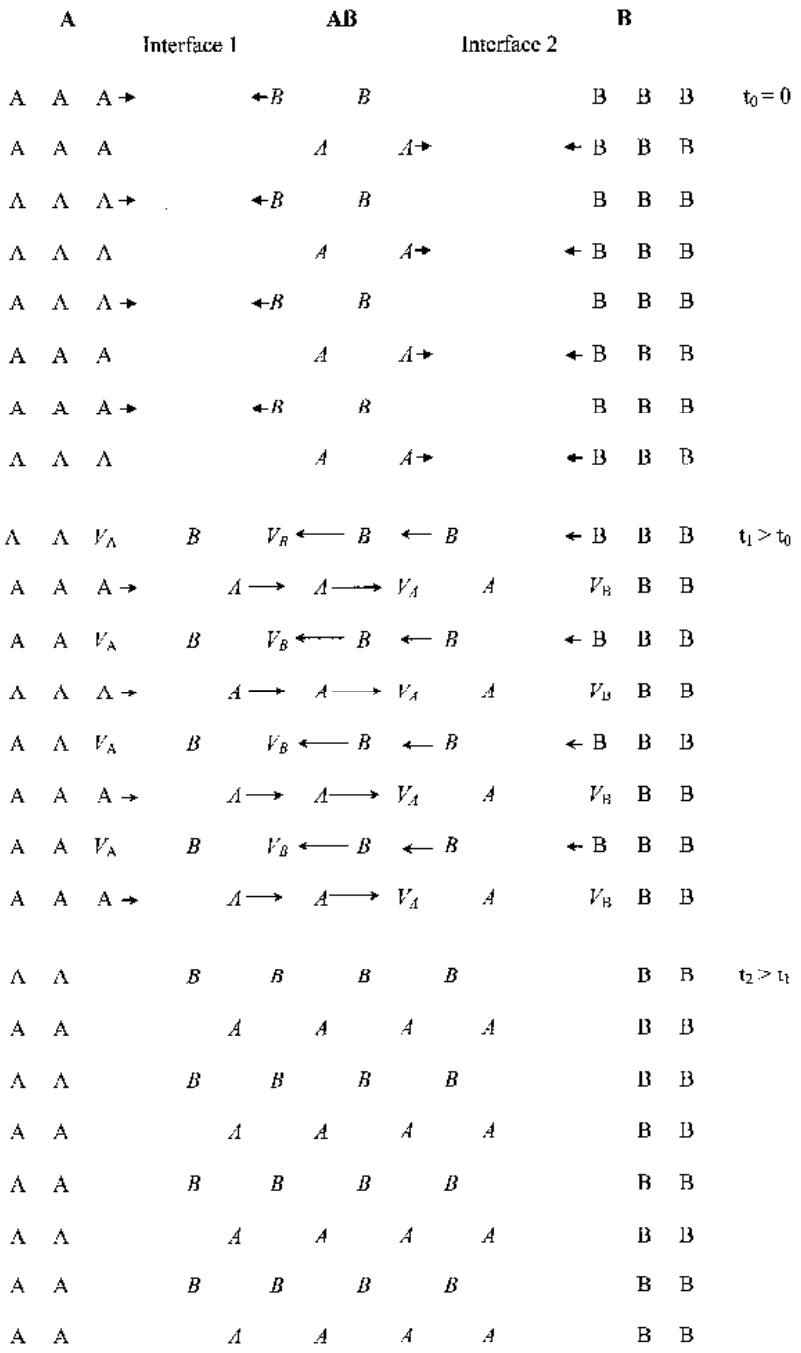

Fig. 2.17. Formation and displacement of rows (planes) of *A* and *B* vacancies across the bulk of the *AB* layer in the course of diffusion of both components. At t_0, chemical reactions start to proceed simultaneously at both interfaces of the *AB* layer with initial phases. As a result of those reactions, a row (a plane) of *A* vacancies and a row (a plane) of *B* vacancies occur in the *AB* layer. Between t_1 and t_2, these move across the *AB* layer in opposite directions towards its interfaces and then are filled with the appropriate atoms from *A* or *B* phases. Arrows of different length indicate the sequence of movement of diffusing atoms. At t_2, the system returns to a new initial state, and all the processes are repeated again and again.

The quantity $\Delta c_A = HR$ is the driving force for the *diffusion* process when two specimens of substance AB with contents of A equal to c_{A1} and c_{A2} are brought into close contact with each other and then allowed to react for some period of time at a constant temperature and pressure. This is in fact the process of formation of a solid solution resulting in complete homogenising the examined diffusion couple (Fig. 2.15c). Such experiments can readily be carried out with chemical compounds having considerable ranges of homogeneity (around a few per cent).

Figure 2.18 shows the concentration profile of Co in a $Co_{54}Ti_{46}$–$Co_{50}Ti_{50}$ diffusion couple (for the CoTi intermetallic compound HR = 4 at.%) [37]. It is like that shown in Fig. 2.15c. Similar plots are obtained for Al in FeAl (HR = 20 at.%) at 1000 °C [38] and for Fe in Pt_3Fe (HR = 3 at.%) at 1060 °C [39]. These concentration profiles are quite different from the straight-line (horizontal if $HR = 0$ or inclined if $HR > 0$) ones that are typical of growing compound layers (compare Figs 2.15a and b with Fig. 2.15c).

Any reaction couple tends with passing time to its equilibrium state. According to the Gibbs phase rule [1-6], in any binary system at most two phases can coexist under equilibrium, if both the temperature and pressure are maintained constant. These are either the compound layer of constant composition and one of initial substances (see Fig. 2.15b) or the compound layer itself, if the initial amounts of reacting substances correspond to its composition.

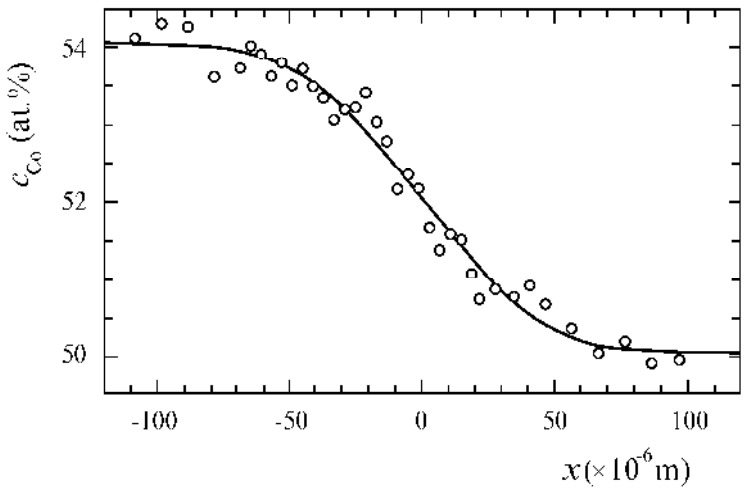

Fig. 2.18. Concentration profile of cobalt in a $Co_{54}Ti_{46}$–$Co_{50}Ti_{50}$ diffusion couple annealed at 1300 °C for 11.4×10^3 s [37].

This is one of two modes of attaining equilibrium, namely, by consumption of an initial phase. It is typical of systems with no solid-state solubility. Another is a smooth homogenisation, as shown in Fig. 2.15c. Figure 2.15a represents a combination of the two extremes. First, phase B is completely consumed and subsequently the AB layer attains the concentration c_{A1} (the upper limit of the range of homogeneity in regard to component A).

2.6.2: Kirkendall effect

The difference in diffusivities of the components in a growing chemical compound layer is often connected, especially in the literature on physics and metallurgy and especially in relation to intermetallics, with the Kirkendall effect. From historical and scientific viewpoints, this does not always appear to be sufficiently substantiated.

The Kirkendall effect was established in 1939-1947. Its final formulation was presented in a paper published in 1947 [40] (see also Refs [21, 23, 34, 41]). This effect arises from the different values of the self-diffusion (intrinsic) coefficients of the components of a *substitutional solid solution*, determined by Matano's method.

Matano's interface (plane) is defined by the condition that as much of the diffusing atoms have migrated away from its one side as have entered the other. To understand the essence of the Kirkendall effect, it suffices to consider a schematic representation of the diffusion processes taking place during annealing of any couple A–B, the components of which are capable of forming an extended or a terminal solid solution under given temperature-pressure conditions. Its initial state is shown in Fig. 2.19a.

If $D_A = D_B$ (Kirkendall effect is missing), the area confined between Matano's interface (MI), the experimental concentration curve and the horizontal line c_{A2} = const, representing the amount of component B that has diffused in time $t_{\text{equilibrium}} > t > 0$, is at any instant equal to the area confined between MI, the concentration curve and the horizontal line c_{A1} = const, representing the amount of component A that has diffused during the same time, as shown in Fig. 2.19b. With increasing time, the concentration curve gradually flattens but the marked initial interface (Kirkendall interface) always coincides with Matano's interface.

In diffusion couples A–B of finite dimensions, a homogeneous solid solution AB is eventually formed, if the components were taken in the proper amount following from the phase diagram of a given binary system. In the process of its formation, both parts of the concentration curve approach the equilibrium composition of this solution at equal rates. If the initial amounts of the components were improper, the excess component will co-exist with the solid solution at equilibrium.

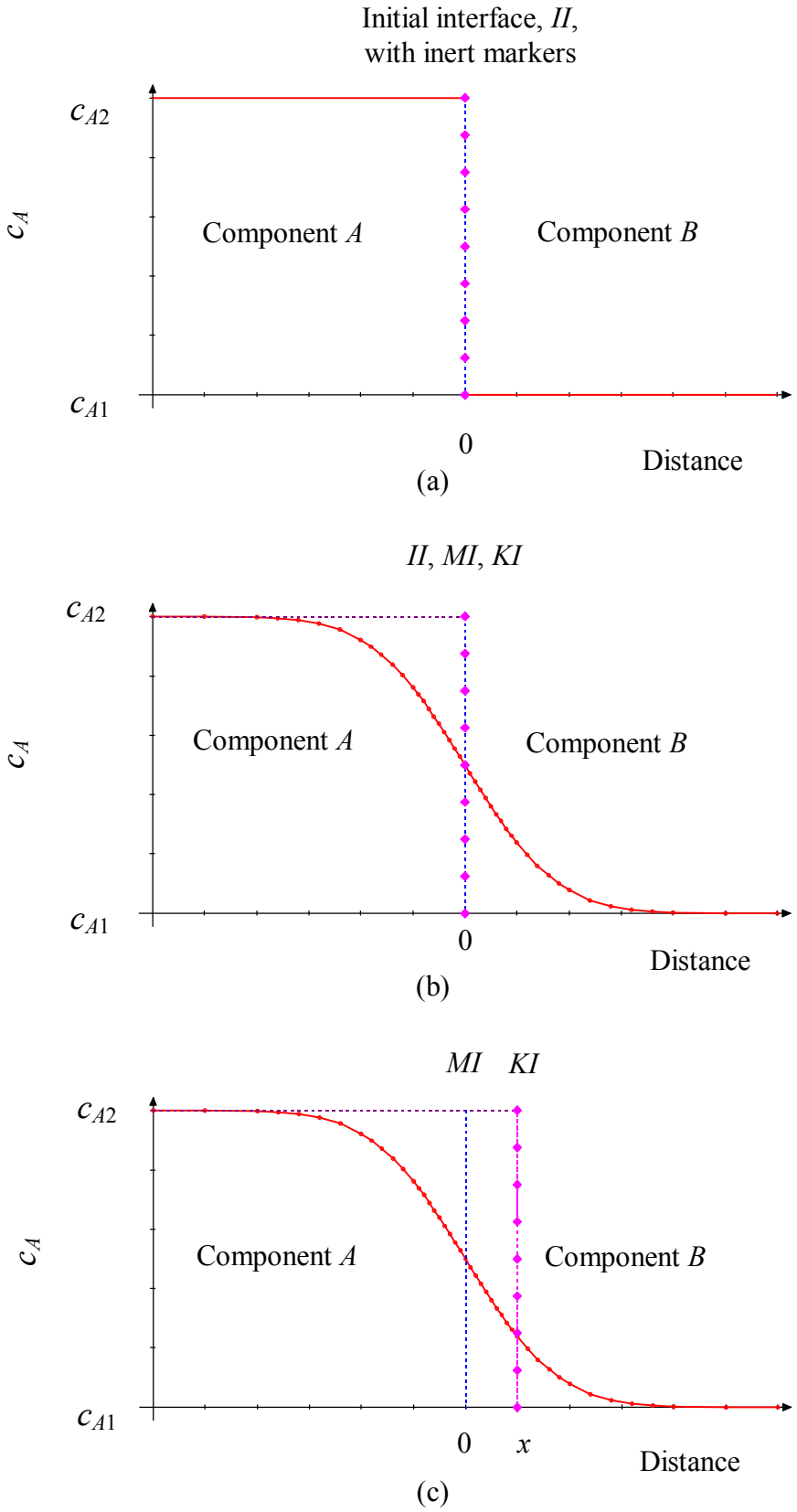

Fig.2.19. Concentration profile of component *A* in the *A–B* diffusion couple in the case of formation of a solid solution. (a) Initial condition, (b) Kirkendall effect is missing, (c) Kirkendall effect is available.

If $D_A \neq D_B$ (Kirkendall effect is present), the final result is the same (formation of a homogeneous solid solution) but with increasing time the diffusion zone not only flattens but also simultaneously displaces as a whole relative to the marked initial interface or Kirkendall interface *KI*. In this case, a certain Kirkendall shift, 0 to *x* in Fig. 2.19c, arises between the Kirkendall interface *KI* and Matano's interface *MI*, so that at any instant, excepting $t = 0$, these do not coincide.

This shift may be considered as a result of either the lattice plastic flow or the movement of excess vacancies arising from the side of a faster diffusing component. In the absence of complicating factors, both approaches produce identical results, enabling to treat the process of diffusion in a two-component solid solution in terms of a single *interdiffusion coefficient*, $D_{\text{interdiffusion}}$ (see, for example, Refs [21, 23, 24, 42, 43].

Note that *interdiffusion* is often called *chemical diffusion*. The former term appears to be more suitable because the *interdiffusion* coefficient characterises the rate of *intermixing* of components *A* and *B* to form a solid solution in the diffusion zone, whereas the latter may even be misleading since the formation of a solid solution is not a chemical process.

The theoretical treatment of interdiffusion in a two-component binary system appears to have been given for the first time by L.S. Darken in 1948 [42] and since is and probably will be cited or reproduced, because of its fundamental nature, in numerous subsequent papers, handbooks, textbooks and monographs where diffusion processes are considered. In this section, it is briefly reproduced, just to show the limits of applicability of Darken's approach to chemical compounds.

According to the second Fick law,

$$\frac{\partial c_A}{\partial t} = \frac{\partial}{\partial x}\left(D_A \frac{\partial c_A}{\partial x} - c_A v_{\text{K}}\right), \tag{2.63}$$

$$\frac{\partial c_B}{\partial t} = \frac{\partial}{\partial x}\left(D_B \frac{\partial c_B}{\partial x} - c_B v_{\text{K}}\right), \tag{2.64}$$

where v_{K} is the velocity of movement of the Kirkendall interface; the concentration *c* of the components *A* and *B* is expressed in number (or moles) of particles per cubic metre and the volume of the diffusion couple is assumed to be constant.

Since the total number of the *A* and *B* atoms in unit volume, $c = c_A + c_B$, in the course of formation of any substitutional solid solution remains unchanged, the sum of these equations must be zero. Hence,

$$\frac{\partial}{\partial t}(c_A + c_B) = \frac{\partial}{\partial x}\left(D_A \frac{\partial c_A}{\partial x} + D_B \frac{\partial c_B}{\partial x} - c v_{\text{K}}\right) = 0. \tag{2.65}$$

From this equation, it follows

$$D_A \frac{\partial c_A}{\partial x} + D_B \frac{\partial c_B}{\partial x} - c v_K = \text{const.} \tag{2.66}$$

At $x = \pm \infty$, the integration constant is equal to zero. Beyond the diffusion zone, the concentration gradients and the Kirkendall velocity are also assumed to be zero. Then, taking into account that for any solid solution $\partial c_A/\partial x = -(\partial c_B/\partial x)$, one obtains

$$v_K = (D_A - D_B)\frac{\partial c_A}{\partial x}\frac{1}{c} = (D_A - D_B)\frac{\partial N_A}{\partial x}, \tag{2.67}$$

where $N_A = c_A/c$ is the mole fraction of component A in the solid solution.

By substituting this expression for v_K into equation (2.63), the following equation is obtained

$$\frac{\partial c_A}{\partial t} = \frac{\partial}{\partial x}[(D_A N_B + D_B N_A)\frac{\partial c_A}{\partial x}] = \frac{\partial}{\partial x}(D_{\text{interdiffusion}}\frac{\partial c_A}{\partial x}), \tag{2.68}$$

where

$$D_{\text{interdiffusion}} = D_A N_B + D_B N_A \tag{2.69}$$

is the *interdiffusion* coefficient.

Written in terms of $D_{\text{interdiffusion}}$, equation (2.68) is seen to be similar to equation (2.52), thus permitting to treat the diffusional formation of any binary solid solution in a mathematically consistent manner by a single interdiffusion coefficient.

Note that, from this derivation, it must be clear that Darken's equations are not applicable at all to chemical compounds without any range of homogeneity because for these the total number of the A and B atoms in unit volume, $c = c_A + c_B$, is not simply constant at any instant, as for solid solutions, but in addition is unable, unlike solid solutions, to vary under any circumstances. Any change of their composition is not allowed by the laws of definite and multiple proportions.

In such a case, there are merely no theoretical grounds to apply Darken's equations. With chemical compounds, Darken's approach is only applicable to diffusion couples formed by two (terminal) solid solutions of different composition, based on one and the same chemical compound of the type A_pB_q having some range of homogeneity, but this case does not differ essentially from that where a couple is formed by two pure components A and B.

To distinguish between different diffusion coefficients, it appears relevant to introduce more detailed designations, namely, $D_A = D_{A\ in\ AB}$ and $D_B = D_{B\ in\ AB}$. Variation of $D_{\text{interdiffusion}}$, $D_{A\ in\ AB}$ and $D_{B\ in\ AB}$ with concentration for an extended solid solution is shown schematically in Fig. 2.20. Generally, these dependences are clearly more complicated than simple straight lines.

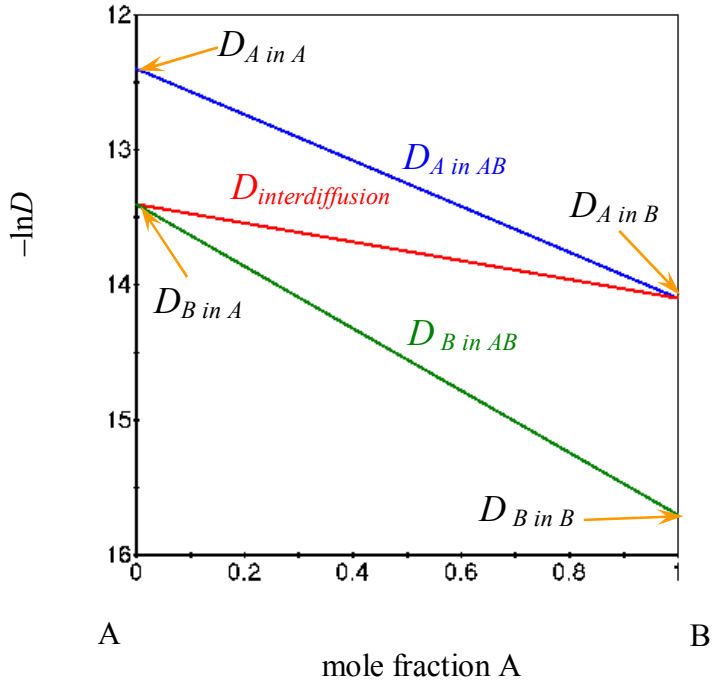

Fig.2.20. Interconnection among various diffusion coefficients in the case of formation of an extended solid solution between components *A* and *B*.

For dilute solutions of *A* in *B* ($N_A \to 0$, $N_B \to 1$), $D_{\text{interdiffusion}} \approx D_{A\ in\ AB}$. In the limit $N_A = 0$, $D_{\text{interdiffusion}} = D_{A\ in\ AB} = D_{A\ in\ B}$, $D_{A\ in\ B}$ being the tracer-diffusion coefficient of *A* in *B*. Similarly, for dilute solutions of *B* in *A* ($N_B \to 0$, $N_A \to 1$), $D_{\text{interdiffusion}} \approx D_{B\ in\ AB}$. In the limit $N_B = 0$, $D_{\text{interdiffusion}} = D_{B\ in\ AB} = D_{B\ in\ A}$, $D_{B\ in\ A}$ being the tracer-diffusion coefficient of *B* in *A*. $D_{A\ in\ A}$ and $D_{B\ in\ B}$ are tracer-diffusion coefficients of *A* in *A* and *B* in *B*, respectively.

It should be emphasised that Kirkendall's discovery was probably indeed a discovery since at that time most researchers in the field of diffusion considered the relation $D_A = D_B$ to hold for *any* solid solution of the substitutional type. Kirkendall's experiments showed that in fact this is not always the case.

At the time of E. Kirkendall, his interpretation of the experimental results obtained was severely criticised. Then, as often happens, the situation changed to the contrary. Now, the Kirkendall effect is found even in those cases to which it has no attitude. In particular, it is so in the case of formation of chemical compound layers at the interface of initial substances *A* and *B*. However, it does not appear to be justified not only from a scientific viewpoint, as stressed above, but also from a historical one.

That the components of a *chemical compound* generally diffuse in its growing solid layer at *different* speeds became known far before the appearance of the works of E. Kirkendall. It suffices to remind marker experiments in tarnishing reactions carried out by L.B. Pfeil in 1929-1931 or the investigation of interaction of silver with liquid sulphur performed by C. Wagner in the early 1930s (see, for example, Refs [17, 21-23, 44]).

Using inert markers, L.B. Pfeil found cations to be the main diffusing species in the oxidation of many metals. C. Wagner showed silver cations to be the only diffusing species in growing layers of α-Ag_2S. In view of these and numerous other well-known experiments carried out with chemical compounds, there are no historical grounds to attribute revealing the difference in the diffusion coefficients of the components in growing compound layers exclusively to E. Kirkendall.

Moreover, it was probably commonplace, at least to chemists, to regard diffusional contributions of the components to the growth process of a *chemical compound layer* as different and not equal. The reasons for this seem to be rather obvious.

Firstly, formation of chemical compounds is typical of the elements strongly differing by their physical and chemical properties including atomic radii and melting points. In view of these differences, equal diffusivities of the components in a growing compound layer could hardly be expected.

Secondly, chemical compounds are ordered phases. Though nature often allows some degree of disorder, each of the components of any chemical compound is free to move on its own sublattice. There are therefore no reasonable grounds to assume that the speeds of such a movement are equal for both components of any compound including intermetallics. Note that in this respect solid solutions of the interstitial type are more similar to chemical compounds than to substitutional solid solutions.

In the light of this short consideration, it appears obvious that different diffusional contributions, for example, of nickel and bismuth to the growth process of the $NiBi_3$ layer (see Section 2.5) must by no means be regarded as a manifestation of the Kirkendall effect. Moreover, in this and similar systems the Kirkendall effect is in principle unobservable since the intermetallic compounds have no range of homogeneity. To reveal this effect, an intermetallic phase must be taken in the form of its two pieces differing by their composition, as shown in Fig. 2.15c. With intermetallics like CoTi, NiAl, $ReAl_4$, $MoIr_3$, *etc*., having relatively wide ranges of homogeneity, such experiments are quite feasible.

2.6.3: Ratio of reaction- and self-diffusion coefficients

Let us now continue an analysis of the interrelation between the reaction- and self-diffusion coefficients. It is obvious that a mere re-calculation using equation (2.59) and substituting into its denominator the total content, c_A, of component A in the chemical compound instead of the concentration difference Δc_A, can hardly produce close values, for example, of the diffusion coefficient of aluminium in the growing Fe_2Al_5 layer on the one hand and in the non-growing one on the other because in this case $c_A/\Delta c_A \approx 20$ [16].

Therefore, the primary contribution to the difference observed in practice appears to arise from the relatively small number of vacancies in non-growing compounds. Note that in non-growing stoichiometric compounds these are mainly thermal. Their relative amount is known to be 10^{-1}-10^{-3} at temperatures close to the melting point of a compound and 10^{-6}-10^{-11} at room temperature (see, for example, Refs [21, 44]).

Seeing at these very small figures on the one hand and at very large values of the ratio of the reaction- to self-diffusion coefficient, like those presented in Table 2.4, on the other, it only remains to assume that the relation [16]

$$\frac{D}{c_v} = \text{const} \tag{2.70}$$

must hold for the components of a given compound, at least to a first approximation.

Table 2.4. Ratios between the reaction- and self-diffusion coefficients for some oxides with the predominant oxygen diffusion at a temperature of 1000 °C, calculated using the experimental data from the book by P. Kofstad [28]

Oxide	SiO_2	ZrO_2	UO_2
$D_O^{(rd)} = k_1$ (m^2 s^{-1})	1.3×10^{-16}	1.7×10^{-13}	1.6×10^{-12}
$D_O^{(sd)}$ (m^2 s^{-1})	1.3×10^{-22}	2.2×10^{-16}	1.6×10^{-15}
$D_O^{(rd)} : D_O^{(sd)}$	1.0×10^{6}	0.8×10^{3}	1.0×10^{3}

When normalised per unit vacancy concentration using the equation

$$\left(\frac{D}{c_v}\right)_{\text{growing compound}} = \left(\frac{D}{c_v}\right)_{\text{non-growing compound}} \tag{2.71}$$

the reaction- and self-diffusion coefficient of any component of a chemical compound may therefore be expected to become close, if not identical, under similar experimental conditions, as it should be from a physical viewpoint.

When applying this relationship, one must be aware of (*i*) all diffusion mechanisms operative in a non-growing compound, (*ii*) the concentration of vacancies of a given component in the solid layer of this compound and (*iii*) the value of its self-diffusion coefficient associated with the vacancy mechanism. In view of the lack of specially planned experiments aimed at obtaining all necessary data for the same compound, including reaction- and self-diffusion coefficients of its components, only evaluations based on the results compiled from several works are at present possible.

The accuracy of such calculations is not too high due mainly to the poor reproducibility of experimental data, especially of the values of the self-diffusion coefficients. As the vacancy concentration in a non-growing compound is strongly dependent upon preparation conditions, presence of impurities and thermal pre-treatment of its sample, the data of different authors, though self-consistent and almost always claimed to be accurate to within ±10% or so, are hardly comparable, with the difference in self-diffusion coefficients reaching a few orders of magnitude. In this respect, the situation with the reaction-diffusion coefficients (diffusional constants) is much more favourable. Against the background of the huge amount of reaction-produced vacancies, the amount of thermal ones as well as those connected with the non-stoichiometry, if not too large, of a compound is negligibly small and has practically no influence on the layer-growth kinetics. Therefore, for any compound, experimental values of the reaction-diffusion coefficients are in general much more accurate than those of the self-diffusion coefficients.

In the case of non-stoichiometric compounds, the vacancy concentration is mainly associated with their degree of deficiency [28, 45]. When comparing the reaction- and self-diffusion coefficients of iron cations in $Fe_{3-\delta}O_4$, satisfactory results can be obtained simply by setting $c_v \approx 3/4$ for the growing $Fe_{3-\delta}O_4$ phase and $c_v \approx \delta$ for the non-growing one. The value of δ characterizing the cation deficiency of the crystal structure of this phase is known to be around 1.0×10^{-2} [28, 45], considerably higher than the concentration of thermal vacancies. The $Fe_{3-\delta}O_4$ layer grows mainly at the expense of diffusion of iron cations. The value of their reaction-diffusion coefficient determined from the $Fe_{3-\delta}O_4$ parabolic-growth kinetics is just two orders of magnitude greater than the value of the self-diffusion coefficient of iron cations in the non-growing compound. It means that equation (2.71) may reasonably be expected to produce a fair agreement between the values of reaction- and self-diffusion coefficients.

To accurately verify the proposed relations, further experimental work is badly needed. It must include

(*i*) choice of a chemical compound with a sufficiently wide range of homogeneity. If a binary system is multiphase, the compound should be the first to occur and grow at the *A–B* interface, while the other compounds should be missing. It is desirable that the stoichiometric composition be located near the middle of the range of homogeneity of the compound.

(*ii*) separate determination of the reaction-diffusion coefficients (diffusional constants) for both components of the compound from the parabolic layer-growth kinetic relationships, as discussed in Section 2.4.3. Comparable values of these constants are clearly desired.

(*iii*) measurement of self-diffusion coefficients of both components in a sample of that compound taken alone using radioactive tracers, with the simultaneous determination of the concentration of the vacancies.

The tracer technique is based on the measurement of concentration or activity of a radioactive element, deposited initially onto the surface of a solid sample, in different sections of the sample after its diffusion treatment at a chosen temperature for a given period of time. In the case of an infinitely thin sufficiently powerful (not changing essentially its intensity during the time of the experiment) tracer layer of concentration $c_{surface}$ on a semi-infinite sample, the concentration varies with the depth of penetration x and time t as (see, for example, [23]

$$c(x,t) = \frac{c_{surface}}{2(\pi Dt)^{1/2}} \exp(-\frac{x^2}{4Dt}). \qquad (2.72)$$

A typical plot of $c(x,t)$ against x at a fixed time is shown in Fig. 2.21a. If ln $c(x,t)$ is plotted against x^2, a straight line is obtained (Fig. 2.21b), from the slope of which the tracer diffusion coefficient D can readily be evaluated. Examples of experimental plots are provided in Fig. 2.21c and d.

(*iv*) investigation of homogenising the diffusion couple consisting of two samples of the compound with the content of the components equal respectively to the upper and lower limit of its range of homogeneity, as shown in Fig 2.15c. This enables revealing the Kirkendall effect, if sufficiently pronounced, calculation of the integrated diffusion coefficient [48] (for more detail, see Chapter 4) and establishment of its concentration dependence.

Such data would give an impact to further development of the theory of reaction-diffusion kinetics. This should by no means be considered in isolation from the general theory of diffusion. It is essential to remember, however, that any consideration has certain limitations. Therefore, for example, application of Wagner's concept of the integrated diffusion coefficient and Darken's equations to growing compound layers does not seem substantiated. In the case of chemical compounds, such an approach is physically meaningless and produces *fictitious* diffusion coefficients of little scientific and practical value.

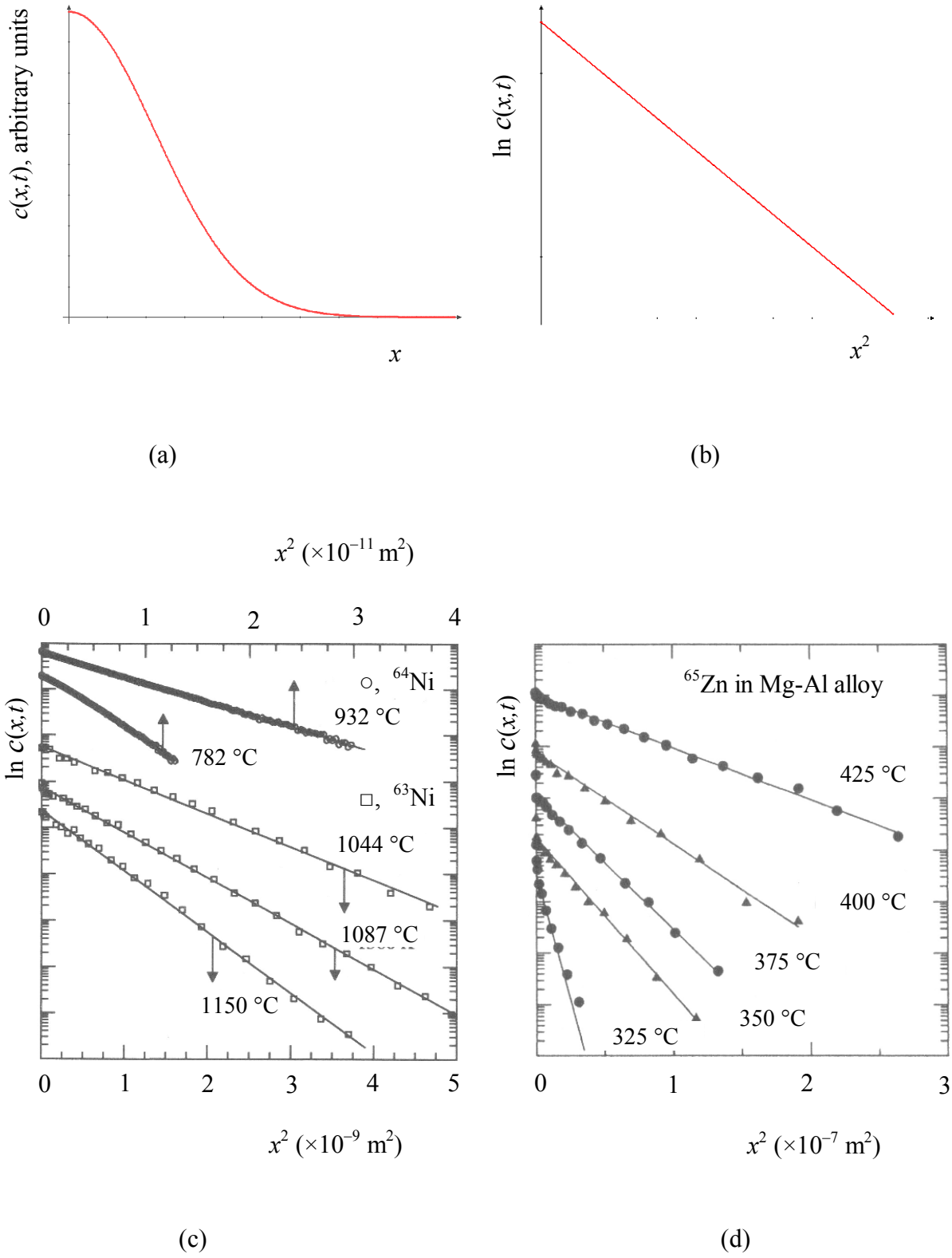

Fig. 2.21. Typical plots of (a) $c(x,t)$ against x and (b) ln $c(x,t)$ against x^2, and examples of experimental penetration profiles for (c) diffusion of ^{63}Ni and ^{64}Ni in NiAl [46]) and (d) diffusion of ^{65}Zn in Mg–Al eutectic alloy [47].

Also, a simple dependence like equation (2.71) can hardly be expected to hold for all chemical compounds without any exceptions under a variety of experimental conditions. The value of the self-diffusion coefficient of any component in the non-growing layer of a chemical compound is known to be strongly affected not only by the amount of vacancies but also by the mode of their formation and interaction with each other, the value of their charge, and other factors. Perhaps, better results might in some cases be obtained using the equation [49, 50]

$$D(c) = D(c_i)\left(\frac{c}{c_i}\right)^{q_v} \tag{2.73}$$

where $D(c)$ and $D(c_i)$ are the values of the diffusion coefficient at the vacancy concentrations c and c_i, respectively, while the exponent q_v is equal to the charge of a vacancy or is its function.

Note that certain care must be taken when using the literature data on the diffusion coefficients for estimating the parameters of technological processes which include the reaction-diffusion process as one of the stages (solid-state synthesis of inorganic compounds, making the composite materials or very-large-scale-integrated circuits for microelectronics, joining the dissimilar metals including welding and brazing, protective coating, corrosion, *etc*.). In view of a wide variety of available (self-diffusion, reaction-diffusion, interdiffusion, intrinsic diffusion, tracer diffusion, chemical diffusion and integrated diffusion) coefficients, not always the choice of a relevant value can be made unambiguously.

It should be emphasised that the main kinetic equations presented in this chapter hold for any mechanism of transfer of the atoms across the bulk of a growing compound layer since the basic assumption “the longer the diffusion path, the greater the time to overcome it” is clearly always fulfilled. Knowledge of the details of this mechanism is only important when establishing a relationship between the transport properties of the layer of a given compound and the diffusion characteristics of its components.

2.7: Single compound layer: comparison of diffusional and physico-chemical approaches

Most essential distinctions between the conventional diffusional approach and the proposed physico-chemical one in the case of solid-state formation of one compound layer are briefly summarised in Table 2.5. A thorough analysis of available experimental and theoretical data provides evidence that the latter is generally more adequate.

For the sake of further visual comparison of the layer-growth mechanism in the case of formation of one, two and multiple compound layers in heterogeneous systems, it would be desirable to remember a schematic diagram of Fig. 2.22 in which a scheme for a homogeneous reaction is also included.

2.8: Interfacial formation of a chemical compound layer: short conclusions

1. The reactants and products of any solid-state heterogeneous reaction exist as non-mixing macroscopic phases (layers) separated from each other by interfaces.

2. Growth of the layer of any chemical compound A_pB_q between two mutually insoluble elementary substances A and B is due to two partial chemical reactions proceeding at its two interfaces, each of which takes place in two consecutive (alternate) steps:

(i) diffusion of atoms of a given component across the bulk of the layer,

(ii) chemical transformations with the participation of these atoms and the surface atoms of another component.

3. Both partial chemical reactions as well as the diffusion fluxes of the components across the bulk of a growing compound layer are assumed to be independent of each other.

4. The layer thickness-time kinetic dependence is in general described by a linear-parabolic equation. Its initial region is close to a straight line, while then there is a gradual transition to a parabola. The higher the temperature, the narrower is the region of linear growth.

5. There are two critical values $x_{1/2}^{(A)}$ and $x_{1/2}^{(B)}$ of the layer thickness, which divide this dependence into the reaction controlled and diffusion controlled regions with regard to components A and B, respectively.

6. For any chemical compound A_pB_q, the reaction-diffusion coefficient and the self-diffusion coefficient of a given component (A or B) are in general different, the former being much greater than the latter.

7. Different diffusional contributions of the components of a chemical compound to the growth process of its layer at the interface between phases A and B should not generally be regarded as a manifestation or result of the Kirkendall effect, the essence of which consists in different diffusivities of the components of a substitutional solid solution.

Table 2.5. Comparison of diffusional and physico-chemical approaches to compound layer-growth kinetics

Diffusional approach	Physico-chemical approach
1. One step: diffusion.	1. Two alternate steps: diffusion and reaction.
2. Layer-growth kinetics are parabolic.	2. Layer-growth kinetics are linear-parabolic.
3. Layer-growth rate is proportional to the width of the range of homogeneity, *HR*, of a given chemical compound.	3. Layer-growth rate depends very slightly upon the width of the range of homogeneity of a given chemical compound.
4. Only a small portion of atoms ($HR << c_{total}$) of a compound is active in the layer-growth process.	4. All available atoms of a compound are active in the layer-growth process.
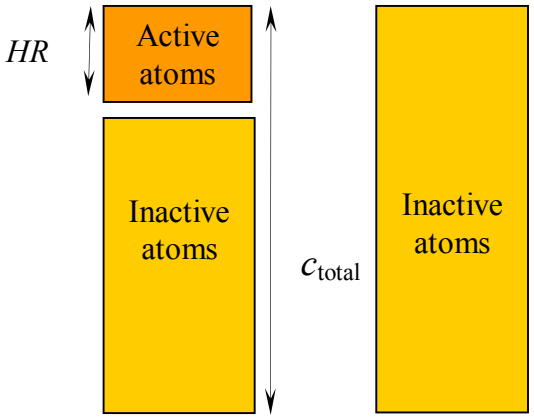	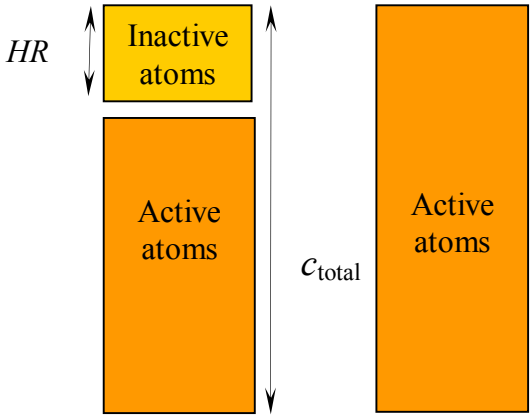
$HR \neq 0$, D is too high	$HR = 0$, D is infinity
$HR \neq 0$, $D \approx k_1$	$HR = 0$, $D = k_1$
5. The *greater* the amount of native structure defects (vacancies) of a compound, the *greater* will be the rate of growth of its layer at the interface of initial substances.	5. The *greater* the amount of native structure defects (vacancies) of a compound, the *less* will be the rate of growth of its layer at the interface of initial substances.

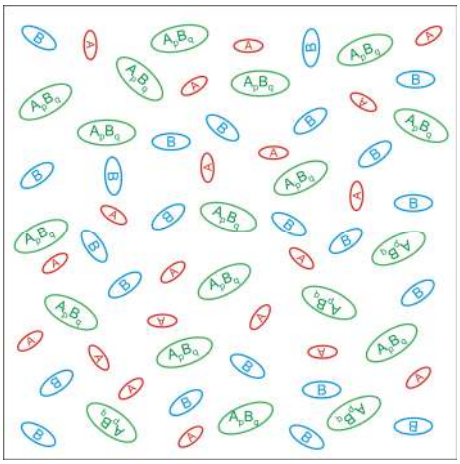

(a)

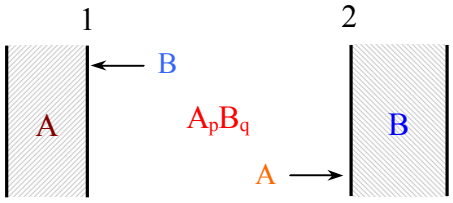

(b)

Fig. 2.22. Schematic diagrams to illustrate the main distinction between (a) homogeneous and (b) heterogeneous chemical reactions of the type $pA + qB = A_pB_q$. Three reacting species A, B and A_pB_q of the homogeneous reaction are intermixed within the reaction volume at the microscopic (molecular) level, while those of the heterogeneous reaction exist as three non-mixing macroscopic phases (layers) separated from each other by interfaces.

3: Growth of two compound layers between elementary substances

Purely diffusional (physical) considerations predict that (*i*) the layers of two compounds available on the *A*–*B* phase diagram must occur between the reactants *A* and *B* simultaneously and (*ii*) the thickness of each of them as well as their total thickness should increase parabolically with passing time. However, available experimental data provide evidence that in most reaction couples the formation of compound layers is sequential rather than simultaneous, while their growth kinetics is not parabolic. Instead, a variety of kinetic laws (linear, asymptotic, paralinear, *etc*.) are observed experimentally. Only a certain portion of the layer thickness-time dependence in the region of long reaction times and hence large layer thicknesses is close to a parabola.

Unambiguous interpretation of these well-known experimental observations in the framework of the diffusional theory is hardly possible. In contrast, from a physico-chemical viewpoint, the phenomena and dependences observed in practice are readily explainable.

To find out a system of two differential equations describing the rate of formation of two solid compound layers at the interface of two elementary substances *A* and *B*, it is necessary:

(*i*) to write down equations of partial chemical reactions taking place at layer interfaces with adjacent phases (there are four such reactions, two for each layer);

(*ii*) to find out relations between the changes in thicknesses of the layers due to those reactions;

(*iii*) to establish mathematical equations relating the differential time dt to the differential changes dx and dy of the layer thicknesses, using the assumption about the summation of the time of diffusion and the time of chemical transformations;

(*iv*) to write down the required general system of differential equations, taking into account the principle of independency of the elementary acts of chemical reactions.

3.1: Partial chemical reactions at layer interfaces

A schematic diagram illustrating the growth process of the layers of two chemical compounds A_pB_q and A_rB_s, with p, q, r and s being positive numbers, at the *A*–*B* interface is shown in Fig. 3.1. Note that the lines showing the concentration profiles of components *A* and *B* in the phases involved into the interaction are parallel to the distance axis since (*i*) formation of the layers of chemical compounds which have no range of homogeneity is considered and (*ii*) initial substances are assumed to be mutually insoluble.

In such a case, immediate application of Fick's equations is clearly impossible. Therefore, it is not surprising that the smooth concentration distributions characteristic of solid solutions

are usually drawn by most theoreticians, while the results obtained are then applied to chemical compounds. Many of them, especially physicists and metallurgists, even do not employ the term *chemical compound*, giving preference to analysing the formation of *a new phase*. No difference is thus made between solid solutions and chemical compounds.

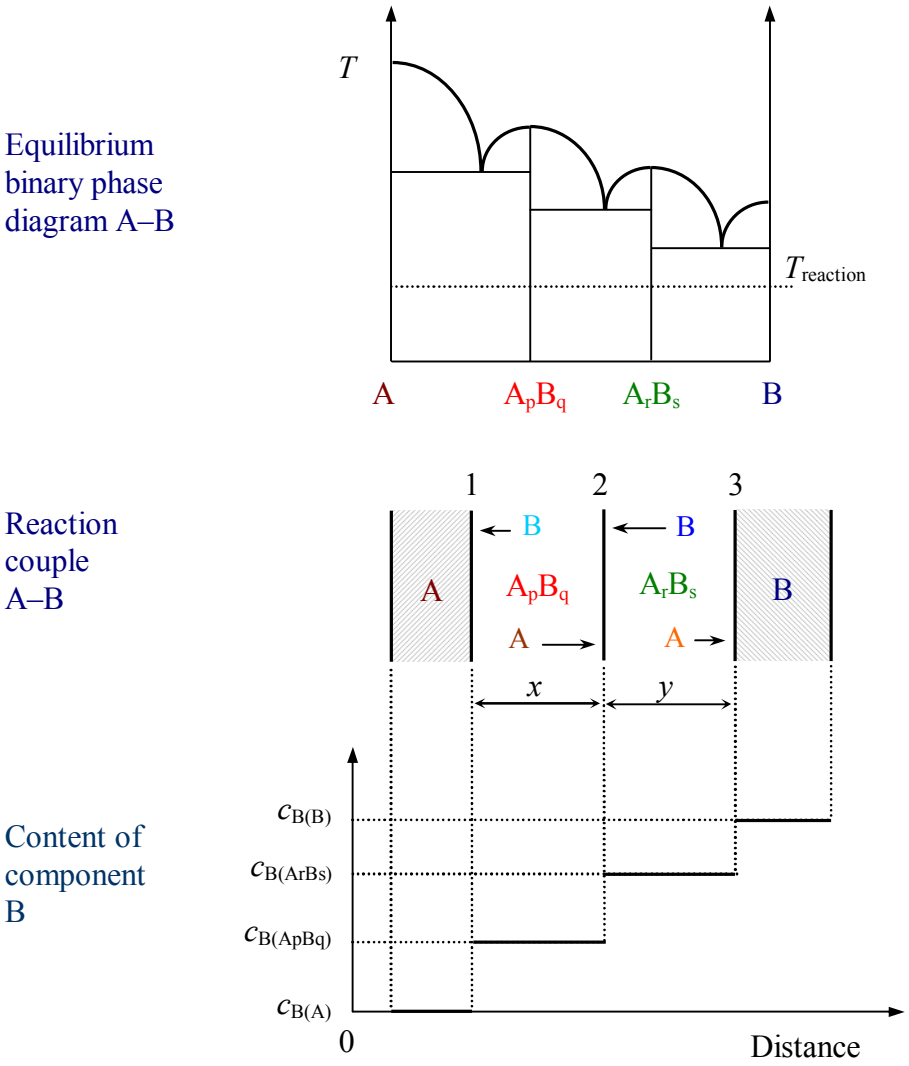

Fig. 3.1. Schematic diagram to illustrate the growth process of the layers of two chemical compounds A_pB_q and A_rB_s at the interface between mutually insoluble elementary substances A and B.

Although in many binary systems there is no clear-cut distinction between a chemical compound and a solid solution, it is nonetheless necessary, as already pointed out in Chapter 1, to distinguish between them on the basis of (*i*) constancy or variability of their composition and (*ii*) degree of ordering their crystal lattices. Also, usually the chemical compound has a crystal lattice different from crystal lattices of parent phases A and B, while the solid solution

has either a similar one or the same. It would be a rough mistake to ignore these differences. As will be seen later, this results in far-reaching misleading conclusions.

Whether a particular phase is a chemical compound or a solid solution can hardly be subject to any doubt in obvious cases such as in the Ni–Bi binary system with the intermetallics NiBi (homogeneity range $HR \leq 0.3$ at.%) and $NiBi_3$ (stoichiometric phase) or in the Ti–Al binary system with the intermetallics Ti_3Al ($HR \approx 12$ at.% at 600 °C), TiAl ($HR \approx 7$ at.%), $TiAl_2$ ($HR \leq 1$ at.%) and $TiAl_3$ (stoichiometric phase).

Definitely, NiBi, $NiBi_3$, $TiAl_2$ and $TiAl_3$ are chemical compounds, not differing, for example, from Bi_2O_3 or TiO_2. Phases like Ti_3Al or TiAl can, of course, be treated ambiguously. This point will be analysed once again in the next chapter.

Also, formation of a solid solution is often considered to be a pre-requisite for the occurrence of a chemical compound layer, with the latter being a result of super-saturation of the former. In fact, however, these are two concurrent, competing processes, if both solid solutions and chemical compounds are present on the phase diagram of a binary system. In any reaction couple *A*–*B* given to itself under conditions of constant temperature and pressure or tending to its equilibrium state from below (from lower to higher temperatures and pressures), no super-saturation is possible.

Clearly, any direct chemical reaction between elementary substances *A* and *B* ceases after the formation of compound layers A_pB_q and A_rB_s a few crystal-lattice units thick, which separate the reacting phases from each other. Subsequently, four partial chemical reactions take place at the layer interfaces. These are as follows:

Layer	Interface	Partial chemical reaction	
A_pB_q	1	$qB_{\text{dif}} + pA_{\text{surf}} = A_pB_q,$	(3.1_1)
	2	$(sp - qr)A_{\text{dif}} + qA_rB_s = sA_pB_q,$	(3.1_2)
A_rB_s	2	$(sp - qr)B_{\text{dif}} + rA_pB_q = pA_rB_s,$	(3.2_1)
	3	$rA_{\text{dif}} + sB_{\text{surf}} = A_rB_s.$	(3.2_2)

The A_pB_q compound layer grows at the expense of diffusion of the *B* atoms to interface 1 where these atoms then enter into reaction (3.1_1) with the surface *A* atoms. It is seen that the same partial chemical reaction takes place at the A–A_pB_q interface in the A–A_pB_q–B (see Section 2.2) and A–A_pB_q–A_rB_s–B heterogeneous systems. The difference between these two systems is that in the former the *B* atoms which have crossed only the bulk of the A_pB_q layer enter into the chemical reaction at interface 1, while in the latter the *B* atoms have to diffuse across the bulks of both layers A_rB_s and A_pB_q before entering into this reaction because the only source of the *B* atoms in both systems is substance *B*.

The thickness of the A_pB_q layer also increases at the expense of diffusion of the A atoms to interface 2 and their subsequent partial chemical reaction with the A_rB_s compound in accordance with equation (3.1_2). Thus, another difference between the A–A_pB_q–B and A–A_pB_q–A_rB_s–B systems is that in the former an increase in thickness of the A_pB_q layer at interface 2 is a result of reaction of the A atoms diffusing across its bulk with phase B, while in the latter with the A_rB_s compound.

Growth of the A_rB_s compound layer is due to both partial chemical reaction (3.2_1) taking place at interface 2 between the diffusing B atoms and the A_pB_q compound and partial chemical reaction (3.2_2) at interface 3 between the diffusing A atoms and the surface B atoms. It must be clear that only the diffusing A atoms which have not entered earlier into reaction (3.1_2) at interface 2 can then enter into reaction (3.2_2) at interface 3.

Note that no reactions proceed within the bulks of both compound layers. Layer bulks only serve as a transport medium for diffusing atoms. Chemical transformations take place exclusively at the phase interfaces that are regarded as transition regions between the interacting phases, whose widths are not very different from the lattice spacing of those phases.

The A_pB_q chemical compound is seen to be a product of reactions (3.1_1) and (3.1_2). At the same time, it is also a reactant of reaction (3.2_1). The A_rB_s chemical compound is a product of reactions (3.2_1) and (3.2_2) and a reactant of reaction (3.1_2). Thus, each of the two compound layers grows not only at the expense of the A and B atoms diffusing from initial phases A and B, but also partly at the expense of an adjacent compound layer. Hence, the change in thickness of the A_pB_q layer is a result of (*i*) growth due to reactions (3.1_1) and (3.1_2) and (*ii*) consumption during the formation of the A_rB_s chemical compound by reaction (3.2_1). Similarly, the A_rB_s layer grows in the course of reactions (3.2_1) and (3.2_2) and is consumed by reaction (3.1_2).

3.2: A system of differential equations describing the rates of formation of two compound layers

During an infinitesimal period of time, dt, the thickness of the A_pB_q layer increases by dx_{B1} at interface 1 as a result of reaction (3.1_1) and by dx_{A2} at interface 2 as a result of reaction (3.1_2), as shown in Fig. 2.2. At the same time, the thickness of the A_rB_s layer increases by dy_{B2} at interface 2 and by dy_{A3} at interface 3 due to reactions (3.2_1) and (3.2_2), respectively.

To establish differential equations relating dt to the increases dx_{B1}, dx_{A2}, dy_{B2} and dy_{A3} in thicknesses of the A_pB_q and A_rB_s layers, use is again made of the assumption about the summation of the time of diffusion of the A or B atoms and the time of subsequent chemical transformations for each of four partial chemical reactions taking place at phase interfaces 1, 2 and 3. It yields

$$\mathrm{d}t = \mathrm{d}t_{\mathrm{dif}}^{(B\to A_pB_q)} + \mathrm{d}t_{\mathrm{chem}}^{(B\to A_pB_q)}, \qquad (3.3_1)$$

$$dt = dt_{dif}^{(A\rightarrow A_pB_q)} + dt_{chem}^{(A\rightarrow A_pB_q)}, \qquad (3.3_2)$$

$$dt = dt_{dif}^{(B\rightarrow A_rB_s)} + dt_{chem}^{(B\rightarrow A_rB_s)}, \qquad (3.4_1)$$

$$dt = dt_{dif}^{(A\rightarrow A_rB_s)} + dt_{chem}^{(A\rightarrow A_rB_s)}, \qquad (3.4_2)$$

where the superscripts of the type $(B\rightarrow A_pB_q)$ in equation (3.3_1) indicate that such a time is required for the diffusion of the B atoms across the bulk of the A_pB_q layer (first term) or for subsequent chemical transformations with their participation (second term).

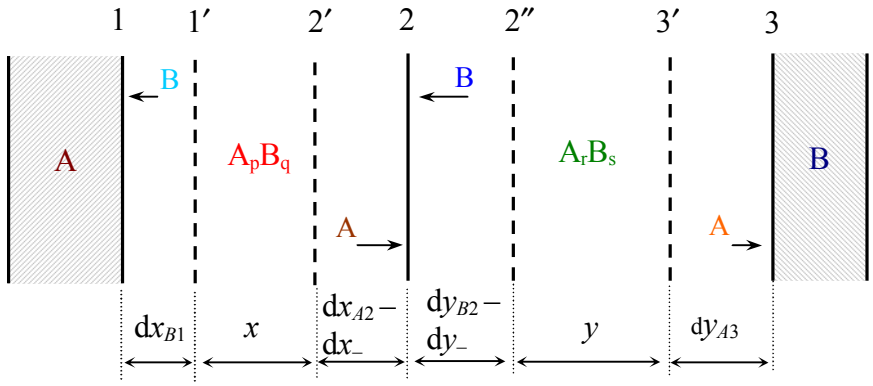

Fig. 3.2. Schematic diagram to illustrate the changes dx_{B1}, dx_{A2}, dy_{B2}, dy_{A3}, dx_{-} and dy_{-} in thicknesses of the A_pB_q and A_rB_s compound layers during the time dt in the general case where both layers grow at the expense of diffusion of both components across their bulks.

Like the case of formation of the layer of a single chemical compound, it is assumed that the time of diffusion is directly proportional to both the increase of the thickness of a given compound layer and its total thickness, whereas the time of chemical transformations is directly proportional to the increase of the thickness of the layer and is independent of its total thickness (see Section 2.3). Hence,

$$dt = \left(\frac{x}{k_{1B1}} + \frac{1}{k_{0B1}}\right)dx_{B1}, \qquad (3.5_1)$$

$$dt = \left(\frac{x}{k'_{1A2}} + \frac{1}{k'_{0A2}}\right)dx_{A2}, \qquad (3.5_2)$$

$$\mathrm{d}t = \left(\frac{y}{k'_{1B2}} + \frac{1}{k'_{0B2}} \right) \mathrm{d}y_{B2}, \qquad (3.6_1)$$

$$\mathrm{d}t = \left(\frac{y}{k_{1A3}} + \frac{1}{k_{0A3}} \right) \mathrm{d}y_{A3}, \qquad (3.6_2)$$

where all k_0 are chemical constants, while all k_1 are physical (diffusional) constants.

The designations with strokes were only introduced to avoid confusion with the results of Chapter 2. Partial chemical reactions at interface 1 are the same in the A–A_pB_q–B and A–A_pB_q–A_rB_s–B systems, whereas at interface 2 these are different. Therefore, equations (2.6) and (3.5_1) are identical, while equations (2.21) and (3.5_2) are different.

Note that not only k'_{0A2} is not equal to k_{0A2}, but also k'_{1A2} is not equal to k_{1A2}, although the diffusion coefficient of the A atoms across the bulk of the A_pB_q layer does not depend on whether this layer borders phase B or A_rB_s. However, different amounts of the diffusing A atoms are necessary to form one molecule of the A_pB_q chemical compound by reactions (2.2) and (3.1_2). In Section 2.4 k_{1A2} was used to denote the physical (diffusional) constant relating to reaction (2.2). From equations (2.2) and (3.1_2), it follows

$$k'_{1A2} = \frac{sp}{sp - qr} k_{1A2}. \qquad (3.7)$$

Relations between different constants will be considered in greater detail, when comparing the growth rates of the same chemical compound layer in various reaction couples of a multiphase binary system (Chapter 4).

On the basis of the principle of independency of the rates of elementary acts of chemical reactions, equations (3.5_1)-(3.6_2) are assumed to be independent of each other. Therefore, the increases of layer thicknesses can explicitly be expressed from these equations as follows

$$\mathrm{d}x_{B1} = \frac{k_{0B1}}{1 + \dfrac{k_{0B1}x}{k_{1B1}}} \mathrm{d}t, \qquad (3.8_1)$$

$$\mathrm{d}x_{A2} = \frac{k'_{0A2}}{1 + \dfrac{k'_{0A2}x}{k'_{1A2}}} \mathrm{d}t, \qquad (3.8_2)$$

$$\mathrm{d}y_{B2} = \frac{k'_{0B2}}{1 + \dfrac{k'_{0B2}y}{k'_{1B2}}} \mathrm{d}t, \qquad (3.9_1)$$

$$dy_{A3} = \frac{k_{0A3}}{1 + \frac{k_{0A3}y}{k_{1A3}}} dt. \qquad (3.9_2)$$

The increase in thickness of the A_pB_q layer during the time dt is

$$dx_+ = dx_{B1} + dx_{A2}, \qquad (3.10)$$

while that of the A_rB_s layer is

$$dy_+ = dy_{B2} + dy_{A3}. \qquad (3.11)$$

During the same period of time, dt, the thickness of the A_pB_q layer decreases by dx_- due to partial chemical reaction (3.2$_1$). The value of this decrease can easily be found using equation (3.2$_1$). Calculations are like conventional ones generally accepted for chemical reactions. The only difference is that the diffusing component must be written in equations (1.48), (1.49), (3.1$_1$)-(3.2$_2$) in that form (atom, ion, *etc*.) in which it diffuses across the bulks of growing compound layers and then reacts at an appropriate phase interface and not in the form in which it exists in an initial substance. Consider a few examples.

The process of growth of the Cu_3Sn and Cu_6Sn_5 intermetallic layers in the Cu–Cu_3Sn–Cu_6Sn_5–Sn system can be represented as follows:

Layer	Interface	Partial chemical reaction	
Cu_3Sn	Cu–Cu_3Sn	$Sn_{dif} + 3Cu_{surf} = Cu_3Sn$,	(3.12$_1$)
	Cu_3Sn–Cu_6Sn_5	$9Cu_{dif} + Cu_6Sn_5 = 5Cu_3Sn$,	(3.12$_2$)
Cu_6Sn_5	Cu_6Sn_5–Cu_3Sn	$3Sn_{dif} + 2Cu_3Sn = Cu_6Sn_5$,	(3.13$_1$)
	Cu_6Sn_5–Sn	$6Cu_{dif} + 5Sn_{surf} = Cu_6Sn_5$.	(3.13$_2$)

In this obvious case, there is no ambiguity in writing partial chemical reactions. It can only be noted that the copper and tin ions, not atoms, are most likely to diffuse across the growing Cu_3Sn and Cu_6Sn_5 intermetallic layers, whereas electrons simply accompany them, so that the final result is such, as if the atoms were the diffusing species. For formal kinetic considerations, such details of the mechanism of atomic transfer are clearly of little importance.

A somewhat different situation arises in the case of formation of the TiO and TiO_2 layers in the Ti–TiO–TiO_2–O_2 reaction system. Most probably, oxygen and titanium diffuse across layer bulks in the form of ions or atoms, whereas in the initial gaseous phase oxygen exists in

the form of molecules O_2. Therefore, the partial chemical reactions taking place at phase interfaces must be written as follows:

Layer	Interface	Partial chemical reaction	
TiO	Ti–TiO	$O_{dif} + Ti_{surf} = TiO,$	(3.14_1)
	TiO–TiO_2	$Ti_{dif} + TiO_2 = 2TiO,$	(3.14_2)
TiO_2	TiO_2–TiO	$O_{dif} + TiO = TiO_2,$	(3.15_1)
	TiO_2–O_2 (gas)	$Ti_{dif} + 2O_{surf} = TiO_2,$	(3.15_2)

but not as

$$2Ti + O_2 = 2TiO \qquad (3.16)$$

and

$$2TiO + O_2 = 2TiO_2. \qquad (3.17)$$

The last two reactions may proceed if very porous layers are formed, not preventing the Ti and TiO surfaces from the direct oxygen attack. However, if the oxide layers are compact and have no macroscopic defects, oxygen can only diffuse across their bulks after its molecules have dissociated into atoms or ions onto the surface of the TiO_2 layer bordering the gaseous phase. Clearly, the time of dissociation of the O_2 molecules into atoms is independent of the thickness of the TiO_2 layer. Therefore, it must be included into the value of the chemical constant corresponding to partial chemical reaction (3.15_2).

If initial phases are chemical compounds, not elementary substances, the growth of the layers of two new chemical compounds in a quasi-binary system takes place as a result of counter diffusion of the same-type ions or atoms of smaller size. The common ion usually does not take active part in the layer-growth process. This does not mean, however, that its presence exerts no influence on the mechanism of formation of the layers. The Rb_2AgI_3 and $RbAg_4J_5$ layers are known to form in the RbI–AgI system [51-53]. Their formation is due to the following partial chemical reactions:

Layer	Interface	Partial chemical reaction	
Rb_2AgI_3	RbI–Rb_2AgI_3	$Ag^+ + 3RbI = Rb_2AgI_3 + Rb^+,$	(3.18_1)
	Rb_2AgI_3–$RbAg_4J_5$	$7Rb^+ + 3RbAg_4J_5 = 5Rb_2AgI_3 + 7Ag^+,$	(3.18_2)
$RbAg_4J_5$	$RbAg_4J_5$–Rb_2AgI_3	$7Ag^+ + 5Rb_2AgI_3 = 3RbAg_4J_5 + 7Rb^+,$	(3.19_1)
	$RbAg_4J_5$–AgJ	$Rb^+ + 5AgJ = RbAg_4J_5 + Ag^+.$	(3.19_2)

It can easily be seen that the total yield of partial chemical reactions (3.18_2) and (3.19_1) is zero. This is caused by the presence of the third, low-mobile component (iodine anions I^-). Because of their presence, rubidium and silver cations are unable to move in the lattices of the growing Rb_2AgI_3 and $RbAg_4J_5$ compounds independently of each other. The fluxes of these cations should necessarily be balanced since partial chemical reactions (3.18_1) and (3.19_2) are mutually dependent. In this respect, the system under consideration and other similar systems differ from binary ones in which all four partial chemical reactions taking place at layer interfaces are independent of each other unless any diffusional constraints arise (see the next chapter).

Thus, the increase in thickness of the Rb_2AgI_3 layer is due to partial chemical reaction (3.18_1), while that of the $RbAg_4J_5$ layer to partial chemical reaction (3.19_2). The overall reaction is the sum of these two partial chemical reactions:

$$3RbI + 5AgJ = Rb_2AgI_3 + RbAg_4J_5. \qquad (3.20)$$

Formally, the final result is such, as if the initial phases RbI and AgI reacted immediately, although they have no direct contact. Similar reactions are likely to take place during the interaction of metal oxides and other chemical compounds.

Let us now return to analysing the process of growth of the A_pB_q and A_rB_s compound layers at the interface between elementary substances A and B. From equation (3.2_1), it follows that the ratio of the mass of the A_pB_q compound entering into partial chemical reaction (3.2_1) to the mass of the A_rB_s compound formed as a result of this reaction is equal to the ratio of the molecular masses of the compounds A_pB_q and A_rB_s with the factors r and p, respectively:

$$\frac{m_{A_pB_q}}{m_{A_rB_s}} = \frac{rM_{A_pB_q}}{pM_{A_rB_s}}, \qquad (3.21)$$

where m is the mass and M is the molecular mass of an appropriate compound. This is a conventional chemical relation.

The mass is equal to the product of the density, ρ, and the volume which in turn is the product of the surface area of the phase interface and the thickness of the growing layer. Since the surface area of the interfaces between all the reacting phases is assumed to be the same and constant during the whole course of layer growth, then

$$\frac{\rho_{A_pB_q}\,dx_-}{\rho_{A_rB_s}\,dy_{B2}} = \frac{rM_{A_pB_q}}{pM_{A_rB_s}}. \qquad (3.22)$$

Taking into account that the quotient of dividing the molecular mass by the density of a given compound is its molar volume, V, one obtains

$$\mathrm{d}x_{\_} = \frac{rg}{p}\mathrm{d}y_{B2}, \tag{3.23}$$

where g stands for the ratio of the molar volumes of chemical compounds A_pB_q and A_rB_s: $g = V_{A_pB_q} / V_{A_rB_s}$.

Similarly, from equation (3.1_2), one finds

$$\mathrm{d}y_{\_} = \frac{q}{sg}\mathrm{d}x_{A2}. \tag{3.24}$$

Equations (3.23) and (3.24) take account of the mutual consumption of the A_pB_q and A_rB_s layers during their simultaneous formation.

The total change in thickness of the A_pB_q layer during the time dt is equal to the difference between the right-hand parts of equations (3.10) and (3.23):

$$\mathrm{d}x = \mathrm{d}x_{B1} + \mathrm{d}x_{A2} - \mathrm{d}x_{\_}\ . \tag{3.25}$$

For the A_rB_s layer, this value is (see equations (3.11) and (3.24))

$$\mathrm{d}y = \mathrm{d}y_{B2} + \mathrm{d}y_{A3} - \mathrm{d}y_{\_}\ . \tag{3.26}$$

Substituting the expressions (3.8_1)-(3.9_2) for the increases in thicknesses of the A_pB_q and A_rB_s compound layers into these equations yields the required general system of two differential equations describing their growth rates at the A–B interface:

$$\frac{\mathrm{d}x}{\mathrm{d}t} = \frac{k_{0B1}}{1+\dfrac{k_{0B1}x}{k_{1B1}}} + \frac{k'_{0A2}}{1+\dfrac{k'_{0A2}x}{k'_{1A2}}} - \frac{rg}{p}\,\frac{k'_{0B2}}{1+\dfrac{k'_{0B2}y}{k'_{1B2}}}, \tag{3.27_1}$$

$$\frac{\mathrm{d}y}{\mathrm{d}t} = \frac{k'_{0B2}}{1+\dfrac{k'_{0B2}y}{k'_{1B2}}} + \frac{k_{0A3}}{1+\dfrac{k_{0A3}y}{k_{1A3}}} - \frac{q}{sg}\,\frac{k'_{0A2}}{1+\dfrac{k'_{0A2}x}{k'_{1A2}}}. \tag{3.27_2}$$

The system of equations (3.27) belongs to the autonomous ones that have been analysed in detail, for example, in Refs [54, 55]. Note, however, that, to avoid misleading conclusions concerning layer-growth kinetics, an approach to its solution should by no means be merely mathematical. Namely, besides the initial conditions $x = 0$ and $y = 0$ at $t = 0$, the existence of the critical values of the thicknesses of the A_pB_q and A_rB_s compound layers must necessarily be taken into account. These are as follows (see equations (2.17) and (2.22) of Chapter 2):

$$x_{1/2}^{(B)} = \frac{k_{1B1}}{k_{0B1}}, \qquad (3.28_1)$$

$$x_{1/2}^{(A)} = \frac{k'_{1A2}}{k'_{0A2}}, \qquad (3.28_2)$$

$$y_{1/2}^{(B)} = \frac{k'_{1B2}}{k'_{0B2}}, \qquad (3.29_1)$$

$$y_{1/2}^{(A)} = \frac{k_{1A3}}{k_{0A3}}. \qquad (3.29_2)$$

They divide the $x - t$ and $y - t$ kinetic dependences into the reaction controlled and diffusion controlled regions with regard to components A and B (in the theoretical definition given in Section 2.3.2 of Chapter 2).

It should be emphasised that, according to the designations accepted throughout the book, the plus sign only indicates an increase of the thickness of an appropriate compound layer, while the minus sign indicates its decrease and not the direction of movement of the interfaces of this layer with adjacent phases relative to some fixed frame of reference. Therefore, the quantities, for example, dx_{B1} and dx_{A2} were taken with the plus sign, although interfaces 1 and 2 (see Fig. 3.1) move in the opposite directions during the course of reactions (3.1_1) and (3.1_2).

Clearly, in such a case x and y correspond to the experimentally measured values of thicknesses of the A_pB_q and A_rB_s compound layers. This form of writing mathematical equations also makes it possible to easily take account of a change in volume of the system resulting from the formation of chemical compounds, which in many cases is too considerable to be neglected without a noticeable error.

The system of equations (3.27) is seen to be rather complicated. Its solution, if obtainable at all in quadratures, must probably be even more complicated. However, in experiments certain conditions which enable the initial equations to be simplified are usually fulfilled. Consider limiting cases of particular interest from both theoretical and practical view-points. The process of growth of the A_pB_q and A_rB_s layers will be analysed following its development with increasing time from the start of interaction of initial substances A and B up to the

establishment of equilibrium at which, according to the Gibbs phase rule no more than two phases should remain in any two-component system at constant temperature and pressure.

3.3: Initial linear growth of the A_pB_q and A_rB_s layers

Evidently, in an initial period of interaction of substances A and B when the thicknesses of the A_pB_q and A_rB_s layers are relatively small, the conditions $k_{0B1} << k_{1B1}/x$, $k'_{0A2} << k'_{1A2}/x$, $k'_{0B2} << k'_{1B2}/y$ and $k_{0A3} << k_{1A3}/y$ are satisfied. Hence, at low t the terms of the type k_0x/k_1 and k_0y/k_1 can be neglected in comparison with unity. Therefore, the system of equations (3.27) is simplified to

$$\frac{\mathrm{d}x}{\mathrm{d}t} = k_{0B1} + k'_{0A2} - \frac{rg}{p}k'_{0B2}, \qquad (3.30_1)$$

$$\frac{\mathrm{d}y}{\mathrm{d}t} = k'_{0B2} + k_{0A3} - \frac{q}{sg}k'_{0A2}. \qquad (3.30_2)$$

Integration with initial conditions $x = 0$ and $y = 0$ at $t = 0$ yields

$$x = \left(k_{0B1} + k'_{0A2} - \frac{rg}{p}k'_{0B2}\right)t, \qquad (3.31_1)$$

$$y = \left(k'_{0B2} + k_{0A3} - \frac{q}{sg}k'_{0A2}\right)t. \qquad (3.31_2)$$

The systems of equations (3.30) and (3.31) describe the reaction controlled stage of growth of the A_pB_q and A_rB_s compound layers, where the rates of diffusion of the atoms across layer bulks are so high that their effect on the overall rates of formation of the layers is negligible in comparison with that of the rates of chemical transformations taking place at phase interfaces. This is that case in which the purely chemical processes are rate-determining (chemical control), for there is a great excess of diffusing atoms of both kinds for both layers to grow.

It does not mean, however, that under such circumstances the A_pB_q and A_rB_s compound layers must necessarily occur at the A–B interface simultaneously. Clearly, their simultaneous occurrence is only possible if the derivatives $\mathrm{d}x/\mathrm{d}t$ and $\mathrm{d}y/\mathrm{d}t$ in equations (3.30) are positive ($\mathrm{d}x/\mathrm{d}t > 0$ and $\mathrm{d}y/\mathrm{d}t > 0$), and consequently the inequalities $k_{0B1} + k'_{0A2} > (rg/p)k'_{0B2}$ and $k'_{0B2} + k_{0A3} > (q/sg)k'_{0A2}$ are satisfied. In such a case, both layers can grow simultaneously from the very start of interaction of phases A and B according to the linear law (3.31), as

illustrated in Fig. 3.3a. Note that they will grow at the highest rates possible under given (constant) temperature-pressure conditions.

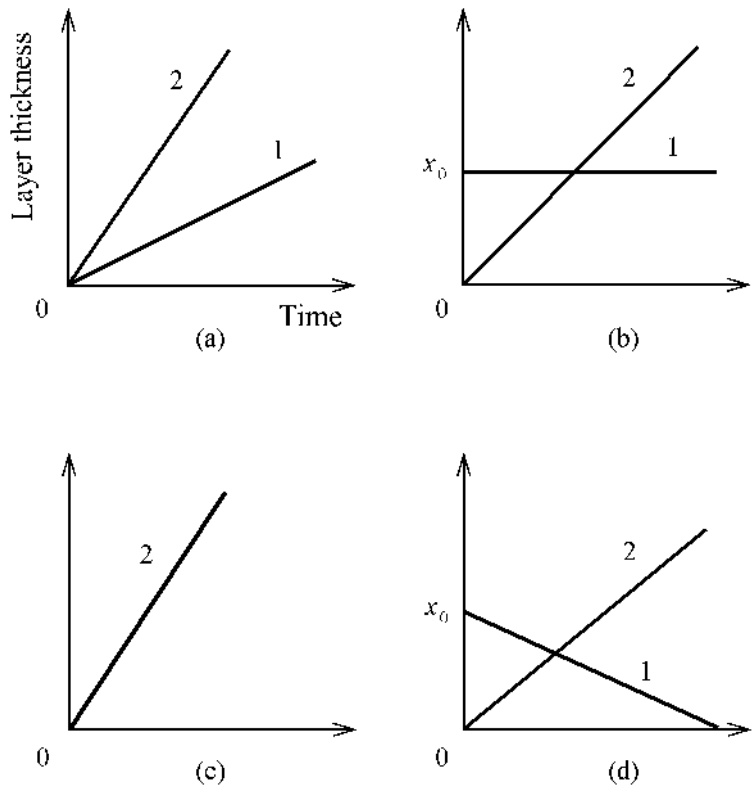

Fig.3.3. Initial stage of formation of the A_pB_q (line 1) and A_rB_s (line 2) compound layers in the course of interaction of elementary substances A and B. (a) Both layers grow simultaneously in accordance with the linear law; (b) thickness of the A_pB_q layer remains constant, while the A_rB_s layer grows linearly; (c) the A_pB_q layer is missing, and only the A_rB_s layer is formed; (d) thickness of the A_pB_q layer decreases until it disappears completely, while the A_rB_s layer grows linearly.

If $k_{0B1} + k'_{0A2} = (rg / p)k'_{0B2}$, then d$x$/d$t$ = 0. This corresponds to the stationary state where the rate of growth of the A_pB_q layer due to partial chemical reactions (3.1_1) and (3.1_2) is equal to the rate of its consumption in the course of formation of the A_rB_s layer by reaction (3.2_1). If the A_pB_q layer were in the initial specimen A–B, then its thickness would remain constant (Fig. 3.3b). At the same time, the A_rB_s layer continues to grow linearly.

If the condition

$$k_{0B1} + k'_{0A2} < \frac{rg}{p} k'_{0B2} \qquad (3.32)$$

is satisfied, the A_pB_q layer cannot form at all ($dx/dt < 0$). Therefore, only the A_rB_s layer will be observed to grow at the A–B interface (Fig. 3.3c). If the A_pB_q layer were in the initial specimen A–B, then its thickness would decrease, and it might eventually disappear completely (Fig. 3.3d). In this case, the A_pB_q compound layer is kinetically unstable since the decrease in its thickness due to the consumption during growth of the A_rB_s layer exceeds the increase due to reactions (3.1_1) and (3.1_2).

From the system of equations (3.30), it follows that the thickness of the A_rB_s layer remains constant or equal to zero if $k'_{0B2} + k_{0A3} = (q/sg)k'_{0A2}$. If the inequality

$$k'_{0B2} + k_{0A3} < \frac{q}{sg} k'_{0A2} \tag{3.33}$$

is satisfied, the A_rB_s layer is missing at the A_pB_q–B interface as kinetically unstable. If present initially, it would be prone to full degradation with passing time.

In cases where the manufacturing technology includes the deposition of the layers of chemical compounds (intermetallics, silicides, oxides, *etc*.) onto a solid substrate and their subsequent annealing as, for example, in fabricating very-large-scale-integrated circuits for microelectronics, their probable kinetic instability in contact with parent and other phases should necessarily be taken into account. Otherwise, during service compound layers will gradually degrade, and this may lead to undesirable consequences, especially in the case of thicknesses of several tens of nanometres. Their long-term stability may prove to be insufficient even at room temperature.

Clearly, in the framework of the proposed physico-chemical approach, it is impossible to predict theoretically the values of chemical constants k_0 for each particular reaction couple A–B. This limitation is known to be characteristic of any phenomenological consideration. Therefore, the inverse task is exercised in practice, namely, the experimentally established kinetic dependences $x - t$ and $y - t$ are employed to calculate appropriate constants.

Note that the kinetic data must necessarily be supplemented by measurements of the displacement of phase interfaces relative to inert markers located within the bulks of growing A_pB_q and A_rB_s layers (Fig. 3.4). Otherwise, it is impossible to find out all four chemical constants, k_{0B1}, k'_{0A2}, k'_{0B2} and k_{0A3}, from the system (3.30) containing only two equations.

To determine the values of the chemical constants, initial linear portions of the plots of layer thicknesses against time, where $x << x_{1/2}^{(B)}$, $x << x_{1/2}^{(A)}$, $y << y_{1/2}^{(B)}$ and $y << y_{1/2}^{(A)}$, must be investigated. By measuring the distance from a marker located inside the A_pB_q layer to the former A–A_pB_q interface 1′ prior to annealing the A–A_pB_q–A_rB_s–B reaction couple and then to its new position 1 after its isothermal annealing during a certain time Δt, one can calculate a value of the chemical constant k_{0B1} from the equation $k_{0B1} = \Delta x_{B1}/\Delta t$.

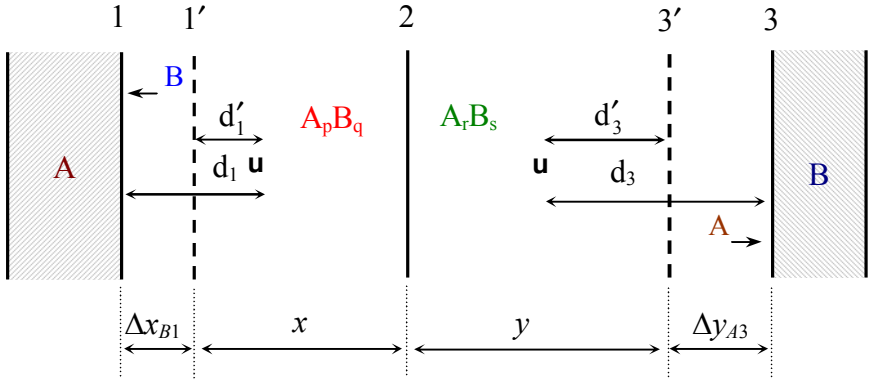

Fig.3.4. Schematic diagram to explain one of the methods of determining the values of the chemical constants k_0 in the system A–A_pB_q–A_rB_s–B. $\Delta x_{B1} = d_1 - d_1'$, $\Delta y_{A3} = d_3 - d_3'$. To simplify the figure, displacement of interface 2 during layer formation is not shown.

Similarly, by measuring the distance from a marker located inside the A_rB_s layer to the former position of the A_rB_s–B interface 3′ and to its new position 3, a value of the chemical constant k_{0A3} is determined from the equation $k_{0A3} = \Delta y_{A3} / \Delta t$. Having obtained the constants k_{0B1} and k_{0A3}, the values of the constants k'_{0B2} and k'_{0A2} can readily be found. In doing so, it is preferable to employ the system of equations (3.31) instead of (3.30) since the total thickness of any compound layer at a certain time t is always measured at a higher accuracy than its increase during Δt.

After measuring the thicknesses of the A_pB_q and A_rB_s layers grown in time t_i, the values of k'_{0B2} and k'_{0A2} are calculated from the system of two algebraic equations with two unknowns

$$k'_{0A2} - \frac{rg}{p} k'_{0B2} = \left(\frac{x}{t} \right)_{t=t_i} - k_{0B1} , \qquad (3.34_1)$$

$$k'_{0B2} - \frac{q}{sg} k'_{0A2} = \left(\frac{y}{t} \right)_{t=t_i} - k_{0A3} . \qquad (3.34_2)$$

The required quantities p, q, r, s and g become known if the phase identity and chemical compositions of growing compound layers as well as the pyknometric and X-ray density of the compounds were determined experimentally.

It should be noted that the separate determination of the chemical constants is yet *terra incognita* because of experimental difficulties associated with putting inert markers and measuring layer thicknesses in very thin films (some tens to some hundreds of nanometres thick). Much work is still to be done in this field.

It must be quite clear that in the vast majority of binary systems with two chemical compounds on equilibrium phase diagrams both layers can hardly be expected to occur at the *A–B* interface simultaneously. Rather, their formation will be sequential. This immediately follows even from a formal probability consideration.

Indeed, of three possible combinations of the signs (+,+; +,–; –,+) of the derivatives dx/dt and dy/dt in equations (3.30), there are two cases of different signs, in which one of the layers is lacking, and only one case of the same sign, in which both layers occur and grow simultaneously from the very beginning of interaction of initial substances *A* and *B*. Hence, if a number of binary systems are considered, the probability of simultaneous formation of two compound layers in any particular reaction couple *A–B* is one-third.

In fact, it is far less in view of too many physico-chemical conditions to be satisfied to make their simultaneous occurrence possible. Therefore, one of the layers almost always occurs at the *A–B* interface somewhat earlier than the other. The absence of one of the layers is thus a physical reality. To explain this phenomenon, there is no need to invoke additional causes like difficulties with nucleating new phases or too slow growth rates yielding invisible compound layers.

It must be clear, however, that on a time scale of their further growth the difference in the times of layer occurrence (incubation or retardation period) can in many cases be very small. If insufficiently thin compound layers are investigated, this difference may remain unnoticed, thereby producing an impression of simultaneous formation of both layers.

3.4: Minimal thickness of the A_rB_s layer necessary for the A_pB_q layer to occur

The absence of the A_pB_q compound layer from the *A–B* reaction couple during some period of time in the initial stage of interaction of substances *A* and *B* does not mean that this compound cannot then occur and grow between *A* and A_rB_s. Indeed, equation (3.27_1) shows that the rate of consumption of the A_pB_q layer gradually decreases with increasing thickness of the A_rB_s layer.

Hence, a certain *minimal* value, $y_{\min}$, of the thickness of the A_rB_s layer is always reached at which the condition

$$k_{0B1} + k'_{0A2} = \frac{rg}{p} \frac{k'_{0B2}}{1 + \dfrac{k'_{0B2} y_{\min}}{k'_{0B2}}} \tag{3.35}$$

is satisfied. Therefore, the derivative dx/dt in equation (3.27_1) becomes first equal to zero and then positive. Hence, the A_pB_q layer will occur at the A–A_rB_s interface after some delay, as shown schematically in Fig. 3.5.

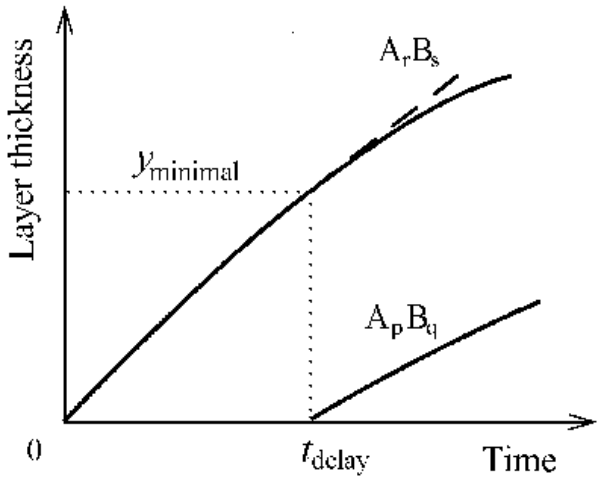

Fig. 3.5. Schematic illustration of the concept of a minimal thickness of the A_rB_s layer necessary for the A_pB_q layer to occur and grow in the A–B reaction couple.

As long as both derivatives dx/dt and dy/dt prove to be positive, the A_pB_q and A_rB_s layers will grow simultaneously until at least one of initial substances A or B is consumed completely. The delay with the formation of the A_pB_q layer is thus due to purely kinetic reasons and is not associated with either the thermodynamic stability of the A_pB_q compound or its nucleation rate. It should be noted that after the appearance of the A_pB_q layer the rate of growth of the A_rB_s layer appreciably decreases because it is partially consumed in the process of formation of the A_pB_q compound.

If the A_rB_s layer was initially missing from the A–B reaction couple, it occurs between A_pB_q and B after the A_pB_q layer has reached a necessary minimal value

$$k'_{0B2} + k_{0A3} = \frac{q}{sg} \frac{k'_{0A2}}{1 + \frac{k'_{0A2} x_{\min}}{k'_{1A2}}}. \qquad (3.36)$$

With transition metal silicides, the minimal necessary thickness may reach a few micrometres. For example, the NiSi layer starts to grow at 300-430 °C only after the Ni_2Si layer between nickel and silicon has reached a thickness of about 2 μm [56, 57]. The first layer to grow in the palladium-aluminium reaction couple at 343-431 °C is that of the Pd_2Al_3 intermetallic compound [58]. After the Pd_2Al_3 layer has reached a thickness of 3.9-6.5 μm (depending on annealing temperature), the $PdAl_3$ intermetallic compound layer starts to grow.

Figure 3.6 shows a plot of the thicknesses of the Pd_2Al_3 and $PdAl_3$ layers against the annealing time of palladium-aluminium specimens at 386 °C [58]. The $PdAl_3$ layer is seen to be missing from the Pd–Al reaction couple over a time period of approximately 500 seconds.

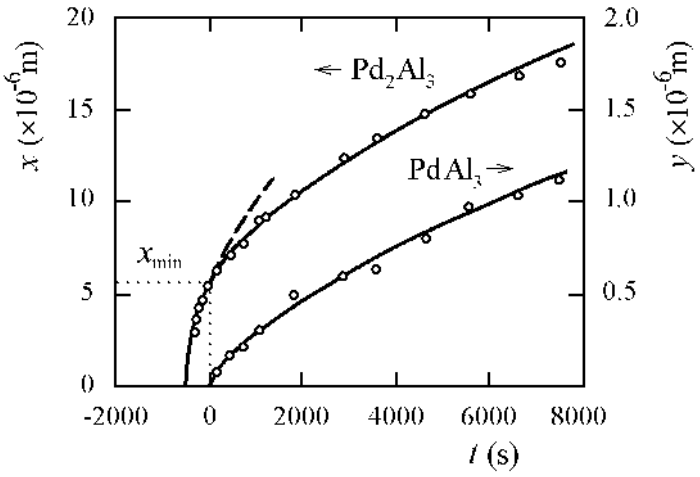

Fig. 3.6. Kinetics of sequential growth of the Pd_2Al_3 and $PdAl_3$ layers in the Pd–Al reaction couple at 386 °C [58]. The $PdAl_3$ layer starts to grow after the Pd_2Al_3 layer has reached a thickness of 5.7 μm. The rate of growth of the Pd_2Al_3 layer is seen to decrease from the point x_{min} on compared to its initial value.

Sequential formation of compound layers is often assumed to be a consequence of the existence of an interfacial barrier preventing the reaction of formation of a given compound. Such an interpretation of this phenomenon is misleading. Indeed, it may seem that after removing this barrier, for example, by artificial depositing the Pd_2Al_3 and $PdAl_3$ layers, both will grow simultaneously in Pd–Pd_2Al_3–$PdAl_3$–Al specimens. However, this is not the case. Even the existing $PdAl_3$ layer of whatever thickness will not grow unless the thickness of the Pd_2Al_3 layer exceeds the minimal necessary value x_{min}, because the consuming reaction is more rapid than the two forming ones.

3.5: Non-linear growth of the A_pB_q layer

Thickening the A_pB_q and A_rB_s layers with increasing time of interaction of initial substances A and B leads to a change in the regimes of their growth (see Sections 2.3.2 and 2.4.1). Let us assume that the regime of growth of the A_pB_q layer with regard to component B became diffusion controlled in the theoretical definition $(x > x_{1/2}^{(B)})$, and consider the case where $x >> x_{1/2}^{(B)}$.

As before in Section 3.3, the regime of growth of the A_pB_q layer with regard to component A and also that of the A_rB_s layer with regard to both components are assumed to be reaction controlled, so that $x << x_{1/2}^{(A)}$, $y << y_{1/2}^{(B)}$ and $y << y_{1/2}^{(A)}$. These conditions can also be written as $k_{0B1} >> k_{1B1}/x$, $k'_{0A2} << k'_{1A2}/x$, $k'_{0B2} << k'_{1B2}/y$ and $k_{0A3} << k_{1A3}/y$. Therefore, the system of equations (3.27) takes the form

$$\frac{dx}{dt} = \frac{k_{1B1}}{x} + k'_{0A2} - \frac{rg}{p}k'_{0B2}, \qquad (3.37_1)$$

$$\frac{dy}{dt} = k'_{0B2} + k_{0A3} - \frac{q}{sg}k'_{0A2}. \qquad (3.37_2)$$

The latter equation of this system indicates that the A_rB_s layer will grow linearly with passing time. The $x - t$ dependence is more complicated. Let us briefly analyse its possible variants.

(1) If the condition $k'_{0A2} = (rg/p)k'_{0B2}$ happens to be satisfied for a particular A–B reaction couple under certain experimental conditions, then equation (3.37_1) becomes $dx/dt = k_{1B1}/x$. Hence, the A_pB_q layer will grow parabolically, as shown schematically in Fig. 3.7a.

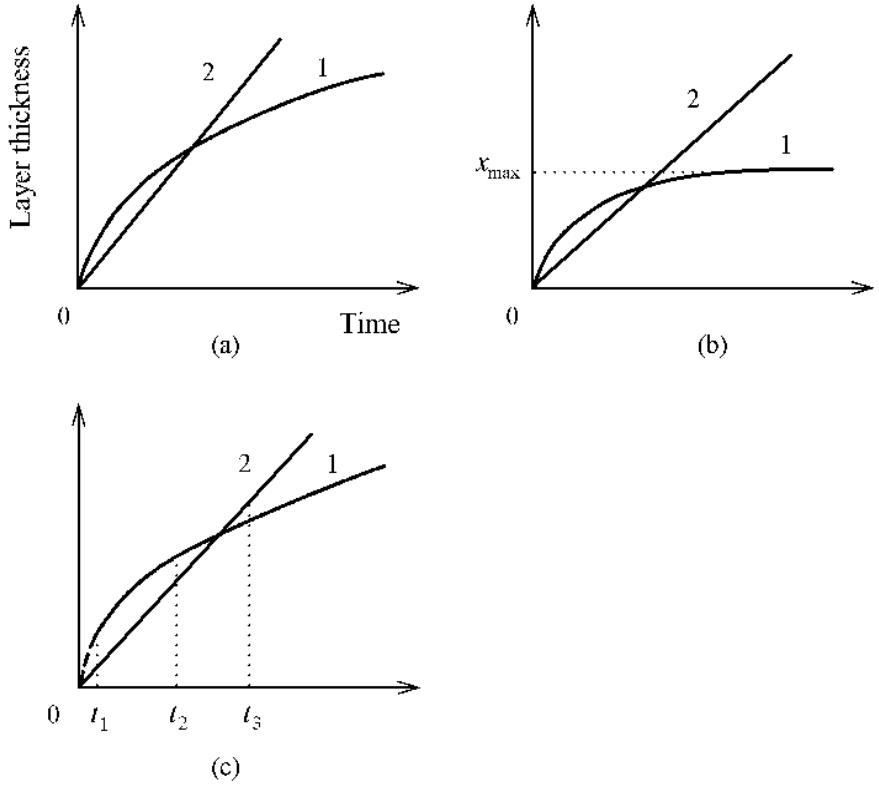

Fig. 3.7. The non-linear–linear stage of simultaneous growth of the A_pB_q (line 1) and A_rB_s (line 2) layers between substances A and A_rB_s. Growth of the A_rB_s layer is linear. Growth of the A_pB_q layer is (a) parabolic, (b) asymptotic or (c) close to parabolic in the t_1– t_2 range and almost linear at $t > t_3$.

(2) If $k'_{0A2} < (rg/p)k'_{0B2}$, then

$$\frac{dx}{dt} = \frac{k_{1B1}}{x} - R, \tag{3.38}$$

where $R = (rg/p)k'_{0B2} - k'_{0A2}$. From equation (3.38), it is easy to conclude that the thickness of the A_pB_q layer will asymptotically tend with passing time to some limiting value x_{max} (Fig. 3.7b). To find this value, it suffices to put $dx/dt = 0$ in equation (3.38), giving

$$x_{max} = \frac{k_{1B1}}{R}. \tag{3.39}$$

Note that a certain portion of the $x - t$ curve, where the condition $k_{1B1}/x >> R$ is satisfied, is close to the parabola $x^2 = 2\,k_{1B1}\,t$.

(3) If $k'_{0A2} > (rg/p)k'_{0B2}$, then the derivative dx/dt is positive, and therefore the A_pB_q layer continuously grows with passing time. That portion of the $x - t$ dependence between t_1 and t_2, where the condition $k_{1B1}/x >> k'_{0A2} - (rg/p)k'_{0B2}$ is fulfilled, is close to a parabola, whereas the region of long times $t > t_3$, where $k_{1B1}/x << k'_{0A2} - (rg/p)k'_{0B2}$, is almost linear (Fig. 3.7c).

Similar considerations clearly apply to the A_rB_s layer if the regime of its growth is diffusion controlled with regard to component A, so that $y >> y^{(A)}_{1/2}$, and reaction controlled with regard to component B ($y << y^{(B)}_{1/2}$), while that of the A_pB_q layer is reaction controlled with regard to both components, so that $x << x^{(A)}_{1/2}$ and $x << x^{(B)}_{1/2}$. Then, the A_rB_s layer will grow non-linearly, while the A_pB_q layer linearly.

3.6: Effect of the critical thickness of the A_pB_q layer with regard to component A on the process of growth of the A_rB_s layer

Due to further thickening the A_pB_q layer, its growth regime becomes diffusion controlled (in the theoretical definition) not only with regard to component B but also with regard to component A ($x > x^{(B)}_{1/2}$ and $x > x^{(A)}_{1/2}$). This case differs essentially from that considered in the previous section. Indeed, if the growth regime of the A_pB_q layer is diffusion controlled with regard to component A, then the A_rB_s layer cannot grow at the expense of diffusion of component A because at $x > x^{(A)}_{1/2}$ all the A atoms crossing the bulk of the A_pB_q layer per unit time are combined into the A_pB_q compound at interface 2 according to partial chemical reaction (3.1_2).

Subsequent increasing the thickness of the A_pB_q layer makes a deficit of the diffusing A atoms progressively large in comparison with the reactivity of the surface of the A_rB_s layer towards these atoms. Therefore, no atom A is able to enter into partial chemical reaction

(3.2$_2$). Interface 2 or, rather, the surface of the A_rB_s layer thus becomes an insurmountable barrier for the A atoms. Hence, at $x > x_{1/2}^{(A)}$ simply there are no diffusing A atoms for the A_rB_s layer to grow. All of them are consumed during the formation of the A_pB_q layer.

It is surprising why this obvious conclusion remained overlooked until the 1980s [16], although in examining the process of layer growth the equations of mass balance at phase interfaces are always written. The answer is that, firstly, the constancy of the composition of any chemical compound is usually not taken into account and, secondly, each interface is examined separately from others, whereas it is necessary to analyse the mutual effect on each other of the physical and chemical processes taking place at the interfaces between all the phases involved in the interaction.

It must be clear that at $x > x_{1/2}^{(A)}$ the term

$$\frac{k_{0A3}}{1+\dfrac{k_{0A3}y}{k_{1A3}}}$$

of the system of equations (3.27), though quite sound from a mathematical viewpoint, nonetheless has no physical meaning and therefore should be omitted whatever y. Hence, the rate of growth of the A_rB_s layer will appreciably decrease after the thickness of the A_pB_q layer has reached its critical value of $x_{1/2}^{(A)}$, as shown schematically in Fig. 3.8.

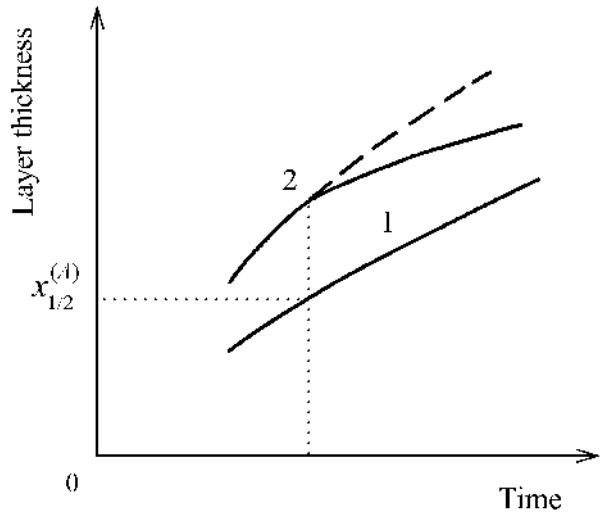

Fig. 3.8. Decreasing the growth rate of the A_rB_s layer after the A_pB_q layer has reached its critical thickness $x_{1/2}^{(A)}$ with regard to component A. 1, thickness of the A_pB_q layer; 2, thickness of the A_rB_s layer.

Indeed, at $x < x_{1/2}^{(A)}$ the A_rB_s layer grows at the expense of diffusion of both components A and B followed by partial chemical reactions (3.2$_1$) and (3.2$_2$), while at $x > x_{1/2}^{(A)}$ it only grows at the expense of diffusion of component B and subsequent partial chemical reaction (3.2$_1$).

Therefore, the $y - t$ curve will exhibit a deviation from its former course reflecting a decrease of the growth rate of the A_rB_s layer. This deviation is due to the existence of the critical thickness $x_{1/2}^{(A)}$ of the A_pB_q layer, which divides the $x - t$ dependence into the reaction controlled and diffusion controlled regions with regard to component A.

Decreasing the growth rate of the A_rB_s layer is clearly smooth and not abrupt since a relative deficit of the diffusing A atoms in comparison with the reactivity of the surface of substance B towards these atoms becomes perceptible somewhat earlier than the thickness of the A_pB_q layer reaches $x_{1/2}^{(A)}$. However, if sufficiently wide portions of the layer thickness-time dependences in the vicinity of the point $x_{1/2}^{(A)}$ of the $x - t$ curve and the corresponding point of the $y - t$ curve are investigated, then a decrease in the growth rate of the A_rB_s layer may readily be noticed.

3.7: Paralinear growth kinetics of two compound layers

If the A_pB_q layer grows in the diffusion controlled regime with regard to components A and B, while the A_rB_s layer grows in the reaction controlled regime with regard to component B, so that $x >> x_{1/2}^{(B)}$, $x >> x_{1/2}^{(A)}$ and $y << y_{1/2}^{(B)}$, then the system of equations (3.27) is simplified to

$$\frac{\mathrm{d}x}{\mathrm{d}t} = \frac{k_{1B1} + k'_{1A2}}{x} - \frac{rg}{p} k'_{0B2}, \qquad (3.40_1)$$

$$\frac{\mathrm{d}y}{\mathrm{d}t} = k'_{0B2} - \frac{q}{sg}\frac{k'_{1A2}}{x}. \qquad (3.40_2)$$

Since equation (3.40_1), similar to equation (3.38), does not contain y, it can be solved separately from equation (3.40_2). It is clear that under constant temperature and pressure conditions the thickness of the A_pB_q layer asymptotically tends with passing time to the maximal possible value (see Section 3.5, equation (3.39))

$$x_{\max} = \frac{(k_{1B1} + k'_{1A2})p}{rgk'_{0B2}}, \qquad (3.41)$$

theoretically never reaching it, whereas the growth of the A_rB_s layer is almost linear if $k'_{0B2} >> (q/sg)k'_{1A2}/x$. If the latter condition is satisfied, then the system of equations (3.40) takes a simpler form

$$\frac{\mathrm{d}x}{\mathrm{d}t} = \frac{k_{1B1} + k'_{1A2}}{x} - \frac{rg}{p} k'_{0B2}, \qquad (3.42_1)$$

$$\frac{\mathrm{d}y}{\mathrm{d}t} = k'_{0B2}. \qquad (3.42_2)$$

A system of differential equations of this type appears to have been first proposed by J. Loriers in 1949 (see Ref. [27]) to describe *paralinear* growth kinetics of two oxide layers. The term *paralinear* growth, being a combination of the words *para*bolic and *linear*, means that some initial portion of the time dependence of the total thickness or mass of two compound layers is almost parabolic and then there is a gradual transition to linear kinetics.

Indeed, from the system of equations (3.42), it is easily seen that at low values of t and consequently x $(k_{1B1} + k'_{1A2})/x >> (rg/p)k'_{0B2}$ and therefore this dependence is close to the parabola $x^2 = 2(k_{1B1} + k'_{1A2})t$ in view of small contribution from the straight line $y = k'_{0B2}t$ to the total thickness of both layers. Its long-time portion, being the sum of two straight lines $x = x_{\max}$ (see equation (3.41)) and $y = k'_{0B2}t$, is linear.

Paralinear kinetics are especially often observed if one of the layers is compact, while the other porous. It should be noted, however, that the presence of pores, cracks or other macroscopic defects in one of the layers is not a necessary condition for employing the system of equations (3.42) to treat the experimental data. Only a large difference in the diffusivities of the components in compound layers, ensuring different regimes of their growth, is important. Also, the duration of experimental observations must be sufficiently long because the final stage of asymptotic growth of one of the layers is extremely slow.

In the oxidation of metals, paralinear growth kinetics of oxide layers are known to be a quite usual phenomenon [27]. Such a dependence is likely to be observed much less frequently with metallic systems due to three reasons. Firstly, the duration of investigation of the process of oxidation of metals is far longer than that in examining the solid-state interaction of two metals. Secondly, the minimal measurable thickness (or mass) of compound layers which can be detected using available techniques is much less in the former case than in the latter. Thirdly, since this “anomalous” dependence has no satisfactory explanation from a diffusional viewpoint, most experimentalists investigating metallic systems probably prefer not to accentuate on it.

Note that the transition from the parabolic to linear kinetics with passing time can take place only in the case of simultaneous growth of the layers of two (or more) chemical compounds. Therefore, if a thermogravimetric curve is well described by paralinear equations (3.42), it provides evidence for the presence of at least two growing compound layers at the interface of reacting substances. If a single compound layer is formed, only the reverse transition where a straight line gradually transforms into a parabola is possible. This must be kept in mind to avoid misleading conclusions regarding the rate-determining step in the layer formation.

Often, the parabolic-to-linear transition is interpreted in such a way, as if initially the diffusion is the rate-determining step, while then (with increasing time) the reaction becomes the rate-determining step. Firstly, during the paralinear growth no change of the rate-determining steps ever occurs. Secondly, if the diffusion is already dominant at a smaller thickness of any compound layer, the reaction can never become dominant at its larger thickness.

3.8: Diffusion controlled growth of the A_pB_q and A_rB_s layers

Increasing the thickness of the A_rB_s layer will inevitably result in a change of its growth regime from reaction to diffusion controlled with regard to component B (at $y > y_{1/2}^{(B)}$). This change immediately affects the growth rate of the A_pB_q layer. Namely, at $y > y_{1/2}^{(B)}$ the A_pB_q layer loses a source of B atoms and consequently its further growth proceeds at the expense of diffusion of only component A.

Thus, at $x > x_{1/2}^{(A)}$ and $y > y_{1/2}^{(B)}$ the A_pB_q layer grows at the expense of diffusing A atoms and subsequent partial chemical reaction (3.1_2), while the A_rB_s layer grows at the expense of diffusing B atoms and subsequent partial chemical reaction (3.2_1). Both reactions take place at their common interface 2 (Fig. 3.9).

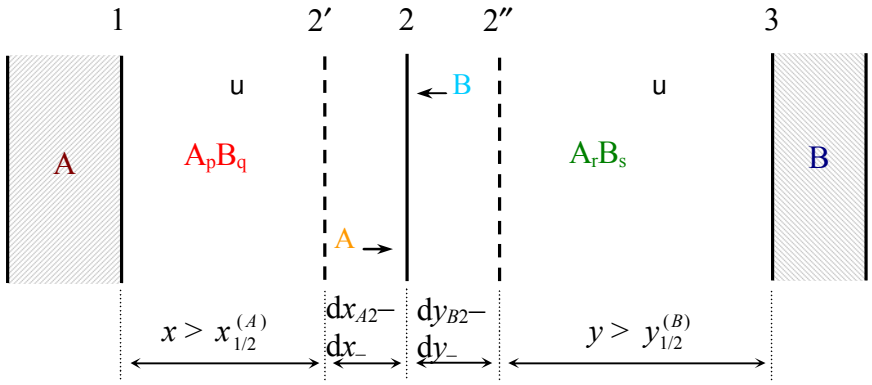

Fig. 3.9. Schematic diagram to illustrate the growth process of two chemical compound layers under conditions of diffusion control ($x > x_{1/2}^{(A)}$ and $y > y_{1/2}^{(B)}$). Only component A is diffusing across the A_pB_q layer, while only component B is diffusing across the A_rB_s layer. Both layers thicken at their common interface 2. No partial chemical reactions take place at interfaces 1 and 3 in view of the lack of appropriate diffusing atoms. The symbol **u** designates an inert marker.

Partial chemical reactions (3.1_1) and (3.2_2) cannot proceed at all in view of the lack of excessive diffusing B and A atoms. These are completely consumed at the A_pB_q– A_rB_s interface. Hence, the terms

$$\frac{k_{0B1}}{1+\dfrac{k_{0B1}x}{k_{1B1}}} \quad \text{and} \quad \frac{k_{0A3}}{1+\dfrac{k_{0A3}y}{k_{1A3}}}$$

of the system of equations (3.27) lose their physical meaning and should be omitted whatever x and y. The time dependence of the total thickness or mass of two compound layers must therefore exhibit two more of less pronounced deviations from their former course, as shown schematically in Fig. 3.10.

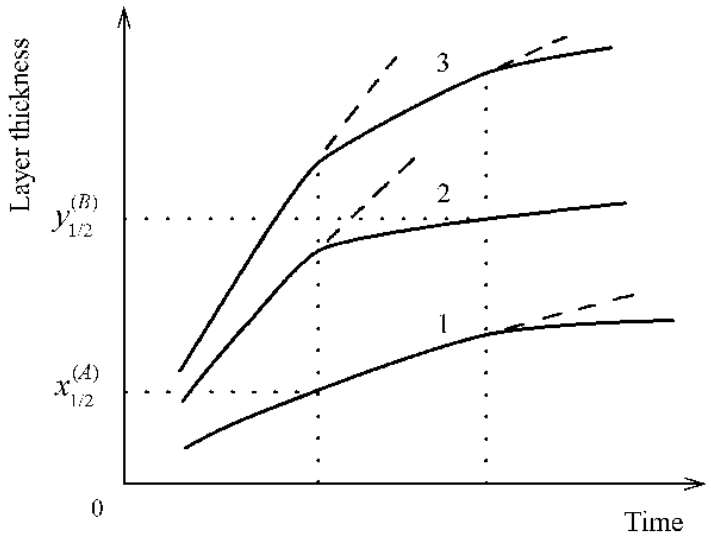

Fig. 3.10. Deviations of the kinetic dependences due to the existence of the critical thicknesses of growing A_pB_q and A_rB_s layers. 1, thickness of the A_pB_q layer; 2, thickness of the A_rB_s layer; 3, total thickness of both layers.

One of these deviations is due to a change of the regime of growth of the A_pB_q layer from reaction (at $x < x_{1/2}^{(A)}$) to diffusion (at $x > x_{1/2}^{(A)}$) controlled with regard to component A. After the A_pB_q layer has reached the thickness $x_{1/2}^{(A)}$, a deviation occurs on the $y - t$ curve describing the time dependence of the thickness of the A_rB_s layer.

Another deviation is due to a change of the regime of growth of the A_rB_s layer from reaction (at $y < y_{1/2}^{(B)}$) to diffusion (at $y > y_{1/2}^{(B)}$) controlled with regard to component B. When the A_rB_s layer reaches the thickness $y_{1/2}^{(B)}$, a deviation occurs on the dependence, $x - t$, of the thickness of the A_pB_q layer upon time. Note that in the case under consideration the deviations observed on the kinetic dependences are caused solely by quantitative changes in thickness of growing compound layers. Neither their number, nor phase identity, nor structure are changed. This is an instructive example of the transformation of quantity into quality.

3.8.1: Late diffusional stage of growth of two compound layers: system of differential equations

The late diffusional stage of growth of the A_pB_q and A_rB_s layers is the one where the conditions $x >> x_{1/2}^{(A)}$ and $y >> y_{1/2}^{(B)}$ are satisfied. This means that $k'_{0A2} >> k'_{1A2}/x$ and $k'_{0B2} >> k'_{1B2}/y$. Therefore, by omitting, as physically meaningless, both the first term of the right-hand side of equation (3.27_1) and the second term of the right-hand side of equation (3.27_2) and neglecting unity in the denominators of the other terms, one obtains

$$\frac{\mathrm{d}x}{\mathrm{d}t} = \frac{k'_{1A2}}{x} - \frac{rg}{p}\frac{k'_{1B2}}{y}, \qquad (3.43_1)$$

$$\frac{\mathrm{d}y}{\mathrm{d}t} = \frac{k'_{1B2}}{y} - \frac{q}{sg}\frac{k'_{1A2}}{x}. \qquad (3.43_2)$$

A similar system of differential equations, differing only by its coefficients, was obtained earlier in the framework of diffusional considerations by V.I. Arkharov [17]. For the late diffusional stage of growth of two compound layers, most frequently observed in practice, the physico-chemical and diffusional approaches give identical kinetic equations because in this stage of interaction the rates of their formation are restricted almost entirely by the rate of diffusion of the A and B atoms across layer bulks, with the rate of chemical transformations at the interfaces being practically instantaneous by comparison. In other words, the time of chemical transformations (chemical reaction as such) is negligible compared to the time of diffusional transport of reacting species to the reaction site.

3.8.2: Late diffusional stage of growth of two compound layers: ratio of their thicknesses

When solving any system of differential equations like (3.43), it is usually assumed that either

$$x \sim t^{1/2} \text{ and } y \sim t^{1/2}$$

or

$$\frac{\mathrm{d}x}{\mathrm{d}t} : \frac{\mathrm{d}y}{\mathrm{d}t} = \text{const}.$$

Therefore, the (parabolic) type of the $x - t$ and $y - t$ dependences becomes predetermined beforehand. Also, the ratio of the growth rates (and thicknesses) of the layers is considered to be unchanged during their formation. It is supposed to follow from the available experimental data. However, this is not the case.

In fact, the ratio of the thicknesses of growing compound layers changes with passing time, but relatively slowly, and not always this change can be noticed in view of the limited duration of experimental observations. To determine the range in which the ratio of the

thickness of the A_pB_q and A_rB_s layers can vary during their growth in the late diffusional stage, let us analyse the system of equations (3.43) in more detail.

Positive values of the derivatives dx/dt and dy/dt are clearly a necessary condition for the simultaneous growth of the A_pB_q and A_rB_s layers. Therefore, instead of the system of equations (3.43), the following system of inequalities is obtained

$$\frac{k'_{1A2}}{x} - \frac{rg}{p}\frac{k'_{1B2}}{y} > 0, \qquad (3.44_1)$$

$$\frac{k'_{1B2}}{y} - \frac{q}{sg}\frac{k'_{1A2}}{x} > 0. \qquad (3.44_2)$$

These inequalities must be satisfied simultaneously. Hence, the limits within which the ratio of the thickness of the A_pB_q and A_rB_s layers can vary are as follows

$$\frac{q}{sg}\frac{k'_{1A2}}{k'_{1B2}} < \frac{x}{y} < \frac{p}{rg}\frac{k'_{1A2}}{k'_{1B2}}. \qquad (3.45)$$

It is seen, firstly, that the ratio of the thicknesses of the A_pB_q and A_rB_s layers depends upon:

(i) values of the physical (diffusional) constants,

(ii) ratio of the molar volumes of the A_pB_q and A_rB_s compounds,

(iii) stoichiometry of these compounds.

Secondly, the closer the compositions of the compounds A_pB_q and A_rB_s to each other, the narrower is the range of variation of the ratio x/y. For example, for chemical compounds of the type AB and AB_2,

$$\frac{1}{2g}\frac{k'_{1A2}}{k'_{1B2}} < \frac{x}{y} < \frac{1}{g}\frac{k'_{1A2}}{k'_{1B2}}. \qquad (3.46)$$

Therefore, in prolonged experiments the x/y ratio can change by as much as 50%. This range (50%) is rather wide in comparison with the experimental error of measuring the thickness of the layers, which is known to be 5 to 25% of the average value. Therefore, in this case a gradual change in the ratio of the thicknesses of the AB and AB_2 layers during their diffusional growth can readily be noticed, if the time of observation is not too short.

For the AB_4 and AB_5 compounds,

$$\frac{4}{5g}\frac{k'_{1A2}}{k'_{1B2}} < \frac{x}{y} < \frac{1}{g}\frac{k'_{1A2}}{k'_{1B2}}. \qquad (3.47)$$

Thus, in the course of diffusional growth of the AB_4 and AB_5 layers the x/y ratio varies only by 20%. Taking into account the limited duration of any experiment, it must be clear that in practice the change of the x/y ratio is much less and therefore can hardly be noticed, especially if the researcher is not aware of its probable existence. This explains why it is often assumed that $x/y = \text{const}$. In fact, the latter is nothing more than an approximation, though sufficiently substantiated in some particular cases.

From the system of equations (3.43), it follows that the layers of the A_pB_q and A_rB_s compounds already present in an A–A_pB_q–A_rB_s–B specimen should not necessarily simultaneously grow during its further isothermal annealing. If their initial thicknesses x_0 and y_0 are such that, for example, the derivative $(\mathrm{d}x/\mathrm{d}t)_{t=t_0}$ is negative and the derivative $(\mathrm{d}y/\mathrm{d}t)_{t=t_0}$ is positive, then the thickness of the A_pB_q layer will decrease, while the thickness of the A_rB_s layer will increase until the x/y ratio falls into the range defined by inequality (3.45). Subsequently, both layers will grow simultaneously.

Thus, the $y - x$ phase plane [54, 55] is divided into three regions, as shown schematically in Fig. 3.11. In regions I and III the thickness of one of the layers increases and that of the other decreases. In region II the thickness of both layers increases.

Region I is separated from region II by the nodal line

$$y = \frac{sgk'_{1B2}}{qk'_{1A2}}x. \qquad (3.48)$$

To obtain this equation, it suffices to put $\mathrm{d}x/\mathrm{d}t = 0$ in equation (3.43_1).

The nodal line between regions II and III is the straight line

$$y = \frac{rgk'_{1B2}}{pk'_{1A2}}x, \qquad (3.49)$$

which is obtained from equation (3.43_2) by putting $\mathrm{d}y/\mathrm{d}t = 0$.

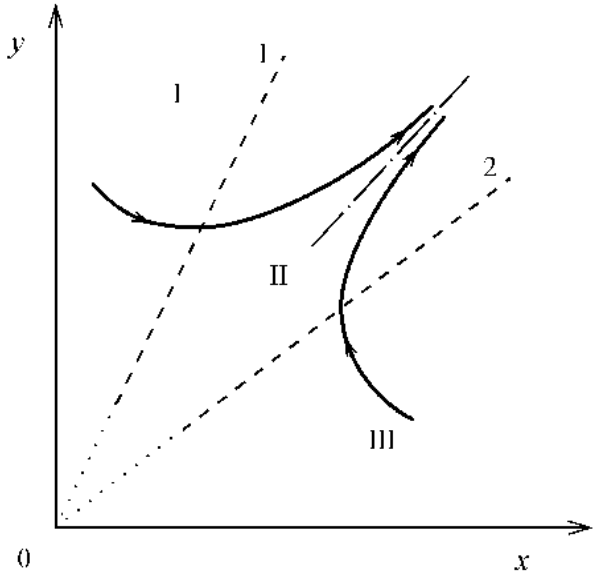

Fig. 3.11. The $y - x$ phase plane in the late diffusional stage of formation of two compound layers. The nodal lines 1 and 2 separate the phase plane into three regions. In regions I and III the thickness of one of the layers increases, while that of the other decreases. In region II both layers grow simultaneously. The arrows at phase trajectories indicate the direction of variation of the layer thicknesses with increasing time.

If the initial thicknesses of the A_pB_q and A_rB_s layers correspond to any point in region I, then with passing time the A_pB_q layer will grow, whereas the A_rB_s layer will shrink until the phase trajectory indicating the direction of growth enters region II in which both layers will grow. If these thicknesses correspond to any point in region III, then the A_rB_s layer will grow, whereas the A_pB_q layer will shrink until again the phase trajectory enters region II where both layers will grow. If the initial thicknesses of the A_pB_q and A_rB_s layers correspond to any point in region II, then the A_pB_q and A_rB_s layers will grow simultaneously from the very beginning of isothermal annealing of an $A–A_pB_q–A_rB_s–B$ specimen.

Both trajectories are seen in Fig. 3.11 to tend asymptotically with increasing time to a straight line corresponding to a constant ratio of the layer thicknesses. Whenever these are sufficiently close to this line, the parabolic growth law becomes a good approximation for both layers and therefore can be employed to treat the experimental kinetic data.

During the natural course of the process of formation of the A_pB_q and A_rB_s layers between elementary substances A and B when an $A–B$ specimen is given to itself at constant temperature and pressure, a correct ratio of their thicknesses is established automatically. However, if an $A–A_pB_q–A_rB_s–B$ specimen was prepared artificially by depositing the A_pB_q and A_rB_s layers of arbitrary thickness, this ratio can hardly be expected to be correct.

Therefore, during subsequent isothermal annealing of the specimen, one of the layers will shrink and can even disappear as occurred before its turn if, of course, by that time the other layer has not reached a minimal thickness required for the former to occur. Such a phenomenon was observed, for example, with the PtSi layer in Pt–Pt_2Si–PtSi–Si specimens [59] and with the CoSi layer in Co–Co_2Si–CoSi–Si specimens [60].

The exact law of growth of the layers of two chemical compounds in the late diffusional stage of their formation can be found, at least in principle, by solving the system of equations (3.43) with initial conditions $x = x_0$ and $y = y_0$ ($x_0 > 0$, $y_0 > 0$) at $t = 0$ (or $t = t_0$) without any additional assumptions. Indeed, dividing the second equation by the first yields an equation of the type $dy/dx = f(x, y)$. By solving this equation, y is obtained as a function of x. By substituting this dependence into equation (3.43_1), the expression $dx/dt = f(x)$ is obtained. Its integration gives x as a function of t. It is then possible to determine the $y - t$ dependence from equation (2.46_2).

Unfortunately, every stage of finding the solution to the system of differential equations (3.43) leads to very complicated expressions. Therefore, the final result can hardly be represented in the form of a single simple function. However, these difficulties are not a serious obstacle for practical applications of the system of equations (3.43).

Indeed, the derivatives dx/dt and dy/dt at $t = t_i$ can readily be determined (for example, by graphic differentiation or any other means) from the experimental data. Then, the system (3.43) transforms into an ordinary system of algebraic equations containing two unknowns k'_{1A2} and k'_{1B2}:

$$\left(\frac{dx}{dt}\right)_{t=t_i} = \frac{k'_{1A2}}{x_i} - \frac{rg}{p}\,\frac{k'_{1B2}}{y_i}, \qquad (3.50_1)$$

$$\left(\frac{dy}{dt}\right)_{t=t_i} = \frac{k'_{1B2}}{y_i} - \frac{q}{sg}\,\frac{k'_{1A2}}{x_i}. \qquad (3.50_2)$$

Therefore, an attempt can be undertaken to describe the experimental dependence of the thickness of the layers upon time in terms of the diffusional constants k'_{1A2} and k'_{1B2}. If these prove to be indeed constant at all experimental values of the thicknesses of the A_pB_q and A_rB_s layers, then the system of equations (3.43) describes properly the process of growth of two chemical compound layers. Otherwise, this portion of the layer thickness-time dependence appears to be not purely diffusional, and use must be made of other mathematical equations giving a more adequate fit to the experimental data.

It is clear that in general the kinetic dependences considered in this chapter gradually transform into each other with passing time. In contrast to the diffusional theory, the physico-chemical approach thus gives a more complicated, not simply parabolic, relationship between the thickness of two chemical compound layers and the time, in accordance with the available experimental data.

Note that the unjustified neglect of the step of chemical transformations in analysing the process of growth of two compound layers immediately leads to the loss of a few growth laws (linear, paralinear, asymptotic, *etc*.). Also, spreading the consequences following from diffusional equations into the region of small layer thicknesses, to which these are inapplicable at all, results in the misleading conclusion about the simultaneous beginning of parabolic growth of both layers in any binary system with two chemical compounds on the equilibrium phase diagram.

In application to chemical compounds, both the diffusional and physico-chemical theories consider the rate of chemical transformations (chemical reaction) in the late diffusional stage of layer formation as very high compared to that of diffusion. But the conclusion made from this *quite correct* premise in the framework of diffusional considerations is *quite incorrect*, namely, the (rapid) step of chemical transformations is considered as non-existing at all.

In fact, chemical transformations taking place at the interfaces between reacting phases are responsible for the occurrence of the barriers to diffusing atoms at the critical values of the thicknesses of the A_pB_q and A_rB_s layers. Their rate is also decisive in determining the sequence of formation of the layers of those compounds in the A–B reaction couple.

Actually, the rate of chemical transformations affects the rate of growth of the layers at all stages from the start of interaction of initial substances to the establishment of equilibrium in the system. The widespread opinion according to which the chemical transformations have no effect on the layer-growth kinetics, except in a very short initial period of time, is thus quite groundless.

As long as the components A and B are insoluble in each other and in the compounds A_pB_q and A_rB_s, equilibrium can only be established by means of sequential consumption of initial phases. After the substance A or B has been completely consumed, either A_pB_q or A_rB_s becomes another initial substance. Depending on the relative amounts of initial substances A and B, the following phases can remain in the equilibrium state:

(*i*) substance A and adjacent layer A_pB_q,

(*ii*) substance B and adjacent layer A_rB_s,

(*iii*) layers of A_pB_q and A_rB_s,

(*iv*) layer of either A_pB_q or A_rB_s.

It should be noted that in general any inert marker only indicates the diffusing species in that compound layer in which it is embedded or with which it borders. From Fig. 3.9, it must be clear that in the case of two compound layers it is necessary to have inert markers inside *both* layers to *directly* decide of the diffusing species in their bulks. Indeed, the fact that the distance between any marker located within the A_rB_s layer growing under conditions of diffusion control and interface 3 remains unchanged, while the distance between this marker and interface 2 steadily increases in the course of reaction means that component B is the only

diffusing species in *this* layer and nothing more, though component *B* is often regarded to be the main diffusing one in *both* layers.

The latter conclusion is incorrect. The very presence of the A_pB_q layer growing under conditions of diffusion control provides *indirect* evidence that component *A* is the *only* diffusing species in this layer since it cannot grow at the expense of diffusion of the *B* atoms in view of their lack.

Evidently, in the course of layer formation the plane of inert markers cannot coincide with the initial interface between substances *A* and *B*. It would mean that compound layers could grow at the expense of *one* component. Chemically, this is impossible since any binary compound consists of two components. Position of the layers relative to the initial interface is mainly dependent upon the stoichiometry of chemical compounds, if both ends of a couple are equally free to move. Coincidence of initial and marker planes provides evidence for the lack of contact between reacting phases at that place.

It must also be clear that in the case of two compound layers, even growing under conditions of diffusion control, the calculation of integrated diffusion coefficients [48] produces fictitious, physically intractable quantities since the real mechanism of layer formation has little in common with the assumptions made when introducing the concept of an integrated diffusion coefficient and deriving basic mathematical equations. In fact, there is no *interdiffusion* during diffusional growth of two compound layers, with only *one* component diffusing across each layer. Any concentration-distance curve like that shown in Fig. 3.1 may of course be divided into two regions of equal area to formally define Matano's interface, but such a division can hardly be considered as sufficiently substantiated.

3.8.3: Simultaneous diffusional growth of the Al_3Mg_2 and $Al_{12}Mg_{17}$ intermetallic layers between aluminium and magnesium

The layers of two intermetallic compounds Al_3Mg_2 and $Al_{12}Mg_{17}$ available on the Al–Mg phase diagram [61-63] are known to grow simultaneously at the interface between aluminium and magnesium at 400 °C [64]. A schematic diagram to illustrate the process of their growth is shown in Fig. 3.12a, while the microstructure of the Al–Mg transition zone in Fig. 3.12b.

Formation of the layers is likely to be due to partial chemical reactions

$$27Al_{dif} + 2Al_{12}Mg_{17} = 17Al_3Mg_2 \qquad (3.51_1)$$

and

$$9Mg_{dif} + 4Al_3Mg_2 = Al_{12}Mg_{17} \qquad (3.51_2)$$

taking place at their common interface 2.

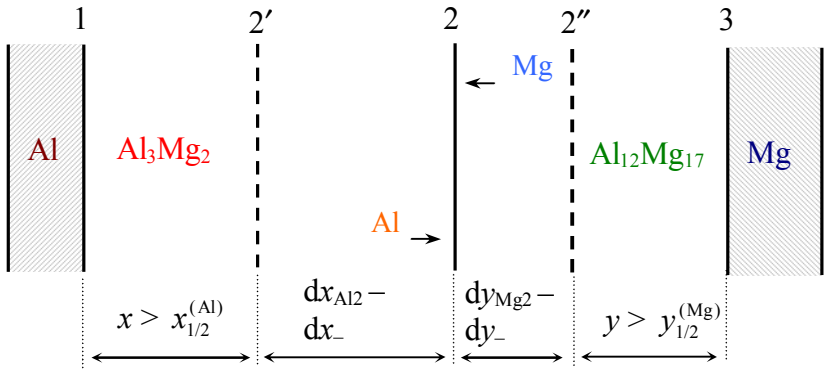

(a)

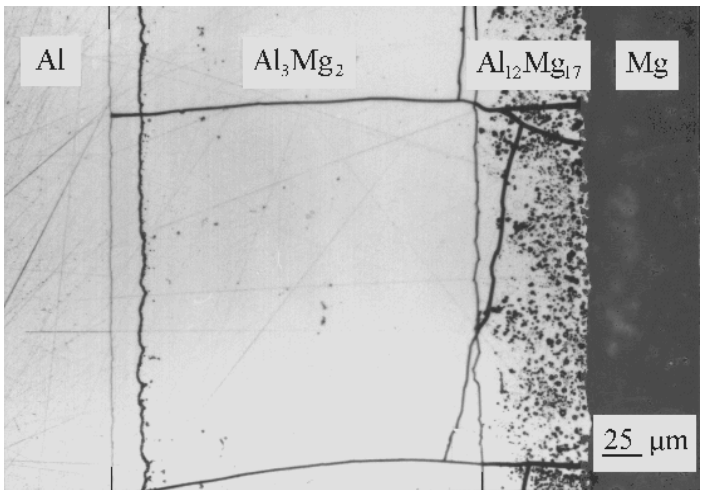

(b)

Fig.3.12. (a) Schematic diagram to illustrate the diffusional stage of the growth process of the Al_3Mg_2 and $Al_{12}Mg_{17}$ intermetallic compound layers and (b) microstructure of the transition zone between aluminium and magnesium after isothermal annealing at 400 °C for 172800 s (48 h) [64].

As seen in Fig. 3.13, the Al_3Mg_2 layer grows much faster than the $Al_{12}Mg_{17}$ layer, though the diffusional theory predicts the opposite relationship since the homogeneity range of Al_3Mg_2 is at least five times less than that of $Al_{12}Mg_{17}$. This provides additional support to the conclusion of Chapter 1 about the lack of direct proportionality between the rate of formation of a chemical compound and the width of its homogeneity range.

The layer-growth kinetics were found to be parabolic for both compounds (Fig. 3.14), indicative of diffusion control. This result could be expected since the thickness of the layers varied from about 10 μm to 300 μm for the $Al_{12}Mg_{17}$ intermetallic compound and from about 80 μm to more than 900 μm for the Al_3Mg_2 intermetallic compound.

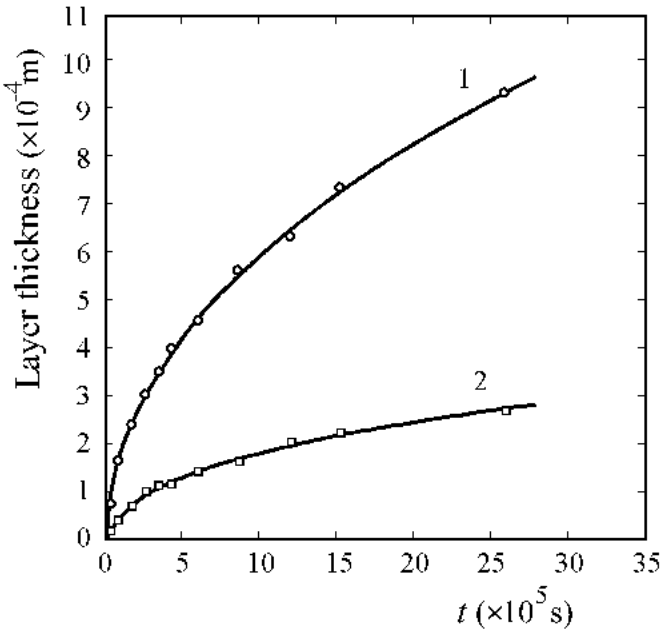

Fig. 3.13. Plots of layer thickness against annealing time of Al–Mg diffusion couples at 400 °C [64]. 1, Al_3Mg_2; 2, $Al_{12}Mg_{17}$.

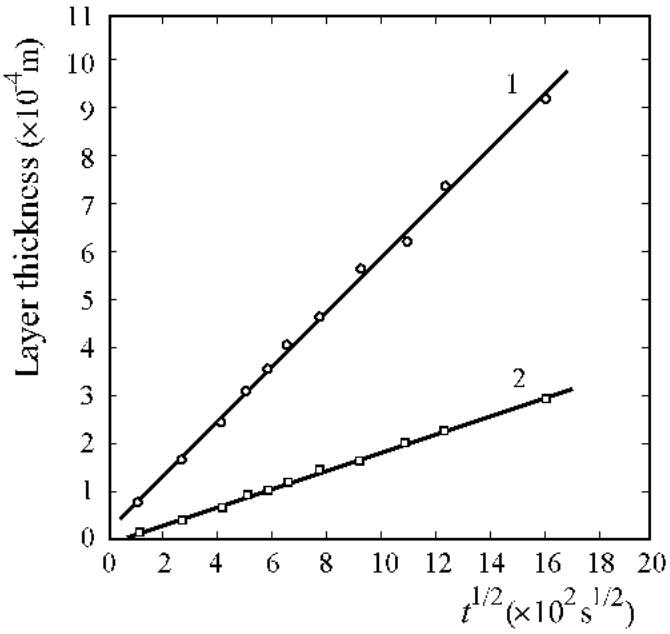

Fig. 3.14. Plots of layer thickness against the square root of the annealing time of Al–Mg diffusion couples at 400 °C [64]. 1, Al_3Mg_2; 2, $Al_{12}Mg_{17}$.

Diffusional constants were calculated using parabolic equations of the type $x^2 = 2k_1 t$. The temperature dependence of the diffusional constants was found to obey the Arrhenius relations [64]

$$k_1^{(Al_3Mg_2)} = 3.5\times10^{-8}\exp\,(-69\ \text{kJ mol}^{-1}/RT)\ \text{m}^2\ \text{s}^{-1}, \qquad (3.52_1)$$

$$k_1^{(Al_{12}Mg_{17})} = 0.1\ \exp\,(-165\ \text{kJ mol}^{-1}/RT)\ \text{m}^2\ \text{s}^{-1}. \qquad (3.52_2)$$

Treatment of the experimental data on the layer-growth kinetics in the Al–Mg system with the use of the system of equations (3.43), which in this case assumes the form

$$\left(\frac{dx}{dt}\right)_{t=t_i} = \frac{k_{1Al2}}{x_i} - \frac{rg}{p}\,\frac{k_{1Mg2}}{y_i}, \qquad (3.53_1)$$

$$\left(\frac{dy}{dt}\right)_{t=t_i} = \frac{k_{1Mg2}}{y_i} - \frac{q}{sg}\,\frac{k_{1Al2}}{x_i}, \qquad (3.53_2)$$

and in which the strokes were omitted for simplicity, yields the following results.

Evaluation of the diffusional constants k_{1Al2} and k_{1Mg2} was first carried out directly using initial experimental values of layer thicknesses at a temperature of 400 °C, listed in Table 3.1 [64]. From the chemical formulae of the Al_3Mg_2 and $Al_{12}Mg_{17}$ compounds, $p = 3$, $q = 2$, $r = 12$ and $s = 17$. The value of g was estimated from the densities of these compounds [63, 65] and their molecular masses as 0.94.

The derivatives dx/dt and dy/dt at each value of time t_i were found by the numerical three-point method (see Section 1.3). The results of calculations are presented in Table 3.1. The average value of k_{1Al2} was determined to be 4.49×10^{-13} m^2 s^{-1} and that of k_{1Mg2} 9.41×10^{-14} m^2 s^{-1}. As seen in Table 3.1, the accuracy of calculations of k_{1Al2} and k_{1Mg2} are strongly dependent upon a scatter of experimental points. To avoid the effect of this scatter on the final results, approximation of the experimental data with any suitable analytical function is therefore advisable.

For example, the use of parabolic relations $x^2 = 2k_1 t$ and equations (3.52), with the parabolic constant $k_1 = 1.57\times10^{-13}$ m^2 s^{-1} for the Al_3Mg_2 compound and $k_1 = 1.63\times10^{-14}$ m^2 s^{-1} for the $Al_{12}Mg_{17}$ compound at a temperature of 400 °C [64], to approximate the layer thickness–time dependences and then to find the derivatives, yields another set of values of k_{1Al2} and k_{1Mg2} (Table 3.2).

Table 3.1. Evaluation of diffusional constants k_{1Al2} and k_{1Mg2} from the system of equations (3.53) for the Al_3Mg_2 and $Al_{12}Mg_{17}$ intermetallic layers at a temperature of 400 °C using the initial experimental data on the layer-growth kinetics from Ref. [64]

t ($\times 10^3$ s)	x ($\times 10^{-4}$ m)	y ($\times 10^{-4}$ m)	k_{1Al2} ($\times 10^{-13}$ m^2 s^{-1})	k_{1Mg2} ($\times 10^{-14}$ m^2 s^{-1})
30	0.58	0.03	-	-
75	1.58	0.18	5.06	4.71
170	2.43	0.53	4.70	9.32
255	3.08	0.88	4.84	12.10
340	3.63	0.98	4.40	9.26
425	4.13	1.03	4.11	8.42
600	4.78	1.33	4.13	9.77
865	5.93	1.53	4.27	9.38
1205	6.73	1.98	4.40	11.20
1525	7.88	2.23	4.53	10.50
2596	10.00	2.73	-	-

Average values: $k_{1Al2} = 4.49\times 10^{-13}$ m^2 s^{-1}, $k_{1Mg2} = 9.41\times 10^{-14}$ m^2 s^{-1}.

Since the experimental dependences become smoothed as a result of this procedure (solid lines of Fig. 3.13), all the values of k_{1Al2} ($k_{1Al2} = 3.40\times 10^{-13}$ m^2 s^{-1}) thus found are identical. The same applies to k_{1Mg2} ($k_{1Mg2} = 9.37\times 10^{-14}$ m^2 s^{-1}).

Comparing these with the average values of k_{1Al2} and k_{1Mg2} found numerically from the experimental points by direct calculations, it may be concluded that both sets of the constants agree fairly well, providing evidence for the validity of the analytical treatment employed. Physically, the value of k_{1Al2} thus obtained is the reaction-diffusion coefficient D_{Al} of aluminium atoms in the Al_3Mg_2 compound lattice, whereas the value of k_{1Mg2} is the reaction-diffusion coefficient D_{Mg} of magnesium atoms in the $Al_{12}Mg_{17}$ compound lattice in the course of simultaneous growth of both compounds.

As the melting points of aluminium (660 °C) and magnesium (651 °C) are very close, the large difference in growth rates of the Al_3Mg_2 and $Al_{12}Mg_{17}$ intermetallic compound layers appears to be due to the difference in atomic radii of those elements. The atomic radius of aluminium (0.143 nm) is less than that of magnesium (0.160 nm) [66, 67]. Therefore, the Al_3Mg_2 layer growing at the expense of diffusion of smaller aluminium atoms can reasonably be expected to grow faster compared to the $Al_{12}Mg_{17}$ layer growing at the expense of diffusion of greater magnesium atoms. Note that both intermetallic compounds have similar (cubic) structures.

Table 3.2. Evaluation of diffusional constants k_{1Al2} and k_{1Mg2} from the system of equations (3.53) for the Al_3Mg_2 and $Al_{12}Mg_{17}$ intermetallic layers at a temperature of 400 °C using the smoothed experimental data on the layer-growth kinetics

t ($\times 10^3$ s)	x ($\times 10^{-4}$ m)	y ($\times 10^{-4}$ m)	k_{1Al2} ($\times 10^{-13}$ m^2 s^{-1})	k_{1Mg2} ($\times 10^{-14}$ m^2 s^{-1})
30	0.97	0.31	3.40	9.37
75	1.54	0.49	3.40	9.37
170	2.31	0.74	3.40	9.37
255	2.83	0.91	3.40	9.37
340	3.27	1.05	3.40	9.37
425	3.66	1.18	3.40	9.37
600	4.34	1.40	3.40	9.37
865	5.21	1.68	3.40	9.37
1205	6.15	1.98	3.40	9.37
1525	6.92	2.23	3.40	9.37
2596	9.03	2.91	3.40	9.37

Average values: $k_{1Al2} = 3.40\times10^{-13}$ m^2 s^{-1}, $k_{1Mg2} = 9.37\times10^{-14}$ m^2 s^{-1}.

The Al–Mg binary system is worth further investigation, especially in the region of non-parabolic layer-growth kinetics. Marker experiments are also desirable, with inert markers embedded in both intermetallic layers, to reveal directly the contributions of the components Al and Mg to the growth process of the Al_3Mg_2 and $Al_{12}Mg_{17}$ intermetallic compound layers.

3.9: Two compound layers: comparison of diffusional and physico-chemical approaches

Main distinctions between the conventional diffusional approach and the proposed physico-chemical one for the case of formation of two compound layers are briefly summarised in Table 3.3. To avoid misleading conclusions, it would be desirable to take account of these distinctions when studying the growth kinetics of two compound layers.

Most significant features of the mechanism of formation of two compound layers are partly visualised in Fig. 3.15 where a scheme for the case of formation of one compound layer is also included for comparison. Note that two compound layers can in principle grow simultaneously, whatever their growth regime (either reaction controlled or diffusion controlled).

From these schemes, it is seen that one compound layer can always grow at the expense of diffusion of both components. Two compound layers can grow at the expense of diffusion of both components across their bulks only under conditions of reaction control. Under conditions of diffusion control, each of them grows exclusively at the expense of diffusion of one component (with which a given layer borders).

3.10: Two compound layers: short conclusions

1. In the reaction controlled regime, the solid layer of each of two chemical compounds A_pB_q and A_rB_s grows at the expense of two partial chemical reactions taking place at its interfaces with adjacent phases.

2. Each of two growing compound layers is a product in the two and a reactant in one of the four partial chemical reactions taking place in the $A–A_pB_q–A_rB_s–B$ system.

3. In most reaction couples, the layer formed first should reach a certain minimal thickness before the second layer can occur. Both compound layers will then grow simultaneously until one of initial substances A or B is entirely consumed.

4. In any binary system, the sequence of formation of compound layers is governed by the rate of chemical transformations (partial chemical reactions) at phase interfaces.

5. The layer thickness-time kinetic relationships are in general rather complicated, not merely parabolic. Depending on the values of the chemical and physical (diffusional) constants, their different portions can be described by linear, paralinear, asymptotic, parabolic and other laws.

6. In the diffusion controlled regime, growth of each of two compound layers is due to one partial chemical reaction taking place at its common interface with another growing layer. In this case, only the A atoms diffuse across the A_pB_q layer adjacent to initial phase A, while only the B atoms diffuse across the A_rB_s layer adjacent to initial phase B. No partial chemical reactions proceed at the $A–A_pB_q$ and $A_rB_s–B$ interfaces in view of the lack of appropriate diffusing atoms.

7. In the case of two compound layers, even growing under conditions of diffusion control, application of Matano's analysis and calculation of integrated diffusion coefficients do not seem to be sufficiently substantiated. Such quantities can hardly have any physical meaning.

Table 3.3. Comparison of diffusional and physico-chemical approaches in the case of two compound layers

Diffusional approach	Physico-chemical approach
1. Both compound layers occur and grow simultaneously.	1. Occurrence of two compound layers is sequential rather than simultaneous.
2. Layer-growth kinetics are parabolic.	2. A variety of kinetic laws may be observed experimentally.
3. Both compound layers can always grow at the expense of diffusion of both components.	3. Under conditions of reaction control, both compound layers can generally grow at the expense of diffusion of both components. Under conditions of diffusion control, each of them grows only at the expense of diffusion of that component with which it borders.

1. Growth of one compound layer: reaction or diffusion control

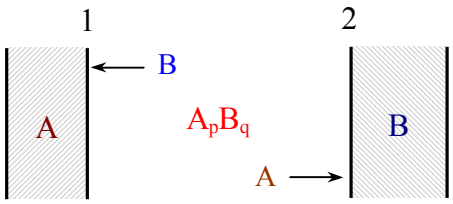

2a. Growth of two compound layers: reaction control

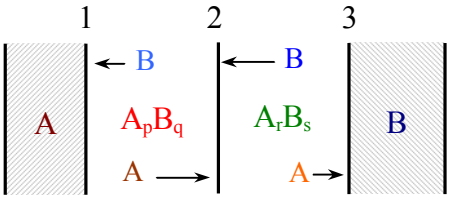

2b. Growth of two compound layers: diffusion control

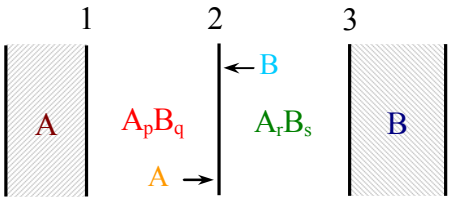

Fig. 3.15. Comparative schematic diagrams to illustrate the process of solid-state growth of one and two compound layers.

4: Occurrence of multiple compound layers at the *A–B* interface

Many binary systems are multiphase, with the number of chemical compounds on the *A–B* equilibrium phase diagram reaching or even exceeding ten [61, 62, 68-72]. Therefore, the primary question the experimentalist faced when starting to investigate a particular reaction couple is how many and what compounds, of their variety shown on the phase diagram, can occur as separate layers at the interface between initial elementary substances *A* and *B* under given conditions of temperature and pressure.

In the framework of diffusional considerations all chemical compounds of a multiphase binary system, whatever their number, are assumed to simultaneously form individual layers which must grow according to a parabolic law during isothermal annealing of the *A–B* reaction couple. This misleading assumption can readily be found in numerous papers, monographs and, unfortunately, even textbooks. Though often stated to follow from the equilibrium phase diagram, in fact it has no reasonable substantiation.

What actually follows from the equilibrium phase diagram of any binary system is (*i*) what compounds *may*, not *should*, form as individual layers at the interface between substances *A* and *B* and (*ii*) the final state of the *A–B* reaction couple after prolonged isothermal annealing, which only depends on the amounts of initial substances taken. The phase diagram by no means dictates that those compound layers must necessarily occur simultaneously. Moreover, from the point of view of phase equilibria, the number of compound layers can be expected to decrease rather than to increase with passing time since only two phases must remain in the equilibrium state.

In most reaction couples, part of compound layers are known to be missing, with only one or two layers growing at the *A–B* interface, irrespective of the number of chemical compounds on the appropriate phase diagram. The cases where three or more compound layers were *present* and the more so *grew simultaneously* between elementary substances *A* and *B* are very rare against the background of the cases where one or two layers were formed. Consider a few instructive examples.

Though there are several oxides in the Ti–O binary system, the TiO_2 layer dominates during oxidation of titanium [27]. Of eight intermetallics of the Zr–Al binary system, only the $ZrAl_3$ layer is known to grow at the Zr–Al interface at temperatures below the melting point of aluminium. This is typical of most transition metal-aluminium binary systems [73]). A single layer of the $CuCd_3$ compound occurs between Cu and Cd (four intermetallics on the Cu–Cd phase diagram) [74].

Two layers Ni_5Sb_2 and NiSb are formed at the Ni–Sb interface (five intermetallics on the phase diagram) [75]. The layers of Mo_5Si_3 and $MoSi_2$ occur in Mo–Si diffusion couples, while the formation of Mo_3Si is not observed [76, 77]. The Cu_5Zn_8 and $CuZn_5$ layers is found to grow between Cu and Zn, with the third intermetallic compound CuZn of the Cu–Zn binary system being missing [78, 79].

Simultaneous growth of two intermetallic layers is observed in Mo–Ni [80] and Mo–Ir [81] diffusion couples (three and four intermetallics on appropriate phase diagrams). Compact layers of one or two compounds are known to form in almost all transition metal-silicon reaction couples [82-84]. The same applies to numerous other heterogeneous systems of different chemical nature [22, 85-87]. Note that even in those cases where multiple compound layers were present at the *A–B* interface, two layers were dominating [88-90].

It should be emphasised that not always the multilayered structure of the transition zone between elementary substances *A* and *B* is a result of simultaneous isothermal formation of chemical compounds. Additional compound layers may readily occur during cooling, if slow, because the reaction usually takes place at elevated temperatures, while the layers grown are then investigated after cooling down to room temperature. Another main reason for the formation of additional layers may be the disruption of contact between the phases involved into the interaction, due to mechanical stresses associated with thermal expansion and volume effect. As a result, the examined reaction couple is split into at least two new independent couples. In those, the other compound layers, lacking from the previous couple, may occur. Clearly, in such a case, at least one of the former layers must shrink, up to its full disappearance, as is observed, for example, with the PtSb compound layer in Pt–Sb diffusion couples [91].

However, as evidenced from the available experimental data, not always even these secondary factors do lead to any significant increase in the number of chemical compound layers at the *A–B* interface. Not only the *simultaneous parabolic growth* of eight or ten compound layers, but even their *simultaneous presence* was never observed experimentally.

To explain the absence of certain compound layers from the interface of initial substances *A* and *B*, the following two reasons are most frequently put forward.

(1) Difficulties with nucleating a new phase (see, for example, Refs [35, 92]). This may take place in particular cases. However, generally the difficulties with nucleating new phases in a heterogeneous system appear to be too exaggerated. If sufficiently clean surfaces of initial phases capable of forming chemical compounds are brought into intimate contact, the interaction resulting in chemical bonding is known to start at relatively low temperatures even in reaction couples consisting of substances with very high melting points.

In this connection, the results of an analysis of the nucleation process, obtained by F.M. d'Heurle [93] for transition-metal silicides, appear to be worth consideration. F.M. d'Heurle evaluated a specific thickness of the layers (an analogue of the critical radius of nuclei in a homogeneous system) for compounds of the Ni–Si binary system.

For Ni_2Si, its value was found to be 0.15 nm, *i.e*. the "nucleus" does not contain even one lattice unit. Although higher values were obtained for other nickel silicides, they never exceeded 1 nm. Therefore, the nucleation process can hardly play any significant role in the formation of most transition-metal silicides. This conclusion is likely to be valid for any other chemical compound layer.

The nucleation process in heterogeneous systems is considered from a physico-chemical viewpoint, for example, in the book edited by W.E. Garner [94]. It might be interesting for the reader to compare it with physical considerations of K.P. Gurov *et al*. [92] and A.M. Gusak *et al*. [35].

(2) The low layer-growth rate due to the small value of the product $D\Delta c$, where D is the diffusion coefficient and Δc is the width of the range of homogeneity of a chemical compound. Firstly, there is no straightforward relation between the width of the homogeneity range and the growth rate of the layer of a chemical compound. Secondly, if the absence of a certain compound layer were a consequence of the low growth rate, its occurrence in the *A–B* reaction couple would only depend on the duration of interaction between initial substances.

The experimental data are known providing evidence that these reasons for the absence of some part of the compounds of a multiphase system at the *A–B* interface are definitely not decisive. For example, F.J.J. van Loo [95] carried out isothermal annealing of Ti–Ti_3Al–TiAl–$TiAl_2$–$TiAl_3$–Al specimens consisting of all the phases of the Ti–Al binary system at 625 °C for 15 hours. Instead of the parabolic growth predicted by the diffusional theory, the layers of Ti_3Al, TiAl and $TiAl_2$ disappeared and only the $TiAl_3$ layer remained.

Note that all these intermetallic compounds are thermodynamically stable at 625 °C. This experiment has convincingly shown that, firstly, all the compound layers of a multiphase system present in the *A–B* reaction couple should not necessarily grow during its isothermal annealing and, secondly, nucleating new phases does not play in the solid-state systems that role which is attributed to them.

In the case under consideration, even the layers of the already existing compounds that clearly need no nucleation did not grow. Only the layer of the $TiAl_3$ intermetallic compound, which is the first to occur at the Ti–Al interface, grew. The layers of the remaining compounds were consumed during its growth and therefore sequentially disappeared with passing time. These findings have been confirmed by subsequent experiments with much thinner artificially prepared Ti–Ti_3Al–Al and Ti–TiAl–Al specimens [96].

It is worth noting that the intermetallic compound $TiAl_3$ is a stoichiometric phase without any noticeable range of homogeneity, whereas the other intermetallics of the Ti–Al binary system have the homogeneity ranges of 1 to 12 at.% [61, 62]. Nonetheless, the $TiAl_3$ layer grows much faster than do those. In such a case, in order that the product $D\Delta c$ be a real reason for the fast growth of the $TiAl_3$ layer, the diffusion coefficient D must clearly have an infinitely high value. Physically, this is hardly possible.

It should be emphasised that according to the diffusional theory any chemical compound layer once formed cannot then disappear during isothermal annealing of the *A–B* reaction couple because its growth rate, $dx/dt \sim \partial c/\partial x$, increases with decreasing thickness and tends to infinity, as $x \to 0$. It is therefore usually assumed that the layers do not disappear completely, but their thickness decreases to such an extent that they become unobservable experimentally.

Until recently, when it was only possible to examine compound layers with a thickness of the order of 1 μm or greater, experimentalists were forced to believe in this explanation. At present, however, when the phase identity, chemical composition, crystallographic structure and rate of formation of chemical compound layers a few nanometers thick can readily be determined, this belief lost any experimental support. At smaller thicknesses of a growing layer the concept *phase* clearly loses its physical meaning since, in order to be identified as such, any phase must accommodate at least a few crystal-lattice units across the layer width.

Therefore, it appears much more reasonable to assume that if the layers of certain compounds cannot be revealed in the *A–B* reaction couple, both in thin films and massive specimens, with the help of sufficiently sensitive experimental techniques then they are in all probability merely *missing* from that couple, and to attempt to find out the real reasons for this phenomenon. Such an attempt will be undertaken in this chapter.

4.1: Partial chemical reactions at the interfaces of the *A–B* reaction couple

To understand the peculiarities of multiple layer formation, it suffices to consider the *A–B* binary system with three chemical compounds A_pB_q, A_rB_s and A_lB_n on the phase diagram (Fig. 4.1). Analysis of the process of their occurrence at the *A–B* interface is similar to that of two compound layers (see Chapter 3). First of all, the equations of partial chemical reactions taking place at phase interfaces must be written. These are as follows.

Layer	Interface	Partial chemical reaction	
A_pB_q	1	$qB_{dif} + pA_{surf} = A_pB_q,$	(4.1_1)
	2	$(sp - qr)A_{dif} + qA_rB_s = sA_pB_q,$	(4.1_2)
A_rB_s	2	$(sp - qr)B_{dif} + rA_pB_q = pA_rB_s,$	(4.2_1)
	3	$(rn - ls)A_{dif} + sA_lB_n = nA_rB_s,$	(4.2_2)
A_lB_n	3	$(rn - ls)B_{dif} + lA_rB_s = rA_lB_n,$	(4.3_1)
	4	$lA_{dif} + nB_{surf} = A_lB_n.$	(4.3_2)

As previously, all these reactions are assumed to be independent in the sense that the elementary act of each of them has no effect on the elementary acts of the others.

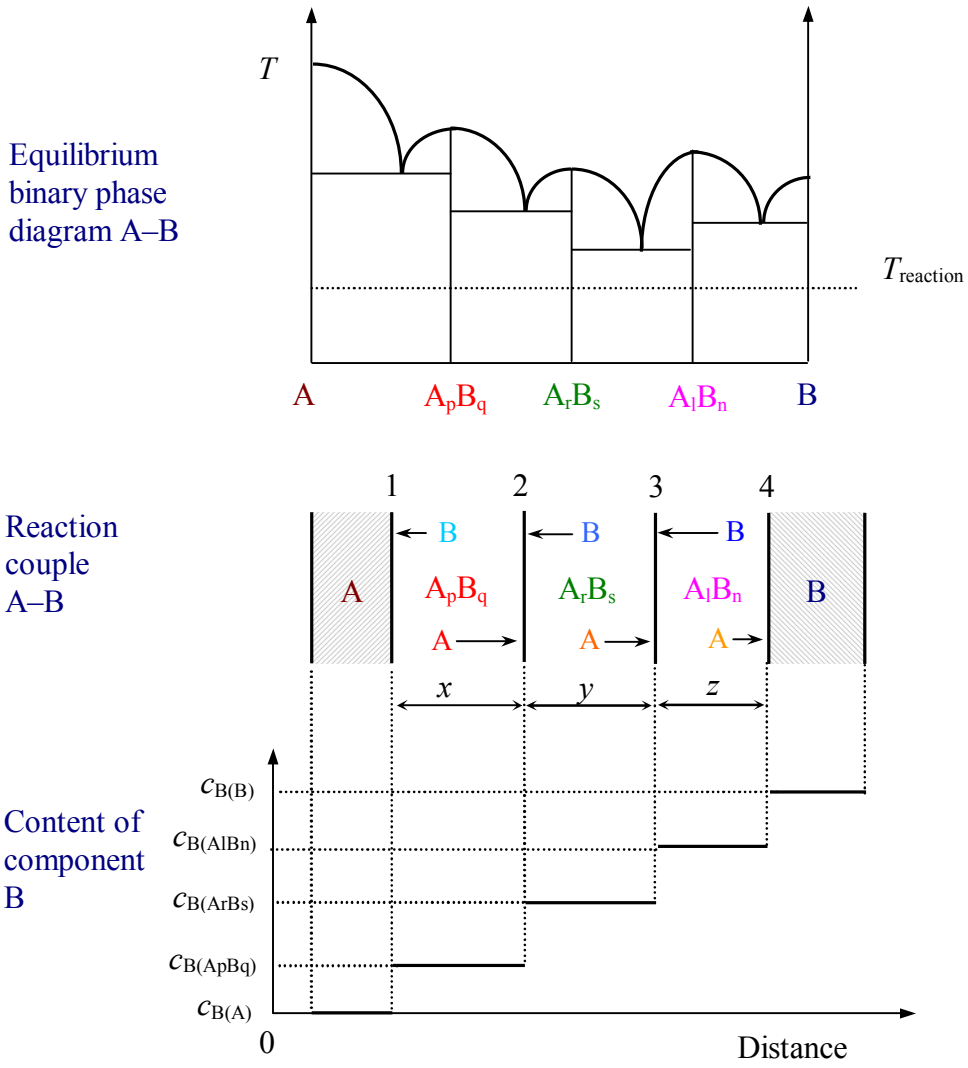

Fig. 4.1. Schematic diagram to illustrate the process of formation of three chemical compound layers A_pB_q, A_rB_s and A_lB_n between mutually insoluble elementary substances A and B.

Partial chemical reactions (4.1_1)-(4.3_2) cause the changes in thickness of appropriate compound layers. During the time dt, reactions (4.1_1) and (4.1_2) lead to the increase of the thickness of the A_pB_q layer by dx_{B1} at interface 1 and by dx_{A2} at interface 2 (Fig. 4.2). Reaction (4.2_1) resulting in the increase of the thickness of the A_rB_s layer by dy_{B2} at interface 2, leads simultaneously to the decrease in thickness of the A_pB_q layer by $dx_{-}^{(2)}$ at the same interface 2. The thickness of the A_rB_s layer also increases by dy_{A3} at interface 3 as a result of reaction (4.2_2). At the same time, its thickness decreases by $dy_{-}^{(2)}$ at interface 2 and by $dy_{-}^{(3)}$ at interface 3 since the A_rB_s phase is consumed in the course of reactions (4.1_2) and (4.3_1). Reactions

(4.3$_1$) and (4.3$_2$) cause the increases of the thickness of the A_lB_n layer during dt by dz_{B3} and dz_{A4} at interfaces 3 and 4, respectively. Again, the thickness of this layer decreases by $dz_{-}^{(3)}$ at interface 3 as a result of reaction (4.2$_2$).

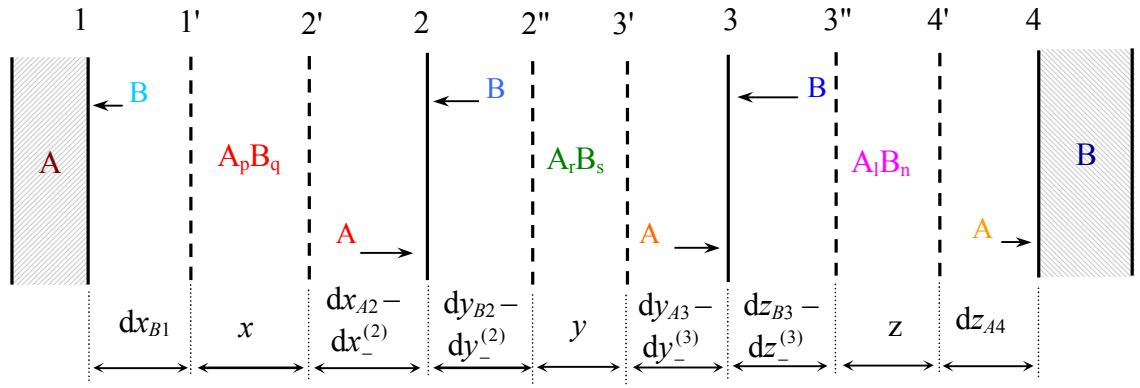

Fig. 4.2. Schematic diagram to illustrate the changes in thickness of three chemical compound layers A_pB_q, A_rB_s and A_lB_n growing between mutually insoluble elementary substances A and B at the expense of diffusion of both components (reaction control).

Position of interface 1 is seen to depend on the occurrence of only one partial chemical reaction (4.1$_1$). Similarly, position of interface 4 only depends on partial chemical reaction (4.3$_2$). Position of interface 2 is determined by two partial chemical reactions (4.1$_2$) and (4.2$_1$) taking place simultaneously. The same applies to position of interface 3, depending on partial chemical reactions (4.2$_2$) and (4.3$_1$).

The thickness of the A_pB_q layer as well as the A_lB_n layer is thus determined by the rate of occurrence of two partial chemical reactions. The thickness of the A_rB_s layer located between them depends on the rate of four partial chemical reactions. The same applies to any other compound layer of a multiphase system, having no direct contact with either of initial phases, if the number of compounds on the phase diagram exceeds three.

4.2: A system of differential equations describing the process of formation of three compound layers between elementary substances *A* and *B*

Application of the postulate about the summation of the time of diffusion of reacting atoms and the time of subsequent chemical transformations with their participation yields

$$\mathrm{d}t = \mathrm{d}t_{\mathrm{dif}}^{(B\to A_pB_q)} + \mathrm{d}t_{\mathrm{chem}}^{(B\to A_pB_q)}, \qquad (4.4_1)$$

$$\mathrm{d}t = \mathrm{d}t_{\mathrm{dif}}^{(A\to A_pB_q)} + \mathrm{d}t_{\mathrm{chem}}^{(A\to A_pB_q)}, \qquad (4.4_2)$$

$$\mathrm{d}t = \mathrm{d}t_{\mathrm{dif}}^{(B\to A_rB_s)} + \mathrm{d}t_{\mathrm{chem}}^{(B\to A_rB_s)}, \qquad (4.5_1)$$

$$\mathrm{d}t = \mathrm{d}t_{\mathrm{dif}}^{(A\to A_rB_s)} + \mathrm{d}t_{\mathrm{chem}}^{(A\to A_rB_s)}, \qquad (4.5_2)$$

$$\mathrm{d}t = \mathrm{d}t_{\mathrm{dif}}^{(B\to A_lB_n)} + \mathrm{d}t_{\mathrm{chem}}^{(B\to A_lB_n)}, \qquad (4.6_1)$$

$$\mathrm{d}t = \mathrm{d}t_{\mathrm{dif}}^{(A\to A_lB_n)} + \mathrm{d}t_{\mathrm{chem}}^{(A\to A_lB_n)}, \qquad (4.6_2)$$

where the subscripts and superscripts have the former meaning (see Section 3.2).

Assuming that the time of diffusion of the *A* or *B* atoms is directly proportional to both the increase in thickness of the layer and its total thickness, while the time of chemical transformations in which these atoms then take part is directly proportional to the increase in thickness of the layer and is independent of its total thickness, one obtains the following relations:

$$\mathrm{d}t_{\mathrm{dif}}^{(B\to A_pB_q)} = \frac{x}{k_{1B1}}\mathrm{d}x_{B1} \quad \text{and} \quad \mathrm{d}t_{\mathrm{chem}}^{(B\to A_pB_q)} = \frac{1}{k_{0B1}}\mathrm{d}x_{B1}, \qquad (4.7_1)$$

$$\mathrm{d}t_{\mathrm{dif}}^{(A\to A_pB_q)} = \frac{x}{k'_{1A2}}\mathrm{d}x_{A2} \quad \text{and} \quad \mathrm{d}t_{\mathrm{chem}}^{(A\to A_pB_q)} = \frac{1}{k'_{0A2}}\mathrm{d}x_{A2}, \qquad (4.7_2)$$

$$\mathrm{d}t_{\mathrm{dif}}^{(B\to A_rB_s)} = \frac{y}{k'_{1B2}}\mathrm{d}y_{B2} \quad \text{and} \quad \mathrm{d}t_{\mathrm{chem}}^{(B\to A_rB_s)} = \frac{1}{k'_{0B2}}\mathrm{d}y_{B2}, \qquad (4.8_1)$$

$$\mathrm{d}t_{\mathrm{dif}}^{(A\to A_rB_s)} = \frac{y}{k'_{1A3}}\mathrm{d}y_{A3} \quad \text{and} \quad \mathrm{d}t_{\mathrm{chem}}^{(A\to A_rB_s)} = \frac{1}{k'_{0A3}}\mathrm{d}y_{A3}, \qquad (4.8_2)$$

$$\mathrm{d}t_{\mathrm{dif}}^{(B\to A_lB_n)} = \frac{z}{k_{1B3}}\mathrm{d}z_{B3} \quad \text{and} \quad \mathrm{d}t_{\mathrm{chem}}^{(B\to A_lB_n)} = \frac{1}{k_{0B3}}\mathrm{d}z_{B3}, \qquad (4.9_1)$$

$$\mathrm{d}t_{\mathrm{dif}}^{(A\to A_lB_n)} = \frac{z}{k_{1A4}}\mathrm{d}z_{A4} \quad \text{and} \quad \mathrm{d}t_{\mathrm{chem}}^{(A\to A_lB_n)} = \frac{1}{k_{0A4}}\mathrm{d}z_{A4}. \qquad (4.9_2)$$

Hence,

$$\mathrm{d}t = \left(\frac{x}{k_{1B1}} + \frac{1}{k_{0B1}}\right)\mathrm{d}x_{B1}, \qquad (4.10_1)$$

$$\mathrm{d}t = \left(\frac{x}{k'_{1A2}} + \frac{1}{k'_{0A2}}\right)\mathrm{d}x_{A2}, \qquad (4.10_2)$$

$$\mathrm{d}t = \left(\frac{y}{k'_{1B2}} + \frac{1}{k'_{0B2}} \right) \mathrm{d}y_{B2}, \tag{4.11$_1$}$$

$$\mathrm{d}t = \left(\frac{y}{k'_{1A3}} + \frac{1}{k'_{0A3}} \right) \mathrm{d}y_{A3}, \tag{4.11$_2$}$$

$$\mathrm{d}t = \left(\frac{z}{k_{1B3}} + \frac{1}{k_{0B3}} \right) \mathrm{d}z_{B3}, \tag{4.12$_1$}$$

$$\mathrm{d}t = \left(\frac{z}{k_{1A4}} + \frac{1}{k_{0A4}} \right) \mathrm{d}z_{A4}. \tag{4.12$_2$}$$

Since equations (4.10$_1$)-(4.12$_2$) are assumed to be independent of each other, the increases in thickness of the A_pB_q, A_rB_s and A_lB_n layers can be expressed from them as follows

$$\mathrm{d}x_{B1} = \frac{k_{0B1}}{1 + \frac{k_{0B1}x}{k_{1B1}}} \mathrm{d}t, \tag{4.13$_1$}$$

$$\mathrm{d}x_{A2} = \frac{k'_{0A2}}{1 + \frac{k'_{0A2}x}{k'_{1A2}}} \mathrm{d}t, \tag{4.13$_2$}$$

$$\mathrm{d}y_{B2} = \frac{k'_{0B2}}{1 + \frac{k'_{0B2}y}{k'_{1B2}}} \mathrm{d}t, \tag{4.14$_1$}$$

$$\mathrm{d}y_{A3} = \frac{k'_{0A3}}{1 + \frac{k'_{0A3}y}{k'_{1A3}}} \mathrm{d}t, \tag{4.14$_2$}$$

$$\mathrm{d}z_{B3} = \frac{k_{0B3}}{1 + \frac{k_{0B3}z}{k_{1B3}}} \mathrm{d}t, \tag{4.15$_1$}$$

$$\mathrm{d}z_{A4} = \frac{k_{0A4}}{1 + \frac{k_{0A4}z}{k_{1A4}}} \mathrm{d}t. \tag{4.15$_2$}$$

The increase of the thickness of the A_pB_q layer during the time dt, due to partial chemical reactions (4.1_1) and (4.1_2), is (see Fig. 4.2)

$$\mathrm{d}x_{+} = \mathrm{d}x_{B1} + \mathrm{d}x_{A2}. \tag{4.16}$$

The decrease of the thickness of this layer during the same time dt as a result of partial chemical reaction (4.2_1) in which the A_pB_q compound is a reactant, is equal to (see Section 3.2)

$$\mathrm{d}x_{-}^{(2)} = \frac{rg_1}{p}\mathrm{d}y_{B2}, \tag{4.17}$$

where $g_1 = V_{A_pB_q} / V_{A_rB_s}$, V is the molar volume of an appropriate compound. Thus, the total change, dx, of the thickness of the A_pB_q layer during the time dt is

$$\mathrm{d}x = \mathrm{d}x_{+} - \mathrm{d}x_{-}^{(2)} = \mathrm{d}x_{B1} + \mathrm{d}x_{A2} - \frac{rg_1}{p}\mathrm{d}y_{B2}. \tag{4.18}$$

For the A_rB_s layer, the increase of its thickness during the time dt is

$$\mathrm{d}y_{+} = \mathrm{d}y_{B2} + \mathrm{d}y_{A3}. \tag{4.19}$$

Unlike the A_pB_q compound which is only consumed by one partial chemical reaction (4.2_1), the A_rB_s compound is a reactant of two partial chemical reactions (4.1_2) and (4.3_1). Therefore, during dt the thickness of the A_rB_s layer decreases by

$$\mathrm{d}y_{-}^{(2)} = \frac{q}{sg_1}\mathrm{d}x_{A2} \tag{4.20}$$

at interface 2 as a result of reaction (4.1_2) and by

$$\mathrm{d}y_{-}^{(3)} = \frac{lg_2}{r}\mathrm{d}z_{B3} \tag{4.21}$$

at interface 3 as a result of reaction (4.3_1), where $g_2 = V_{A_rB_s} / V_{A_lB_n}$.

Hence, the total change, dy, of the thickness of the A_rB_s layer during the time dt is

$$\mathrm{d}y = \mathrm{d}y_{B2} + \mathrm{d}y_{A3} - \frac{q}{sg_1}\mathrm{d}x_{A2} - \frac{lg_2}{r}\mathrm{d}z_{B3}\ . \tag{4.22}$$

Evidently, for the A_lB_n layer,

$$\mathrm{d}z_{+} = \mathrm{d}z_{B3} + \mathrm{d}z_{A4} \tag{4.23}$$

and

$$\mathrm{d}z_{-}^{(3)} = \frac{s}{ng_2}\mathrm{d}y_{A3}, \tag{4.24}$$

with the total change, dz, of its thickness during the time dt being

$$\mathrm{d}z = \mathrm{d}z_{B3} + \mathrm{d}z_{A4} - \frac{s}{ng_2}\mathrm{d}y_{A3}. \tag{4.25}$$

The required system of non-linear differential equations describing the growth rates of three chemical compound layers A_pB_q, A_rB_s and A_lB_n at the interface between two mutually insoluble solid elementary substances A and B is obtained by inserting the expressions for the changes in layer thicknesses from equations (4.13$_1$)-(4.15$_2$) into equations (4.18), (4.22) and (4.25), giving

$$\frac{\mathrm{d}x}{\mathrm{d}t} = \frac{k_{0B1}}{1+\dfrac{k_{0B1}x}{k_{1B1}}} + \frac{k'_{0A2}}{1+\dfrac{k'_{0A2}x}{k'_{1A2}}} - \frac{rg_1}{p}\frac{k'_{0B2}}{1+\dfrac{k'_{0B2}y}{k'_{1B2}}}, \tag{4.26$_1$}$$

$$\frac{\mathrm{d}y}{\mathrm{d}t} = \frac{k'_{0B2}}{1+\dfrac{k'_{0B2}y}{k'_{1B2}}} + \frac{k'_{0A3}}{1+\dfrac{k'_{0A3}y}{k'_{1A3}}} - \frac{q}{sg_1}\frac{k'_{0A2}}{1+\dfrac{k'_{0A2}x}{k'_{1A2}}} - \frac{lg_2}{r}\frac{k_{0B3}}{1+\dfrac{k_{0B3}z}{k_{1B3}}}, \tag{4.26$_2$}$$

$$\frac{\mathrm{d}z}{\mathrm{d}t} = \frac{k_{0B3}}{1+\dfrac{k_{0B3}z}{k_{1B3}}} + \frac{k_{0A4}}{1+\dfrac{k_{0A4}z}{k_{1A4}}} - \frac{s}{ng_2}\frac{k'_{0A3}}{1+\dfrac{k'_{0A3}y}{k'_{1A3}}}. \tag{4.26$_3$}$$

Undertaking no attempt to find a general solution to this rather complicated system, let us analyse the most important consequences resulting immediately from the differential equations and their solutions in a few simplest limiting cases.

4.3: Initial linear growth of three compound layers

During certain initial period of time, the rates of diffusion of the A and B atoms do not play any significant role in determining the rates of formation of the A_pB_q, A_rB_s and A_lB_n layers. Their growth rates are only restricted by the rates of chemical transformations at the phase

interfaces, both types of the diffusing atoms being in great excess for the growth of each of the layers. This does not necessarily mean, however, that they will all occur and grow simultaneously in any reaction couple *A*–*B*.

At small thicknesses of the A_pB_q, A_rB_s and A_lB_n layers, the terms of the type k_0x/k_1 are evidently negligible in comparison with unity. Hence, the system of equations (4.26) is simplified to

$$\frac{\mathrm{d}x}{\mathrm{d}t} = k_{0B1} + k'_{0A2} - \frac{rg_1}{p}k'_{0B2}, \qquad (4.27_1)$$

$$\frac{\mathrm{d}y}{\mathrm{d}t} = k'_{0B2} + k'_{0A3} - \frac{q}{sg_1}k'_{0A2} - \frac{lg_2}{r}k_{0B3}, \qquad (4.27_2)$$

$$\frac{\mathrm{d}z}{\mathrm{d}t} = k_{0B3} + k_{0A4} - \frac{s}{ng_2}k'_{0A3}. \qquad (4.27_3)$$

From the system of equations (4.27), it follows that there may be a few ways of occurrence and further growth of the A_pB_q, A_rB_s and A_lB_n layers, depending on the values of the chemical constants k_0, the stoichiometry of the compounds and the ratio of their molar volumes.

(1) If the derivatives d*x*/d*t,* d*y*/d*t* and d*z*/d*t* are positive, then all three layers will occur and grow simultaneously according to a linear law from the very beginning of interaction of initial substances *A* and *B* (Fig. 4.3a).

(2) If the condition $k_{0B1} + k'_{0A2} = (rg_1/p)k'_{0B2}$ happens to be satisfied, then the thickness of the A_pB_q layer, if present, remains constant (Fig. 4.3b) or is equal to zero if this layer was lacking in the initial *A*–*B* couple.

(3) If $k_{0B1} + k'_{0A2} < (rg_1/p)k'_{0B2}$, then the thickness of the A_pB_q layer present initially will decrease up to its disappearance because d*x*/d*t* < 0 (Fig. 4.3c). Only the A_rB_s and A_lB_n layers will grow between initial substances *A* and *B*. In the absence of the A_pB_q layer, their growth kinetics are described by a system of two differential equations similar to (3.30)

$$\frac{\mathrm{d}y}{\mathrm{d}t} = k_{0B2} + k'_{0A3} - \frac{lg_2}{r}k_{0B3}, \qquad (4.28_1)$$

$$\frac{\mathrm{d}z}{\mathrm{d}t} = k_{0B3} + k_{0A4} - \frac{s}{ng_2}k'_{0A3}. \qquad (4.28_2)$$

Note that k_{0B2} is not equal to k'_{0B2} since the chemical reactions at the *A*–A_rB_s and A_pB_q–A_rB_s interfaces in the reacting systems *A*–A_rB_s–A_lB_n–*B* and *A*–A_pB_q–A_rB_s–A_lB_n–*B* are different. Indeed, in the former system the *B* atoms diffusing across the A_rB_s layer react at interface 2 with phase A, while in the latter with phase A_pB_q. In order that not to change the

numeration of all the interfaces shown in Fig. 4.1, both interfaces were designated by the same digit 2.

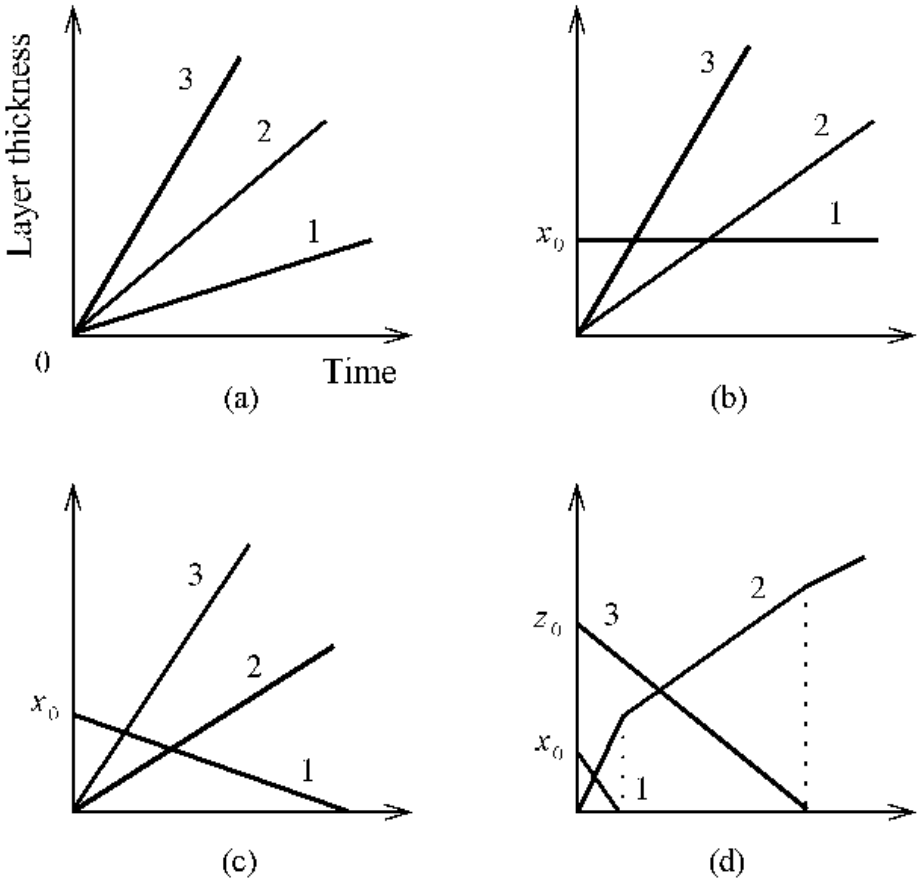

Fig. 4.3. Typical dependences of the thickness of the layers of three chemical compounds A_pB_q (line 1), A_rB_s (line 2) and A_lB_n (line 3) upon the time in an initial period of interaction of elementary substances A and B: (a) simultaneous linear growth of all three layers; (b) thickness of the A_pB_q layer remains constant, while the A_rB_s and A_lB_n layers grow linearly; (c) thickness of the A_pB_q layer decreases up to its complete disappearance, while the A_rB_s and A_lB_n layers grow linearly; (d) only the A_rB_s layer grows, while the A_pB_q and A_lB_n layers are gradually consumed until their disappearance.

(4) If $dx/dt < 0$ and $dz/dt < 0$, then the A_pB_q and A_lB_n layers cannot occur at all and therefore only the A_rB_s layer will grow at the interface between substances A and B according to a linear law (Fig. 4.3d). If the layers of all three compounds are present in initial specimens, the thickness of the A_pB_q and A_lB_n layers should decrease and they will disappear completely after some time, if of course the thickness of the A_rB_s layer does not exceed the minimal values necessary for the growth of these layers to start.

It should be noted that the disappearance of each of the A_pB_q and A_lB_n layers considerably reduces the rate of linear growth of the A_rB_s layer, as shown schematically in Fig. 4.3d, because the closer the compositions of adjacent non-growing phases to the composition of any growing compound layer, the greater is the growth rate of that layer. This question will be considered in more detail in Chapter 5.

4.4: Transition from linear to non-linear layer-growth kinetics

It is clear that the layer which has disappeared or was missing at the linear stage of reaction between substances A and B can then occur and grow again in the A–B reaction couple. Assume that the A_pB_q layer present initially has disappeared (Fig. 4.4).

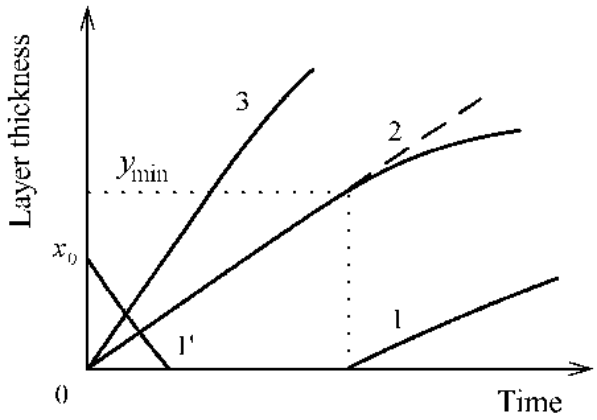

Fig. 4.4. Schematic illustration of the transition from the linear to non-linear stage of formation of the A_pB_q (lines 1′ and 1), A_rB_s (line 2) and A_lB_n (line 3) layers between elementary substances A and B. The A_pB_q layer present initially first disappears and then occurs and grows again after the A_rB_s layer has reached the minimal necessary thickness y_{min}.

Since the A_rB_s and A_lB_n layers gradually thicken with increasing reaction time, at a certain moment of time the term $k'_{0B2}y/k'_{1B2}$ in the denominator of equation (4.26_1) becomes significant in comparison with unity and therefore should be taken into account. This may lead to a change in the number of growing compound layers.

Indeed, increasing the thickness y of the A_rB_s layer reduces the value of the third term

$$\frac{rg_1}{p}\frac{k'_{0B2}}{1+\dfrac{k'_{0B2}y}{k'_{1B2}}}$$

on the right-hand side of equation (4.26_1). As its first two terms still remain almost constant and equal to k_{0B1} and k'_{0A2}, it is obvious that at a certain thickness $y_{\min}$ of this layer the equality

$$k_{0B1} + k'_{0A2} = \frac{rg_1}{p} \frac{k'_{0B2}}{1 + \frac{k'_{0B2} y_{\min}}{k'_{1B2}}} \tag{4.29}$$

will inevitably be satisfied.

Therefore, the derivative dx/dt becomes positive. This means that the A_pB_q layer will start to grow between the A and A_rB_s phases if, of course, the substance A is not consumed completely by that moment of time. The value $y_{\min}$ is again a minimal thickness of the A_rB_s layer to be attained before the A_pB_q layer can start growing (see Section 3.4).

4.5: Critical thicknesses of compound layers and their influence on layer-growth kinetics

It seems more likely, however, that the number of growing compound layers will decrease, not increase, with increasing time of interaction of initial substances A and B. This is due to the existence of critical layer thicknesses (see Sections 2.3.1 and 3.2).

Evidently, at some thickness, say of the A_pB_q layer, the flux of the A atoms across its bulk and the reactivity of the surface of the A_rB_s layer towards these atoms become equal. This is a critical thickness of the A_pB_q layer at which the equality

$$\mathrm{d}t_{\mathrm{dif}}^{(A \to A_pB_q)} = \mathrm{d}t_{\mathrm{chem}}^{(A \to A_pB_q)}$$

is satisfied for the reacting A atoms.

By applying similar equalities to equations (4.7_1)-(4.9_2), one obtains the expressions for the critical layer thicknesses

$$x_{1/2}^{(B)} = \frac{k_{1B1}}{k_{0B1}}, \tag{4.30_1}$$

$$x_{1/2}^{(A)} = \frac{k'_{1A2}}{k'_{0A2}}, \tag{4.30_2}$$

$$y_{1/2}^{(B)} = \frac{k'_{1B2}}{k'_{0B2}}, \tag{4.31_1}$$

$$y_{1/2}^{(A)} = \frac{k'_{1A3}}{k'_{0A3}}, \tag{4.31_2}$$

$$z_{1/2}^{(B)} = \frac{k_{1B3}}{k_{0B3}}\ , \qquad (4.32_1)$$

$$z_{1/2}^{(A)} = \frac{k_{1A4}}{k_{0A4}}\ . \qquad (4.32_2)$$

By comparing equations (2.17), (2.22), (3.28_1)-(3.29_2) and (4.30_1)-(4.32_2), it is easy to understand that some of the critical layer thicknesses are practically the same in all three reacting systems $A–A_pB_q–B$, $A–A_pB_q–A_rB_s–B$ and $A–A_pB_q–A_rB_s–A_lB_n–B$, while the others are different. Practically and not precisely the same, because the value of any critical thickness is dependent, though probably to a negligible extent, upon where the reacting atoms are diffusing from.

For example, the critical thicknesses of the A_pB_q layer with regard to component B are the same since in all the systems the B atoms diffusing across its bulk react with the same phase A. However, the critical thicknesses of the same A_pB_q layer with regard to component A in the reacting systems $A–A_pB_q–B$ and $A–A_pB_q–A_rB_s–B$ are different, while in the reacting systems $A–A_pB_q–A_rB_s–B$ and $A–A_pB_q–A_rB_s–A_lB_n–B$ they are the same. To avoid confusion, in some cases it would be necessary to use more complicated designations for the critical layer thicknesses. For brevity, the simplified designations are nonetheless employed throughout, relying upon the comprehension of the reader.

At $x = x_{1/2}^{(A)}$, all the A atoms diffusing across the A_pB_q layer are combined by the surface of the A_rB_s layer into the A_pB_q compound at interface 2 according to reaction (4.1_2). Therefore, at $x \geq x_{1/2}^{(A)}$ none of these atoms is available for reaction (4.2_2) leading to the growth of the A_rB_s layer and even more so for reaction (4.3_2) resulting in the formation of the A_lB_n layer. Thus, the A_rB_s and A_lB_n layers cannot grow at the expense of diffusion of component A if the growth regime of the A_pB_q layer is diffusion controlled with regard to this component in the theoretical definition, *i.e.* if $x > x_{1/2}^{(A)}$.

An unambiguous criterion to distinguish between the growth regimes of any compound layer is the availability or lack of a given kind of diffusing atoms for other layers of a multiphase binary system. Under conditions of reaction (chemical) control these atoms are still available, while under conditions of diffusion control already not, and this is all that is necessary to explain the absence of some part of compound layers from the $A–B$ reaction couple.

If $x > x_{1/2}^{(A)}$, then the second terms of equations (4.26_2) and (4.26_3) and also the third term of equation (4.26_3) simply have no physical meaning and therefore should be omitted whatever y and z. At $x >> x_{1/2}^{(A)}$, the system of equations (4.26) becomes

$$\frac{\mathrm{d}x}{\mathrm{d}t}=\frac{k_{0B1}}{1+\dfrac{k_{0B1}x}{k_{1B1}}}+\frac{k'_{1A2}}{x}-\frac{rg_1}{p}\frac{k'_{0B2}}{1+\dfrac{k'_{0B2}y}{k'_{1B2}}}, \qquad (4.33_1)$$

$$\frac{\mathrm{d}y}{\mathrm{d}t}=\frac{k'_{0B2}}{1+\dfrac{k'_{0B2}y}{k'_{1B2}}}-\frac{q}{sg_1}\frac{k'_{1A2}}{x}-\frac{lg_2}{r}\frac{k_{0B3}}{1+\dfrac{k_{0B3}z}{k_{1B3}}}, \qquad (4.33_2)$$

$$\frac{\mathrm{d}z}{\mathrm{d}t}=\frac{k_{0B3}}{1+\dfrac{k_{0B3}z}{k_{1B3}}}. \qquad (4.33_3)$$

The growth process of the A_lB_n layer is seen to be quite independent of those of two other layers because equation (4.33_3) contains neither x, nor y. Note that in this case all three layers can still grow simultaneously. The A_pB_q layer will grow at the expense of diffusion of both components, whereas the A_rB_s and A_lB_n layers will grow only at the expense of diffusion of component B, as illustrated in Fig. 4.5.

4.6: Diffusional stage of formation of compound layers

The conditions of formation of the A_pB_q, A_rB_s and A_lB_n layers are changed drastically when at $z > z_{1/2}^{(B)}$ the growth regime of the A_lB_n layer becomes diffusion controlled with regard to component B. In such a case, all the B atoms crossing the A_lB_n layer are combined by the surface of the A_rB_s layer into the A_lB_n compound at interface 3 (Fig. 4.6). Therefore, the A_pB_q and A_rB_s layers lose a source of B atoms for their growth.

It is clear that at $x > x_{1/2}^{(A)}$ and $z > z_{1/2}^{(B)}$ the A_pB_q layer can still grow at the expense of diffusion of component A, whereas the A_rB_s layer having no source of diffusing A and B atoms cannot grow at all. Thus, in the diffusional stage the A_pB_q layer grows at the expense of diffusion of the A atoms across its bulk from interface 1 to interface 2 and subsequent partial chemical reaction (4.1_2), while the A_lB_n layer grows at the expense of diffusion of the B atoms across its bulk from interface 4 to interface 3 and subsequent partial chemical reaction (4.3_1). The middle layer A_rB_s is consumed during their growth until it entirely disappears (Fig. 4.7).

In the late diffusional stage of formation of three compound layers ($x >> x_{1/2}^{(A)}$ and $z >> z_{1/2}^{(B)}$), the system of equations (4.26) becomes

$$\frac{\mathrm{d}x}{\mathrm{d}t}=\frac{k'_{1A2}}{x}, \qquad (4.34_1)$$

$$\frac{\mathrm{d}y}{\mathrm{d}t}=-\frac{q}{sg_1}\frac{k'_{1A2}}{x}-\frac{lg_2}{r}\frac{k_{1B3}}{z}, \qquad (4.34_2)$$

$$\frac{\mathrm{d}z}{\mathrm{d}t}=\frac{k_{1B3}}{z}. \qquad (4.34_3)$$

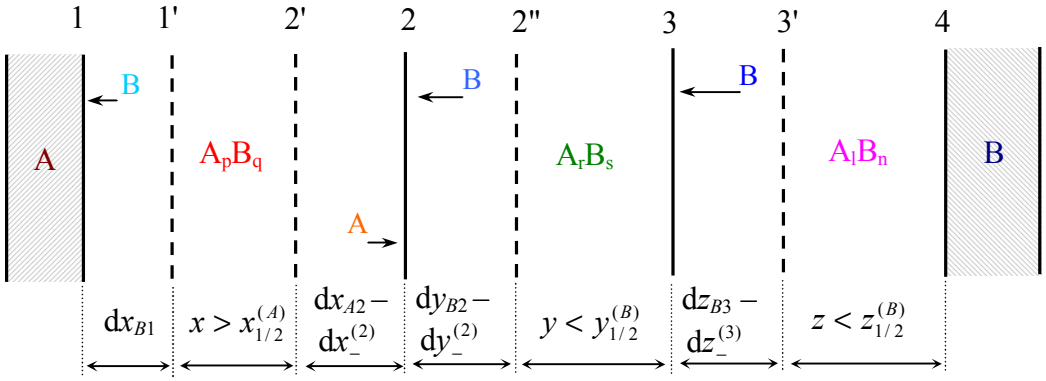

Fig. 4.5. Schematic diagram to illustrate the case where the A_pB_q layer grows at the expense of diffusion of both components, while the A_rB_s and A_lB_n layers grow at the expense of diffusion of only component B. The only source of diffusing A atoms for all the layers to grow is substance A. Since the growth regime of the A_pB_q layer adjacent to phase A is diffusion controlled with regard to component A ($x > x_{1/2}^{(A)}$), the A_rB_s and A_lB_n layers lose the source of diffusing A atoms and therefore grow no longer at the expense of diffusion of this component, whatever their thicknesses and growth regimes. The growing compound layers readily supply to each other only the remaining diffusing atoms not consumed during their own growth process. In regards to the supply of diffusing A atoms, the A_lB_n layer is seen to be in the most unfavourable position.

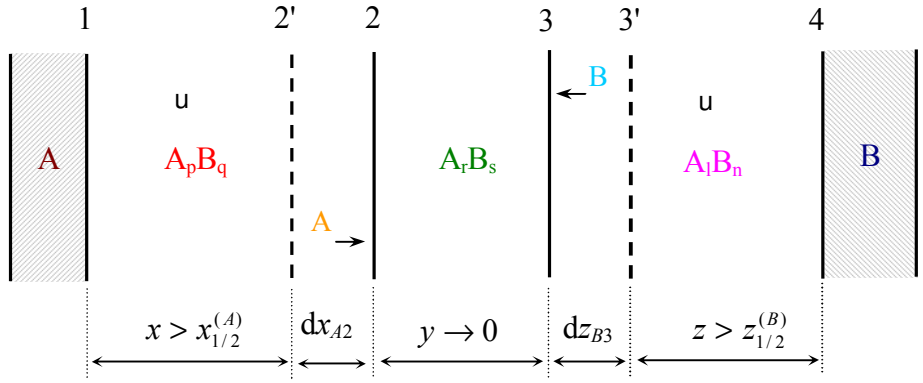

Fig. 4.6. Diffusional stage of formation of three chemical compound layers when $x > x_{1/2}^{(A)}$ and $z > z_{1/2}^{(B)}$. The A_pB_q layer grows only at interface 2 at the expense of diffusion of component A. At interface 1 its thickness does not increase because of the lack of diffusing B atoms. The A_lB_n layer grows only at interface 3 at the expense of diffusion of component B. At interface 4 its thickness does not increase because of the lack of diffusing A atoms. The A_rB_s layer having no source of both A and B atoms cannot grow at all and is therefore consumed until its full disappearance. The symbol u designates an inert marker.

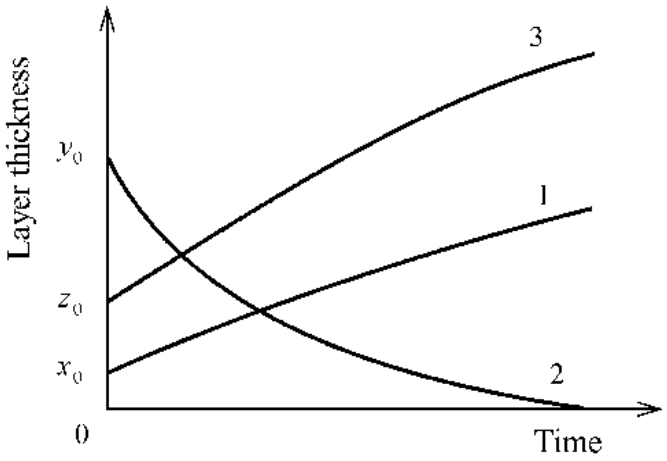

Fig. 4.7. Layer thickness-time plots for the A_pB_q, A_rB_s and A_lB_n layers in the diffusional stage of their formation at $x > x_{1/2}^{(A)}$ and $z > z_{1/2}^{(B)}$. The A_pB_q and A_lB_n layers grow (parabolically at $x >> x_{1/2}^{(A)}$ and $z >> z_{1/2}^{(B)}$), while the A_rB_s layer shrinks and eventually disappears completely.

The A_pB_q and A_lB_n layers are seen to grow parabolically, whereas the thickness of the A_rB_s layer will gradually decrease with passing time. Eventually, this layer disappears. It is easy to notice that in this case the values of the diffusional constants k'_{1A2} and k_{1B3} can readily be determined from the experimental dependences $x^2 - t$ and $z^2 - t$, respectively, using an artificially prepared specimen $A–A_pB_q–A_rB_s–A_lB_n–B$ or $A–A_rB_s–B$.

It is essential to note that both the A_pB_q and A_lB_n layers must be the first to occur at the $A–B$ interface. The diffusional constant k'_{1A2} thus obtained is the reaction-diffusion coefficient of the A atoms in the A_pB_q lattice, while the diffusional constant k_{1B3} is the reaction-diffusion coefficient of the B atoms in the A_lB_n lattice.

After the disappearance of the A_rB_s layer, the system $A–A_pB_q–A_lB_n–B$ remains. Growth kinetics of two compound layers have already been considered in Chapter 3.

During further isothermal holding, the A_pB_q and A_lB_n layers will grow until one of initial substances A or B is consumed completely. The A_rB_s layer can then form and grow either in the $A_pB_q–A_rB_s–A_lB_n–B$ system or in the $A–A_pB_q–A_rB_s–A_lB_n$ system.

To avoid any misunderstanding and confusion, it should be emphasised that it is only the *growth* of the third compound layer *between* the two compound layers already growing in the diffusion controlled regimes with regard to appropriate components, that is impossible. If, for example, the A_rB_s and A_lB_n layers grow between substances A and B, then the A_pB_q layer having an immediate contact with a source of A atoms, *i.e.* with substance A, may in principle occur and grow at the $A–A_rB_s$ interface, whatever the growth regimes of the A_rB_s and A_lB_n layers. However, when the growth regimes of the A_pB_q and A_lB_n layers become diffusion

controlled with regard to components A and B, respectively, then the A_rB_s layer proves "superfluous" and must inevitably disappear with passing time.

It is clear that if A_pB_q is the most A-rich compound and A_lB_n is the most B-rich compound of a binary multiphase system, then no other compound layer can grow in the A–B reaction couple until the full consumption of one of initial phases A or B, provided that the A_pB_q layer grows in the diffusion controlled regime with regard to component A and the A_lB_n layer grows in the diffusion controlled regime with regard to component B. Since in practice relatively thick layers of chemical compounds, already growing in the diffusion controlled regimes with regard to both components, are investigated, it becomes clear why in the vast majority of the A–B reaction couples the dominant growth of at most two layers is observed, irrespective of the total number of chemical compounds on the equilibrium phase diagram of a given multiphase binary system.

4.7: Sequence of compound-layer formation at the *A–B* interface

From a theoretical viewpoint, predicting the sequence of layer occurrence at the A–B interface would present no difficulties if the values of all the chemical constants entering into a system of differential equations of the type (4.27) were known. For any multiphase binary system A–B, these values are determined by the physical and chemical properties of the elements A and B and their compounds. With their dependence on those properties established, the sequence of formation of compound layers would readily be predicted from the system of equations (4.27) or similar. Unfortunately, the theory of solid-state heterogeneous kinetics has not yet reached this stage of its development.

It is obvious that the simultaneous occurrence of all compound layers at the A–B interface is highly unlikely even from a formal statistical viewpoint. For example, with three compounds, the total probability of the cases where the derivatives dx/dt, dy/dt and dz/dt have different signs (+,–,–; –,+,–; –,–,+; +,+,–; +,–,+; –,+,+) is evidently much greater than the probability of the case in which all three derivatives are positive (+,+,+), with their ratio being 6:1. Therefore, formation of the A_pB_q, A_rB_s and A_lB_n layers must be sequential rather than simultaneous, in accordance with experimental observations.

Exact laws governing the sequence of occurrence of compound layers in a particular reaction couple have not so far been established. What is available is a few empirical rules predicting this sequence at a probability level of about 60 to 90%. These are based either (*i*) on the main features of the equilibrium phase diagram of a binary system A–B or (*ii*) on the thermodynamic properties of its constituting phases (for more detail, see ref. [16]).

4.8: Reasons of formation of multiple compound layers at the *A–B* interface

The simultaneous presence of multiple compound layers at the A–B interface is sometimes observed experimentally. Therefore, just as in the framework of diffusional considerations it is necessary to explain why the number of compound layers is in most cases so small, so in the framework of the proposed physico-chemical approach it is necessary to explain why in

certain cases the number of those layers is so large. There are a few reasons for the formation of multilayered structures at the *A–B* interface. These may be summarised as follows.

(1) If the growth regimes of all the layers are reaction controlled (in the theoretical definition given in Chapter 2) at least with regard to one component, then they can in principle grow simultaneously, whatever their number. Note that in this case the layer-growth kinetics can hardly be expected to obey a parabolic law. This is characteristic of very thin compound layers, at most a few hundreds of nanometres thick.

Thus, many compound layers may occur in the *A–B* reaction couple of a multiphase system in the initial reaction controlled rather than in the late diffusion controlled stage of their formation, although this seems to be somewhat paradoxical. Furthermore, initially their number may even happen to exceed the number of chemical compounds on the equilibrium phase diagram of a given binary system. This is so in the case of compounds with wide ranges of homogeneity. The layers of such compounds may consist of two sublayers of different composition.

For example, the number of the separate layers present simultaneously between nickel and aluminium in thin-film nickel-aluminium couples at 220 °C was found to be equal to six [97], whereas according to the equilibrium phase diagram there are only four intermetallic compounds Ni_3Al, NiAl, Ni_2Al_3 and $NiAl_3$ in the Ni–Al binary system [61, 62]. However, since the NiAl and Ni_2Al_3 phases have considerable ranges of homogeneity, each of them forms two sublayers of limiting compositions. These sublayers had the atomic percentages $Ni_{60}Al_{40}$ and $Ni_{44}Al_{56}$ for NiAl and $Ni_{40}Al_{60}$ and $Ni_{35}Al_{65}$ for Ni_2Al_3 [97].

The upper and lower limits of the homogeneity range of the NiAl intermetallic compound are equal to 60 at.% and 45 at.% of nickel, respectively [61]. For Ni_2Al_3, these values are 40.8 at.% and 36.3 at.% of nickel. As the accuracy of measuring the width of the homogeneity range is within ±1 at.%, the agreement between the two sets of contents of aluminium and nickel should be regarded as fairly good for both compounds NiAl and Ni_2Al_3. Subsequent growth of the intermetallic layers is accompanied by a redistribution of the concentrations of the components in their bulks from stepwise to smooth, and eventually the distribution close to linear is established. At the layer interfaces those concentrations correspond to the limiting values of the homogeneity range of a given compound.

(2) Restrictions on the number of simultaneously growing compound layers, following from physico-chemical considerations, are not applicable to the phases with extremely wide ranges of homogeneity, similar to the ε-phase of the Ag–Zn binary system. This phase has a homogeneity range extending from 55.1 to 81.6 % Zn [61].

For such phases, the condition of a quasi-stationary distribution of the concentrations of the components across the width of the layer formed is usually not fulfilled. Note that this type of phase is not regarded as chemical compounds. During their formation, considerable part of diffusing atoms may either remain within the layer due to the existence of a wide range of homogeneity or leave that layer without the loss of stability of a given phase.

Therefore, firstly, the physical (diffusional) constants become strongly dependent upon the layer thickness and consequently vary with annealing time. Secondly, the chemical constants also become time-dependent due to the variation of boundary concentrations of the components in that layer.

In such a case, growth of other layers is possible not only at the expense of consumption of a given phase, but also at the expense of variation of the average composition of its layer. The latter is clearly impossible with typical chemical compounds having no homogeneity ranges. Since the phases with a very wide range of homogeneity are something intermediate between chemical compounds and extended solid solutions, the description of their growth kinetics requires a more detailed consideration, the theoretical basis of which is still obscure.

(3) Since compound layers are polycrystalline, grain boundary diffusion may to some extent affect both their morphology and growth kinetics. Grain boundary diffusivities of the components of any compound are known to be a few orders of magnitude higher than appropriate lattice ones.

Therefore, an excess of diffusing atoms may build up in the vicinity of the boundaries of any grain adjacent to the other phase. Part of these atoms, not consumed completely at a given interface in view of its insufficient local combining ability, are then able to diffuse further and are consumed in the formation of additional compound layers.

This must result in the formation of the layers with uneven interfaces, *i.e.* the layer thickness becomes irregular. The effect of grain boundary diffusion is clearly most profound in compound layers of columnar structure, with the grains extending from one layer interface to another. In fine-grained structures of equal grain size, it can hardly play any significant role.

(4) The effect produced by cracks in growing layers, located in the direction of atomic diffusion, is largely similar to that of grain boundary diffusion, with the main contribution to mass transport in the vicinity of any crack arising from surface diffusion. Less obvious and predictable is the effect of cracks located along and at the layer interfaces, especially of those continuously forming and disappearing in the course of annealing the reaction couples. Such cracks appear to be the main reason for the occurrence of thick multiple compound layers at the *A–B* interface. Therefore, this point will be analysed in more detail.

Consider first the primary causes of crack formation. These appear to be (*i*) the difference in the coefficients of thermal expansion of the constituents of a given reaction couple and (*ii*) the volume effect associated with the formation of a chemical compound, the volume of the reaction products formed being in general not equal to that of the reactants consumed.

The difference of thermal expansion coefficients of the interacting phases causes their considerable lateral displacement relative to each other, if the temperature is changed. As these are usually not free either to move laterally or to bend, great mechanical stress arisen results in the formation of cracks, mainly at the layer interfaces. Clearly, the cracks due to this cause most frequently occur during heating the reaction couples from room temperature up to

a temperature at which the experiment is carried out and then during their cooling down from that temperature again to room temperature.

The couples like Ni–Bi (room-temperature coefficients of thermal expansion are equal for both metals, $\alpha_{20} = 13.5\times10^{-6}$ K^{-1}) readily withstand a few heating-cooling cycles without any indication of rupture, whereas those like Ni–Zn ($\alpha_{20} = 30.0\times10^{-6}$ K^{-1} for zinc) crack along one of the interfaces between reacting phases during the first cooling-down from experimental temperatures to room temperature.

The formation of chemical compounds is usually accompanied by a decrease of the couple volume and relatively rarely by its increase. The volume change gives rise to considerable mechanical stress. If the *A–B* couple is allowed to freely contract, this results in the occurrence of numerous regular cracks across the layer bulks. If not, the couple will in all probability rupture along the whole reaction front. In the latter case, a continuous crack may be located either at one of the interfaces or in the bulk of one of the compound layers formed.

Note that the cracks due to volume changes occur immediately in the course of layer growth. To prevent their formation, external pressure is often applied. It is not so easy, however, to choose its optimum value. If insufficient, it will obviously produce no desirable effect. If too high, compound layers may simply be crushed.

During the whole course of annealing the *A–B* couple under pressure, contacts between initial and occurring phases may be lost and re-newed several times, giving rise to a complicated and hardly tractable microstructure of the *A–B* transition zone. Thus, in many cases the compound-layer formation actually takes place in a few independent couples. Though in each of those couples no more than two compound layers can grow simultaneously under conditions of diffusion control, multiple compound layers will ultimately be seen between *A* and *B*. Clearly, the newly-occurred layers can only grow at the expense of the former ones whose thickness must therefore decrease.

In some cases the crack is apparent (Fig. 4.8), while in the others not (Fig. 4.9a). Shown in Fig. 4.8 is the microstructure of the transition zone between cobalt and silicon after annealing at 800 °C for 64 h in vacuum [98]. All the phases available on the Co–Si phase diagram [99] are readily seen as distinct layers. However, since the Co_2Si and CoSi layers are known to be the first to occur, with Co_2Si being the very first [100, 101], the $CoSi_2$ layer is most probably formed after the occurrence of a crack between Co and Co_2Si. The growth process of this layer is always accompanied by a decrease of the thickness of either the Co_2Si or CoSi layer or both [100]. In the absence of cracks all these compound layers cannot occur simultaneously. Note that up to 500-600 nm the silicide layers are found to grow linearly.

When without the plots of Fig. 4.9b, the microstructure of Fig. 4.9a [102] might provide indisputable evidence for the simultaneous occurrence of all the platinum antimonides between platinum and antimony in the course of isothermal annealing the Pt–Sb reaction couple. Layer thickness-time plots clearly indicate, however, that this is far from being the case. The PtSb layer is seen to shrink.

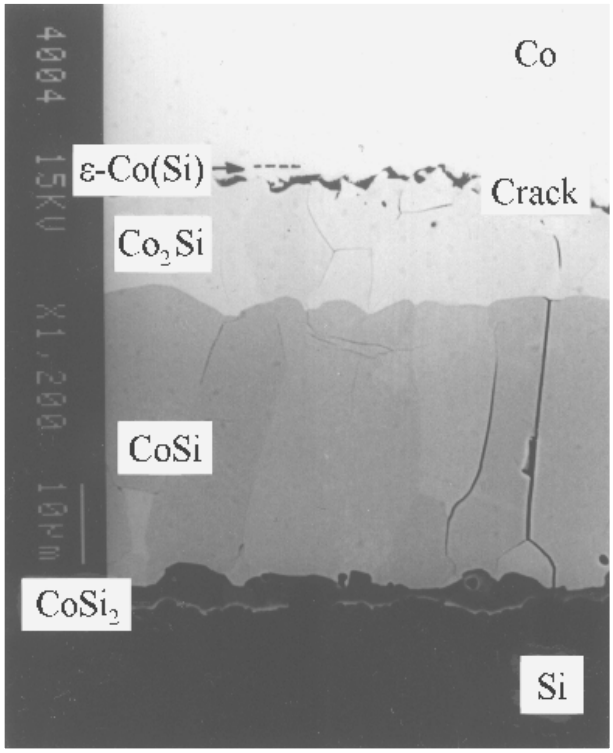

Fig. 4.8. Backscattered electron image of the transition zone between cobalt and silicon after annealing at 800 °C for 230400 s (64 h) in vacuum [98]. The microstructure reveals all the phases available on the equilibrium phase diagram of the Co–Si binary system. A continuous crack is seen between Co and Co_2Si.

Therefore, though no crack is visible due to the application of pressure, the Pt–Sb couple was probably split at some (uncertain) moment of time into at least two independent couples in which the other platinum antimonide layers could readily occur. Generally, in perfect reaction couples any compound layer survived in the initial linear stage of interaction can hardly be expected to shrink on its own during the further course of the reaction.

Microstructures like those of Figs 4.8 and 4.9 are often invoked to oppose massive specimens with multiple compound layers to thin-film ones with one or two compound layers. For binary systems without any considerable solubility in the solid state, however, the dimensions of reaction couples, if of course not of the order of the lattice spacing, play no role in determining layer-growth kinetics. Growing compound layers can scarcely feel whether a particular reaction couple is 100 nm or 1 cm thick, if the difference in chemical composition of its constituents is insignificant.

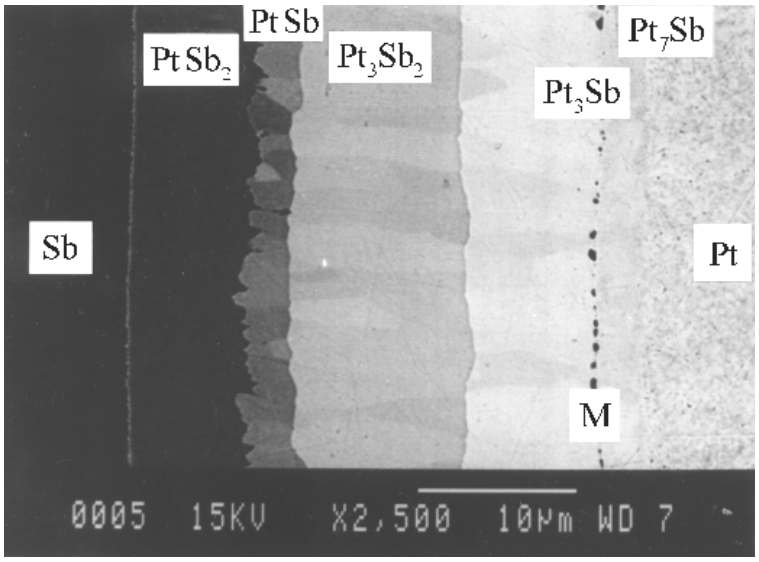

(a)

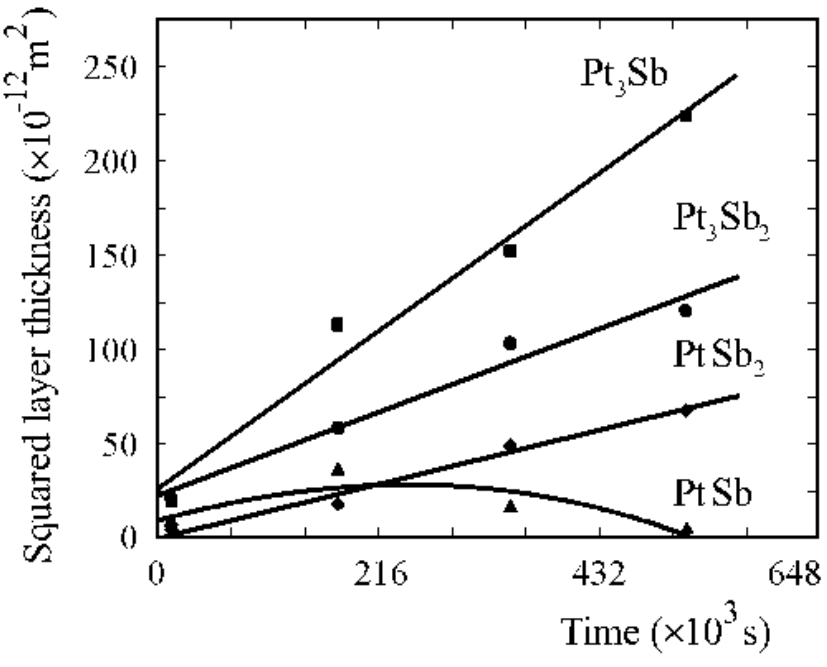

(b)

Fig. 4.9. (a) Microstructure of the transition zone between platinum and antimony after annealing at 500 °C for 345600 s (96 h) and (b) plots of the squared layer thickness against time [102]. The Pt_7Sb layer is extremely thin. The letter M designates inert markers.

Though often invoked, the Kirkendall effect has in fact no relation to the crack occurrence in multi-layered structures where some part of compound layers grow at the expense of diffusion of only one component, while the other part do not grow at all. Also, in the case of multiple layers occurring in the actually independent couples any calculations of interdiffusion coefficients prove to be meaningless.

This is so even with perfect *A–B* couples. Initially, when interdiffusion is still taking place, layer-growth kinetics are non-parabolic and therefore the purely diffusional considerations are inapplicable. Then, when the layer growth becomes diffusion controlled, there is no interdiffusion in any of the layers present, and in some of them there is no diffusion at all, excepting the random walk of atoms never resulting in compound formation.

In the diffusional stage of interaction of initial substances, interdiffusion is only possible if a single compound layer is formed between *A* and *B*. With two compound layers, only monodiffusion in each of the layers takes place. With multiple compound layers, even monodiffusion in all the layers is not possible. It takes place only in two of them.

To visualise the diffusing species, inert markers should be embedded in each of compound layers. From Figs 4.2 and 4.6, it must be clear that one marker is insufficient to make far-reaching conclusions regarding the diffusing species in multiple layers.

Position of the layers grown relative to the initial *A–B* interface only depends upon the amounts of *A* and *B* consumed or, in other words, upon the stoichiometry of chemical compounds and layer thicknesses. It does not indicate whether *A* or *B* is diffusing faster.

4.9: Mutiple compound layers: comparison of diffusional and physico-chemical approaches

Most essential distinctions between the conventional diffusional approach and the proposed physico-chemical one for the case of formation of multiple compound layers at the interface of elementary substances *A* and *B* are briefly listed in Table 4.1. These are partly visualised in Fig. 4.10.

4.10: Multiple compound layers: short conclusions

1. Though there are no restrictions on the number of compound layers growing simultaneously in the reaction controlled regimes, from a physico-chemical viewpoint their formation in the *A–B* reaction couple of any multiphase binary system is likely to be sequential and not simultaneous.

2. The sequence of occurrence of compound layers is determined by the rates of chemical transformations at the interfaces. It cannot yet be theoretically predicted with confidence for any particular reaction couple *A–B*. Having sufficient information on the equilibrium phase diagram, thermodynamics of chemical reactions, and the crystallographic structure and physico-chemical properties of the compounds, it is possible to indicate those of them, which are most likely to occur and grow first at the *A–B* interface.

3. The layers of no more than two compounds can grow simultaneously in the diffusion controlled regimes. The layer adjacent to substance *A* or the *A*-enriched phase only grows at the expense of diffusion across its bulk of *A* atoms. The layer bordering substance *B* or the *B*-enriched phase only grows at the expense of diffusion across its bulk of *B* atoms. Both layers thicken at their common interface by pushing each other in the opposite direction.

4. Under conditions of diffusion control, all other compound layers of a multiphase binary system, located between the two growing ones, are kinetically unstable. If these other layers were initially missing from the *A–B* couple, they will not occur in it until at least one of initial substances (either *A* or *B*) is completely exhausted. If present, they must disappear completely during further isothermal annealing.

5. In general, there can be no full correspondence between the equilibrium phase diagram of a multiphase binary system and the microstructure of the *A–B* transition zone occurred after isothermal annealing of the *A–B* reaction couple.

6. If observed, formation of multiple compound layers at the *A–B* interface is most likely a result of secondary reactions taking place after the occurrence of cracks in and between reacting phases. Crack formation is due to volume changes accompanying layer growth and the difference in the coefficients of thermal expansion of the couple constituents. Though often invoked, the Kirkendall effect is in principle unobservable with growing compound layers and therefore has no relation to the crack occurrence both in layer bulks and at the interfaces between reacting phases.

7. One inert marker only indicates the diffusing species in that compound layer in which it is embedded or with which it borders. If this layer grows under conditions of diffusion control, then the very presence of other compound layers provides in itself evidence that another component is diffusing across their bulks.

8. In view of the lack of interdiffusion in the course of multiple layer formation at the *A–B* interface and because of complicated mechanism of this process, calculation of integrated diffusion coefficients appears in most cases to be quite formal and hence meaningless, yielding figures of doubtful physical significance.

Table 4.1. Comparison of diffusional and physico-chemical approaches in the case of formation of multiple compound layers

Diffusional approach	Physico-chemical approach
1. All compound layers, whatever their number on the *A–B* phase diagram, can occur and grow simultaneously.	1. Compound layers occur in sequence that can as yet hardly be predicted with confidence theoretically.
2. Layer-growth kinetics are parabolic for all the layers, whatever their thickness.	2. Kinetic laws are rather complicated and in general can hardly be expressed by any simple mathematical relation.
3. All compound layers always can grow at the expense of diffusion of both components.	3. All compound layers always can grow at the expense of diffusion of both components only under conditions of reaction control. Under conditions of diffusion control, at most two compound layers will grow simultaneously, each at the expense of diffusion of one component. Artificially prepared "superfluous" layers must disappear with time.

1. Formation of one compound layer: reaction or diffusion control

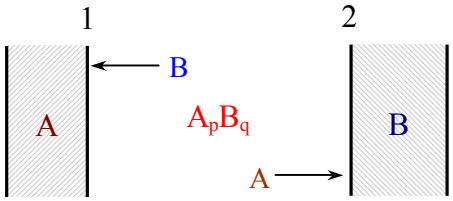

2a. Formation of two compound layers: reaction control

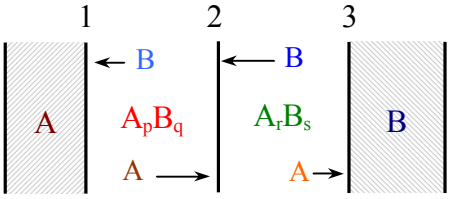

2b. Formation of two compound layers: diffusion control

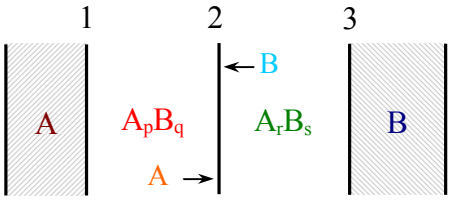

3a. Formation of three compound layers: reaction control

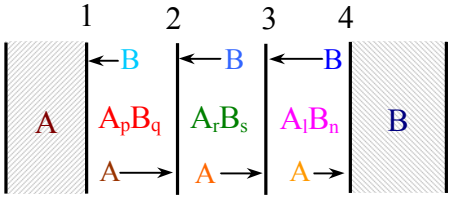

3b. Formation of three compound layers: diffusion control

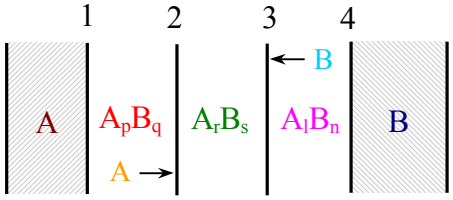

Fig. 4.10. Comparative schematic diagrams to illustrate the distinctions in the processes of formation of one, two and three compound layers. No restrictions on the growth of any layer under conditions of reaction control. No restrictions on the growth of one layer A_pB_q under conditions of diffusion control. Restricted diffusional growth of the layers A_pB_q and A_rB_s in the case of two compound layers. No growth (only the consumption) of the middle layer A_rB_s in the case of three compound layers, while the A_pB_q and A_lB_n layers grow.

5: Formation of the same compound layer in various reaction couples

If a binary system is multiphase, then the layer of the same chemical compound can obviously grow in different reaction couples consisting of elementary substances A and B and their other compounds. To show how its growth rate depends on the composition of initial phases, it suffices to consider a binary system with three compounds A_pB_q, A_rB_s and A_lB_n on the equilibrium phase diagram (see Fig. 4.1).

If the A_rB_s layer is the first to occur at the A–B interface, then in a certain range of temperature its growth can readily be observed between

(*i*) elementary substances A and B (reaction couple A–B),

(*ii*) one of the two other compounds and one of the elementary substances (reaction couples A_pB_q–B and A–A_lB_n),

(*iii*) two other compounds (reaction couple A_pB_q–A_lB_n).

Note that in this chapter the A_rB_s layer will be assumed to be the only one in all possible reaction couples of the A–B multiphase binary system under given experimental conditions.

5.1: Growth of the A_rB_s layer in the A–B reaction couple

It is most convenient to compare the growth rates of the layer of the same chemical compound in various reaction couples with the rate of its growth at the interface of elementary substances. Therefore, let us first briefly analyse the case in which the A_rB_s compound layer is formed at the A–B interface (Fig. 5.1). To avoid considerable changes in the designations of the reaction-diffusion constants describing the layer-growth kinetics, the numeration of the interfaces of the A_rB_s layer, shown in Fig. 4.1, will be retained.

Solid-state growth of the A_rB_s layer at the interface between elementary substances A and B is due to two partial chemical reactions each of which occurs in two consecutive, alternate steps (see Chapter 2). Firstly, the B atoms diffuse across the layer bulk and then react at the A–A_rB_s interface (interface 2) with the surface A atoms in accordance with the equation

$$sB_{\text{dif}} + rA_{\text{surf}} = A_rB_s. \qquad (5.1)$$

Secondly, the A atoms diffuse in the opposite direction and then react at the A_rB_s–B interface (interface 3) with the surface B atoms

$$rA_{\text{dif}} + sB_{\text{surf}} = A_rB_s. \qquad (5.2)$$

During the time dt, the thickness of the A_rB_s layer increases by dy_{B2} at the A–A_rB_s interface. As a result, this interface moves from position 2′ into position 2. Simultaneously, it increases by dy_{A3} at the A_rB_s–B interface, so that this interface moves from position 3′ into position 3. A kinetic equation describing the growth rate of the A_rB_s layer at the interface of mutually insoluble elementary substances A and B has the form

$$\left(\frac{\mathrm{d}y}{\mathrm{d}t}\right)_{A-B} = \frac{k_{0B2}}{1+\dfrac{k_{0B2}y}{k_{1B2}}} + \frac{k_{0A3}}{1+\dfrac{k_{0A3}y}{k_{1A3}}}. \qquad (5.3)$$

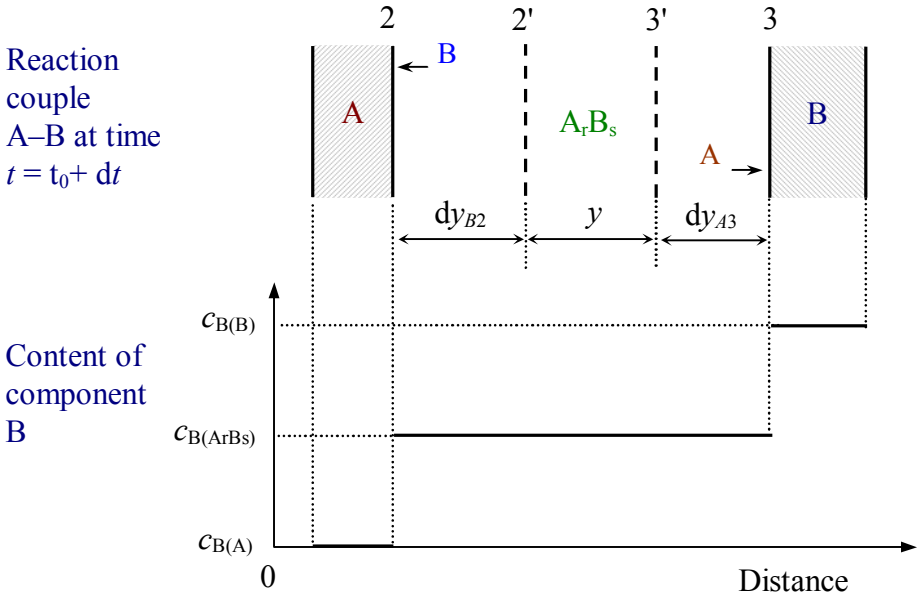

Fig. 5.1. Schematic diagram to illustrate the growth process of the A_rB_s layer between mutually insoluble elementary substances A and B at the expense of diffusion of both components.

When comparing the chemical constants in the systems A–A_rB_s–B and A–A_pB_q–A_rB_s–A_lB_n–B (see Chapter 4), it should be kept in mind that k_{0B2} is not equal to k'_{0B2} and k_{0A3} is not equal to k'_{0A3} since different partial chemical reactions take place in those systems at the interfaces of the A_rB_s layer with the adjacent phases. Though the rate of transport of any component across the bulk of the A_rB_s layer is an intrinsic property of this layer, not depending on the composition of the adjacent phases, the diffusional constants k_{1B2} and k'_{1B2} as well as k_{1A3} and k'_{1A3} are also not identical because in the systems A–A_rB_s–B and A–A_pB_q–

A_rB_s–A_lB_n–B different numbers of the A_rB_s molecules are formed per one diffusing atom A or B. Therefore, the constants k_{1B2} and k'_{1B2} differ by a constant multiplier. The same applies to the constants k_{1A3} and k'_{1A3}.

5.2: Growth of the A_rB_s layer in the A_pB_q–B reaction couple

The mechanism of formation of the A_rB_s layer at the A_pB_q–B interface is essentially dependent upon which component (either A or B) has a higher mobility in the crystal lattice of the A_rB_s compound. Comparing the systems A–A_rB_s–B and A_pB_q–A_rB_s–B, it can easily be concluded that the same physico-chemical processes take place in both systems at the interface of the A_rB_s and B phases.

It does not mean, however, that if the diffusion of component A prevails in the A_rB_s layer, then the growth rates of this layer in the A_pB_q–B and A–B reaction couples will be identical. Consider this case in more detail.

5.2.1: Growth of the A_rB_s layer between A_pB_q and B at the expense of diffusion of only component A

Schematic diagram to illustrate the growth process of the A_rB_s layer at the interface between the A_pB_q and B phases at the expense of diffusion of component A is shown in Fig. 5.2. If the A_pB_q compound has a considerable range of homogeneity, then the content of component A in the initial phase A_pB_q will be assumed to be constant and equal to the lower limit of this range according to the equilibrium phase diagram of the A–B binary system.

During the time dt, the thickness of the A_rB_s layer increases by dy_{A3} at interface 3 as a result of diffusion of the A atoms from interface 2 to interface 3 and their subsequent partial chemical reaction (5.2) with the surface B atoms. In the A_pB_q–B reaction couple, the A_pB_q phase serves as a source of diffusing A atoms. It must be clear, however, that the content of component A in this phase cannot be less than the lower limit of its homogeneity range. Hence, as reaction (5.2) proceeds, the A_pB_q compound becomes unstable and therefore should undergo a partial transformation into another compound of the A–B multiphase binary system. To reveal the essence of this transformation, let us consider one of the simplest cases in which the layer of the chemical compound AB grows between the A_2B and B phases.

If a molecule A_2B loses one atom A which then diffuses across the AB layer and reacts with B to form a molecule AB at the AB–B interface, it transforms into a molecule AB. Appropriate chemical reactions are

$$A_2B = AB + A_{\text{dif}} \tag{5.4}$$

and

$$A_{\text{dif}} + B_{\text{surf}} = AB. \tag{5.5}$$

Thus, one molecule AB is formed at the AB–B interface as a result of reaction (5.5). At the same time, an additional molecule AB is formed at the A_2B–AB interface as a result of the phase transformation inevitably following the reaction diffusion of component A. Consequently, enhanced growth of the AB layer must be observed in the A_2B–AB–B system in comparison with its growth in the A–AB–B system. The ratio of the growth rates of the AB layer in those systems is seen to be equal to 2.

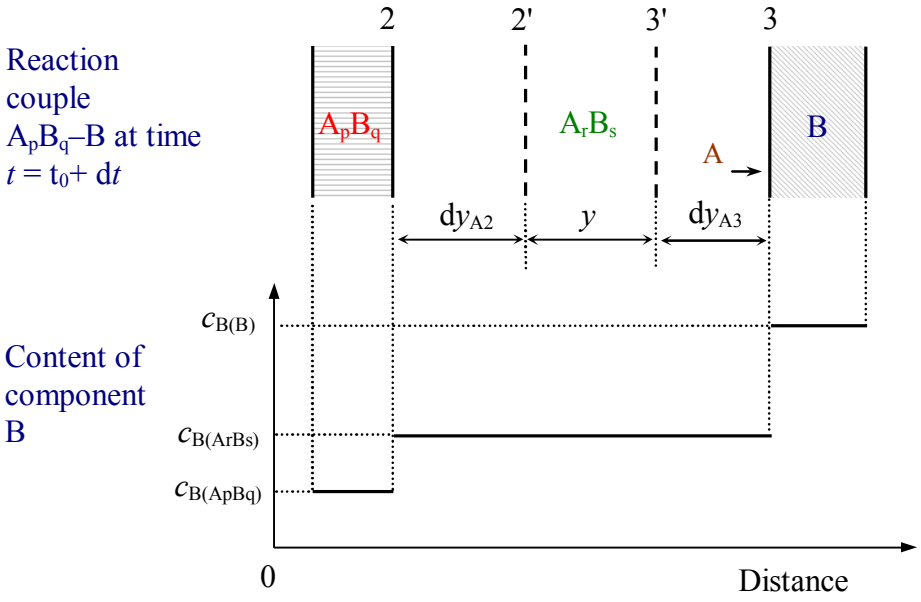

Fig. 5.2. Schematic diagram to illustrate the growth process of the A_rB_s layer in the A_pB_q–B reaction couple due to the diffusion of component A to interface 3 and the simultaneous partial decomposition of the A_pB_q phase at interface 2.

This result can easily be generalised. It appears reasonable to assume that a most likely transformation is that in which an initial phase loses the minimum number of atoms and therefore transforms into an adjacent phase of the A–B equilibrium phase diagram. Therefore, the phase transformation of A_pB_q into A_rB_s taking place at the A_pB_q–A_rB_s interface under the influence of reaction diffusion of the A atoms to the A_rB_s–B interface can be represented as follows

$$sA_pB_q = qA_rB_s + (sp - qr)A_{\text{dif}} . \qquad (5.6)$$

Hence, during the same time dt, the thickness of the A_rB_s layer must also increase by dy_{A2} at interface 2 due to reaction (5.6). It is obvious that the values dy_{A2} and dy_{A3} are directly proportional

$$\mathrm{d}y_{A2} = \alpha\, \mathrm{d}y_{A3}. \tag{5.7}$$

The proportionality coefficient, α, can readily be found from equations (5.2) and (5.6). Indeed, according to reaction (5.2) an increase of the thickness of the A_rB_s layer at interface 3 is a result of diffusion of r A atoms. However, from reaction (5.6) it is seen that the loss of s A_pB_q molecules ($sp - qr$) A atoms is accompanied by the formation of q A_rB_s molecules at interface 2. Hence, from the proportion

$$\frac{\alpha}{q} = \frac{r}{sp - qr}, \tag{5.8}$$

it follows

$$\alpha = \frac{1}{\beta - 1}, \tag{5.9}$$

where $\beta = sp/qr$. Note that sp is always greater than qr because the A_pB_q compound is enriched in component A in comparison with the A_rB_s compound. Therefore, $\beta > 1$.

The total increase in thickness of the A_rB_s layer due to both the reaction diffusion of A atoms and the phase transformation of A_pB_q into A_rB_s under the influence of this reaction diffusion is

$$\mathrm{d}y_A = \mathrm{d}y_{A2} + \mathrm{d}y_{A3} = \frac{\beta}{\beta - 1}\mathrm{d}y_{A3}. \tag{5.10}$$

If only component A diffuses across the A_rB_s layer, then the rate of its growth in the A–B reaction couple is (see equation (5.3))

$$\left(\frac{\mathrm{d}y_A}{\mathrm{d}t}\right)_{A-B} = \frac{k_{0A3}}{1 + \dfrac{k_{0A3}y}{k_{1A3}}}, \tag{5.11}$$

because in this case $dy_A = dy_{A3}$.

From equation (5.10), it follows that the growth rate of the A_rB_s layer in the A_pB_q–B reaction couple is

$$\left(\frac{dy_A}{dt}\right)_{A_pB_q-B} = \frac{\beta}{\beta-1}\frac{k_{0A3}}{1+\dfrac{k_{0A3}y}{k_{1A3}}}. \qquad (5.12)$$

Therefore, the ratio of the rate of growth of the A_rB_s layer in the A_pB_q–A_rB_s–B system to the rate of its growth in the A–A_rB_s–B system is

$$\frac{\left(\dfrac{dy_A}{dt}\right)_{A_pB_q-B}}{\left(\dfrac{dy_A}{dt}\right)_{A-B}} = \frac{\beta}{\beta-1}. \qquad (5.13)$$

This ratio is seen to depend only upon the stoichiometry of the compounds A_pB_q and A_rB_s.

Equation (5.13) shows that the rate of growth of the A_rB_s layer in the A_pB_q–A_rB_s–B system is greater than the rate of its growth in the A–A_rB_s–B system because β always exceeds unity. The closer the composition of A_pB_q to that of A_rB_s (β tends to unity), the greater is the rate of growth of the A_rB_s layer in the A_pB_q–B reaction couple.

To illustrate the magnitude of this effect, consider a few numerical examples. If the growth rate of the AB_3 layer in the A–AB_3–B system is taken as unity, then its growth rate in the AB–AB_3–B system is equal to 3/2 and in the AB_2–AB_3–B system to 3. The rate of growth of the A_2B_3 layer in the AB–A_2B_3–B system should be three times the rate of its growth in the A–A_2B_3–B system.

If the A_pB_q compound has a considerable range of homogeneity, the growth rate of the A_rB_s layer in the A_pB_q–B reaction couple depends upon the composition of initial phase A_pB_q. The growth kinetics of the A_rB_s layer between the A_pB_q phase enriched in component A and elementary substance B is more complicated than the growth kinetics of this layer between the A_pB_q phase enriched in component B and substance B. In the former case, simultaneously with the consumption of the A_pB_q phase as a whole, a lowering of the content of component A in its bulk is likely (but not necessarily) to occur. If not, the ratio of the growth rates of the A_rB_s layer in the reaction couples consisting of substance B and the A_pB_q phase of different composition can readily be found from equation (5.13) simply by expressing its composition in atomic fractions or atomic percent. Note that equation (5.13) also holds if the initial phase is a solid solution that is consumed as a whole, *i.e.* without any change of its composition, during growth of the A_rB_s layer.

Although in the case under consideration only component A diffuses across the bulk of the A_rB_s layer, the thickness of this layer nevertheless increases at its both interfaces. The final result is thus similar to that which would be observed if both components diffused simultaneously. This should be taken into account when interpreting the experimental data on diffusional contributions of components A and B to the growth process of any chemical compound layer, obtained using inert markers. In the case of reaction couples of the A_pB_q–B type, their interpretation is not always unambiguous.

Indeed, if an inert marker is initially placed at the interface between A_2B and B and the movement of the A_2B–AB and AB–B interfaces during growth of the AB layer is then observed, it will be found that the distances from the marker to those interfaces gradually increase with passing time and remain equal to one another. On the basis of these observations, the researcher might have concluded, from a diffusional viewpoint, that (*i*) both components A and B are diffusing across the AB layer in the opposite direction and (*ii*) the rates of their diffusion are equal. In fact, however, component B does not diffuse in the AB layer at all.

5.2.2: Growth of the A_rB_s layer between A_pB_q and B at the expense of diffusion of both components

Consider now the general case of growth of the A_rB_s layer between A_pB_q and B at the expense of diffusion of both components A and B (Fig. 5.3). Then, the additional increase, dy_{B2}, in thickness of the A_rB_s layer at interface 2 is caused by the diffusion to this interface of the B atoms and subsequent occurrence of partial chemical reaction (4.2_1). It is obvious that the values of this increase in the A_pB_q–A_rB_s–B and A–A_rB_s–B systems are different.

Clearly, the transport ability of the A_rB_s layer in regard to diffusing B atoms as well as in regard to diffusing A atoms does not depend upon with which phase this layer borders in each particular reaction couple and also upon which phase is a source of either B or A atoms. This ability only depends upon the number of diffusion paths in the A_rB_s lattice and upon the rate of travel of the atoms along those paths.

It should be taken into account, however, that the formation of one molecule of A_rB_s by reaction (5.1) requires s diffusing B atoms, whereas according to reaction (4.2_1) the interaction of (sp–qr) diffusing B atoms with r A_pB_q molecules results in the occurrence of p A_rB_s molecules at interface 2. If the elementary acts of partial chemical reactions (5.1) and (4.2_1) had the same rate, the increase of the thickness of the A_rB_s layer in the A_pB_q–A_rB_s–B system at this interface per unit time would be $sp/(sp–qr) = \beta/(\beta–1)$ times greater than that in the A–A_rB_s–B system.

In general, however, these rates appear to be different. If only component B diffuses in the A_rB_s layer, then from equations (4.11_1), (4.14_1) and (5.3) it can be found that the growth rate of this layer is

$$\left(\frac{dy_B}{dt}\right)_{A_pB_q-B} = \frac{\beta}{\beta-1}\frac{k''_{0B2}}{1+\frac{k''_{0B2}y}{k_{1B2}}}, \qquad (5.14)$$

where $k'_{0B2} = \frac{\beta}{\beta-1}k''_{0B2}$ and $k'_{1B2} = \frac{\beta}{\beta-1}k_{1B2}$.

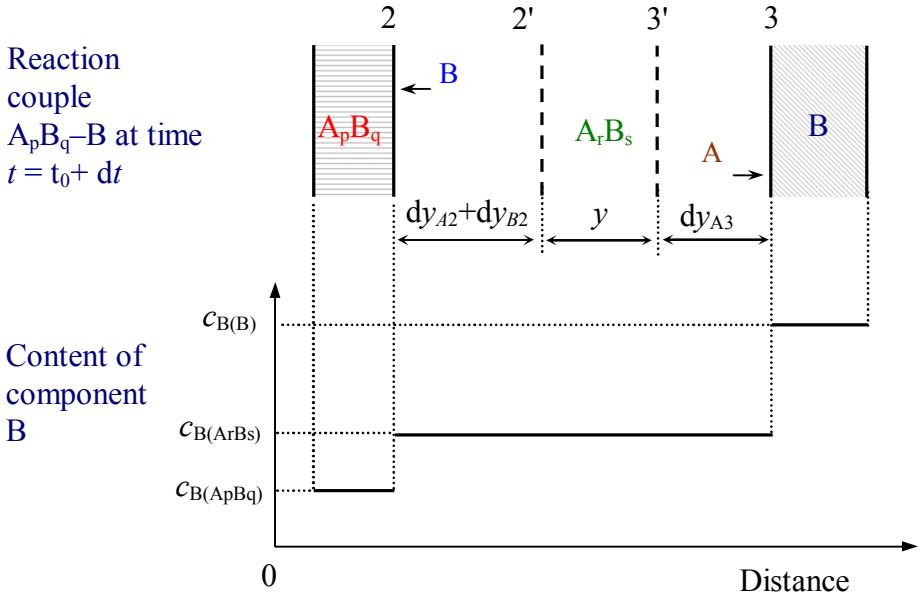

Fig. 5.3. Schematic diagram to illustrate the growth process of the A_rB_s layer in the A_pB_q–B reaction couple due to counter-diffusion of both components and partial decomposition of the A_pB_q phase at interface 2.

Thus, in the case of diffusion of both components A and B, there are three velocities of movement of the interfaces of the A_rB_s layer with the adjacent phases of the A_pB_q–A_rB_s–B system (see Fig. 5.3):

(1) movement of interface 2 to the left as a result of partial chemical reaction (4.2_1);

(2) movement of interface 3 to the right as a result of partial chemical reaction (5.2);

(3) movement of interface 2 to the left as a result of the phase transformation of A_pB_q into A_rB_s according to reaction (5.6).

Summation of the right-hand parts of equations (5.12) and (5.14) yields a general kinetic equation describing the growth rate of the A_rB_s layer between the A_pB_q and B phases in the case where both components are diffusing in its bulk

$$\left(\frac{\mathrm{d}y}{\mathrm{d}t}\right)_{A_pB_q-B} = \frac{\beta}{\beta-1}\left(\frac{k''_{0B2}}{1+\frac{k''_{0B2}y}{k_{1B2}}}+\frac{k_{0A3}}{1+\frac{k_{0A3}y}{k_{1A3}}}\right), \qquad (5.15)$$

or in the form more convenient for subsequent comparisons

$$\left(\frac{\mathrm{d}y}{\mathrm{d}t}\right)_{A_pB_q-B} = \frac{sp}{sp-qr}\left(\frac{k''_{0B2}}{1+\frac{k''_{0B2}y}{k_{1B2}}}+\frac{k_{0A3}}{1+\frac{k_{0A3}y}{k_{1A3}}}\right). \qquad (5.16)$$

Evidently, there is no significant difference between the growth kinetics of the A_rB_s layer in the A_pB_q–B reaction couple and its growth kinetics in the A–A_lB_n reaction couple. The growth rate of this layer in the latter couple (Fig. 5.4) is in general described by the equation

$$\left(\frac{\mathrm{d}y}{\mathrm{d}t}\right)_{A-A_lB_n} = \frac{rn}{rn-ls}\left(\frac{k_{0B2}}{1+\frac{k_{0B2}y}{k_{1B2}}}+\frac{k''_{0A3}}{1+\frac{k''_{0A3}y}{k_{1A3}}}\right). \qquad (5.17)$$

Its derivation is similar to that of equation (5.16). Note that in the A–A_lB_n reaction couple the phase transformation of A_lB_n into A_rB_s

$$rA_lB_n = lA_rB_s + (rn - ls)B_{\mathrm{dif}} \qquad (5.18)$$

takes place at interface 3 under the influence of reaction diffusion of the B atoms from interface 3 to interface 2. Hence, in this couple an increase in thickness of the A_rB_s layer at interface 3 is due to two reactions (4.2_2) and (5.18), while that at interface 2 only to one reaction (5.1). Appropriate changes of the A_rB_s layer thickness during the time dt are shown in Fig. 5.4.

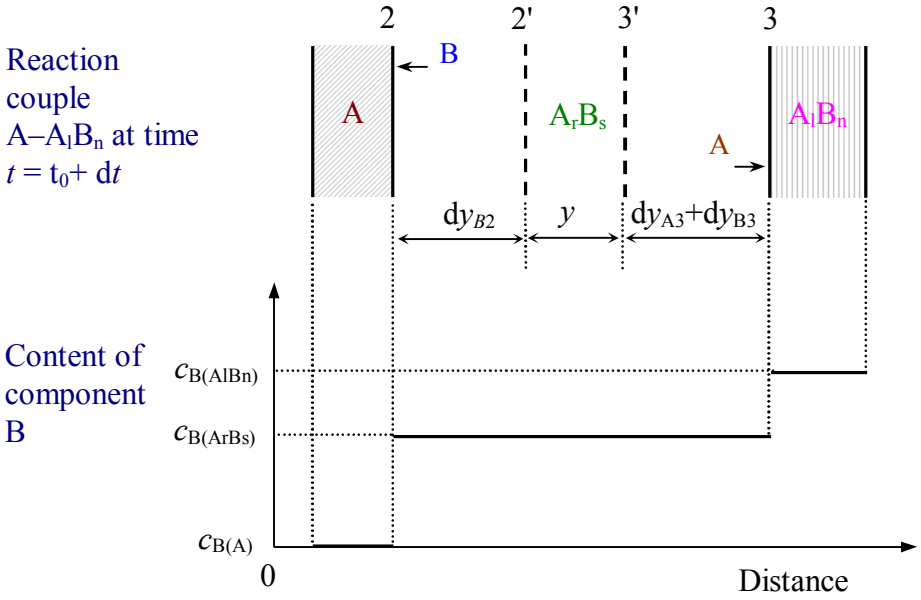

Fig. 5.4. Schematic diagram to illustrate the growth process of the A_rB_s layer in the $A–A_lB_n$ reaction couple due to the counter-diffusion of both components and the partial decomposition of the A_lB_n phase at interface 3.

5.3: Growth of the A_rB_s layer in the A_pB_q–A_lB_n reaction couple

Schematic diagram illustrating the growth process of the A_rB_s layer between the A_pB_q and A_lB_n phases is shown in Fig. 5.5. As seen from equation (5.14), its thickness increases at interface 2 in the course of reaction (4.2_1) at a rate of

$$\left(\frac{\mathrm{d}y_{B2}}{\mathrm{d}t}\right)_{A_pB_q-A_lB_n} = \frac{sp}{sp-qr}\,\frac{k''_{0B2}}{1+\dfrac{k''_{0B2}y}{k_{1B2}}}. \qquad (5.19)$$

Simultaneously, the A_rB_s layer thickness increases at interface 3 as a result of the phase transformation of A_lB_n into A_rB_s by reaction (5.18). The diffusional constant k_{1B2} characterizes partial chemical reaction (5.1) in which s diffusing B atoms take part. Again, according to equation (5.18) the loss of r A_lB_n molecules $(rn–ls)$ B atoms results in the formation of l A_rB_s molecules. Therefore, the growth rate of the A_rB_s layer at interface 3 is

$$\left(\frac{dy_{B3}}{dt}\right)_{A_pB_q-A_lB_n} = \frac{ls}{rn-ls}\frac{k''_{0B2}}{1+\frac{k''_{0B2}y}{k_{1B2}}}. \qquad (5.20)$$

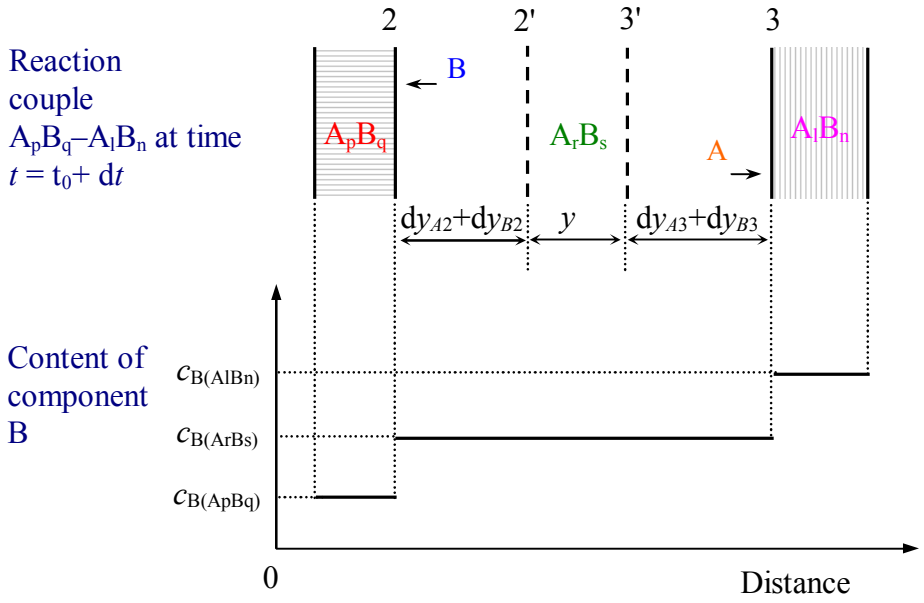

Fig. 5.5. Schematic diagram to illustrate the growth process of the A_rB_s layer in the A_pB_q–A_lB_n reaction couple in the case of simultaneous diffusion of both components.

Hence, if only component B diffuses in the A_rB_s layer, then the rate of growth of this layer in the A_pB_q–A_lB_n reaction couple is

$$\left(\frac{dy_B}{dt}\right)_{A_pB_q-A_lB_n} = \frac{rs(pn-ql)}{(sp-qr)(rn-ls)}\frac{k''_{0B2}}{1+\frac{k''_{0B2}y}{k_{1B2}}}. \qquad (5.21)$$

This equation is a result of term-by-term summation of equations (5.19) and (5.20).

Partial chemical reaction (4.2_2) proceeds at interface 3 between the A atoms diffusing across the A_rB_s layer and the A_lB_n compound. Accordingly, the phase transformation of A_pB_q into A_rB_s takes place at interface 2 by reaction (5.6). The growth rate of the A_rB_s layer at interface 3 is

$$\left(\frac{\mathrm{d}y_{A3}}{\mathrm{d}t}\right)_{A_pB_q-A_lB_n} = \frac{rn}{rn-ls}\frac{k''_{0A3}}{1+\dfrac{k''_{0A3}y}{k_{1A3}}}. \qquad (5.22)$$

Derivation of this equation is analogous to that of equation (5.14).

The growth rate of the A_rB_s layer at interface 2 can readily be found from equations (5.2) and (5.6). Indeed, the diffusional constant k_{1A3} characterises partial chemical reaction (5.2) in which r diffusing A atoms take part. On the other hand, $(sp–qr)$ diffusing A atoms occur per q A_rB_s molecules formed as a result of decomposition of the A_pB_q phase by reaction (5.6). Therefore,

$$\left(\frac{\mathrm{d}y_{A2}}{\mathrm{d}t}\right)_{A_pB_q-A_lB_n} = \frac{qr}{sp-qr}\frac{k''_{0A3}}{1+\dfrac{k''_{0A3}y}{k_{1A3}}}. \qquad (5.23)$$

Thus, if only component A diffuses across the A_rB_s layer, then the growth rate of this layer in the A_pB_q–A_lB_n reaction couple is

$$\left(\frac{\mathrm{d}y_{A}}{\mathrm{d}t}\right)_{A_pB_q-A_lB_n} = \frac{rs(pn-ql)}{(sp-qr)(rn-ls)}\frac{k''_{0A3}}{1+\dfrac{k''_{0A3}y}{k_{1A3}}}. \qquad (5.24)$$

Term-by-term summation of equations (5.21) and (5.24) yields a general equation describing the growth kinetics of the A_rB_s layer between the A_pB_q and A_lB_n phases in the case of counter-diffusion of components A and B across its bulk at comparable rates

$$\left(\frac{\mathrm{d}y}{\mathrm{d}t}\right)_{A_pB_q-A_lB_n} = \frac{rs(pn-ql)}{(sp-qr)(rn-ls)}\left(\frac{k''_{0B2}}{1+\dfrac{k''_{0B2}y}{k_{1B2}}}+\frac{k''_{0A3}}{1+\dfrac{k''_{0A3}y}{k_{1A3}}}\right). \qquad (5.25)$$

Consider the consequences following from equations (5.3), (5.16), (5.17) and (5.25). It is more convenient to do this separately for the linear and parabolic regions of growth of the A_rB_s layer.

5.4: Comparison of the growth rates of the A_rB_s layer in various reaction couples of the A–B multiphase binary system

Initially, conditions of the type $k_0 << k_1/y$ are satisfied. The growth kinetics of the A_rB_s layer is therefore linear in all four reaction couples:

$$\left(\frac{\mathrm{d}y}{\mathrm{d}t}\right)_{A-B} = k_{0B2} + k_{0A3}, \tag{5.26}$$

$$\left(\frac{\mathrm{d}y}{\mathrm{d}t}\right)_{A_pB_q-B} = \frac{sp}{sp-qr}\left(k''_{0B2} + k_{0A3}\right), \tag{5.27}$$

$$\left(\frac{\mathrm{d}y}{\mathrm{d}t}\right)_{A-A_lB_n} = \frac{rn}{rn-ls}\left(k_{0B2} + k''_{0A3}\right), \tag{5.28}$$

$$\left(\frac{\mathrm{d}y}{\mathrm{d}t}\right)_{A_pB_q-A_lB_n} = \frac{rs(pn-ql)}{(sp-qr)(rn-ls)}\left(k''_{0B2} + k''_{0A3}\right). \tag{5.29}$$

If only the A atoms diffuse across the A_rB_s layer ($k_{0B2} = 0$ and $k''_{0B2} = 0$), then from equations (5.26) and (5.27) it follows that the ratio of the rate of linear growth of this layer in the A_pB_q–B reaction couple to the rate of its linear growth in the A–B reaction couple is

$$\frac{sp}{sp-qr},$$

whereas according to equations (5.28) and (5.29) for the A_pB_q–A_lB_n and A–A_lB_n couples this ratio is

$$\frac{s(pn-ql)}{n(sp-qr)}.$$

If only the B atoms diffuse across the A_rB_s layer ($k_{0A3} = 0$ and $k''_{0A3} = 0$), then from equations (5.26) and (5.28) it follows that the ratio of the rate of linear growth of this layer in the A–A_lB_n reaction couple to the rate of its linear growth in the A–B reaction couple is

$$\frac{rn}{rn-ls},$$

whereas according to equations (5.27) and (5.29) for the A_pB_q–A_lB_n and A_pB_q–B couples this ratio is

$$\frac{r(pn-ql)}{p(rn-ls)}.$$

It is clear that in the case of comparable mobility of components A and B in the A_rB_s lattice it is impossible to make any definite theoretical prediction because an exact relation between k_{0A3} and k''_{0A3} as well as between k_{0B2} and k''_{0B2} is not known *a priori*. It might be expected, however, that the constant k''_{0B2} characterising the rate of chemical interaction taking place in the A_pB_q–A_rB_s–B system at the A_pB_q–A_rB_s interface between the diffusing B atoms and the A_pB_q compound is at least not less than the constant k_{0B2} which characterises the rate of chemical interaction taking place in the A–A_rB_s–B system at the A–A_rB_s interface between the diffusing B atoms and the surface A atoms, since the A_rB_s phase is closer in composition to the A_pB_q than to A phase. In any case, therefore, the rate of linear growth of the A_rB_s layer in the A_pB_q–A_lB_n and A_pB_q–B couples must be higher than the rate of its linear growth in the A–B couple.

The same applies to a relation between k_{0A3} and k''_{0A3}. Moreover, it may happen that an increase in the rate of growth of the A_rB_s layer in a series of the reaction couples A–B, A_pB_q–B, A–A_lB_n, A_pB_q–A_lB_n is even greater than that which would be expected merely putting $k_{0B2} = k''_{0B2}$ and $k_{0A3} = k''_{0A3}$ in equations (5.26)-(5.29). Undoubtedly, influence of the structure of the crystal lattices of reacting phases is important. To find out an exact relationship between all the chemical constants and, accordingly, the ratio of the growth rates of the A_rB_s layer in various reaction couples of the A–B multiphase binary system, it would be desirable to carry out thorough experimental investigations with thin films

It can easily be seen that the ratio of the rates of parabolic (diffusional) growth of the A_rB_s layer in the reaction couples under consideration is unambiguously determined by the chemical composition of the interacting phases. Indeed, conditions of the type $k_0 >> k_1/y$ are fulfilled in the diffusional stage of layer formation. Therefore, equations (5.3), (5.16), (5.17) and (5.25) become

$$\left(\frac{\mathrm{d}y}{\mathrm{d}t}\right)_{A-B} = \frac{k_{1B2} + k_{1A3}}{y}, \tag{5.30}$$

$$\left(\frac{\mathrm{d}y}{\mathrm{d}t}\right)_{A_pB_q-B} = \frac{sp}{sp-qr}\frac{k_{1B2} + k_{1A3}}{y}, \tag{5.31}$$

$$\left(\frac{\mathrm{d}y}{\mathrm{d}t}\right)_{A-A_lB_n} = \frac{rn}{rn-ls}\frac{k_{1B2} + k_{1A3}}{y}, \tag{5.32}$$

$$\left(\frac{\mathrm{d}y}{\mathrm{d}t}\right)_{A_pB_q-A_lB_n} = \frac{rs(pn-ql)}{(sp-qr)(rn-ls)}\frac{k_{1B2} + k_{1A3}}{y}. \tag{5.33}$$

From these equations, it follows that

(*i*) the ratio of the growth rates of the A_rB_s layer in the *A–B*, A_pB_q–*B*, *A*–A_lB_n and A_pB_q–A_lB_n reaction couples only depends on the stoichiometry of the compounds;

(*ii*) the growth rate of this layer is least in the *A–B* couple and highest in the A_pB_q–A_lB_n couple;

(*iii*) if the rate of growth of the A_rB_s layer in any one of the reaction couples is known from the experimental data or assumed, then the rate of its growth in all other couples can be predicted exactly.

For example, if some binary system *A–B* contains three chemical compounds A_2B, *AB* and AB_2 and the *AB* layer is the first to form in the *A–B* reaction couple, then the ratio of the rate of diffusional (parabolic) growth of this layer in the A_2B–*B* couple to the rate of its diffusional growth in the *A–B* couple must be equal to 2. For the A_2B–AB_2 and *A–B* couples, this ratio is 3. For the A_2B–AB_2 and A_2B–*B* couples, it is 3/2.

It is worth noting that both purely diffusional considerations and equations (5.30)-(5.33) yield the same ratio for the rates of parabolic growth of the A_rB_s layer in the *A–B*, A_pB_q–*B*, *A*–A_lB_n and A_pB_q–A_lB_n reaction couples. According to C. Wagner [48], this ratio can be calculated using the concept of the integrated diffusion coefficient $D_{\text{int}}^{(i)}$

$$D_{\text{int}}^{(i)} = \int_{N^{(i)''}}^{N^{(i)'}} D\mathrm{d}N, \qquad (5.34)$$

where *N* is the mole fraction of one of the components in the *i*-th phase having the limits of the homogeneity range $N^{(i)'}$ and $N^{(i)''}$.

If the range of homogeneity is very narrow and there is no mutual solubility of the components in the solid state, then [48, 95]

$$D_{\text{int}}^{(i)} = \frac{(N^{+} - N^{(i)})(N^{(i)} - N^{-})}{N^{+} - N^{-}} \left[k_1^{(i)}\right]_{N^{+}/N^{-}}, \qquad (5.35)$$

where N^{+} and N^{-} are the mole fractions of the same component in initial phases, $N^{(i)}$ is its mole fraction in the growing phase, $\left[k_1^{(i)}\right]_{N^{+}/N^{-}}$ is the parabolic growth-rate constant for the *i*-th phase of a given reaction couple found from a plot of the squared layer thickness upon time.

Calculation of $D_{\text{int}}^{(i)}$, for example, for the *AB* phase $(N_A^{+} = 1/2)$ growing in the reaction couples *A–B* $(N_A^{+} = 1,\ N_A^{-} = 0)$, A_2B–*B* $(N_A^{+} = 2/3,\ N_A^{-} = 0)$ and A_2B–AB_2 $(N_A^{+} = 2/3,\ N_A^{-} = 1/3)$ yields the following relations.

System	$D_{\text{int}}^{(i)}$
A–AB–B	$\frac{1}{4}\left[k_1^{(AB)}\right]_{A-B}$,
A_2B–AB–B	$\frac{1}{8}\left[k_1^{(AB)}\right]_{A_2B-B}$,
A_2B–AB–AB_2	$\frac{1}{12}\left[k_1^{(AB)}\right]_{A_2B-AB_2}$.

The quantity $D_{\text{int}}^{(i)}$ is an intrinsic characteristic of the i-th phase and must therefore be the same in all couples in which this phase occurs. Hence, the ratio of the parabolic growth-rate constants for the AB layer in the A_2B–AB_2, A_2B–B and A–B reaction couples is 3:2:1, in agreement with the calculations on the basis of equations (5.30), (5.31) and (5.33). That this is not an occasional coincidence can readily be verified by carrying out calculations for other chemical compounds of different stoichiometry. Similar results follow, for example, from the data by F.J.J. van Loo on the integrated diffusion coefficients for the Ti–Al system [95].

It should be emphasised, however, that the diffusional theory and hence the concept of the integrated diffusion coefficient is quite inapplicable to the region of linear growth of chemical compound layers. By contrast, the physico-chemical approach makes it possible not only to explain qualitatively the existence of linear growth region but in certain cases allows precise quantitative calculations of the ratio of the growth rates for the same compound layer in different reaction couples of the A–B multiphase system to be carried out.

Note that the mechanism of formation of the A_rB_s layer in reaction couples of the A_pB_q–B type by the decomposition of the A_pB_q compound under the influence of reaction diffusion of the A atoms to the A_rB_s–B interface, described in this chapter, has numerous experimental verifications. The growth process of the NiSi layer between Ni_2Si and single crystals of silicon is found to proceed mainly by means of partial decomposition of Ni_2Si [103, 104]:

$$Ni_2Si = NiSi + Ni_{dif}.$$

The nickel atoms released as a result of this reaction diffuse across the NiSi layer to the NiSi–Si interface and interact there with the surface silicon atoms to form additional molecules of NiSi

$$Ni_{dif} + Si_{surf} = NiSi.$$

Contribution of the reaction

$$Si_{dif} + Ni_2Si = 2NiSi$$

to the process of formation of the NiSi layer appears to be insignificant.

Similar growth mechanism is also typical of the $NiSi_2$ layer occurring between NiSi and Si [104]. Its thickening at the NiSi–$NiSi_2$ interface is due to two partial chemical reactions

$$2NiSi = NiSi_2 + Ni_{dif}$$

and

$$Si_{dif} + NiSi = NiSi_2,$$

while that at the $NiSi_2$–Si interface is a result of one reaction

$$Ni_{dif} + 2Si_{surf} = NiSi_2.$$

This kind of chemical reactions takes place in other systems, if one of the two constituents of a reaction couple is a chemical compound and another is an elementary substance. Since the diffusional stage of growth of the layers of transition-metal silicides has been studied thoroughly, it becomes possible to compare quantitative theoretical predictions with available experimental data.

Consider the Co–Si binary system in which three compounds Co_2Si, CoSi and $CoSi_2$ exist at temperatures up to 1170 ºC as an example [61, 99]. The Co_2Si layer is known to be the first to occur between cobalt and silicon. As seen from Fig. 5.6, at 460 ºC its growth kinetics are parabolic [60].

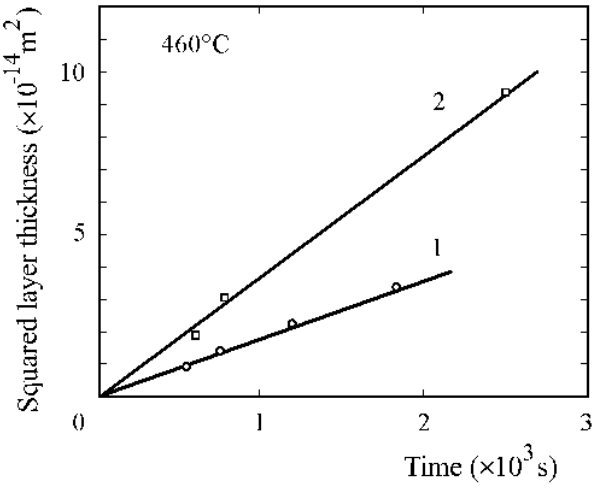

Fig. 5.6. Plots of the squared thickness of the Co_2Si layer in the Co–Si (1) and Co–CoSi (2) diffusion couples against annealing time at 460 ºC [60].

Schematic diagrams illustrating the growth process of the Co_2Si layer in the Co–Si and Co–CoSi couples are shown in Figs 5.7 and 5.8, separately for the two hypothetical cases in which only one component is diffusing.

If diffusion of cobalt is dominant, as in Fig. 5.7, then the growth of the Co_2Si layer in the Co–Si couple is due to partial chemical reaction between the diffusing cobalt atoms and the surface silicon atoms

$$2Co_{dif} + Si_{surf} = Co_2Si \qquad (5.36)$$

taking place at the Co_2Si–Si interface. During the time dt, it causes the increase in thickness of the Co_2Si layer by dy_{Co3} at interface 3. Note that in the Co–Si couple one Co_2Si molecule is formed per two diffusing cobalt atoms.

Partial chemical reaction

$$Co_{dif} + CoSi = Co_2Si \qquad (5.37)$$

proceeds at interface 3 in the Co–CoSi diffusion couple. Hence, during the same time dt, the thickness of the Co_2Si layer must increase by $2dy_{Co3}$ at interface 3 because in this couple one Co_2Si molecule is formed per one diffusing atom of cobalt. Therefore, the ratio of the rate of growth of the Co_2Si layer in the Co–CoSi diffusion couple to the rate of its growth in the Co–Si diffusion couple is equal to 2.

If diffusion of silicon prevails, as in Fig. 5.8, then partial chemical reaction at interface 2 is the same in both couples:

$$Si_{dif} + 2Co_{surf} = Co_2Si. \qquad (5.38)$$

During the time dt, it causes the increase in thickness of the Co_2Si layer by dy_{Si2} at this interface. Since in the Co–CoSi diffusion couple the CoSi compound is a source of silicon atoms, two CoSi molecules lose one silicon atom and thus one Co_2Si molecule is produced at interface 3

$$2CoSi = Co_2Si + Si_{dif}, \qquad (5.39)$$

whereas this released silicon atom diffuses across the Co_2Si layer and reacts at interface 2 with two surface cobalt atoms to form one more Co_2Si molecule.

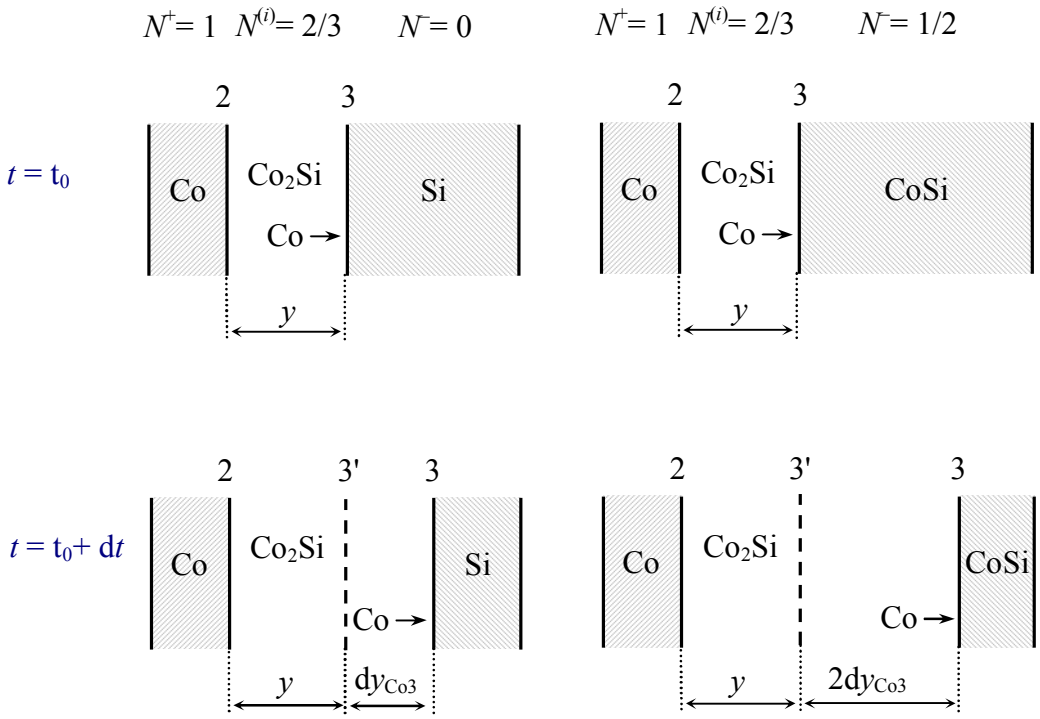

Fig. 5.7. Schematic diagram to illustrate the growth process of the Co_2Si layer in the Co–Si and Co–CoSi diffusion couples in the hypothetical case where only cobalt is the diffusing species.

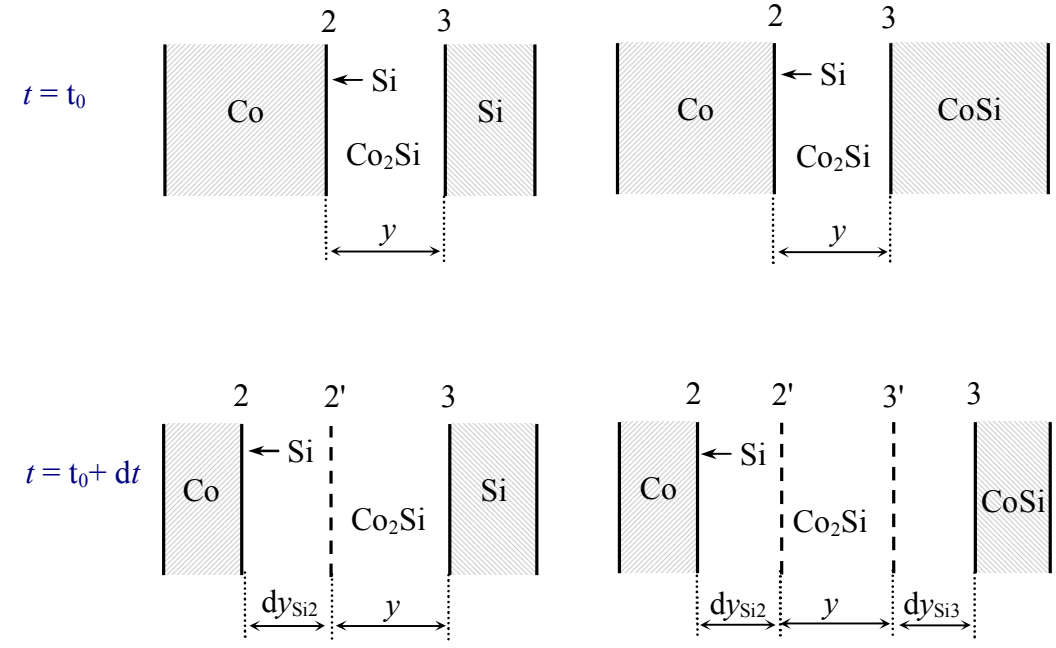

Fig. 5.8. Schematic diagram to illustrate the growth process of the Co_2Si layer in the Co–Si and Co–CoSi diffusion couples in the hypothetical case where only silicon is the diffusing species.

Again, the growth rate of the Co_2Si layer in the Co–CoSi couple is seen to be twice that in the Co–Si couple. Clearly, the same also applies to the general case of comparable mobility of the components in the Co_2Si layer. This result can readily be obtained merely by putting $r = 2$, $s = l = n = 1$ in equation (5.32) and then dividing this equation by equation (5.30).

As seen in Fig. 5.6, for the Co–CoSi couple the slope of a plot of the squared thickness of the Co_2Si layer against annealing time is in fact twice that of such a plot for the Co–Si couple. If the layer thickness is plotted against the square root of the time, $\sqrt{t}$, then the ratio of the slopes of straight lines for the couples of this type should be $\sqrt{2}$. During growth of the Pt_2Si layer the ratio of the slopes of the $y - \sqrt{t}$ dependences for the Pt–PtSi and Pt–Si couples is about 1.5, in fairly good agreement with a theoretical value of $\sqrt{2} = 1.41$ [59].

In the case of parabolic growth of the Co_2Si layer in the Co–Si couple (see Fig. 5.7), $N^+ = 1$, $N^{(i)} = 2/3$ and $N^- = 0$, where N is the mole fraction of cobalt in appropriate phases. Hence, the integrated diffusion coefficient

$$D_{\text{int}}^{(\text{Co}_2\text{Si})} = \frac{2}{9}\left[k_1^{(\text{Co}_2\text{Si})}\right]_{\text{Co-Si}}. \tag{5.40}$$

For the Co–Co_2Si–CoSi system, $N^+ = 1$, $N^{(i)} = 2/3$ and $N^- = 1/2$. Therefore,

$$D_{\text{int}}^{(\text{Co}_2\text{Si})} = \frac{1}{9}\left[k_1^{(\text{Co}_2\text{Si})}\right]_{\text{Co-CoSi}}. \tag{5.41}$$

Thus,

$$\left[k_1^{(\text{Co}_2\text{Si})}\right]_{\text{Co-CoSi}} = 2\left[k_1^{(\text{Co}_2\text{Si})}\right]_{\text{Co-Si}} \tag{5.42}$$

if the constant $k_1^{(\text{Co}_2\text{Si})}$ is determined from the $y^2 - t$ plots for both reaction couples.

Note that the silicide layer can grow not only between silicon and a transition metal, but also between a silicon-containing phase and a transition metal or an intermetallic compound [105-108]. For example, at temperatures above 700 ºC nickel reacts with silicon carbide to form Ni_2Si and C. As the nickel atoms are the dominant diffusing species in the Ni_2Si layer, the thickness of this layer increases mainly at the Ni_2Si–SiC interface by the reaction

$$2\text{Ni}_{\text{dif}} + \text{SiC} = \text{Ni}_2\text{Si} + \text{C}.$$

Since carbon is insoluble in the Ni_2Si phase, it forms fine-grained graphite inclusions in the bulk of the Ni_2Si layer. These inclusions are often seen in the microstructure as the regular bands parallel to the layer interfaces [106].

Formation of silicides in reaction couples, for example, of the Me_3Al–SiC type where Me is a transition metal, is more complicated. In this case, in addition to the Me_2Si layer, the MeAl layer (or some other aluminide layer) also occurs, *i.e.* the Me_3Al–MeAl–(Me_2Si+C)–SiC system is formed. Probably, the mechanism of its formation is as follows. The Me_3Al phase is decomposed at the Me_3Al–MeAl interface by the reaction

$$Me_3Al = MeAl + 2Me_{dif},$$

while two released transition metal atoms then diffuse across the layers of MeAl and (Me_2Si+C) to the (Me_2Si+C)–SiC interface where they enter into the reaction with SiC: $2Me_{dif}$ + SiC = Me_2Si + C, causing an increase of the (Me_2Si+C) layer at this interface. Clearly, in such a case the ratio of the thicknesses of the MeAl and (Me_2Si+C) layers must remains unchanged with passing time. Unfortunately, available literature data are insufficient to make an unambiguous comparison of the growth rates of the Me_2Si layer in reaction couples of the type Me–Si, Me–SiC and Me_3Al–SiC.

It might seem that the A_rB_s layer could grow in the A–A_pB_q–A_rB_s–A_lB_n–B system by the same mechanism as in the A_pB_q–A_rB_s–B and A_pB_q–A_rB_s–A_lB_n systems, *i.e.* at the expense of the phase transformation of A_pB_q into A_rB_s under the influence of reaction diffusion of the A atoms. However, this is not the case. If the growth regime of the A_pB_q layer in the A–A_pB_q–A_rB_s–A_lB_n–B system is reaction controlled with regard to component A ($x < x_{1/2}^{(A)}$), then there is an excess of A atoms in comparison with the reactivity of the A_rB_s surface towards these atoms and therefore no transformation will take place.

Assume that with time the growth regime of the A_pB_q layer with regard to component A became diffusion controlled ($x > x_{1/2}^{(A)}$), while the A_pB_q phase was partly transformed into the A_rB_s one by reaction (5.6). The A atoms released as a result of this transformation cannot, however, cross the A_pB_q–A_rB_s interface in the A–A_pB_q–A_rB_s–A_lB_n–B system in the same manner as in the A_pB_q–A_rB_s–B or A_pB_q–A_rB_s–A_lB_n system. Those A atoms will immediately be combined into the A_pB_q compound at this interface (onto the surface of the A_rB_s phase from the side of A_pB_q) by reaction (4.1_2) which is opposite to reaction (5.6). It is clear that the net result of these reactions is zero.

The behaviour of the same A_pB_q layer in relation to its neighbors in various reaction systems is thus seen to depend on whether it is growing or non-growing. In the A–A_pB_q–A_rB_s–A_lB_n–B system, the A_pB_q layer is a *growing* one. Therefore, it tends to consume all diffusing A atoms for its own growth. By contrast, in the A_pB_q–A_rB_s–B and A_pB_q–A_rB_s–A_lB_n systems, this layer is a *non-growing* one. Therefore, it not only readily supplies the adjacent A_rB_s layer with diffusing A atoms but in addition partly transforms into the latter. This

difference in the behavior of the A_pB_q layer is in turn due to the presence or absence of the A phase.

Obviously, the A_rB_s layer cannot grow in the $A–A_pB_q–A_rB_s–A_lB_n–B$ system by means of the phase transformation of A_lB_n into A_rB_s under the influence of reaction diffusion of the B atoms by reaction (5.18), as is the case in the $A–A_rB_s–A_lB_n$ and $A_pB_q–A_rB_s–A_lB_n$ systems. In the $A–A_pB_q–A_rB_s–A_lB_n–B$ system, the released B atoms are immediately combined onto the surface of the A_rB_s phase into the A_lB_n compound by reaction (4.2_2) opposite to reaction (5.18).

From these considerations, it becomes clear why, for example, the Mo_2B layer, missing from the Mo–B diffusion couple, readily occurs and grows under the same experimental conditions in the Mo–MoB diffusion couple. Though there are four stable molybdenum borideson the Mo–B phase diagram, J. Brandstötter and W. Lengauer [109] found that only the MoB layer 450 μm thick is formed onto the surface of a molybdenum sheet during its boriding at 1450 ºC for 2.5 h (Fig. 5.9a).

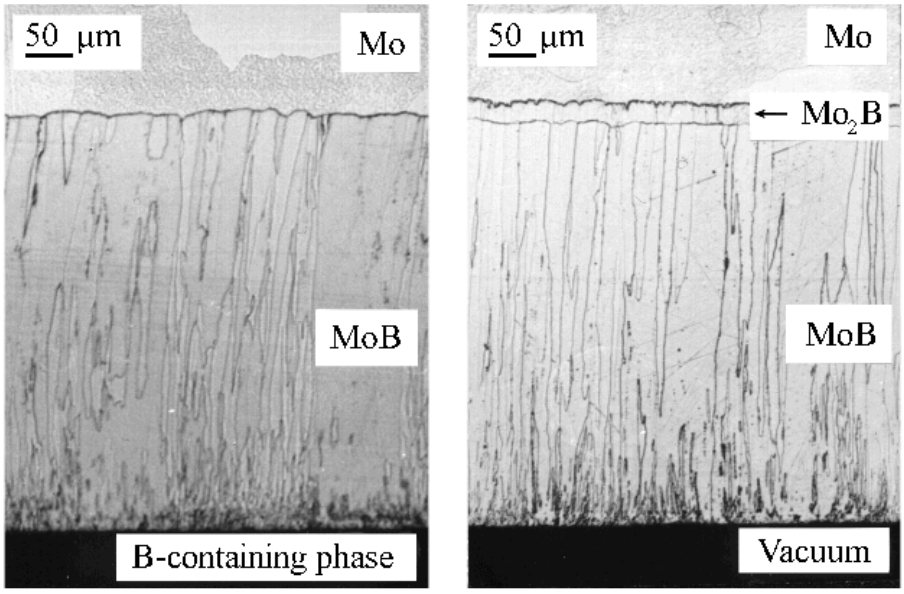

Fig. 5.9. Formation of molybdenum boride layers between (a) Mo and B-containing phase and (b) between Mo and MoB [109]. Reaction temperature 1450 ºC. Time: (a), 9000 s (2.5 h); (b), 7200 s (2 h).

However, if this same specimen is re-annealed at 1450 ºC for 2 h in vacuum in the absence of the B-containing phase, the Mo_2B layer about 19 μm thick occurs between Mo and MoB (Fig. 5.9b). Its formation is due to the decomposition of MoB

$$2MoB = Mo_2B + B_{dif}$$

and the subsequent reaction

$$B_{dif} + 2Mo_{surf} = Mo_2B.$$

It should be stressed that the processes of the phase transformation of A_pB_q into A_rB_s in the A_pB_q–A_rB_s–B and A_pB_q–A_rB_s–A_lB_n systems and the reaction diffusion of the A atoms across the A_rB_s layer from the A_pB_q–A_rB_s interface to the A_rB_s–B or A_rB_s–A_lB_n interface are inseparably linked with each other. Neither of them can occur without the other. It is clear, however, that their rates, when each is taken alone, are not identical.

The results presented in this chapter were obtained assuming that the rate of transformation of A_pB_q into A_rB_s is not less than the rate of diffusion of the A atoms across the A_rB_s layer. For thick layers, this appears to be rather substantiated. In thin layers of chemical compounds, especially if the structures of the A_pB_q and A_rB_s crystal lattices differ considerably, rearrangement of the A_pB_q into A_rB_s lattice may be the rate-determining step. Therefore, the growth kinetics of the A_rB_s layer will be dependent upon the rate of this transformation.

In such a case, the region of reaction control for the formation of the A_rB_s layer will merely be more extended in time. More essential differences between the kinetic dependences describing the growth rates of this layer in different reaction couples of the A–B multiphase binary system can hardly be expected.

Note that the driving force for the reaction between initial phases, *i.e*. the difference of the chemical potentials of the components in those phases, decreases in the series A–B, A_pB_q–B, A_pB_q–A_lB_n. This can easily be seen from the distribution of the content of component B in interacting phases, shown in Figs 5.1, 5.2 and 5.5, the concentration difference of component B being highest between A and B and least between A_pB_q and A_lB_n. Nevertheless, the growth rate of the A_rB_s layer increases in this series.

It seems therefore relevant to emphasise that great care is necessary in application of the usually unconditionally accepted thesis about a directly proportional relationship between the driving force behind any physical or chemical process and its rate. This example clearly shows that without a detailed knowledge of the mechanism of that process, starting only from "apparent general considerations", so beloved by many theoreticians, it is hardly possible to accurately describe its peculiarities, even qualitatively. In the case under consideration, "general considerations" would definitely lead to the opposite, misleading result because the highest growth rate of the A_rB_s layer is observed in the A_pB_q–A_lB_n reaction couple where the driving force for the reaction-diffusion process is least.

5.5: Duplex structure of the A_rB_s layer

Since in the A–A_lB_n, A_pB_q–B and A_pB_q–A_lB_n reaction couples the mechanisms of formation of the A_rB_s layer at its interfaces with adjacent phases are different, in many cases the duplex (dual) structure of this layer, shown schematically in Fig. 5.10, can readily be formed and observed experimentally.

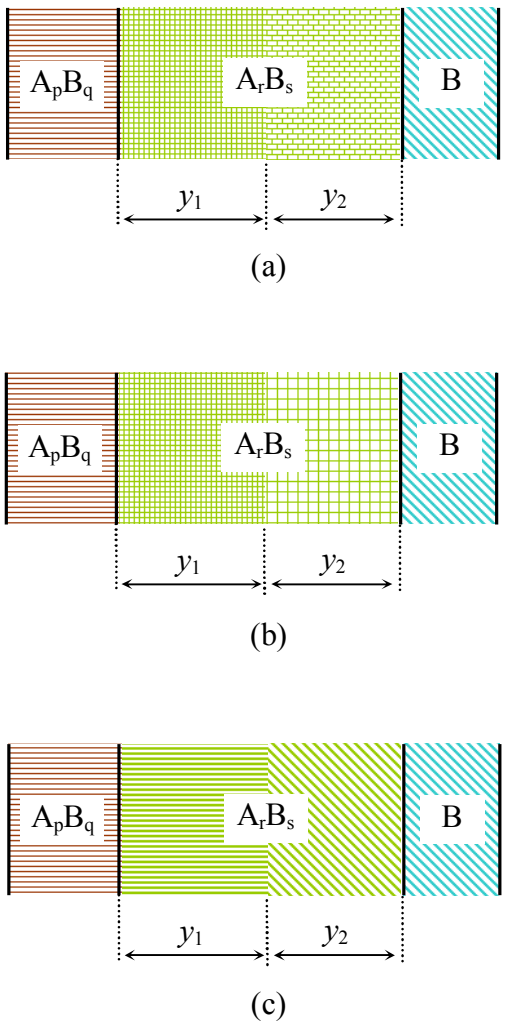

Fig. 5.10. Schematic representation of the duplex structure of the A_rB_s layer in which its sublayers differ by (a) shape, (b) size or (c) crystallographic orientation of grains.

The term *duplex structure* means that in the microstructure of the transition zone between reacting phases the layer of the same chemical compound looks like the layers of two quite different chemical compounds. Its sublayers having a distinct common interface can differ by the shape, size or orientation of grains.

Using the results of the preceding section, it is easy to show that if only component A is diffusing, then the ratio, y_1/y_2, of the thicknesses of these sublayers in the A_pB_q–B reaction couple is

$$\frac{y_1}{y_2} = \frac{1}{\beta - 1} = \frac{qr}{sp - qr}. \qquad (5.43)$$

Note that although the mechanisms of formation of the A_rB_s layer by reactions (5.6) and (4.2_1) are different, the products of these reactions are hardly distinguishable in the microstructure because both reactions take place at the same interface A_pB_q–A_rB_s. Therefore, if the A_rB_s layer grows in the A_pB_q–A_rB_s–B system by means of diffusion of both components, then reaction (4.2_1) also contributes to the value of y_1 of the duplex structure (see Fig. 5.3), thereby causing an additional increase of the y_1/y_2 ratio compared to the case where only component A is diffusing.

Duplex structures often occur in metallic, oxide, salt and other binary and multi-component systems. For example, the duplex structure of the Co_3O_4 oxide layer is observed in the CoO–Co_3O_4–O_2 system [110]. It consists of fine grains in the outer sublayer bordering the oxygen phase and coarse elongated grains in the inner sublayer bordering CoO. At 700-800 ºC, the thickness of the outer sublayer is 10.3 to 23.4% of the total thickness of the Co_3O_4 layer. The growth kinetics of this layer are parabolic.

If only cobalt diffused, then an increase of the thickness of the Co_3O_4 layer at the Co_3O_4–O_2 interface would be due to the partial chemical reaction

$$3Co_{dif} + 2O_2 = Co_3O_4,$$

while that at the CoO–Co_3O_4 interface to the phase transformation of CoO into Co_3O_4 by the reaction

$$4CoO = Co_3O_4 + Co_{dif}.$$

In the latter of these reactions, the number of CoO molecules formed per one diffusing Co atom is seen to be three times greater than in the former. Consequently, the ratio of the thicknesses of the outer and inner sublayers should be 1:3, *i.e.* the thickness of the outer sublayer must be equal to 25% of the total thickness of the Co_3O_4 layer. At 800 ºC, this value is close to the experimental one (23.4%).

At other temperatures, experimental values were found to be much lower than the predicted value 25%. It means that the contribution of oxygen diffusion to the growth process of the Co_3O_4 layer through the reaction

$$O_{dif} + 3CoO = Co_3O_4$$

is considerable at those temperatures. This partial chemical reaction leads to additional thickening the Co_3O_4 layer at the CoO–Co_3O_4 interface, thereby affecting the ratio of sublayer thicknesses.

If only component *B* is diffusing in the A_rB_s layer, then in the A–A_lB_n reaction couple the ratio of the thickness of the sublayer bordering the A_lB_n phase to the thickness of the sublayer bordering the *A* phase is seen from equations (5.1) and (5.18) to be $ls/(rn–ls)$. Couples of this type are Fe–$FeSn_2$ [111] and Nb–Nb_6Sn_5 [112].

The duplex structure of the FeSn layer between Fe and $FeSn_2$ consists of two sublayers of equal thickness. The sublayer adjacent to iron consists of fine-grained polyhedrons with approximately equal length of their sides. By contrast, the sublayer bordering the $FeSn_2$ phase consists of elongated grains aligned at almost right angles to the FeSn–$FeSn_2$ interface.

The ratio of the thicknesses of the sublayers of the FeSn layer can readily be found immediately from the equations of chemical reactions

$$Sn_{dif} + Fe_{surf} = FeSn$$

and

$$FeSn_2 = FeSn + Sn_{dif}$$

that occur in the Fe–FeSn–$FeSn_2$ system at the Fe–FeSn and FeSn–$FeSn_2$ interfaces, respectively. Since the same number (one at each) of the FeSn molecules is formed during these reactions at the interfaces of the FeSn layer, it is clear that the ratio of the thicknesses of the sublayers should be 1:1, provided that this layer grows entirely at the expense of diffusion of tin atoms.

Formation of the duplex structure of the Nb_3Sn layer is also observed between niobium and the Nb_6Sn_5 intermetallic compound [112]. The sublayer adjacent to niobium possesses a fine-grained structure, while that bordering Nb_6Sn_5 a coarse-grained one. The ratio of their thicknesses is close to the theoretical value 2:3, resulting from the equations of chemical reactions under the assumption of dominant diffusion of tin atoms in the Nb_3Sn lattice ($r = 3$, $s = 1$, $l = 6$, $n = 5$, $ls/(rn–ls) = 2/3$).

Duplex structures are also formed in reaction couples of the type A_pB_q–A_lB_n. In the Ni–Sn binary system, such a structure is typical of the Ni_3Sn_2 layer occurring between the Ni_3Sn and Ni_3Sn_4 phases [111]. In the Ni_3Sn_2 lattice, the nickel atoms diffuse much faster than the tin atoms. Therefore, the Ni_3Sn_2 layer grows mainly by means of the reaction

$$2Ni_3Sn = Ni_3Sn_2 + 3Ni_{dif}$$

that takes place at the Ni_3Sn–Ni_3Sn_2 interface, and of the reaction

$$3Ni_{dif} + Ni_3Sn_4 = 2Ni_3Sn_2$$

proceeding at the Ni_3Sn_2–Ni_3Sn_4 interface.

The number of Ni_3Sn_2 molecules formed per unit time at the Ni_3Sn_2–Ni_3Sn_4 interface is seen to be twice their number formed at the Ni_3Sn–Ni_3Sn_2 interface. Therefore, the ratio of the thicknesses of the sublayers in the duplex structure of the Ni_3Sn_2 layer must be 1:2. In this case, the shape of the grains is similar, while their sizes are different. The sublayer adjacent to the Ni_3Sn_4 phase consists of much larger grains than the sublayer bordering the Ni_3Sn phase.

Figure 5.11 shows the microstructure of the Ni_5Si_2 layer grown between the Ni_3Si and δ-Ni_2Si phases [108]. The diffusion coefficient of nickel in the Ni_5Si_2 lattice is reported to be much higher than that of silicon.

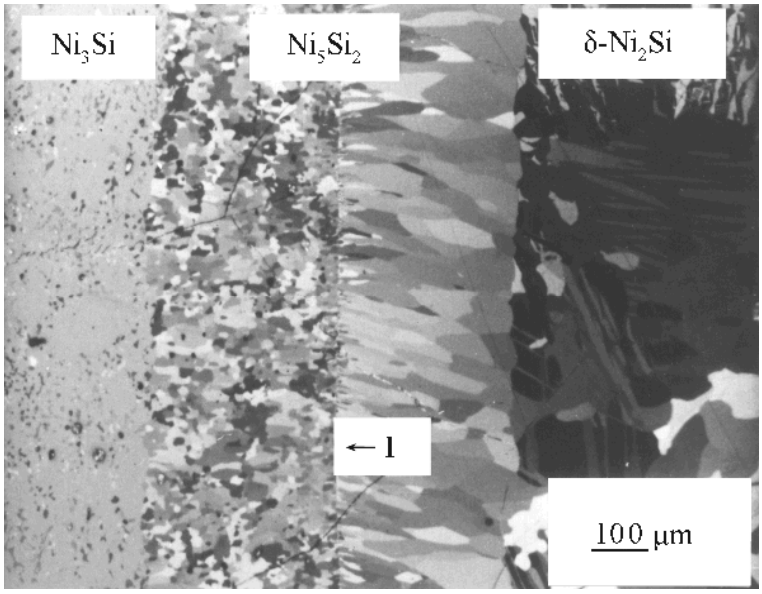

Fig. 5.11. Optical micrograph in the polarised light of the transition zone between Ni_3Si and δ-Ni_2Si phases [108]. Temperature 900 °C, reaction time 176400 s (49 h). The Ni_5Si_2 layer formed has an easily distinguishable duplex structure. The thicknesses of its sublayers are almost equal. Their interface is denoted by I.

Therefore, growth of the Ni_5Si_2 layer is due to reactions

$$2Ni_3Si = Ni_5Si_2 + Ni_{dif}$$

and

$$Ni_{dif} + 2Ni_2Si = Ni_5Si_2$$

taking place at the Ni_3Si–Ni_5Si_2 and Ni_5Si_2–Ni_2Si interfaces, respectively.

As seen in Fig. 5.11, the ratio of the thicknesses of the sublayers is about 1:1. The same value follows from the equations of chemical reactions because the numbers of Ni_5Si_2 molecules formed per unit time at the layer interfaces with the adjacent phases are equal.

It is clear that in cases like this, there is even no need to do marker experiments to reveal the main diffusing species. Formation of duplex structures provides by itself evidence for the dominant diffusion of one of two components. If, in addition, the ratio of sublayer thicknesses coincides with a theoretically predicted value, then it can be concluded that the layer growth undoubtedly takes place exclusively at the expense of diffusion of that component.

Note that the duplex structure of the layer of a chemical compound, observed in the quasi-binary systems formed by the oxides or salts with a common ion, may be of somewhat different nature, frequently being simply a result of different crystallographic orientation of the grains of initial phases. A suitable example is the process of formation of the $NiAl_2O_4$ spinel between the NiO and Al_2O_3 oxide phases [113].

If the crystallographic orientations of the NiO and Al_2O_3 single crystals are identical, then the newly-formed crystals of $NiAl_2O_4$ have the same orientation, and no duplex structure occurs, as shown schematically in Fig. 5.12a. If different, however, two sublayers of the same composition $NiAl_2O_4$ but of different crystallographic orientations of their crystals, readily distinguishable, for example by means of electron microscopy, are formed (Fig. 5.12b). The orientation of crystals of each sublayer is close to the orientation of crystals of the adjacent phase NiO or Al_2O_3.

The ratio, y_1: y_2 = 1 : 3, of the thicknesses of the sublayers follows immediately from the equations of chemical reactions

$$2Al^{3+}_{dif} + 4NiO = NiAl_2O_4 + 3Ni^{2+}_{dif}$$

and

$$3Ni^{2+}_{dif} + 4Al_2O_3 = 3NiAl_2O_4 + 2Al^{3+}_{dif}$$

taking place at the NiO–$NiAl_2O_4$ and $NiAl_2O_4$–Al_2O_3 interfaces, respectively. Growth of the $NiAl_2O_4$ layer is thus due to the counter-diffusion of the aluminium and nickel ions, while its grains at different interfaces tend to retain the crystallographic orientation of the parent phase.

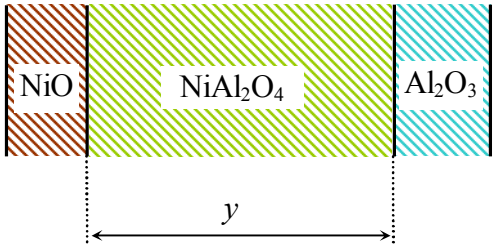

(a)

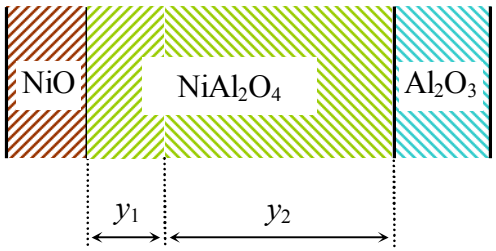

(b)

Fig. 5.12. Schematic representation of the growth process of the $NiAl_2O_4$ spinel layer between the oxides NiO and Al_2O_3. (a) All the phases have the same crystallographic orientation of their grains and therefore no duplex structure occurs. (b) The initial NiO and Al_2O_3 oxide phases have different crystallographic orientations of their grains. The $NiAl_2O_4$ layer assumes a duplex structure. Its sublayer adjacent to NiO retains the crystallographic orientation of this phase and is three times thinner than the sublayer bordering Al_2O_3, which retains the crystallographic orientation of the Al_2O_3 phase.

5.6: Formation of the same compound layer in various reaction couples: short conclusions

1. The growth rate of the layer of any chemical compound in reaction couples consisting of one of elementary substances *A* or *B* and another compound of a multiphase binary system or of two other compounds, is higher than the rate of its growth between pure components, provided that this layer is the only one in all reaction couples under comparison.

2. The closer the chemical compositions of the initial phases of a given reaction couple, the greater is the layer-growth rate compared to that in the *A*–*B* reaction couple, even though the driving force of the reaction-diffusion process changes in the opposite direction, as illustrated schematically in Fig. 5.13.

3. The ratio of the rates of diffusional (parabolic) growth of the same compound layer in various reaction couples can be predicted exactly knowing only the stoichiometry of all compounds of a multiphase binary system. In this case, diffusional and physico-chemical approaches yield identical results which are in good agreement with available experimental data.

4. The physico-chemical approach allows also certain predictions regarding the layer-growth rate in the linear region to be made, whereas in the framework of diffusional considerations the linear growth cannot be explained, even qualitatively.

5. If diffusion of one of the two components prevails in the growing layer of a chemical compound, then in the reaction couples consisting of one of other compounds of a multiphase system and the non-diffusing component or of two other compounds this layer may be expected to have a duplex structure. Its sublayers differ by the shape, size or orientation of their grains.

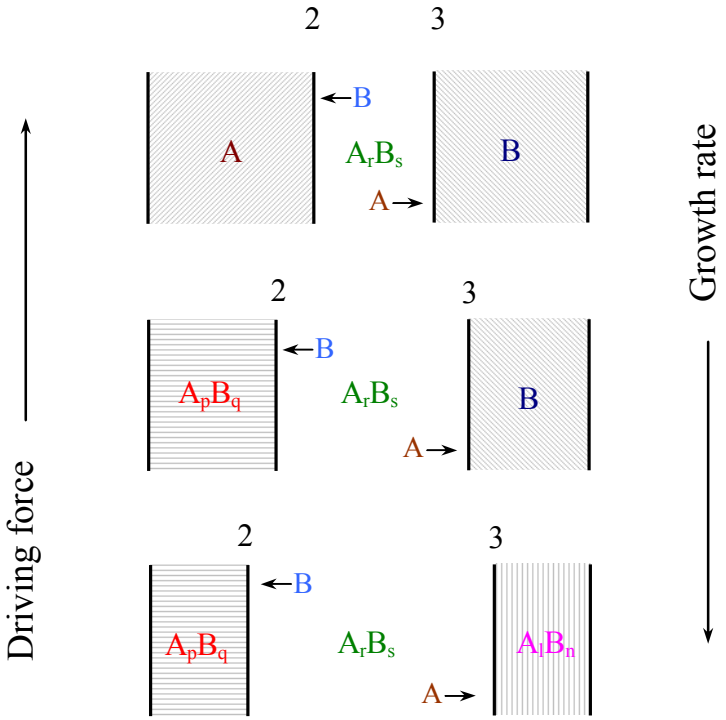

Fig. 5.13. Schematic comparison of the growth rate of the A_rB_s layer and the driving force of the reaction-diffusion process in three main types of reaction couples of a multiphase system *A–B*.

6: Formation of a compound layer in solid-liquid and solid-gas reactions

The melting points of the components of a reaction couple are most frequently different. Therefore, there is a certain range of temperature in which one of the components is in the solid state, while the other in the liquid state. If soluble, the solid substance will dissolve in the liquid phase. The dissolution process should clearly affect the growth kinetics of a chemical compound layer at the solid-liquid interface.

If a solid interacts with a gas, the reaction product may happen to be appreciably volatile at a given temperature. Then, the rate of its evaporation must also be taken into account in kinetic equations.

The effect of dissolution in the solid-liquid system and of evaporation in the solid-gas system on the growth rate of a chemical compound layer will be established in this chapter. Substance A will be assumed to have a higher melting point than substance B. As before, substance B is considered to be insoluble in phase A.

6.1: Main relationships governing dissolution of solids in liquids

It seems relevant to briefly consider first the main features of the process of dissolution of a solid substance in a liquid. Assume that the interaction of substances A and B takes place at temperature T_2 (see Fig. 2.1). The solubility of component A in liquid B at this temperature is c_s, kg m^{-3} or mol m^{-3}. If the instantaneous concentration c of A in B is below this value, then solid A will dissolve in liquid B.

Consider first the case where the chemical compound A_pB_q is not formed between initial substances A and B during dissolution. The rate of dissolution of any solid in the well-agitated liquid phase is described by an equation of the form

$$\frac{\mathrm{d}c}{\mathrm{d}t} = k\frac{S}{v}(c_s - c) \qquad (6.1)$$

where c is the concentration of the dissolved substance in the bulk of the liquid phase at time t, c_s is the saturation concentration (solubility) of A in B at a given temperature, k is the dissolution-rate constant, S is the surface area of the solid in contact with the liquid, and v is the volume of the liquid.

This type of equation of was first proposed to describe the process of dissolution of solids in liquids by A. Shchukarev in 1896 [114]. According to W. Nernst [115], the dissolution-rate constant can be expressed as follows

$$k = \frac{D_A}{\delta} \tag{6.2}$$

where D_A is the coefficient of diffusion of the atoms of the dissolving substance A across the diffusion boundary layer adjacent to the surface of the solid into the liquid phase, and δ is the thickness of the diffusion boundary layer.

Note that equation (6.1) follows immediately from Fick's laws on the assumption of a quasi-stationary distribution of the concentration of components within the diffusion boundary layer. Indeed, if in this layer $\partial c_A/\partial t \approx 0$, then the second Fick law yields $\partial c_A/\partial x \approx$ const. It means that the distribution of the concentration of component A within the diffusion boundary layer is close to linear (Fig. 6.1).

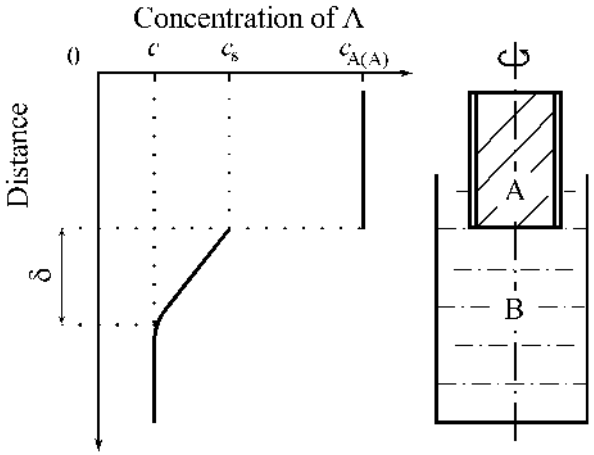

Fig. 6.1. Schematic diagram to illustrate the process of dissolution of a solid A in a liquid B in the case where no chemical compound layer is formed at their interface. Not to scale; in fact, the thickness, δ, of the diffusion boundary layer is very small in comparison with the height of the column of the liquid phase.

Anywhere outside, the concentration of A is assumed to be the same and equal to an instantaneous value, c. Clearly, this implies sufficiently intensive agitation of the liquid. In such a case, the flow of A atoms across the diffusion boundary layer under the condition of constancy of the surface area of the dissolving solid is

$$j_A = -D_A\left(\frac{\partial c_A}{\partial x}\right)_S = -D_A\frac{c_s - c}{\delta}\ . \qquad (6.3)$$

In terms of the concentration of substance A in the bulk of liquid B the flow, j_A, can be written as follows

$$j_A = \frac{v}{S}\frac{\mathrm{d}c}{\mathrm{d}t}. \qquad (6.4)$$

Equation (6.1) is then obtained by combining equations (6.2)-(6.4).

Clearly, this derivation of equation (6.1) is valid only in the case of the diffusional regime of dissolution of substance A in liquid B when the overall rate of the process is limited by the rate of transition of the A atoms across the diffusion boundary layer. However, the equation itself is also applicable in the case of another, interface (decomposition) controlled regime of dissolution when the rate-determining step is the rate of separation of the A atoms from the solid surface due to their interaction with the B atoms at the solid-liquid interface.

Indeed, it appears obvious that a variation of the concentration of any dissolving solid substance in a liquid is directly proportional to both the area of its surface contacting with the liquid and the difference between the saturation concentration (solubility) at a given temperature and the instantaneous concentration of A in B, and is inversely proportional to the volume of the liquid phase. Therefore, the general form of equation (6.1) remains unchanged for either dissolution regime of any solid in any liquid. The difference lies in the character of the dependence of the dissolution-rate constant k upon the thickness δ of the diffusion boundary layer.

It is clear that under conditions of interfacial (decomposition) control the rate of dissolution of a solid in a liquid is independent of the thickness of the diffusion boundary layer and hence of the intensity of agitation of the liquid. By contrast, in the case of diffusional control the intensity of agitation of a liquid exerts a strong influence on the thickness of the diffusion boundary layer, thus affecting the value of the dissolution-rate constant k.

Most frequently, the process of dissolution of solid substances in liquids is investigated using the rotating disc technique [116-120]. The main advantage of this method is an equal accessibility of the rotating disc surface, *i.e.* the dissolution of its surface (or the deposition of any reaction product on it) takes place uniformly.

According to V.G. Levich [116], the thickness of the diffusion boundary layer at the rotating disc surface is expressed by the equation

$$\delta = 1.61 D^{1/3}\nu^{1/6}\omega^{-1/2} \qquad (6.5)$$

where v is the kinematic viscosity of the liquid phase, $m^2\ s^{-1}$; ω is the angular speed of the disc rotation, rad s^{-1}. For simplicity, the subscript A at D_A was omitted.

From equations (6.2) and (6.5), it follows

$$k = 0.62 D^{2/3} \nu^{-1/6} \omega^{1/2} \ . \qquad (6.6)$$

This equation allows the determination of the diffusion coefficient, D, of the atoms of the dissolving substance across the diffusion boundary layer, knowing the value of the dissolution-rate constant k and *vice versa*. It is essential to note, however, that equation (6.6) only holds for Schmidt's numbers Sc exceeding 1000.

The Schmidt number is a dimensionless parameter equal to the quotient of dividing the kinematic viscosity by the diffusion coefficient: Sc = v/D (for more detail, see Refs [116, 117, 119]). Usually, for liquids Sc is less than 1000. In such a case, more accurate calculations can be carried out using the equation

$$k = 0.554 I^{-1} D^{2/3} \nu^{-1/6} \omega^{1/2} \qquad (6.7)$$

in which the factor I is a (slight) function of the Schmidt number: $I = f(\mathrm{Sc})$. The dependence of I upon Sc is provided in Table 6.1 [117, 121].

Equation (6.7) was proposed by T.F. Kassner [121]. It is valid for Sc > 4. In the range $10 < \mathrm{Sc} < 10^3$ typical of liquid metals the difference in the results of calculations with the use of equations (6.6) and (6.7) varies from 3-17%.

In many cases, the solid disc indeed dissolves in a liquid uniformly over the entire surface, as in Fig. 5.2a [122]. Sometimes, however, spiral etch patterns reproducing the lines of laminar flow of the liquid are seen on the disc surface after its dissolution in the liquid phase. An example is shown in Fig. 5.2b. It takes place when the velocity of movement of the solid-liquid interface relative to its initial position exceeds a certain limiting value.

It is clear that the occurrence of visible etch patterns provides evidence for the violation of the condition of an equal accessibility of the rotating disc surface. Therefore, when investigating the dissolution process, the diameter of a disc is to be chosen in such a way as to ensure that, for the pre-determined volume of a liquid, the depth of dissolution of the disc should not exceed a critical value for that particular system.

Table 6.1. Dependence of the correction factor I of the Kassner equation upon the Schmidt number Sc [117, 121]

Sc^{-1}	I	Sc^{-1}	I	Sc^{-1}	I
0.001	0.9209	0.010	0.9564	0.100	1.0368
0.002	0.9286	0.020	0.9747	0.110	1.0412
0.003	0.9341	0.030	0.9877	0.120	1.0451
0.004	0.9385	0.040	0.9981	0.130	1.0488
0.005	0.9424	0.050	1.0068	0.140	1.0521
0.006	0.9457	0.060	1.0143	0.150	1.0552
0.007	0.9487	0.070	1.0209	0.160	1.0580
0.008	0.9515	0.080	1.0268	0.180	1.0631
0.009	0.9541	0.090	1.0321	0.200	1.0675

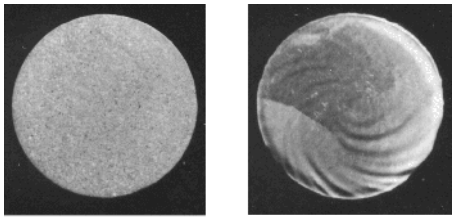

(a) (b)

Fig. 6.2. (a) Niobium and (b) molybdenum discs (12 mm diameter) after their dissolution in liquid aluminum at 700 ºC and an angular rotational speed of 25.0 rad s^{-1}. Dissolution time is 7200 s, while St/v is 19440 s m^{-1} [122].

Diameter values between 1 and 2 cm are practicable. With smaller discs, edge effects become significant. Greater discs are unsuitable from the point of view of experimental set-up.

The volume of the liquid phase usually varies between 10 and 50 cm^3. The diameter of the column of the liquid phase is 2 to 3 times greater than that of the disc. The distance between the disc surface and the bottom of the liquid-phase column is on the order of the disc diameter or a little greater. The depth of immersion of the disc into the liquid is around half the disc diameter. Typical rotational speeds ω lie in the range 5-100 rad s^{-1}.

Note that both a small disc in the large volume of a liquid and a large disc in the small volume of a liquid will hardly produce reliable data on the dissolution kinetics of the solid in the liquid. In the former case, the small disc will not ensure sufficient convective agitation of the liquid phase. In the latter, the turbulence threshold may happen to be exceeded.

Turbulence is known to occur at Reynolds numbers in excess of 10^5. Reynolds number $\mathrm{Re} = \omega r^2/\nu$, r being the disc radius, is a dimensionless parameter characterising the hydrodynamic regime of flow of liquids [116, 117]. Reproducible results are only obtained if the flow is laminar.

It should be emphasised that the simplest way of avoiding the formation of deep etch patterns, namely, by reducing the time of the solid-with-liquid interaction, does not appear to be the best because it only masks the phenomenon, not eliminating its cause. Therefore, it appears to be much more reasonable to increase the disc diameter and to reduce the volume of the liquid phase (within acceptable limits and taking account of other restrictions [116, 117]), so that during dissolution from zero up to the saturation concentration (solubility) of A in B no etch patterns will occur onto the disc surface.

Integration of equation (6.1) with the initial condition $c = 0$ at $t = 0$ yields

$$c = c_s\left[1 - \exp\left(-\frac{kSt}{\nu}\right)\right] \tag{6.8}$$

or in another form

$$\ln\frac{c_s}{c_s - c} = k\frac{St}{\nu}. \tag{6.9}$$

If the initial concentration of the dissolving substance in the liquid is equal to c_0, then

$$\ln\frac{c_s - c_0}{c_s - c} = k\frac{St}{\nu}. \tag{6.10}$$

Equations (6.1), (6.8)-(6.10) indicate that the process of dissolution of a solid in a liquid is characterised by two quantities, namely, the saturation concentration or solubility c_s and the dissolution-rate constant k. At constant pressure, the former only depends upon temperature. The latter is in addition dependent upon the hydrodynamic conditions of flow of the liquid.

6.2: Experimental investigation of the dissolution process of a solid in a liquid

The process of dissolution of a solid in a liquid can readily be investigated using a rapid-quenching device like that shown in Fig. 6.3 [122]. Depending on the nature of substances to be studied, this may be carried out either in vacuum, or in a protective atmosphere (inert gases, hydrogen, nitrogen, *etc*.), or under a flux.

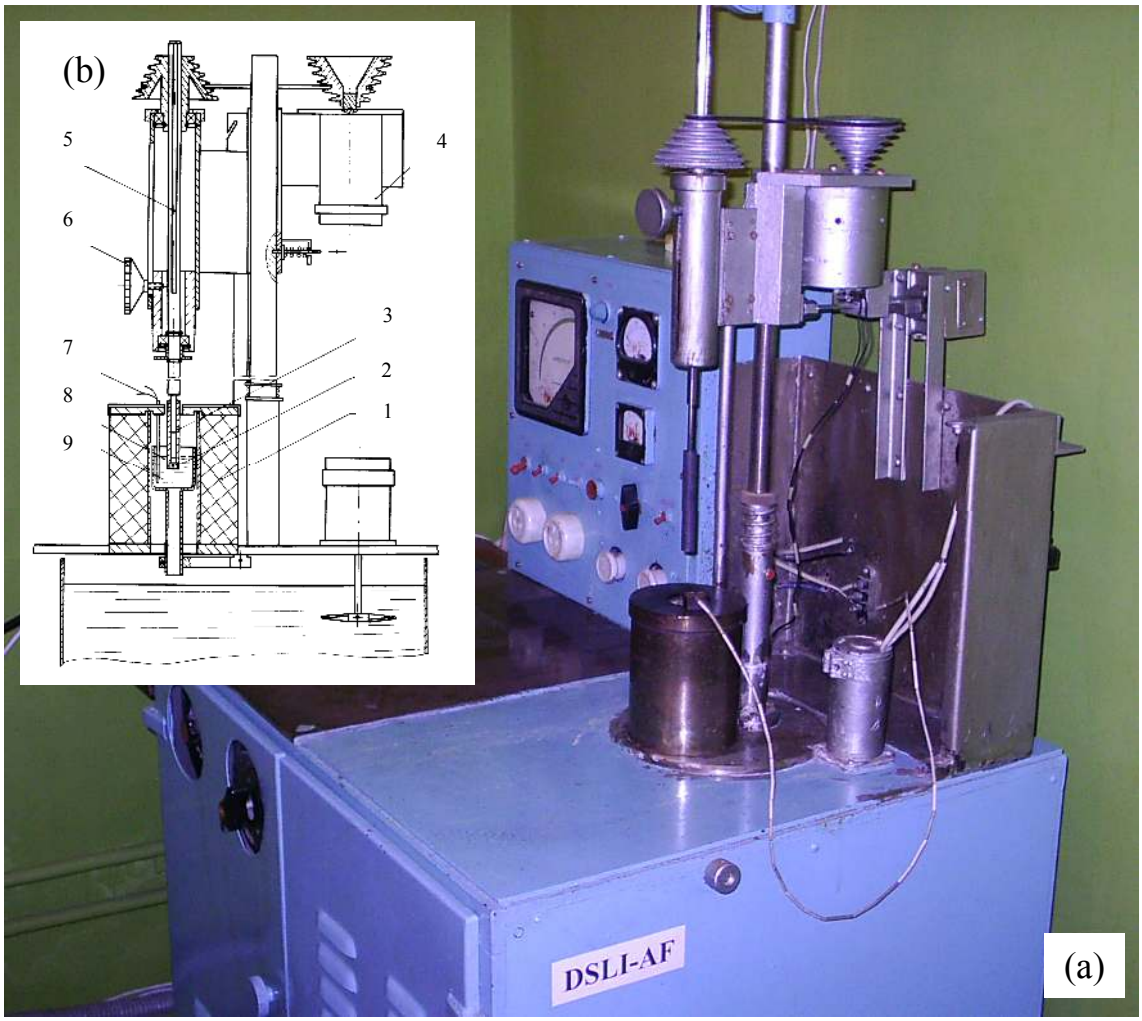

Fig. 6.3. (a) General view and (b) scheme of the rapid-quenching device for investigating the process of dissolution of a solid in a liquid by the rotating disc technique [122]. 1, electric-resistance furnace; 2, solid specimen; 3, protective tube; 4, electric motor; 5, rotating shaft; 6, stopper; 7, thermocouple; 8, flux; 9, liquid.

To heat the materials under investigation to the required temperature and to maintain it, the electric-resistance furnace 1 is employed. The specimen 2 of a solid substance is connected, by means of the protective tube 3, with the shaft 5, being rotated by the electric motor 4. The shaft is free to move in the vertical direction and can be fixed in the required position by the stopper 6. The temperature is measured with the help of the thermocouple 7.

The flux 8 is used both to pre-heat the solid specimen to the experimental temperature and to protect the liquid 9 from oxidation by atmospheric air.

Consider the main features of the process of dissolution of some transition metals in liquid aluminium as an typical example [122]. Cylindrical specimens of a transition metal, 11.28±0.01mm in diameter and 5-6 mm high, were machined from 12-13 mm diameter rods prepared by arc melting the metal under investigation. The disc surface was then ground flat and polished mechanically.

Immediately before the experiment, the solid specimen is rinsed with ethanol and dried. Then, it is pressed into a high-purity graphite tube, 16 mm diameter, to protect its lateral surface from contact with the metallic melt. Therefore, only the disc surface, 1 cm^2 area, dissolvs in liquid aluminium during the run. If a larger surface area is desirable (for example, when determining the solubility values), while its instantaneous value is unimportant, the specimens with unprotected lateral surfaces are used. In such cases, graphite tubes serve only as holders for transition-metal specimens.

A special flux consisting of the halides of alkali metals with the addition of sodium and aluminium fluorides is employed both to protect the aluminium melt from oxidation and to pre-heat the solid specimen to the required temperature. First, the flux is melted in a 26 mm inner diameter alumina crucible. Melting starts at about 350 °C. The height of the flux column is around 15 mm. Aluminium pieces are then melted under the flux layer. The amount of aluminium taken is usually equivalent to a volume of the liquid metal of 10 cm^3. At 700-900 ºC, it is approximately 24 g.

For pre-heating, the disc specimen rotating at a low angular speed (6.45.0 rad s^{-1} or less) is lowered into the flux bulk, so that the distance between its surface and the top surface of the liquid-aluminium column is around 10 mm. After the temperature has equilibrated (typically, it takes around 500 s), the specimen rotating at the required speed is lowered into the bulk of molten aluminium, so that the distance from the disc surface to the bottom of the crucible is 15.0±0.5 mm. This is the start of the run. The rotating disc is held in the melt for a pre-determined period of time. The run is then completed in one of two following ways.

1. When studying the dissolution process, the solid transition-metal specimen is lifted from the aluminium melt into the middle of the flux column, and then the crucible, together with the melt, the flux and the specimen, is rapidly cooled down in a water bath located below the electric furnace. After cooling down to room temperature, the major portion of the aluminium alloy adhering to the surface of the transition-metal specimen is removed mechanically. The remainder is dissolved in a 20% aqueous solution of NaOH at a slow heating. The specimen, free of both aluminium and intermetallic layers, is then washed with water and alcohol, dried and weighed. Because the specimen has also been weighed before the run, its mass loss during dissolution in liquid aluminium can thus be determined.

Samples of the aluminium alloys obtained are analysed chemically to determine their transition-metal contents. Use is usually made of photometric methods. The results are then compared with those found from mass loss measurements.

2. When studying the growth kinetics of intermetallic layers, after the run the crucible, together with the flux, the melt and the solid specimen, is "shot" into cold water to arrest the reactions at the transition metal-aluminium interface. Note that the solid specimen is being rotated until melt solidifies entirely. It is especially essential in examining the formation of the intermetallic layers under conditions of their simultaneous dissolution in the liquid phase (with undersaturated aluminium melts). The time of cooling the experimental cell from the experiment temperature down to room temperature usually does not exceed 2 s.

After cooling, the bimetallic specimen obtained is cut along the cylindrical axis, ground flat and polished electrolytically. The cross-sections prepared are examined by metallography, X-ray diffraction, electron probe microanalysis and other techniques.

6.2.1: Determination of the saturation concentration

The saturation concentration is equal to the solubility of a solid in a liquid at a given temperature. Therefore, its value can in principle be extracted from the liquidus curve of the equilibrium phase diagram of the *A–B* binary system (see Fig. 2.1).

However, in the great majority of cases the accuracy of determining the position of this curve on the phase diagrams is too far from being satisfactory. The data obtained by various authors may differ very considerably, especially in the case of low solubility values (< 1 %). Meanwhile, to obtain reasonable results in calculating the dissolution parameters from equations (6.1) and (6.8)-(6.10), the solubility (saturation concentration) should be known with a relative error not exceeding 5 %. For this reason, it is advisable to begin studying the dissolution process with its experimental determination by saturating a liquid with a solid using, for example, the same rotating disc technique.

Figure 6.4 shows a plot of the tungsten concentration in the aluminium melt against St/v (often called the reduced dissolution time, even though it is measured in s m^{-1}) at 700-850 °C. It is seen that at a constant temperature the tungsten content in aluminium gradually increases up to some limiting value and then remains unchanged. This is just the quantity c_s entering into equations (6.1) and (6.8)-(6.10). The solubility values of some transition metals in liquid aluminium are presented in Table 6.2 [120].

The solubility of various metals is seen to differ considerably. For example, at 700 °C the solubility of nickel in the aluminium melt is 10 %, while that of niobium is only about 0.02 %. For other transition metals, appropriate values are more close, although iron and cobalt also stand apart in this respect. To reveal the causes of such differences, detailed investigations of the structure of liquid alloys are badly needed.

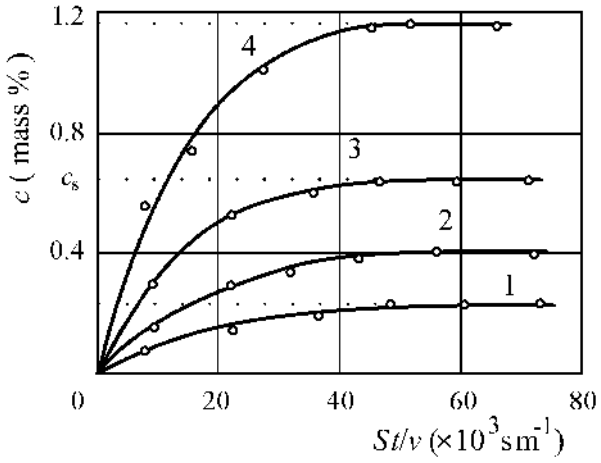

Fig. 6.4. Concentration of tungsten in liquid aluminium plotted against St/v to determine its solubility (saturation concentration) at a given temperature [122]. Angular disc rotational speed $\omega = 25.0$ rad s^{-1}. Temperature: 1, 700 °C; 2, 750; 3, 800; 4, 850.

Table 6.2. Solubility values (%) of transition metals in liquid aluminium [120]

Metal	700 °C	750°C	800°C	850 °C
Ti	0.214	0.33	0.51	0.73
V	0.28	0.46	0.73	0.96
Cr	0.72	1.29	2.5	4.1
Fe	2.5	3.4	5.3	7.9
Co	1.6	2.4	4.2	6.9
Ni	10.0	13.5	19.5	27.0
Zr	0.156	0.276	0.46	0.66
Nb	0.0197	0.0337	0.057	0.101
Mo	0.215	0.44	0.71	1.14
Ta	0.105	0.17	0.25	0.37
W	0.23	0.40	0.84	1.16
Re	0.24	0.61	1.21	1.8

If a binary or multi-component alloy is undergoing the liquid-metal attack, then its dissolution can be either selective or non-selective. In the former case, the more soluble component dissolves at a higher rate.

Hence, the solid phase becomes depleted, while the liquid enriched in this component. In the latter case, the ratio of the alloy components in both phases remains unchanged during dissolution.

On the one hand, selective dissolution of transition-metal alloys in liquid aluminium might be expected in view of considerable differences in their solubility in respective binary systems. On the other, however, in these alloys the atoms of different elements are connected together by metallic bonds of nearly equal strength. Any of the elements can therefore scarcely be expected to leave the alloy lattice at a rate that significantly exceeds the rates of transition of other elements into liquid aluminium.

Iron-nickel alloys are known to dissolve in the aluminium melts non-selectively. The same applies to Fe–Cr alloys and even such a complicated material as an 18Cr–10Ni stainless steel (for more detail, see Ref. [16].

6.2.2: Evaluation of the dissolution-rate constant

To determine the accurate values of the dissolution-rate constant, thorough investigations of initial portions of the $c - St/v$ curves like those shown in Fig. 6.4 are to be carried out. Figure 6.5 shows the experimental data for tungsten single crystals of different crystallographic orientation as an example.

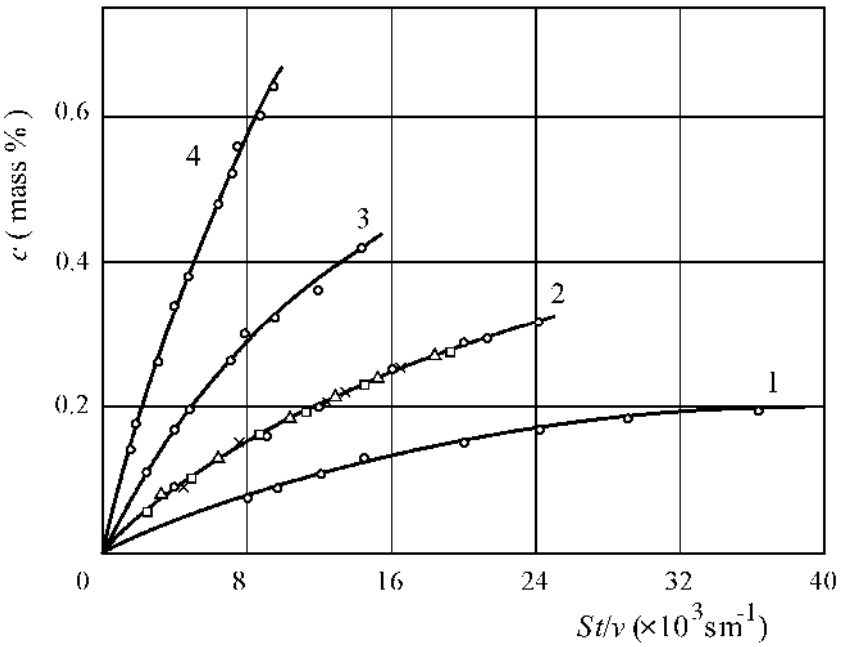

Fig. 6.5. Tungsten concentration in liquid aluminium plotted against St/v at ω = 25.0 rad s^{-1}. Temperature: 1, 700 °C; 2, 750; 3, 800; 4, 850. Crystallographic orientation of single crystals: □, (001); ×, (101); ○, (111); Δ, (112) [122].

Clearly, under conditions of diffusion control the rate of dissolution expressed in terms of the concentration of dissolving elements in the melt does not depend upon the atomic packing density of the crystallographic faces of any substance under investigation. Therefore, dissolution of single crystals of different orientation (line 2 in Fig. 6.5.) is characterised by the same value of the dissolution-rate constant found from equation (6.9) or (6.10). Note, however, that if the dissolution process is followed by measuring the decrease in the disc height, then the faces of looser package will have a higher decrease compared to those of denser package.

Strictly speaking, when using equations (6.1) and (6.8)-(6.10), both the instantaneous and the saturation concentration (solubility) should be expressed in kilograms or moles per cubic metre. However, in this particular case the content of tungsten in aluminium is relatively small (oo the order of 1 % or less). Therefore, it can be expressed in any units because a directly proportional relationship is retained between them with sufficient accuracy.

From equations (6.9) and (6.10), it follows that the experimental points plotted in the coordinates

$$\ln\frac{c_s}{c_s - c} - \frac{St}{v}$$

or

$$\ln\frac{c_s - c_0}{c_s - c} - \frac{St}{v},$$

if the initial concentration is $c_0 \neq 0$, should produce a straight line of the slope equal to the dissolution-rate constant of a solid substance in a liquid at a given temperature and hydrodynamic conditions of flow of the liquid phase.

As seen in Fig. 6.6, for tungsten this relationship is indeed linear. The same applies to other transition metals and alloys hitherto investigated. For some of them, values of the dissolution-rate constant in liquid aluminium at an angular disc rotational speed of 25.0 rad s^{-1} are presented in Table 6.3.

In contrast to the solubility, the values of the dissolution-rate constants of different metals and alloys in liquid aluminium are rather close. At least, they are of the same order of magnitude, namely 10^{-5} m s^{-1}, although the solubility values may differ by two orders of magnitude or more (see Table 6.2). This is also typical of dissolution of other solid substances in liquids [116-118].

Note that the values of the dissolution-rate constant rarely reveal any regular change over the compositional range of a binary alloy (see Ref. [16]), indicative of the complicated nature of interaction in the liquid state. For example, in the case of dissolution in liquid aluminium at 700 °C and ω = 24.0 rad s^{-1} $k = 3.8\times10^{-5}$ m s^{-1} for iron, 6.5×10^{-5} m s^{-1} for nickel and 5.5×10^{-5} m s^{-1} for chromium.

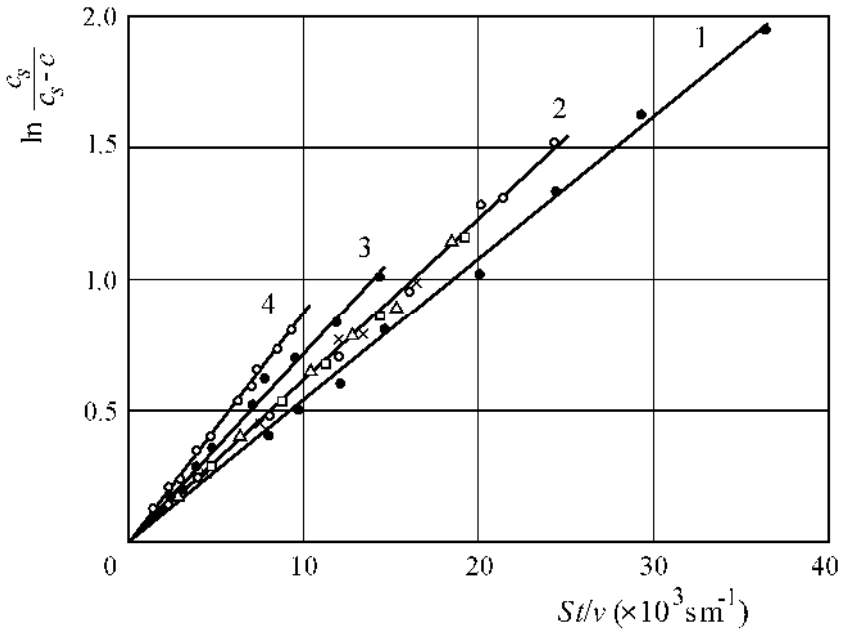

Fig. 6.6. A plot of $\ln[c_s/(c_s - c)]$ against St/v for the data of Fig. 6.5 [122].

Table 6.3. Values of the dissolution-rate constant, k ($\times 10^{-5}$ m s^{-1}), of transition metals in liquid aluminium at an angular disc rotational speed of 25 rad s^{-1} [120]

Metal	700°C	750°C	800°C	850°C
Ti	5.8	6.9	8.2	9.3
V	3.0	3.6	4.5	5.0
Cr	5.5	6.5	7.5	8.5
Co	6.1	7.0	7.5	8.1
Ni	6.5	9.1	10.0	10.7
Zr	5.4	6.1	7.1	7.7
Nb	4.6	5.1	6.2	6.8
Mo	5.4	6.0	7.4	8.0
Ta	4.6	5.5	6.4	7.3
W	5.4	6.1	7.6	8.5
Re	5.3	6.0	7.0	7.5

Under the same conditions, $k = 5.9\times10^{-5}$ m s^{-1} for a 90% Fe–10% Ni alloy and 6.0×10^{-5} m s^{-1} for a 75% Fe–25% Ni alloy. For 90% Fe–10% Cr and 75% Fe–25% Cr alloys, appropriate values are 4.2×10^{-5} m s^{-1} and 3.0×10^{-5} m s^{-1}. The dissolution-rate constant of any Fe–Ni alloy in liquid aluminium tends to slightly decrease with increasing time, while that of Fe–Cr alloys and a 18%Cr–10% Ni stainless steel is indeed constant, being 4.8×10^{-5} m s^{-1} for the latter.

It should be emphasised that accurate calculations of the dissolution-rate constant, k, can only be carried out if the difference between c and c_s is sufficiently large. The error in calculating this constant rapidly increases as c approaches c_s due to the low value of the denominator ($c_s - c$) in equations (6.9) and (6.10). In such a case, even a small inaccuracy in determining the instantaneous concentration c that is clearly practically unavoidable yields a very large error in calculating the value of k.

At the real accuracy of determining the concentration c with a relative error of 2-5%, its upper limit should not exceed $(0.6\text{-}0.7)c_s$. The lower limit depends on the sensitivity and accuracy of experimental methods employed to investigate the process of dissolution of a solid in a liquid.

Although the assumption of a quasi-stationary distribution of the concentration of component A within the diffusion boundary layer seems to be very rough, nevertheless under conditions of sufficiently intensive convection the dissolution kinetics of solids in liquids is well described by equations (6.1) and (6.8)-(6.10). Clearly, these equations are only applicable at a low solubility of the solid in the liquid phase, typically about 10-100 kg m^{-3} or up to 5%.

Note that in some cases they may also describe fairly well the dissolution process in systems of much higher solubility. An example is the Al–Ni binary system in which the solubility of nickel in aluminium amounts to 10 % even at a relatively low temperature of 700 °C (in comparison with the melting point of aluminium, 660 °C).

At a high solubility of the solid in the liquid phase, account must be taken of a variation of the volume of their solution with passing time, due to the transition of the dissolving substance into the bulk of the liquid. For most systems, an exact dependence of the volume of the solution upon its concentration is not known. In such cases, use is made of various approximate methods of determining this dependence. Usually, satisfactory results may be obtained by assuming a linear relation between the solution volume and the concentration of the dissolved substance

$$v = v_0(1+\gamma c), \quad \gamma = (v_s - v_0)/v_s c_s, \tag{6.11}$$

where v_0 is the initial volume of the liquid and v_s is the volume of the liquid after its saturation with the dissolving substance.

Substitution of this expression for the volume into equation (6.1) and subsequent integration with the initial condition $c = 0$ at $t = 0$ yields an equation for calculating the dissolution-rate constant

$$k_v = \frac{v_s}{St}\left[\ln\frac{c_s}{c_s - c} - \frac{v_s - v_0}{v_s c_s}\right]. \qquad (6.12)$$

It is easy to estimate the error associated with neglecting a variation of the volume of the liquid phase due to the dissolution of a solid substance. Indeed, term-by-term dividing of equation (6.12) by (6.9) shows that

$$\frac{k_v}{k} \to 1, \quad \text{as} \quad c \to 0, \qquad (6.13_1)$$

and

$$\frac{k_v}{k} \to 1 + \frac{v_s - v_0}{v_0}, \quad \text{as} \quad c \to c_s. \qquad (6.13_2)$$

Hence, this error does not exceed the value

$$\frac{v_s - v_0}{v_0} \times 100\%$$

of the relative change in volume of the liquid phase during dissolution of a solid from the zero concentration up to the saturation of the solvent.

The result obtained makes it possible to decide whether it is necessary to take account of a variation of the volume of any liquid due to the dissolution of a solid substance or it can be neglected in comparison with other possible uncertainties. To do this, one must know an experimental value of the density of the saturated solution. If not available, it may readily be estimated using the rule of additivity of the reciprocals: $1/\rho_{solution} = 1/\rho_A + 1/\rho_B$.

From equations (6.6) and (6.7), it follows that under conditions of diffusion control the dissolution-rate constant should depend linearly on the square root of the angular disc rotational speed. As seen in Fig. 6.7, this is indeed the case.

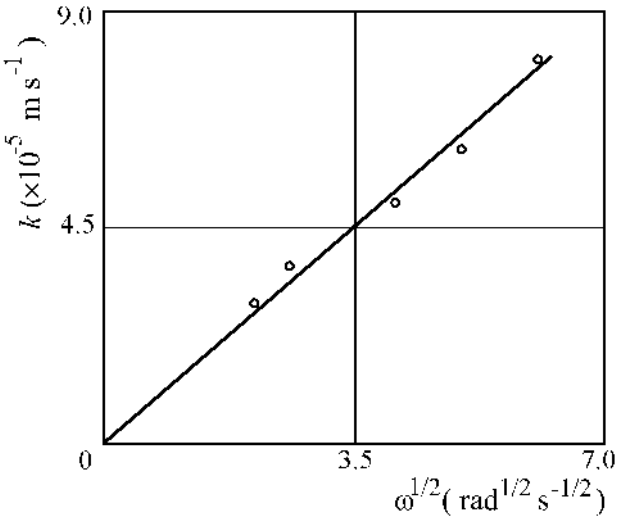

Fig. 6.7. A plot of the dissolution-rate constant of tungsten in liquid aluminium against the square root of the angular disc rotational speed at 750 °C [122].

6.2.3: Estimation of the diffusion coefficient

Knowing an experimental value of k, it is possible to evaluate the diffusion coefficient of the atoms of a dissolving solid substance across the diffusion boundary layer at the solid-liquid interface into the bulk of the liquid phase by using equations (6.6) and (6.7). Its calculation includes two steps.

To begin, an approximate value of D is calculated from equation (6.6). Next, the Schmidt number Sc and the correction factor I is found (see Table 6.1). Finally, a more accurate value is calculated from equation (6.7). In most cases, the results of these calculations do not differ by more than 10%. Values of the diffusion coefficient of some transition metals in liquid aluminium thus found are presented in Table 6.4 as an example [120].

Since even at the zero initial concentration of component A in the solution its average concentration in the diffusion boundary layer at the solid-liquid interface varies during dissolution from $c_s/2$ to c_s, the values in Table 6.4 characterise the diffusion in saturated solutions rather than in the pure solvent. It must therefore be quite clear that the rotating disc method cannot be employed to establish the concentration dependence of the diffusion coefficient of A in B.

As illustrated in Fig. 6.8, the temperature dependence of the diffusion coefficient of transition metals into liquid aluminium is well described by the Arrhenius equation $D = D_0 \exp(-E/RT)$, giving a linear plot of ln D against T^{-1}. Values of the pre-exponential factor D_0 and the activation energy E for some of them are provided in Table 6.5.

Table 6.4. Diffusion coefficients of transition metals, D ($\times 10^{-9}$ $m^2 s^{-1}$), across the diffusion boundary layer at the solid-liquid interface into liquid aluminium [120]

Metal	700 °C	750 °C	800 °C	850 °C
Ti	2.3	3.0	3.8	4.6
V	0.83	1.1	1.4	1.8
Cr	2.0	2.7	3.5	4.0
Co	2.5	3.0	3.5	3.7
Ni	2.7	4.3	4.8	5.4
Zr	2.1	2.5	3.1	3.5
Nb	1.6	1.9	2.5	2.9
Mo	2.0	2.5	3.3	3.8
Ta	1.6	2.1	2.6	3.2
W	2.1	2.5	3.4	4.0
Re	2.0	2.4	2.9	3.5

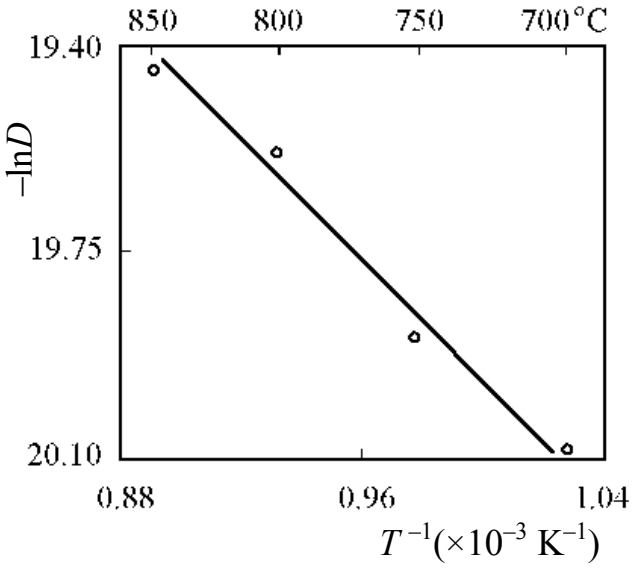

Fig. 6.8. Temperature dependence of the diffusion coefficient of the tungsten atoms across the diffusion boundary layer at the solid-liquid interface into the bulk of liquid aluminium [122].

Table 6.5. Parameters of the Arrhenius equation $D = D_0 \exp(-E/RT)$, describing the temperature dependence of the diffusion coefficient of some transition metals into liquid aluminium [120]

Metal	Temperature range (K)	D_0 ($\times 10^{-7}$ m^2 s^{-1})	E (kJ mol^{-1})
Ti	973–1173	4.5±0.7	42.8±1.5
V	973–1173	2.8±0.3	47.4±0.8
Cr	973–1173	2.6±1.3	39.1±3.8
Co	973–1173	0.43±0.13	22.8±2.4
Ni	973–1173	6.2±3.5	43.5±5.8
Zr	973–1173	0.80±0.22	29.5±2.1
Nb	973–1123	1.50±0.89	36.9±4.0
Mo	973–1123	2.82±0.90	40.2±2.7
Ta	973–1123	2.62±0.55	41.2±1.7
W	973–1123	3.54±1.80	41.9±5.0
Re	973–1173	2.1±0.6	37.8±2.3

6.3: Growth kinetics of the chemical compound layer under conditions of its simultaneous dissolution in the liquid phase

The processes of growth of a chemical compound layer at the solid-liquid interface and its dissolution into the liquid phase take place simultaneously. Depending on the sign of the difference of the growth and dissolution rates, the layer is formed (at a positive value of this difference) or is not formed (at a negative value) between interacting substances.

Equations (6.1) and (6.8) describe the dissolution process in terms of the concentration of component A in liquid B. Let us now describe it in terms of a variation of linear dimensions of a solid disc specimen. Since the concentration is the mass divided by the volume, then

$$c = \frac{\rho_A S x_d}{v}, \qquad (6.14)$$

where ρ_A is the density of substance A, kg m^{-3}, and x_d is the thickness of the dissolved part of the solid specimen, m. Substituting this expression into equations (6.1) and (6.8) yields

$$\frac{dx_d}{dt} = \frac{c_s k}{\rho_A} \exp\left(-\frac{kSt}{v}\right) \tag{6.15}$$

and

$$x_d = \frac{c_s v}{\rho_A S}\left[1 - \exp\left(-\frac{kSt}{v}\right)\right] . \tag{6.16}$$

It is assumed that the volume of the liquid phase does not change significantly during dissolution, so that $v_0 \approx v \approx v_s$.

If the chemical compound A_pB_q and not substance A is dissolving in the liquid (Fig. 6.9), two alternatives are possible.

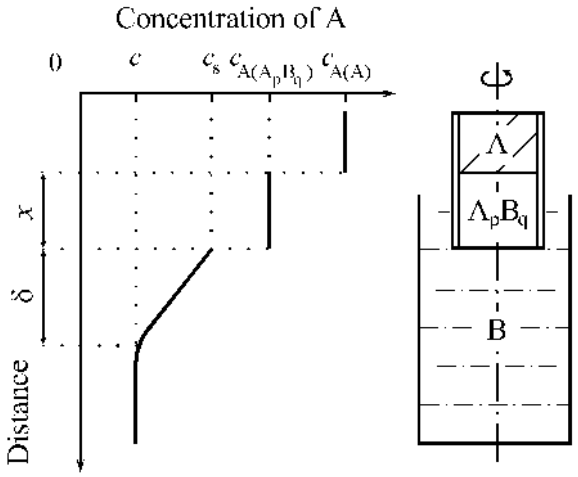

(a)

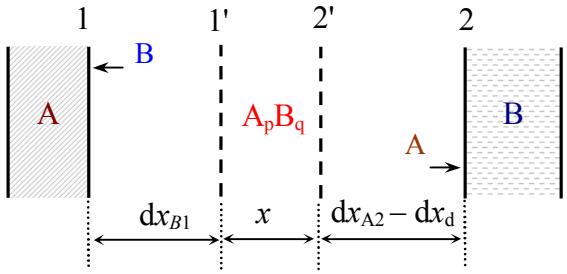

(b)

Fig. 6.9. Schematic diagrams to illustrate the growth process of the A_pB_q layer under conditions of its simultaneous dissolution in the liquid phase. Not to scale.

1. The A_pB_q compound does not decompose during dissolution in the liquid phase. In such a case, equations (6.15) and (6.16) retain their form, but the density of A should be replaced by

that of A_pB_q (kg m^{-3}), while the saturation concentration (solubility) c_s should be expressed in kilograms of A_pB_q, not A, per cubic metre of the solution.

2. During dissolution, the A_pB_q compound entirely decomposes to atoms or ions. Then, equations (6.15) and (6.16) become

$$\frac{\mathrm{d}x_\mathrm{d}}{\mathrm{d}t} = \frac{c_\mathrm{s}k}{\rho_{A_pB_q}\varphi}\exp\left(-\frac{kSt}{v}\right) \tag{6.17}$$

and

$$x_\mathrm{d} = \frac{c_\mathrm{s}v}{\rho_{A_pB_q}\varphi S}\left[1-\exp\left(-\frac{kSt}{v}\right)\right], \tag{6.18}$$

where φ is the content of A in A_pB_q in mass fractions. In these equations, c_s is the amount of A, not A_pB_q, per unit volume of the liquid phase. Note that in the case of a linear dependence of the volume of the liquid solution upon the content of component A equations (6.15)-(6.18) are also valid, but v should be replaced with v_s.

To derive an equation describing the growth kinetics of the A_pB_q layer under conditions of its simultaneous dissolution in liquid B, use will again be made of the principle of independency of the rates of all elementary physical or chemical processes taking place simultaneously. In the case under consideration, these are

(*i*) increase in thickness of the A_pB_q layer as a result of diffusion of component B across its bulk to the A–A_pB_q interface and subsequent occurrence of partial chemical reaction (2.1) (see Chapter 2 and Fig. 6.9b),

(*ii*) increase in thickness of the A_pB_q layer as a result of diffusion of component A across its bulk to the A_pB_q–B interface and subsequent occurrence of partial chemical reaction (2.2),

(*iii*) decrease in thickness of the A_pB_q layer at the A_pB_q–B interface due to its dissolution in the liquid phase B undersaturated with component A.

The growth rate of the A_pB_q layer is described by equation (2.24), while its dissolution rate by equation (6.17). Term-by-term subtracting of the latter equation from the former yields the required equation describing the rate of formation of this layer at the interface between solid A and liquid B

$$\frac{\mathrm{d}x}{\mathrm{d}t} = \frac{k_{0B1}}{1+\dfrac{k_{0B1}x}{k_{1B1}}} + \frac{k_{0A2}}{1+\dfrac{k_{0A2}x}{k_{1A2}}} - b\exp(-at), \tag{6.19}$$

where $a = k\mathrm{S}/v$ and $b = c_\mathrm{s}k/\rho_{A_pB_q}\varphi$.

Consider most important practical consequences following from equation (6.19). First of all, a criterion for the absence of the A_pB_q layer between the A and B phases will be established.

It is clear that the third term of equation (6.19) has the highest possible value equal to b if at is close to 0. This condition is satisfied in the following cases.

(1) At $t \to 0$, *i.e.* in the very initial period of dissolution that is a trivial case. To evaluate the time during which the dissolution rate can be regarded as almost constant and highest, it is necessary to take into account that its variation can only be revealed if the value of this variation becomes comparable with the accuracy of measurements.

Upon expanding the exponential function of equation (6.17) into a power sign-alternate series and retaining only its first two terms, one obtains

$$\frac{\mathrm{d}x_\mathrm{d}}{\mathrm{d}t} = b(1 - at). \qquad (6.20)$$

It is known that in this case the error does not exceed the value of the first rejected term, *i.e.* $a^2t^2/2$ [123, 124]. In percentage to at, it is $(at/2)\times 100\%$.

Let the relative error of determining the dissolution-rate constant be equal to $\Delta\%$. Consequently, a decrease in the dissolution rate will be noticeable, if $\Delta \approx 100at$. During dissolution of solid metals in liquid ones, $\Delta \approx 5\%$. The dissolution-rate constant is known to vary in the range $(2\text{-}10)\times 10^{-5}$ m s^{-1} at angular disc rotational speeds of 5-80 rad s^{-1} [16]. The value of S/v is usually of the order of 10 m^{-1}. Then, assuming that on the average $k = 5\times 10^{-5}$ m s^{-1}, one obtains $a = 5\times 10^{-4}$ s^{-1}. Consequently, $t \approx 100$ s.

Hence, at least during the first two minutes since the start of the interaction of solid A with liquid B, the dissolution rate of the A_pB_q layer can with sufficient accuracy be considered to be constant and equal to b. It should be noted that in this case the error resulting from replacing $\exp(-at)$ with $(1 - at)$ is about 2.5×10^{-2} %. Hence, such a substitution is quite justified.

(2) At $S/v \to 0$. This condition is evidently satisfied for systems of forced circulation, in which the surface of a solid is continuously washed with a pure solvent. Note that if the concentration of A in B is $c_0 \neq 0$, then the dissolution rate of the A_pB_q layer will be constant, but less than b:

$$\frac{\mathrm{d}x_\mathrm{d}}{\mathrm{d}t} = \frac{(c_\mathrm{s} - c_0)k}{\rho_{A_pB_q}\varphi}. \qquad (6.21)$$

If the dissolution rate remains constant and equal to b, equation (6.19) is simplified to

$$\frac{\mathrm{d}x}{\mathrm{d}t} = \frac{k_{0B1}}{1 + \dfrac{k_{0B1}x}{k_{1B1}}} + \frac{k_{0A2}}{1 + \dfrac{k_{0A2}x}{k_{1A2}}} - b. \qquad (6.22)$$

From this equation, a condition for the absence of the A_pB_q layer at the interface between solid A and liquid B can readily be derived. Indeed, the highest value of the first two terms of the right-hand side of equation (6.22) is equal to the sum $k_{0B1} + k_{0A2}$. Therefore, at

$$k_{0B1} + k_{0A2} < b \qquad (6.23)$$

the A_pB_q layer cannot occur between A and B since $\mathrm{d}x/\mathrm{d}t < 0$, *i.e.* the rate of growth of this layer is less than the rate of its dissolution in the liquid phase.

This result is of importance for practice because too rapid formation of compound layers at the interface of reacting substances is often undesirable. An example is the occurrence of thick layers of intermetallic compounds during welding or brazing dissimilar metals, whose presence is known to strongly deteriorate the mechanical strength of the joint (see, for example, Refs [125, 126]).

To simplify the further analysis of equations (6.19) and (6.22), instead of the sum of two terms

$$\frac{k_{0B1}}{1 + \dfrac{k_{0B1}x}{k_{1B1}}} + \frac{k_{0A2}}{1 + \dfrac{k_{0A2}x}{k_{1A2}}}$$

only one term with constants k_0 and k_1 will be retained. Then, equation (6.22) takes the form

$$\frac{\mathrm{d}x}{\mathrm{d}t} = \frac{k_0}{1 + \dfrac{k_0 x}{k_1}} - b. \qquad (6.24)$$

Its solution at the initial condition $x = 0$ at $t = 0$ is

$$-\frac{k_1}{b^2}\ln\left[1 - \frac{k_0 b x}{k_1(k_0 - b)}\right] - \frac{x}{b} = t. \qquad (6.25)$$

By setting dx/dt = 0 in equation (6.24), the highest value x_{max} of the thickness of the A_pB_q layer possible under conditions of its simultaneous dissolution in the liquid phase at a rate b is found:

$$x_{max} = \frac{k_1(k_0 - b)}{k_0 b}. \qquad (6.26)$$

At a constant dissolution rate, the time dependence of the A_pB_q layer thickness is seen to be similar that shown in Fig. 3.7b (line 1). After a certain period of time, the thickness of the layer reaches the value x_{max} and then it grows no longer because the stationary state is established when an increase in layer thickness becomes just equal to a decrease due to its dissolution in the liquid phase. The process of an asymptotic approach of the thickness of the A_pB_q layer with passing time to its highest value possible under given dissolution conditions is described by equation (6.25).

If the growth rate of the A_pB_q layer is restricted by the rate of diffusion of components A and B across its bulk, so that $k_0 >> k_1/x$, while the rate of chemical transformations (partial chemical reactions) far exceeds the dissolution rate ($k_0 >> b$), equations (6.19), (6.22), (6.25) and (6.26) take a simpler form:

$$\frac{dx}{dt} = \frac{k_1}{x} - b\exp(-at), \qquad (6.27)$$

$$\frac{dx}{dt} = \frac{k_1}{x} - b, \qquad (6.28)$$

$$-\frac{k_1}{b^2}\ln\left(1 - \frac{bx}{k_1}\right) - \frac{x}{b} = t, \qquad (6.29)$$

$$x_{max} = \frac{k_1}{b}. \qquad (6.30)$$

Using these equations, the thickness of the layer of any chemical compound under conditions of dissolution of a solid in a liquid can readily be estimated. It should be remembered, however, that at very low t and x equations (6.27)-(6.29) become inapplicable in view of the assumptions on which their derivation rests.

Since equation (6.27) can hardly be integrated precisely [127], calculations are carried out with the use of different approximate methods. For example, the piecemeal-analytical method may successfully be employed. It is based on dividing the examined time range into a finite number of sufficiently short intervals and the subsequent application of equation (6.29) to each of them. Also, equation (6.27) can be transformed into a transcendental equation [128] that is then solved by numerical methods.

To carry out any calculations, it is clearly necessary to know the values of the chemical and physical (diffusional) constants and also of the parameters characterising the dissolution rate of a solid in a liquid. At present, all these quantities can only be determined experimentally or evaluated from other experimental data.

The chemical and physical constants can be found when investigating the growth kinetics of the A_pB_q layer between solid A and liquid B saturated with component A, *i.e.* experiments should be carried out under conditions excluding the process of dissolution of the solid phase in the liquid one. Other steps of the determination of these quantities are identical to those described in Chapter 2.

It should be noted that in many works the degree of saturation of liquid B with the dissolving component A is not taken into account, and even in cases where a pure solvent is used, the experimental data are treated using a linear, parabolic, logarithmic or some other dependence in order to establish the so-called growth law of a chemical compound layer. It is clear, however, that both the academic and practical value of such "laws" is not too high because each of them holds only under particular experimental or technological dissolution conditions which most frequently remain unspecified.

It is therefore sufficient to change, for example, the dimensions of a solid specimen or the volume of the liquid or its agitation conditions, and the parameters of the "layer-growth law" thus found will at best assume other numerical values or at worst even the shape of the layer thickness-time dependence will change considerably, in spite of the lack of any essential changes in the mechanism of formation of the layer of that chemical compound.

It should be emphasised that in following the rate of dissolution of solid A in liquid B by the mass loss of a solid specimen of substance A, measured by weighing the specimen before and after the experiment, errors may arise due to the formation of a chemical compound layer at the solid-liquid interface. On the one hand, dissolution of the solid phase A in the liquid phase B reduces the mass of the solid specimen. On the other, however, formation of the A_pB_q compound layer adhering to the surface of the solid specimen results in an increase of its mass (at $k_0 > b$). Hence, the experimentally determined change in mass of the solid specimen is a consequence of the two simultaneously occurring processes, namely, growth and dissolution of the A_pB_q layer.

If the thickness of the dissolved part of the solid specimen far exceeds the thickness of the A_pB_q layer formed at the solid-liquid interface in the course of dissolution, the error of determination of the mass loss by weighing the specimen before and after the experiment will

be negligibly small. However, at low t and $k_0 > b$ the increase in the specimen mass due to the formation of the A_pB_q layer may prove greater than its decrease caused by dissolution. In such a case, instead of decreasing, the mass of the specimen will increase, as is observed, for example, during dissolution of titanium in the stainless-steel melt [129].

From these considerations, it follows that in the case of formation of the layer of a chemical compound under conditions of simultaneous dissolution of a solid in a liquid, the shape of the layer thickness-time dependence may be rather complicated. Evolution of this dependence in the course of interaction of initial substances from the moment of their contact to the establishment of equilibrium in the A–B system will now be analysed. The time of wetting the solid surface by the liquid phase will not be taken into account, *i.e.* this process is assumed to be instantaneous.

After solid A and liquid B undersaturated with component A are brought into contact with each other, two somewhat different ways of their interaction are possible.

1. The layer of the A_pB_q chemical compound immediately occurs and then grows between the A and B phases. It happens if

$$k_{0B1} + k_{0A2} > b, \tag{6.31}$$

i.e. when the sum of the rates of chemical reactions at layer interfaces with initial substances exceeds the dissolution rate. Since in the initial period of time (in the region of small layer thicknesses) $k_{0B1} << k_{1B1}/x$ and $k_{0A2} << k_{1A2}/x$, while the dissolution rate does not yet change appreciably, equation (6.19) indicates that in this stage of the growth process the time dependence of the layer thickness is close to linear

$$x = \left(k_{0B1} + k_{0A2} - b\right)t. \tag{6.32}$$

As the thickness of the A_pB_q layer increases with passing time, its growth rate must gradually decrease. If $k_{0B1} + k_{0A2} >> b$, $k_{0B1} >> k_{1B1}/x$, $k_{0A2} >> k_{1A2}/x$ and $(k_{1B1} + k_{1A2})/x >> b$, then the growth kinetics of the A_pB_q layer will be almost parabolic. The abundance of necessary conditions to be satisfied indicates that this is a rather rare case. Strictly speaking, the initial portion of the layer thickness-time dependence can in general hardly be expected to be either linear or parabolic.

If the dissolution rate is maintained constant, after reaching its highest thickness (see equation (6.26)), the A_pB_q layer simply moves as a whole into the bulk of solid phase A until it is consumed entirely (if liquid B is taken in excess). Most frequently, however, the dissolution rate decreases from b to 0 with increasing time. Therefore, the effect of dissolution on the

process of formation of the A_pB_q layer gradually weakens, and the layer thickness-time dependence steadily approaches the parabola $x^2 = 2(k_{1B1} + k_{1A2})/t$.

2. If $k_{0B1} + k_{0A2} < b$, then the A_pB_q layer is not formed at the interface of substances A and B during a certain initial period of their interaction. Since the dissolution rate steadily decreases, a time t_0 is always reached when the dissolution and growth rates of the layer become equal, *i.e.*

$$k_{0B1} + k_{0A2} = b\exp(-at_0). \tag{6.33}$$

This corresponds to the start of formation of the A_pB_q layer at the A–B interface. Subsequently,

$$k_{0B1} + k_{0A2} > b\exp(-at)_{t>t_0}. \tag{6.34}$$

Therefore, after a time delay, often referred to as the incubation or latent period, the A_pB_q layer occurs and grows between the solid and liquid phases. Note that, knowing both the time t_0 of occurrence of the compound layer at the A–B interface and the dissolution rate b, the sum $k_{0B1} + k_{0A2}$ of the chemical constants can readily be estimated from equation (6.33). It is another method of its determination, in addition to that described in Chapter 2.

Thus, the reason for the absence of the layer of a chemical compound between reacting substances follows in a natural way from the proposed physico-chemical equations. Note that according to diffusional views the A_pB_q layer should grow at the interface between A and B at *any* finite dissolution rate. It is easily seen from equations (6.27)-(6.30). Indeed, whatever the dissolution rate, the thickness of the layer will never be less than $x_{\max} = k_1/b$. Clearly, this value is always positive.

Hence, the diffusional theory does not "allow" any existing compound layer to disappear during dissolution. Intuitively, this conclusion appears to be quite evident because an increase in the dissolution rate, resulting in a decrease of the layer thickness, automatically leads to an increase in its growth rate (see equations (6.27) and (6.28) in which x is in the denominator of the term k_1/x responsible for the layer-growth rate). Due to such a compensation effect, the thickness of the A_pB_q layer exceeds zero at any real values of the diffusion coefficients of the components across its bulk.

In the framework of the diffusional approach the absence of the layer of a chemical compound in the course of interaction of a solid with a liquid is thus unexplainable. The reason for this is therefore sought outside of this approach. In most cases, it is assumed to be the difficulty with the formation of nuclei of a new phase (see, for example, Ref. [92]).

Perhaps, in some (very limited) number of solid-liquid systems the rate of nucleation indeed plays a significant role. However, such an explanation can hardly be expected to be valid in all cases of absence of the layers of chemical compounds from the solid-liquid interface.

Note that in practice the actual role of nucleation in each particular system can be revealed very simply. It suffices to carry out experiments, preferably at a constant dissolution rate, on specimens where a chemical compound layer is already present. If the compound layer disappears during interaction of those specimens with the liquid phase, then it becomes quite clear that its absence between the A and B phases is due to the effect of dissolution and not to the difficulties of nucleation.

It is worth noting that the condition of constancy of the dissolution rate is rather essential. If the dissolution rate decreases during the experiment, as is often the case, it may happen that the conditions under which inequality (6.34) is satisfied are established even before the full disappearance of the A_pB_q layer due to its dissolution in the liquid. Therefore, after some temporary reduction, the layer thickness will again start to increase. Both equations (6.19) and (6.27) allow such a form of the layer thickness-time dependence. Hence, under varying dissolution conditions it is not so easy to unambiguously decide whether the absence of the A_pB_q layer is due to the difficulties of phase nucleation or to its too high dissolution rate exceeding the rate of interfacial chemical reactions.

With passing time, liquid B becomes more and more saturated with component A. Therefore, dissolution of the A_pB_q layer in the liquid phase eventually ceases, while its growth between A and B continues until at least one of the initial substances is consumed completely. Depending on the amounts of substances A and B taken, phases A and A_pB_q, or A_pB_q and B, or only one phase A_pB_q remain in the equilibrium state.

Analysis of the effect of dissolution on the growth kinetics of the layers of two or more chemical compounds is carried out in a similar way. To take account of this effect, it is necessary to subtract the dissolution rate $b \exp(-at)$ from the right-hand side of a differential equation describing the growth rate of a compound layer bordering liquid B (see equation (3.27_2) in Chapter 3 and (4.26_3) in Chapter 4).

6.4: Kinetics of growth of intermetallic layers at the transition metal-liquid aluminium interface

Consider a few examples of formation of intermetallic layers between a transition metal or an alloy of transition metals and molten aluminium. Let us begin with iron, a metal most widely used in practice.

The main aim of this section is to illustrate the influence of dissolution on the layer-growth kinetics. Therefore, for each pair of initial substances, experiments with saturated and non-saturated aluminium melts will be described.

6.4.1: Formation of the Fe_2Al_5 layer between Fe and Al

At 700 °C, a single-phase layer of the Fe_2Al_5 intermetallic compound is formed at the interface of solid iron or steels and liquid aluminium (Fig. 6.10). It has a readily distinguishable structure consisting of elongated grains orientated in the direction of growth [130, 131]. The growth kinetics of the Fe_2Al_5 layer between iron and iron-saturated aluminium melts follow the parabolic law $x^2 = 2k_1t$, with $k_1 = 1.0\times10^{-10}$ m^2 s^{-1} [130].

To reveal the effect of dissolution on the layer-growth, experiments were carried out with the melts of pure aluminium at an angular disc rotational speed of 24.0 rad s^{-1}, as described in Section 6.2. The first experiment was a check-up one. After pre-heating under a flux, the rotating iron specimen was immersed into the aluminium melt at 700 °C, and immediately the crucible, together with the specimen and the melt, was "shot" into a water bath.

Examination of the bimetalic specimen obtained showed a continuous Fe_2Al_5 intermetallic layer around 1 μm thick to form at the Fe–Al interface. Since the time of cooling from 700 °C down to room temperature was at most 2 s, it is evident that wetting and nucleation were relatively fast processes that could hardly be expected to have any significant influence on the layer-growth kinetics. This time, 2 s, was a small portion of the total experiment duration (50–300 s), and the thickness, 1 μm, of the intermetallic layer formed during cooling was a small portion of the measured layer thicknesses, 40–90 μm. It will become clear later how essential it is to count all these seconds and micrometres in order to avoid incorrect conclusions regarding the actual time of layer formation.

The average value of the maximum height of the Fe_2Al_5 crystallites was used as a measure of the intermetallic layer thickness. The experimental points are shown in Fig. 6.11 by open circles [131]. The relative error of determining the layer thickness was around 15 %.

The theoretical thickness-time dependence (solid line 2) was calculated from equation (6.29), using the following quantities:

(1) $c_s = 60\pm3$ kg m^{-3} [132];

(2) $s = 1$ cm^2, $v = 10$ cm^3, $s/v = 10.0\pm0.2$ m^{-1};

(3) $k = (3.8\pm0.1) \times 10^{-5}$ m s^{-1};

(4) $\rho_{int} = (4.1\pm0.1) \times 10^3$ kg m^{-3} (density of Fe_2Al_5) [62];

(5) $\varphi = 0.453$ (mass fraction of Fe in Fe_2Al_5).

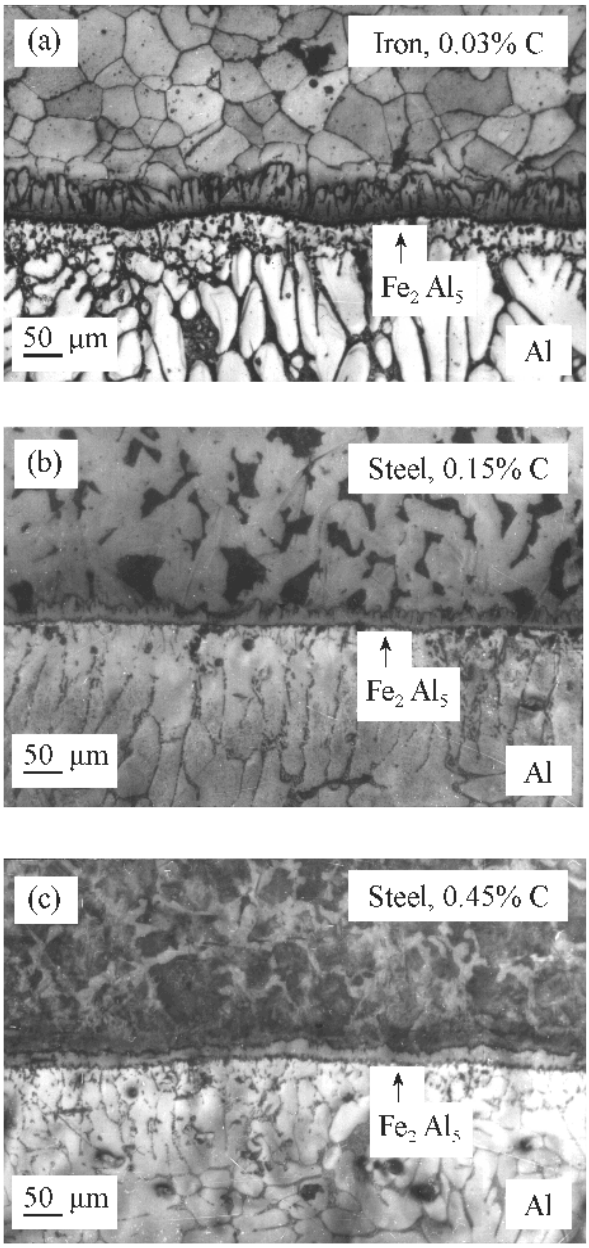

Fig. 6.10. Optical micrographs of the transition zone between (a) commercial purity iron or (b, c) steel and aluminium. The Fe_2Al_5 intermetallic layer becomes progressively flatter and thinner with increasing carbon content of steels. The "Al + an intermetallic compound" eutectic is seen at grain boundaries of aluminium solid solutions.

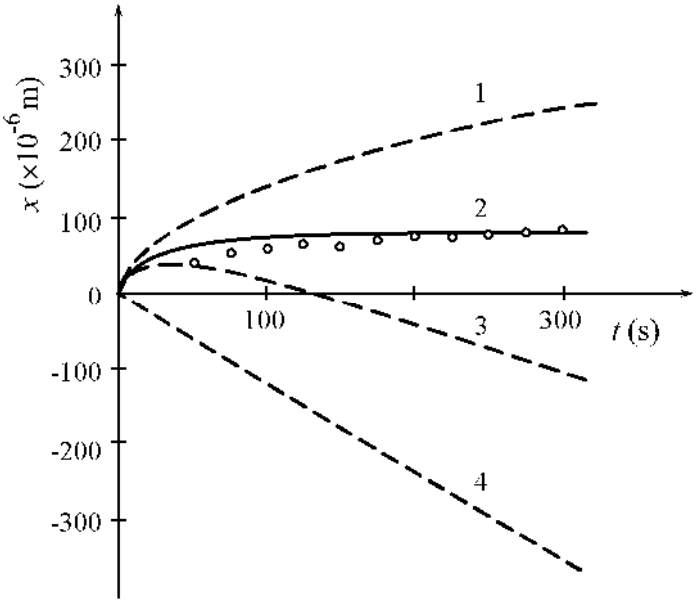

Fig. 6.11. Thickness–time relationships for the Fe_2Al_5 intermetallic layer at 700 °C [131]: 1, parabolic growth kinetics of the layer in the case of the Fe-saturated aluminium melt; 2, theoretical dependence of the thickness of the layer upon time under conditions of its simultaneous dissolution in the aluminium melt (c_0 = 0), calculated from equation (6.29); 3, difference between the dependences represented by lines 1 and 4; 4, thickness of the dissolved portion of the layer plotted against dipping time. Open circles are experimental values of the thickness of the Fe_2Al_5 layer formed at the Fe–Al interface under conditions of its simultaneous dissolution in the aluminium melt at an angular disc rotational speed of 24.0 rad s^{-1}.

The dissolution rate of the Fe_2Al_5 layer was assumed to be constant and equal to its average value in the 0–300 s range. Expressed in terms of the thickness of the Fe_2Al_5 layer dissolved, it is

$$b = \frac{c_s k}{\rho_{int}\varphi} = 1.23\times10^{-6}\ \text{m s}^{-1}\ \text{at}\ t = 0$$

and

$$b\exp(-at)_{t=300} = 1.10\times10^{-6}\ \text{m s}^{-1}\ \text{at}\ t = 300\ \text{s}.$$

Deviations from the average value, 1.16×10^{-6} m s^{-1}, are seen not to exceed ±6%. Therefore, equation (6.29) may reasonably be expected to describe the growth kinetics of the Fe_2Al_5 layer with a sufficient degree of accuracy.

To make the further discussion more illustrative, shown in Fig. 6.11 also are

(*i*) kinetic dependence for the case of growth of the Fe_2Al_5 layer at the interface of iron with the iron-saturated aluminium melt (line 1);

(*ii*) kinetic dependence expressing the thickness of the dissolved portion of the Fe_2Al_5 layer (line 4);

(*iii*) difference of the first two dependences (line 3).

The agreement between the calculated theoretical dependence (line 2) and the experimental points is seen to be fairly good. A certain disagreement is only observed near the initial, abruptly ascending part of the curve 2. The reasons for this appear to be the following.

(1) The rate of dissolution of the Fe_2Al_5 layer was assumed to be constant, whereas in fact it decreases almost linearly from 1.23×10^{-6} m s^{-1} to 1.10×10^{-6} m s^{-1}. As a result, the theoretical curve overestimates the thickness of the intermetallic layer for the first half (0–150 s) and underestimates it for the second half (150–300 s) of the examined time range. Clearly, this reason alone cannot lead to the observed disagreement because the error arising from such an assumption is small compared to the experimental error of measuring the layer thickness.

(2) Growth of the Fe_2Al_5 crystallites is known to be anisotropic. Each elongated crystallite (see Fig. 6.10) is a single crystal whose axis coincides with the *c*-axis of the orthorhombic unit cell of the Fe_2Al_5 intermetallic compound [130]. The highest value of the growth rate of the crystallites is just observed in the direction of the *c*-axis. This is due to the peculiarities of the Fe_2Al_5 lattice structure (for more detail, see Ref. [130]).

However, the maximum values of the growth rates of the crystallites are only observed if the angle between the *c*-axis and the initial Fe–Al interface is 90°. If this angle considerably differs from 90°, then neighboring crystallites hinder each other's growth. The early stage of interaction of solid iron with liquid aluminium is characterised by the formation of a number of randomly orientated nuclei of the Fe_2Al_5 phase. Therefore, in this stage the growth-rate constant k_1 of the layer is probably somewhat less than the accepted value 1.0×10^{-10} m^2 s^{-1}. Hence, the experimental points might be expected to lie below the calculated curve 2 in its initial portion. This was indeed observed experimentally.

During dissolution, the unfavorably orientated Fe_2Al_5 crystallites gradually disappear, while the favorably orientated ones continue to grow. As a result, the morphology of the Fe_2Al_5 layer becomes more and more regular, with its crystallites being almost parallel to each other, and eventually the growth-rate constant k_1 attains its maximum value which then changes no longer. Therefore, the agreement between the calculated and experimental dependences for the second half of the 0–300 s time range is much better than for the first

half. This is another (masked) aspect of the influence of dissolution on the growth kinetics of the Fe_2Al_5 layer. Clearly, its precise quantitative evaluation is hardly possible.

Comparison of the curves 1 and 2 in Fig. 6.11 demonstrates how significant the effect of dissolution on the layer-growth kinetics is. It should be noted that of all intermetallic compounds formed by transition metals with aluminium under similar conditions, the Fe_2Al_5 layer has the highest growth rate [120, 122]. This causes serious difficulties in welding of aluminium and its alloys with iron and steels, in hot-dip protective coating, and in producing composite materials. By increasing the rate of dissolution, it is possible to reduce significantly the thickness of the Fe_2Al_5 layer, but its formation can scarcely be fully prevented at any real dissolution rate.

Note that, when taking account of the effect of dissolution on the growth kinetics of a chemical compound layer, in some works the integrated quantities are simply subtracted from each other. This yields a dependence shown schematically in Fig. 6.11 by line 3 which is the difference between the parabola $x = (2k_1t)^{1/2}$ expressing the layer thickness in the absence of dissolution and equation (6.18) giving the dissolved portion of its thickness. Such an approach is clearly misleading. It is not surprising, therefore, that the dependence thus obtained has nothing in common with the experimental curve 2, excepting a narrow region near the origin of co-ordinates, where $k_1/x >> b$.

6.4.2: Occurrence of the $MoAl_4$ layer between Mo and Al

Figure 6.11 shows a micrograph of the transition zone between solid molybdenum and liquid aluminium saturated with molybdenum. As established by X-ray diffraction, electron probe microanalysis and chemical analysis, the intermetallic layer formed consists of the $MoAl_4$ compound [122].

In contrast to the Fe_2Al_5 layer with its ragged Fe_2Al_5–Fe interface, the $MoAl_4$ intermetallic layer is seen to have relatively even interfaces with both initial phases. In the case of the Mo-saturated aluminium melt, its growth kinetics follow the parabolic law $x^2 = 2k_1t$ (Fig. 6.13).

In the 750-850 °C range, the temperature dependence of the layer growth-rate constant k_1 is described by the equation

$$k_1 = (9.2 \pm 1.2) \times 10^{-6} \exp\left[-\frac{(145 \pm 1) \times 10^3}{RT} \right] \text{ m}^2 \text{ s}^{-1}$$

where the pre-exponential factor is expressed in $m^2\ s^{-1}$ and the activation energy in J mol^{-1}.

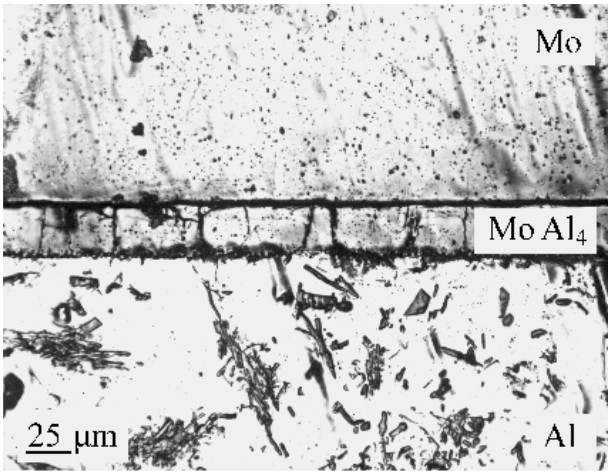

Fig. 6.12. A micrograph of the transition zone formed between molybdenum and the Mo-saturated aluminium melt [122]. Temperature 750 ºC, reaction time 1800 s. Inclusions in the aluminium matrix are crystals of $MoAl_4$ that are formed during cooling the melt.

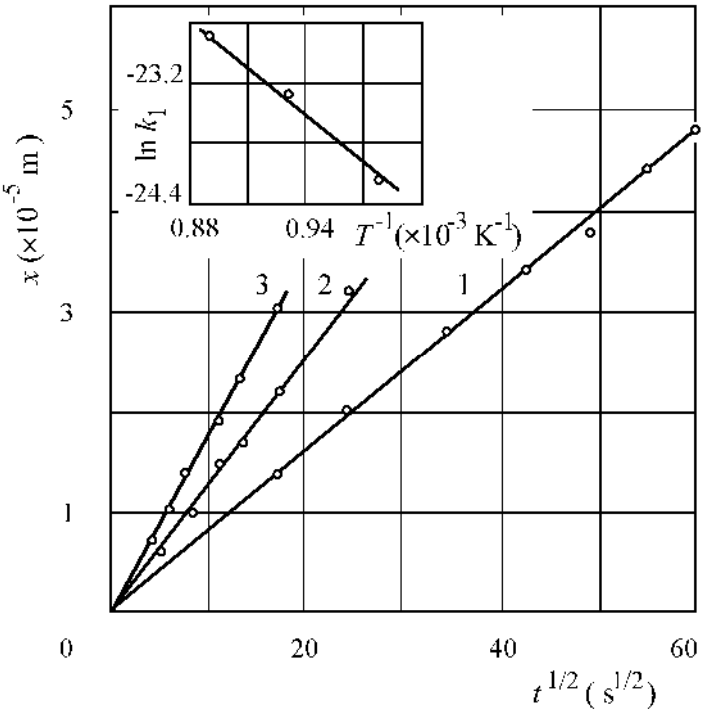

Fig. 6.13. Thickness of the $MoAl_4$ layer formed at the interface of molybdenum with the Mo-saturated aluminium melt plotted against the square root of the time, and the temperature dependence of layer growth-rate constant [122]. Temperature: 1, 750 °C; 2, 800; 3, 850.

The effect of dissolution on the growth rate of the $MoAl_4$ layer will be estimated at a temperature of 750°C, using the following quantities:

(1) $k_l = 3.2\times10^{-13}$ m^2 s^{-1} [122];

(2) $c_s = 10.6$ kg m^{-3} [122];

(3) $s = 1$ cm^2, $v = 10$ cm^3, $s/v = 10.0$ m^{-1};

(3) $k = 3.8\times10^{-5}$ m s^{-1}[122];

(4) $\rho_{int} = 4.35\times10^3$ kg m^{-3} [65];

(5) $\varphi = 0.47$.

The initial dissolution rate of molybdenum discs in liquid aluminum is seen from equation (6.17) to be 1.97×10^{-7} m s^{-1}. After 300 s, it drops to 1.77×10^{-7} m s^{-1}. Assume that in the 0–300 s time range the dissolution rate is constant and equal to the latter value. Then, according to equation (6.30), after 300 s holding the thickness of the $MoAl_4$ layer at the Mo–Al interface cannot exceed

$$x_{max} = \frac{3.2\times10^{-13}}{1.77\times10^{-7}} = 1.8\times10^{-6} \text{ m}.$$

Note that in the case of the aluminum melt saturated with molybdenum the thickness of the $MoAl_4$ layer at $t = 300$ s is 14×10^{-6} m. In welding dissimilar metals, the highest permissible thickness of an intermetallic layer is known to be 2–5 μm. Thus, the dissolution conditions in question ensure the formation of the Mo–Al transition zone with a $MoAl_4$ layer thickness not exceeding this value.

It should be remembered that equation (6.30) significantly overestimates the layer thickness. Its experimental value is less than half the value obtained from this equation. In the case of the Mo-saturated aluminum melt, it takes only 5 s for the $MoAl_4$ layer to reach a thickness of 1.8×10^{-6} m. For this reason, when investigating the effect of dissolution on the growth rate of any chemical compound layer it is so important to ensure sufficiently rapid cooling-down the melt.

This example clearly shows that a few seconds of layer formation during cooling, when the process of dissolution has already ceased but the temperature of the experimental cell has not yet dropped considerably and therefore the layer growth-rate constant still retains its former value, may happen to exert the same effect on thickening the compound layer as do a few minutes of its growth under conditions of simultaneous dissolution in the melt.

6.4.3: Formation of intermetallics at the interface of Fe–Ni and Fe–Cr alloys with liquid aluminium

Aluminium is known to form a number of binary and ternary intermetallic compounds with iron and nickel or chromium [61, 62, 133]. In this section, results on the intermetallic-layer formation and dissolution at the interface between a solid iron-nickel or iron-chromium alloy and aluminium melts will be considered [134-137] (for more detail, see Ref. [16]). Also, the effect of dissolution in the liquid phase on the process of layer growth will be illustrated.

Note that in contrast to binary systems where only one-phase compound layers can occur at the interface between two elementary substances, in ternary systems, when a two-component alloy or a binary compound reacts with a third metal or non-metal (either solid or liquid), the formation of both compact one-phase layers and two-phase reaction zones is observed. These may have a different morphology, possible types of which are considered, for example, in works by F.J.J. van Loo [138] and J.E. Morrel *et al*. [139].

To illustrate the influence of dissolution of the Fe-Ni alloy base into liquid aluminium on the process of layer formation, two sets of experiments were carried out at 700 ºC and a reaction time of 900 s. In the first set, the saturated aluminium melts were used, so that the dissolution of the solid in the liquid phase did not occur. In the second, pure liquid aluminium was employed. In this case, the solid disc specimen was rotated at an angular speed of 24.0 rad sec^{-1} to ensure its sufficiently rapid dissolution in liquid aluminium. In the first set of experiments, the thickness of intermetallic layers formed at interface of Fe–Ni alloys and liquid aluminium was a few times greater than that in the second (Fig. 6.14). Moreover, with some Fe–Ni alloys even the number of the layers was different.

As seen in Fig. 6.14a, three layers ($NiAl_2$, $NiAl_3$ and $FeNiAl_9$) are present at the interface between a 25% Fe–75% Ni alloy and the saturated aluminium melt, whereas only two of them ($NiAl_3$ and $FeNiAl_9$) survive under conditions of simultaneous dissolution in liquid aluminium (Fig. 6.14b), the total thickness of the layers being around 30 and 10 μm, respectively.

Note that a phase of composition close to $NiAl_2$ rather than Ni_2Al_3 has been found to occur at the interface between a 25% Fe–75% Ni alloy and the aluminium melt saturated with the alloy constituents. This phase formed a compact layer with even interfaces, adjacent to the Fe–Ni alloy base. In this connection, it seems relevant to remind that, in investigating the Al–Ni binary phase diagram, the formula $NiAl_2$, not Ni_2Al_3, was first ascribed to an equilibrium phase enriched in nickel compared to $NiAl_3$ [61, 62]. Probably, under non-equilibrium conditions $NiAl_2$ forms first and then it gradually transforms into Ni_2Al_3.

Similar experiments have also been carried out with Fe–Cr alloys containing 10 and 25% chromium. The micrographs illustrating a profound effect of dissolution on the rate of growth of intermetallic layers are provided in Fig. 6.15. The dominating phase is seen to be Fe_2Al_5. The minor phases are Fe_2Al_7, $FeAl_6$ and $CrAl_7$.

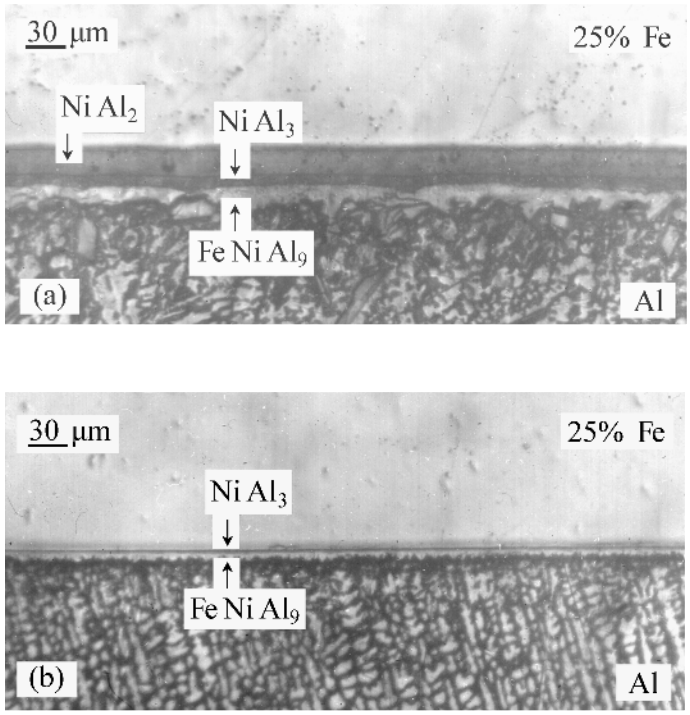

Fig. 6.14. Optical micrographs of the transition zone between a 25% Fe–75% Ni alloy and aluminium. Temperature 700 ºC, reaction time 900 s. Initial liquid phase: (a) aluminium melt saturated with the alloy constituents, (b) pure aluminium (ω = 24.0 rad s^{-1}).

Of two intermetallic layers formed at the interface between Fe–Cr alloys and aluminium, the layer adherent to the alloy base is compact, while that bordering the aluminium matrix is porous. In many cases, the latter actually consisted of separate grains weakly linked or not linked at all with each other. This means that, whenever present, its formation might be partly a result of a solid-state chemical reaction and partly a consequence of crystallisation from the melt. On the contrary, the layer adjacent to the alloy base was formed exclusively in the course of another solid-state chemical reaction.

The effect of dissolution on the process of intermetallic-layer formation is graphically visualised in Fig. 6.16 where the layer thickness-time dependence for a 90% Fe–10% Cr alloy and the saturated (1) and undersaturated (2) melt is shown. Dissolution is seen to cause about a three-fold decrease in layer thickness.

Equation (6.30) was again employed to evaluate the thickness of the Fe_2Al_5 layer at the interface of a Fe–Cr alloy and aluminium during dissolution of the alloy base in the undersaturated melt. When employing this equation, the main difficulty to overcome is evaluating the layer growth-rate constant k_1. It can be done as follows.

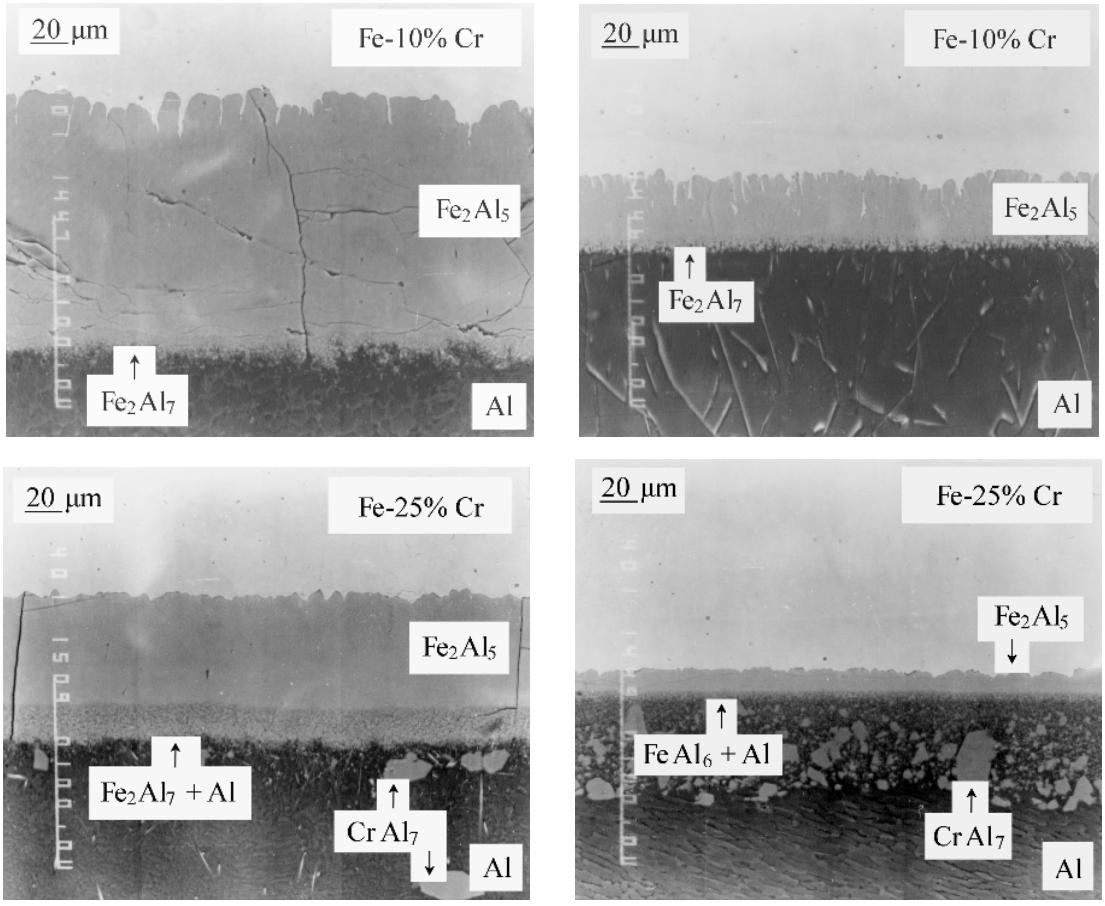

(a) (b)

Fig. 6. 15. Secondary electron image (SEI) of the transition zone between Fe–Cr alloys and aluminium. Temperature 700 ºC, reaction time 3600 s. Initial liquid phase: (a) aluminium melt saturated with the alloy constituents, (b) pure aluminium (ω = 24.0 rad s^{-1}).

1. If a single-phase intermetallic layer occurs in the case of both saturated and undersaturated melts, its value is found from the experimental layer thickness-time dependence for the saturated melt.

2. The layer growth-rate constant is evaluated by equation (6.30) using one or a few initial thickness values of an experimental thickness-time dependence for the undersaturated melt. Then, other values of the layer thickness can readily be calculated from this equation, thereby significantly reducing the amount of experimental work.

3. If the data on the solid-state layer-growth rate are available, a value of k_1 can be estimated by extrapolation from the temperature dependence. Clearly, the temperature values must not differ considerably in both cases.

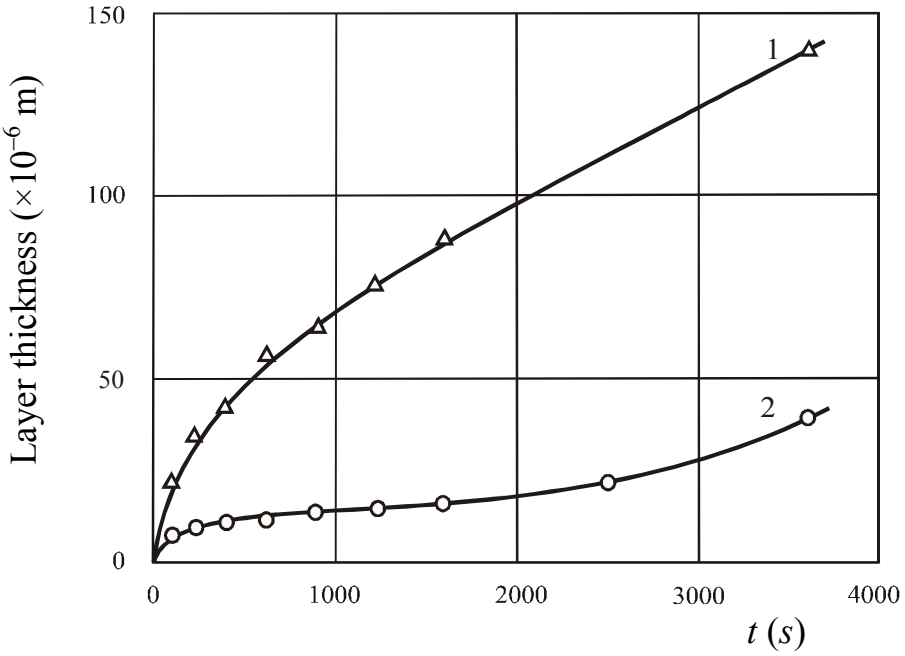

Fig. 6.16. The effect of dissolution on the process of intermetallic compound-layer formation at 700 ºC for a 90% Fe–10% Cr alloy [137]. 1, total thickness of the Fe_2Al_5 and Fe_2Al_7 layers, saturated aluminium melt; 2, thickness of the Fe_2Al_5 layer (Fe_2Al_7 layer is missing), undersaturated aluminium melt, angular disc rotational speed $\omega = 24.0$ rad s^{-1}.

With the Fe–Cr alloys investigated, the number of intermetallic layers growing from saturated and undersaturated melts is different (two, namely Fe_2Al_5 and Fe_2Al_7, in the case of the saturated aluminium melt, and only one, Fe_2Al_5, from the undersaturated melt). Therefore, the layer-growth constant, k_1, can only be calculated using a few experimentally determined points of the layer thickness-time dependence for the undersaturated melt, preferably at short times. This makes the calculation of other points of that dependence possible.

Since the dissolution rate diminishes exponentially from b_0 to b_t in the time range $0 - t$, calculations are carried out twice for each point by putting in the denominator of equation (6.30) first equal to $(b_0 + b_t)/2$ and then b_t. Thus, two sets of the Fe_2Al_5 layer thickness are obtained. The first set represents the underestimated values x_{under}, whereas the second set gives the overestimated ones x_{over}. Experimental values x_{exp} must clearly lie somewhere in between.

For both Fe–Cr alloys investigated, the layer growth-rate constant k_1 was calculated from equation (6.30) using the first two points $t = 100$ s and $t = 225$ s, with $x_{exp} = 9\times10^{-6}$ m and $x_{exp} = 10\times10^{-6}$ m for a 90% Fe–10% Cr alloy and $x_{exp} = 5.0\times10^{-6}$ m and $x_{exp} = 5.2\times10^{-6}$ m for a 75% Fe–25% Cr alloy. Appropriate values of k_1 were found to be 14.1×10^{-12} m^2 s^{-1} and

5.5×10^{-12} m^2 s^{-1}. These are the average of b_0x_{100} and $b_{100}x_{225}$ (subscripts designate the time). Other necessary quantities were as follows [136].

1. 90% Fe–10% Cr alloy:

(1) $k = 4.2\times10^{-5}$ m s^{-1},

(2) $c_s = 66.72$ kg m^{-3} (2.5% Fe + 0.28% Cr),

(3) $a = 4.2\times10^{-4}$ s^{-1},

(4) $b_0 = 1.51\times10^{-6}$ m s^{-1};

2. 75% Fe–25% Cr alloy:

(1) $k = 3.0\times10^{-5}$ m s^{-1},

(2) $c_s = 70.08$ kg m^{-3} (2.2% Fe + 0.72% Cr),

(3) $a = 3.0\times10^{-4}$ s^{-1},

(4) $b_0 = 1.13\times10^{-6}$ m s^{-1}.

The final results are presented in Tables 6.6 and 6.7. From these tables, it follows that equation (6.30) yields a quite satisfactory fit to the experimental data obtained.

Note that the growth-rate constant of the intermetallic layer k_1 tends to rise slightly with increasing time because of the anisotropy of growth of the Fe_2Al_5 phase. Therefore, as might be expected, the experimental values of the Fe_2Al_5 layer thickness, calculated with the use of a smaller value of this constant determined from the initial points of the layer thickness-time plots, are more close to the overestimated than to underestimated ones.

6.5: Interfacial interaction of nickel and cobalt with liquid Pb-free soldering alloys

Since lead falls into the range of toxic metals, conventional Sn-Pb solders are gradually being replaced with other soldering alloys that do not contain appreciable amounts of this metal. Most frequently employed components of new Pb-free solders are Ag, Au, Cu, Bi, In, Sb, Sn and Zn (see, for example, Refs [140, 141]).

In this section, dissolution kinetics and the effect of dissolution on the growth rate of intermetallic layers at the interface of solid nickel and cobalt with liquid bismuth- and tin-based alloys will be considered [142-147]. Experimental procedure did not differ essentially from that described in preceding sections.

Table 6.6. Calculated and experimental thicknesses x of the Fe_2Al_5 intermetallic layer for a 90% Fe–10% Cr alloy and the undersaturated aluminium melt at 700 ºC and ω = 24.0 rad s^{-1}.

Time (s)	$(b_0 + b_t)/2$ ($\times 10^{-6}$ m s^{-1})	x_{under} ($\times 10^{-6}$ m)	b_t ($\times 10^{-6}$ m s^{-1})	x_{over} ($\times 10^{-6}$ m)	x_{exp} ($\times 10^{-6}$ m)
100	1.48	-	1.45	-	9.0
225	1.44	-	1.37	-	10.0
400	1.39	10.1	1.28	11.0	11.0
625	1.33	10.6	1.16	12.2	12.0
900	1.27	11.1	1.03	13.7	13.5
1225	1.20	11.8	0.90	15.7	15.0
1600	1.14	12.4	0.77	18.3	16.0
2500	1.02	13.8	0.53	26.6	22.5
3600	0.92	15.3	0.33	42.7	40.0

Table 6.7. Calculated and experimental thicknesses x of the Fe_2Al_5 intermetallic layer for a 75% Fe–25% Cr alloy and the undersaturated aluminum melt at 700°C and ω = 24.0 rad s^{-1}.

Time (s)	$(b_0 + b_t)/2$ ($\times 10^{-6}$ m s^{-1})	x_{under} ($\times 10^{-6}$ m)	b_t ($\times 10^{-6}$ m s^{-1})	x_{over} ($\times 10^{-6}$ m)	x_{exp} ($\times 10^{-6}$ m)
100	1.11	-	1.10	-	5.0
225	1.10	-	1.06	-	5.2
400	1.06	5.2	1.00	5.5	5.5
625	1.03	5.3	0.94	5.9	6.0
900	1.00	5.5	0.86	6.4	6.5
1225	0.95	5.8	0.78	7.1	7.0
1600	0.91	6.0	0.70	7.9	8.0
2500	0.83	6.6	0.53	10.4	9.5
3600	0.75	7.3	0.38	14.5	12.0

6.5.1: Interaction of solid nickel with liquid bismuth and bismuth-based alloys

The investigation was aimed mainly at (*i*) determining the parameters characterizing dissolution kinetics of solid nickel in bismuth and 51 % Bi–42 % Sn–5 % In–2 % Zn alloy melts, (*ii*) establishing which of the intermetallic compounds (NiBi or $NiBi_3$ or both) are formed as separate layers between solid nickel and liquid bismuth or its alloy, (*iii*) visualising the effect of dissolution on the rate of growth of an intermetallic-compound layer and its morphology.

Equations (6.8)-(6.10) was found to give a good fit to the experimental data on dissolution kinetics of nickel in liquid bismuth and its alloy. The Ni solubility in bismuth is 0.32±0.02% at 300 ºC and 0.39±0.03% at 350 ºC. Somewhat unexpectedly, much lower solubility values, namely 0.0053±0.0009% at 300 ºC and 0.015±0.003% at 350 ºC, were obtained for a 51% Bi–42% Sn–5% In–2% Zn alloy. Therefore, experiments were also carried out at 250, 400 and 450 ºC to establish the solubility temperature dependence and then to find from it by extrapolation the solubility value at temperatures close to the melting point of the alloy. This dependence was found to obey a relation of the Arrhenius type

$$c_s = (3.5^{+0.4}_{-0.3})\times 10^3 \exp\,[-(63.5 \pm 0.5)\ \text{kJ mol}^{-1}/RT]\ \%.$$

From this equation, a value of 0.00005% is obtained by extrapolation for the solubility of nickel in the alloy at 150 ºC. Low solubility values, 0.00005 to 0.094% in the 150–450 ºC temperature range, of nickel in the alloy could hardly be expected judging from the solubility values in binary systems of nickel with the main alloy constituents bismuth (for example, at 300 ºC c_s = 0.32% Ni) and tin (c_s = 0.26% Ni at that temperature [148]). In view of their relatively low content, the influence of indium and zinc cannot be essential. Probably, a large drop in solubility arises because the alloy composition is close to that of the binary eutectic Bi-Sn (57% Bi and 43% Sn) [61, 62].

Differential thermal analysis showed that the alloy starts melting at 139 ºC. This is just the eutectic temperature of the Bi-Sn binary system. It still remains to find out whether lowering the solubility of a transition metal in low-melting alloys of near-eutectic composition, compared to its solubility in pure alloy components, is characteristic only of the system investigated or of others as well.

Though at a given temperature the solubility values of nickel in liquid bismuth and the alloy differ considerably, appropriate dissolution-rate constants are close. For example, at 350 ºC c_s is 0.39% Ni for bismuth and 0.015% Ni for the alloy, while k is 4.0×10^{-5} m s^{-1} for the former and 3.8×10^{-5} m s^{-1} for the latter at ω = 24.0 rad s^{-1} (Table 6.8). Listed in Table 6.8 are also diffusion coefficients of nickel into liquid bismuth and a 51% Bi–42% Sn–5% In–2% Zn alloy.

Table 6.8. Dissolution-rate constants at $\omega = 24.0$ rad s^{-1} and diffusion coefficients of nickel into liquid bismuth and a 51% Bi–42% Sn–5% In–2% Zn alloy

Temperature (°C)	Liquid phase	k ($\times 10^{-5}$ m s^{-1})	D ($\times 10^{-9}$ m^2 s^{-1})
300	Bi	1.5	0.23 ± 0.03
350	Bi	4.0	1.0 ± 0.1
300	alloy	1.2	0.17 ± 0.04
350	alloy	3.8	0.96 ± 0.09

With bismuth as a melt material, a single-phase layer of $NiBi_3$ intermetallic compound was found to form from both saturated and undersaturated melts, as illustrated in Fig. 6.17. No evidence of the presence of the NiBi intermetallic compound at the interface of nickel and molten bismuth was found.

From Fig. 6.17, it is seen that the $NiBi_3$ layer thickness is much less in the case of the undersaturated melt compared to the case of the saturated melt, other experimental conditions being identical. Thus, the effect of dissolution on the layer-growth rate is very appreciable.

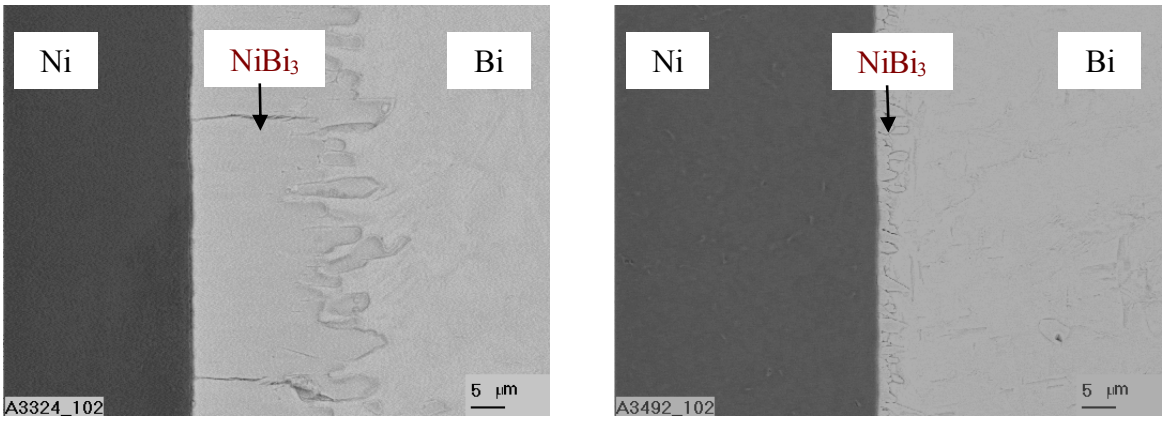

(a) (b)

Fig. 6.17. Backscattered electron image (BEI) of the transition zone formed between nickel and bismuth at a temperature of 350 °C and a reaction time of 3600 s. (a) saturated melt, (b) undersaturated melt, $\omega = 24.0$ rad s^{-1}.

It should be noted that thick $NiBi_3$ layers tend to be destroyed under the influence of the saturated bismuth melts. Clearly, in such a case it was hardly possible to establish a reliable layer thickness-time dependence. Therefore, a value of the layer growth-rate constant k_1, necessary for calculations of layer thicknesses using equation (6.30), was evaluated by extrapolation from its temperature dependence [149]

$$k_1 = 0.49\times10^{-6} \exp(-67100/RT)\ \mathrm{m^2\ s^{-1}}$$

where R is in J mol^{-1} K^{-1} and T in K.

This dependence was obtained when investigating the $NiBi_3$ layer-growth kinetics between two solid phases (nickel and bismuth) in the 150-250 ºC temperature range. Extrapolation yields for k_1 a value of 3.7×10^{-13} m^2 s^{-1} at 300 ºC and 1.2×10^{-12} m^2 s^{-1} at 350 ºC. The other quantities used in calculations were as follows.

1. 300 ºC:

(1) $k_1 = 3.7\times10^{-13}$ m^2 s^{-1}

(2) $k = 1.5\times10^{-5}$ m s^{-1}

(3) $c_s = 27.04$ kg m^{-3} (0.32% Ni in Bi [142])

(4) $\rho_{int} = 10.1\times10^3$ kg m^{-3} [150]

(5) $s/v = 10.0$ m^{-1}

(6) $a = 1.5\times10^{-4}$ s^{-1}

(7) $b_0 = 4.70\times10^{-7}$ m s^{-1}

2. 350 ºC:

(1) $k_1 = 1.2\times10^{-12}$ m^2 s^{-1}

(2) $k = 4.0\times10^{-5}$ m s^{-1}

(3) $c_s = 32.76$ kg m^{-3} (0.39% Ni in Bi [142])

(4) $\rho_{int} = 10.1\times10^3$ kg m^{-3} [150]

(5) $s/v = 10.0$ m^{-1}

(6) $a = 4.0\times10^{-4}$ s^{-1}

(7) $b_0 = 1.52\times10^{-6}$ m s^{-1}

Final results are presented in Table 6.9. Application of equation (6.30) again produces a quite satisfactory fit to the experimental data. It is also worth noting that the range in which the intermetallic-layer thickness can vary is rather narrow, even though the time interval (600-3600 s) is relatively wide.

Table 6.9. Comparison of experimental thicknesses of the $NiBi_3$ layer grown from undersaturated bismuth melts at $\omega = 24.0$ rad s^{-1} with those calculated from equation (5.30)

Temperature (°C)	Time (s)	x_{under} ($\times 10^{-6}$ m)	x_{exp} ($\times 10^{-6}$ m)	x_{over} ($\times 10^{-6}$ m)
300	600	0.82	0.85 ± 0.10	0.86
	3600	1.00	1.25 ± 0.15	1.35
350	600	0.88	0.90 ± 0.15	1.00
	3600	1.3	2.5 ± 0.5	3.3

With a 51% Bi–42% Sn–5% In–2% Zn alloy as a melt material, a thin intermetallic layer occurs at the Ni-alloy interface. After 10800 s (3 h) holding at 350 °C and an angular disc rotation speed of 6.45 rad s^{-1}, its thickness is around 1.5 μm (Fig.6.18). With saturated melts, the layer thickness varies at this temperature from about 0.8 μm at a holding time of 600 s to 2.0 μm at 3600 s. From those values, the layer growth-rate constant can be estimated from a parabolic relation of the type $k_1 = x^2/2t$ as 5.5×10^{-16} m^2 s^{-1}.

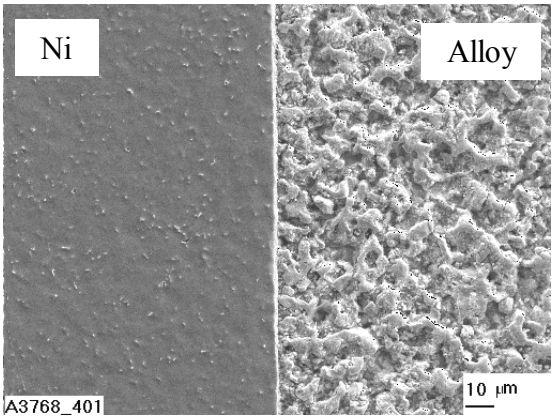

Fig. 6.18. Secondary electron image (SEI) of the transition zone formed between nickel and a 51% Bi–42% Sn–5% In–2% Zn alloy after 3h holding at 350 °C and an angular disc rotational speed of 6.45 rad s^{-1} [142].

At a temperature of 300 and 350 ºC, an angular disc rotational speed of 24.0 rad s^{-1} and reaction times up to 3600 s, no intermetallic layer was found to form at the solid-liquid interface under conditions of dissolution of nickel in the undersaturated 51% Bi–42% Sn–5% In–2% Zn alloy melt [142]. It means that the rate of chemical interaction at the layer interfaces, resulting in the growth of the layer, is less than the rate of its dissolution in the melt, so that in equation (6.26) $k_0 < b$ at any value of t in the 600-3600 s range.

Hence, in the case under consideration the layer formation can readily be prevented, if the rate of dissolution is maintained sufficiently high. Small additions of Sb (1%), Te and Se (0.5% each), instead of corresponding amounts of Sn and Zn, do not change significantly the intermetallic-layer thickness.

6.5.2: Interaction of solid nickel with liquid Sn–Bi–In–Zn–Sb alloys

A brief account of investigation of interfacial reactions of nickel with 87.5% Sn–7.5% Bi–3% In–1% Zn–1% Sb and 80% Sn–15% Bi–3% In–1% Zn–1% Sb alloys is presented in this section [143-145]. As evidenced in Fig. 6.19, temperature dependence of the solubility of nickel in those alloys obeys a relation of the Arrhenius type.

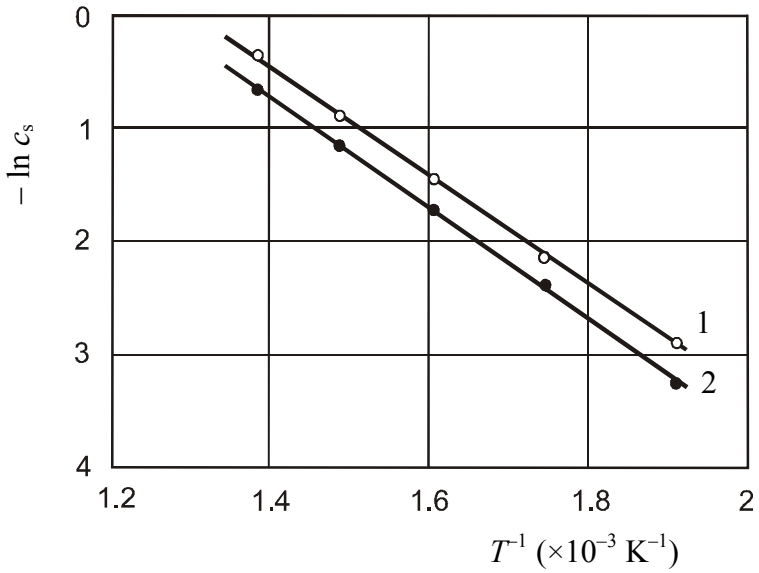

Fig. 6.19. Temperature dependence of the solubility of nickel in liquid soldering alloys. 1, 87.5% Sn–7.5% Bi–3% In–1% Zn–1% Sb alloy; 2, 80% Sn–15% Bi–3% In–1% Zn–1% Sb alloy.

Application of the least-squares fit method yields the following equations:

$$c_s = 4.94\times10^2 \exp(-39500/RT)\ \%$$

for a 87.5% Sn–7.5% Bi–3% In–1% Zn–1% Sb alloy,

$$c_s = 4.19\times10^2 \exp(-40200/RT)\ \%$$

for a 80% Sn–15% Bi–3% In–1% Zn–1% Sb alloy,

where R is in J mol^{-1} K^{-1} (8.314 J mol^{-1} K^{-1}) and T in K. The linear regression coefficient is 0.99963 for the former alloy and 0.99969 for the latter.

Note that relatively small amounts of additives produce a very considerable effect on the solubility of nickel in tin-based soldering alloys. The temperature dependence of the nickel solubility in pure tin in the 300-700 ºC range is reported to obey the equation [148]

$$c_s = 5.34\times10^2 \exp(-36900/RT)\ \%.$$

Comparison of the solubility values calculated from these three temperature dependences is provided in Table 6.10. Twenty percent of additives (Bi, In, Zn and Sb) are seen to produce more than a two-fold decrease in nickel solubility values. Such a large drop could not be expected judging from the solubility values in binary systems of nickel with the main alloy constituents tin and bismuth.

Table 6.10. Comparison of nickel solubility values in liquid tin and soldering alloys

Temperature (ºC)	Nickel solubility, c_s (%)		
	100% Sn [148]	87.5% Sn…	80% Sn…
250	0.11	0.056	0.040
300	0.23	0.12	0.091
350	0.43	0.24	0.18
400	0.73	0.42	0.32
450	1.15	0.69	0.52

For example, at 350 ºC c_s is 0.43% Ni for tin [148] and 0.39% Ni for bismuth [142]. In view of their relatively low content in soldering alloys, the influence of indium, zinc and antimony is insignificant. Note that for a similar alloy containing 51% Bi, 42% Sn, 5% In and 2% Zn the nickel solubility at 350 ºC is much lower, namely, 0.015%. These data again provide evidence that the solubility of nickel decreases as the solder composition approaches that of the binary Bi–Sn eutectic.

Probably, lowering the nickel solubility with increasing bismuth content of the alloys is connected with the increasing degree of ordering of the liquid structure that becomes most perfect at the eutectic composition. In the structure corresponded to the eutectic composition, little room remains to accommodate foreign (nickel) atoms. Direct experimental evidence, for example from X-ray diffraction, is needed to verify this viewpoint.

Dissolution-rate constants of nickel in Sn–Bi–In–Zn–Sb soldering alloys at an angular rotational speed of 24.0 rad s^{-1} are presented in Table 6.11. Also included in the table are appropriate diffusion coefficients.

Table 6.11. Dissolution-rate constants at ω = 24.0 rad s^{-1} and diffusion coefficients of nickel in liquid Sn–Bi–In–Zn–Sb soldering alloys

Alloy	Temperature (ºC)	k ($\times 10^{-5}$ m s^{-1})	D ($\times 10^{-9}$ m^2 s^{-1})	
			Eq. (6.6)	Eq. (6.7)
87.5% Sn…	250	1.3	0.20	0.22
	300	2.7	0.55	0.59
	350	4.6	1.21	1.33
	400	5.4	1.52	1.68
	450	6.2	1.82	2.02
80% Sn…	250	1.1	0.15	0.16
	300	2.6	0.52	0.56
	350	4.5	1.17	1.28
	400	5.3	1.48	1.63
	450	6.1	1.77	2.02

Two sets of experiments, with saturated and undersaturated melts, were again carried out to visualize the effect of dissolution on the process of intermetallic-layer formation at the interface between nickel and liquid soldering alloys. In the case of undersaturated melts, the nickel disc was being rotated during the run at an angular speed of 24.0 rad s^{-1}.

With both soldering alloys, the Ni_3Sn_4 intermetallic layer was found to form from both saturated and undersaturated melts, as illustrated in Fig. 6.20. Like $NiBi_3$, the Ni_3Sn_4 intermetallic-compound layer also tends to be destroyed under the influence of the liquid phase.

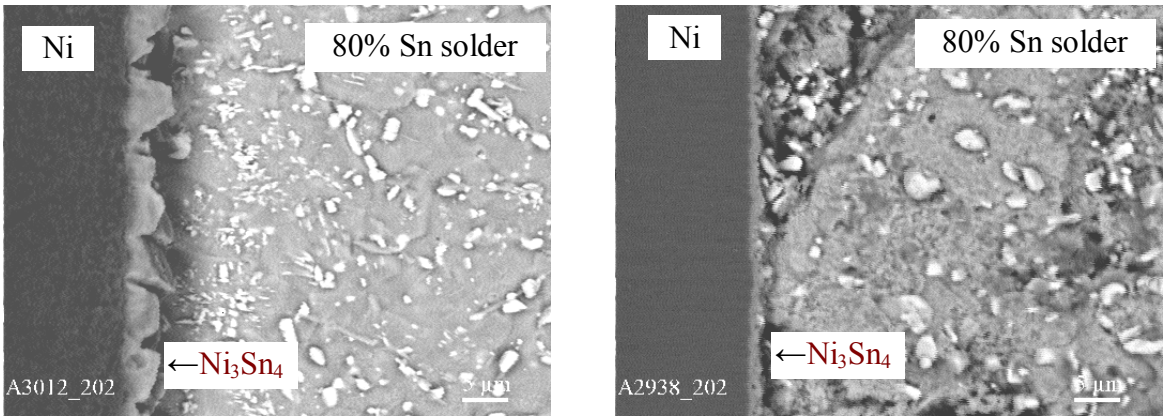

(a) (b)

Fig. 6.20. Backscattered electron image (BEI) of the transition zone formed between nickel and a 80% Sn–15% Bi–3% In–1% Zn–1% Sb alloy at a temperature of 350 ºC and a reaction time of 1800 s. (a) saturated melt, (b) undersaturated melt (ω = 24.0 rad s^{-1}) [142].

This effect is typical of thick layers formed from saturated melts. Nonetheless, from Fig. 5.23 it is seen that the Ni_3Sn_4 layer thickness is much less in the case of the undersaturated melt compared to the case of the saturated melt, indicative of the profound effect of dissolution on the layer-growth kinetics.

To estimate the magnitude of this effect, calculations of the thickness of the Ni_3Sn_4 layer grown from undersaturated solder melts were again carried out using equation (6.30). For example, in the case of the saturated 87.5% Sn–7.5% Bi–3% In–1% Zn–1% Sb alloy melt, the experimental value of the Ni_3Sn_4 layer thickness (whenever it has not been destroyed under the influence of the liquid phase) was found to be 16.0×10^{-6} m at 450 ºC and a reaction time of 300 s. Hence, $k_1 = x^2/2t = 4.3\times10^{-13}$ m^2 s^{-1}.

Other quantities necessary for calculations are $k = 6.2\times10^{-5}$ m s^{-1} at ω = 24.0 rad s^{-1}, c_s = 48.5 kg m^{-3} (0.69% Ni in the soldering alloy), $\rho_{int} = 8.68\times10^3$ kg m^{-3}, φ = 0.27, s/v = 10.0 m^{-1}, $b_0 = 1.28\times10^{-6}$ m s^{-1}. Using these data, one obtains the limiting values, $x_{under} = 0.6\times10^{-6}$ m and $x_{over} = 1.5\times10^{-6}$ m, for the thickness of the Ni_3Sn_4 layer grown from the undersaturated solder melt at 450 ºC and a reaction time of 2400 s. The experimental value x_{exp} is $(1.2\pm0.2)\times10^{-6}$ m. The agreement of these values appears to be quite sufficient for practical purposes to roughly evaluate the intermetallic layer thickness at the solid-liquid interface.

Whenever the layer growth-rate constant k_1 could not be determined from the layer thickness-time dependence for the saturated melt, it was estimated from that for the undersaturated melt. For example, in the case of the undersaturated 87.5% Sn–7.5% Bi–3% In–1% Zn–1% Sb alloy melt at 350 ºC, $k = 4.6\times10^{-5}$ m s^{-1} at ω = 24.0 rad s^{-1}, c_s = 17.0 kg m^{-3} (0.24% Ni in the soldering alloy [145]), $b_0 = 3.34\times10^{-6}$ m s^{-1}; ρ_{int}, φ and s/v are as before.

The experimental value x_{exp} of the Ni_3Sn_4 layer thickness at this temperature and a reaction time of 300 s is 1.0×10^{-6} m. By assuming $x_{exp} = x_{max}$, one obtains from equation (6.30) $k_1 = x_{max}\,(b_0 + b_{300})/2 = 3.13\times10^{-13}$ m^2 s^{-1}. Note that the accuracy of this estimation is rather high, with the overestimated value of k_1 being 3.34×10^{-13} m^2 s^{-1} and the underestimated one 2.91×10^{-13} m^2 s^{-1}.

Comparison of calculated and experimental values of the Ni_3Sn_4 layer thickness is provided in Table 6.12. Also included in the table are the results for a 80% Sn–15% Bi–3% In–1% Zn–1% Sb alloy melt, obtained using the following quantities: $k = 4.5\times10^{-5}$ m s^{-1} at $\omega = 24.0$ rad s^{-1}, $c_s = 13.0$ kg m^{-3} (0.18% Ni in the soldering alloy [145]), $b_0 = 2.50\times10^{-6}$ m s^{-1}, $x_{exp} = 0.9\times10^{-6}$ m at $t = 300$ s, $k_1 = 2.11\times10^{-13}$ m^2 s^{-1}. Again, the agreement of experimental and calculated layer thicknesses is fairly good.

Table 6.12. Comparison of experimental thicknesses of the Ni_3Sn_4 layer grown from undersaturated bismuth melts at 350°C and $\omega = 24.0$ rad s^{-1} with those calculated using equation (6.30)

Soldering alloy	Time (s)	x_{under} ($\times10^{-6}$ m)	x_{exp} ($\times10^{-6}$ m)	x_{over} ($\times10^{-6}$ m)
87.5% Sn…	600	1.06	1.1 ± 0.1	1.24
	900	1.13	1.3 ± 0.1	1.42
	1200	1.19	1.5 ± 0.2	1.63
	1800	1.30	1.8 ± 0.2	2.14
	2400	1.40	2.2 ± 0.3	2.82
80% Sn…	600	0.95	1.0 ± 0.1	1.10
	900	1.01	1.2 ± 0.1	1.26
	1200	1.07	1.3 ± 0.1	1.46
	1800	1.17	1.5 ± 0.2	1.90
	2400	1.26	1.8 ± 0.2	2.48

6.5.3: Reactions of solid cobalt with liquid Sn–Bi–In–Zn–Sb alloys

Like nickel, reactions of cobalt with 87.5% Sn–7.5% Bi–3% In–1% Zn–1% Sb and 80% Sn–15% Bi–3% In–1% Zn–1% Sb soldering alloys have also been studied [146, 147]. As evidenced in Fig. 6.21, temperature dependence of the solubility of cobalt in those alloys obeys a relation of the Arrhenius type.

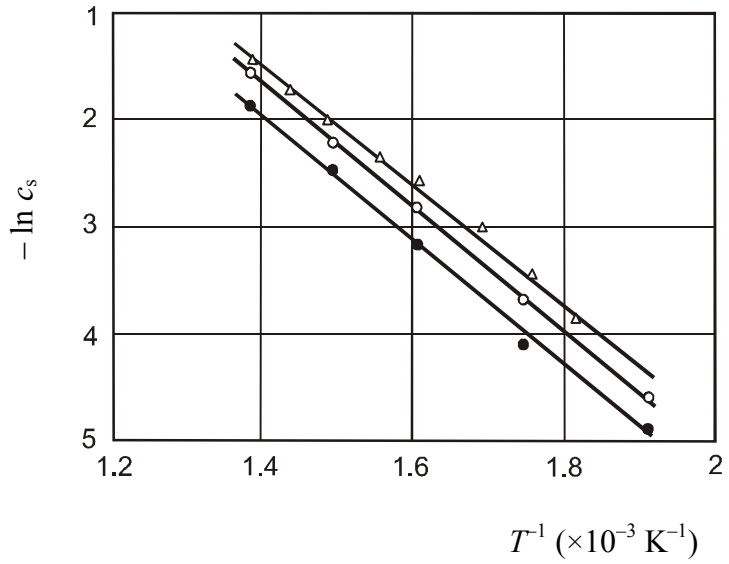

Fig. 6.21. Temperature dependence of the solubility of cobalt in tin and liquid soldering alloys. Δ, tin; ○, 87.5% Sn–7.5% Bi–3% In–1% Zn–1% Sb alloy; ●, 80% Sn–15% Bi–3% In–1% Zn–1% Sb alloy.

The least-squares fit method yields the following equations:

$$c_s = 4.08\times10^2 \exp(-45200/RT)\ \%$$

for tin,

$$c_s = 4.06\times10^2 \exp(-46300/RT)\ \%$$

for a 87.5% Sn–7.5% Bi–3% In–1% Zn–1% Sb alloy,

$$c_s = 5.46\times10^2 \exp(-49200/RT)\ \%$$

for a 80% Sn–15% Bi–3% In–1% Zn–1% Sb alloy,

where R is in J mol^{-1} K^{-1} and T in K. Appropriate linear regression coefficients are 0.9966, 0.9987 and 0.9963.

Comparison of the solubility values calculated from these temperature dependences (smoothed solubilities) is provided in Table 6.13. The additives Bi, In, Zn and Sb are seen to produce a considerable decrease of the cobalt solubility in the solder melts.

Table 6.13. Comparison of smoothed cobalt solubility values in tin and soldering alloys in the temperature range of 250-450 ºC

Temperature (°C)	Cobalt solubility, c_s (%)		
	100% Sn	87.5% Sn…	80% Sn…
250	0.012	0.0092	0.0067
300	0.031	0.024	0.018
350	0.066	0.053	0.041
400	0.13	0.10	0.083
450	0.22	0.18	0.15

From the data of Table 6.13, it must be clear why conventional methods employed to investigate phase equilibria, for example differential scanning calorimetry, do not yield satisfactory results in the liquidus determination with systems like Co–Sn. Firstly, the solubility values of cobalt in liquid tin are rather small. Secondly, the liquidus curve ascends very abruptly from the eutectic point to the peritectic temperature of formation of the $CoSn_2$ compound. For these reasons, any arrests on the thermal heating-cooling curves, corresponding to the cobalt solubility in tin (and the soldering alloys) at a given temperature, can hardly be determined with confidence.

In contrast, kinetic methods yield much more accurate results because the degree of saturation of the liquid can readily be controlled by chemical and physical means. Since the experiment is carried out at constant temperature and pressure, no supersaturation of the liquid is possible. Sooner or later, an equilibrium intermetallic phase is to be formed at the cobalt-solder interface (see Section 4.2). At prolonged reaction times, the layer of this (and perhaps some other) phase will grow until all the cobalt (the solder is usually taken in excess) is consumed completely.

Note that for the liquid-tin phase to reach saturation, it does not matter whether the saturation process is carried out from the cobalt phase, or from the nearest (to tin) intermetallic compound, or from any other intermetallic compound of the Co–Sn binary system because cobalt exists in the saturated metallic melt in the form of atoms, and therefore any initial phase decomposes during its dissolution in tin. No compounds can occur within the liquid-tin bulk unless the temperature is lowered enough to cause supersaturation of the melt (pressure is usually constant in the course of experiments).

Dissolution-rate constants of cobalt in Sn–Bi–In–Zn–Sb soldering alloys at an angular disc rotational speed of 24.0 rad s^{-1} are presented in Table 6.14. Also listed in the table are appropriate diffusion coefficients. As seen from Tables 6.11 and 6.14, both quantities are

close to those for nickel. It is not surprising because many physical and chemical properties of cobalt and nickel are similar.

Table 6.14. Dissolution-rate constants at $\omega = 24.0$ rad s^{-1} and diffusion coefficients of cobalt in liquid Sn–Bi–In–Zn–Sb soldering alloys

Alloy	Temperature (ºC)	k ($\times 10^{-5}$ m s^{-1})	D ($\times 10^{-9}$ m^2 s^{-1})	
			Eq. (6.6)	Eq. (6.7)
87.5 % Sn…	250	1.2	0.17	0.19
	300	2.7	0.55	0.59
	350	4.5	1.17	1.28
	400	5.2	1.44	1.58
	450	6.2	1.82	2.02
80 % Sn…	250	1.1	0.15	0.16
	300	2.4	0.46	0.49
	350	4.4	1.14	1.24
	400	5.2	1.44	1.58
	450	6.2	1.82	2.02

To visualise the effect of dissolution on the intermetallic layer-growth kinetics, experiments with both saturated and undersaturated Sn–Bi–In–Zn–Sb alloy melts were carried out. A few backscattered electron images of the cobalt-solder transition zone are shown in Fig. 6.22 as an example. With both solders, a single layer of the $CoSn_3$ intermetallic compound was found to form from saturated and undersaturated melts at 250°C and reaction times up to 1800 s. The layer of $CoSn_2$ occurs at 350 and 450 ºC. Besides, formation of an additional layer of the CoSn intermetallic compound around 1.5 μm thick was observed at a temperature of 450 ºC and a reaction time of 1800 s.

It is worth noting that, in addition to four known equilibrium intermetallic compounds Co_3Sn_2, CoSn, $CoSn_2$ and $CoSn_3$, formation of the $CoSn_4$ layer was observed by Chao-hong Wang and Sinn-wen Chen at the corners of the Co-Sn diffusion couples reacted at 180-190 ºC, as shown in Fig. 6.23 [151]. It is yet unclear whether the $CoSn_4$ phase is stable or metastable.

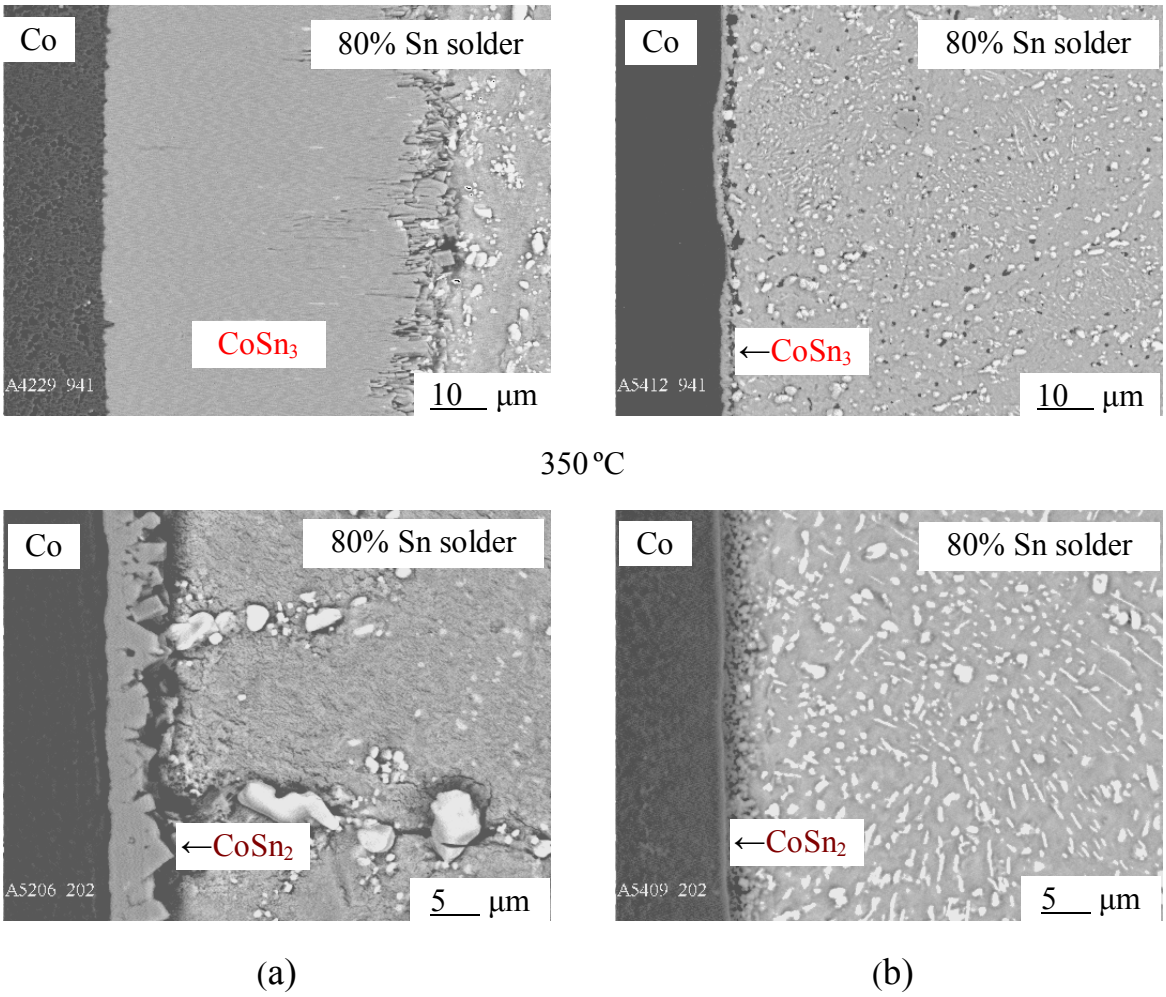

Fig. 6.22. Backscattered electron images (BEI) of the transition zone formed between cobalt and liquid soldering alloys at a reaction time of 1800 s: (a) saturated melts; (b) undersaturated melts ($\omega = 24.0$ rad s^{-1}).

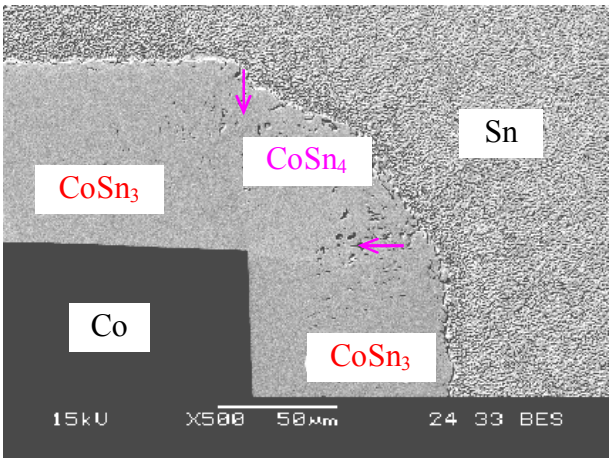

Fig. 6.23. Micrograph (BEI) of the Co–Sn diffusion couple reacted at a temperature of 180 °C for 432×10^3 s (120 h) [151].

Most probably, occurrence of this phase is a result of the secondary reaction $Sn_{dif} + CoSn_3 = CoSn_4$ taking place at the $CoSn_3$–$CoSn_4$ interface where any contact between Co and $CoSn_3$ is lacking, *i.e.* actually in the $CoSn_3$–Sn diffusion couple. In the Co–$CoSn_3$–Sn couple, the $CoSn_4$ layer can hardly compete with the fast-growing $CoSn_3$ layer and is therefore missing.

The absence of the $CoSn_4$ compound from the equilibrium phase diagram might be due to the difficulty of attaining the equilibrium state of Co–Sn alloys during their annealing at low temperatures. Further wok is required to establish phase equalibria in Sn-rich alloys of the Co–Sn binary system. Investigation of reaction kinetics in $CoSn_3$–Sn diffusion couples might be helpful in this respect.

Effect of dissolution on the growth rate of the intermetallic layers is seen in Fig. 6.22 to be very profound. To estimate its magnitude, calculations of the thickness of the layers grown from undersaturated solder melts were again carried out using equation (6.30). For example, in the case of the saturated 80% Sn–15% Bi–3% In–1% Zn–1% Sb alloy melt, the experimental value of the $CoSn_2$ layer thickness was found to be 33.0×10^{-6} m at 450 ºC and a reaction time of 1800 s. Hence, $k_1 = x^2/2t = 3.0\times10^{-13}$ m^2 s^{-1}. Other quantities necessary for calculations are $k = 6.2\times10^{-5}$ m s^{-1} at $\omega = 24.0$ rad s^{-1}, $c_s = 10.74$ kg m^{-3} (0.15 % Co in the soldering alloy [146]), $\rho = 8.91\times10^3$ kg m^{-3} [152], $\varphi = 0.1989$ (19.89 % Co in $CoSn_2$), $s/v = 10.0$ m^{-1}, $b_0 = 3.76\times10^{-7}$ m s^{-1}.

Comparison of calculated values of the $CoSn_2$ layer thickness, x_{under} and x_{over}, with experimental ones is provided in Table 6.15. Since the duration of the soldering procedure rarely exceeds a few minutes, the agreement of these values appears to be quite sufficient for practical purposes to estimate the intermetallic-layer thickness at the solid-liquid interface.

Table 6.15. Comparison of experimental thicknesses of the $CoSn_2$ layer grown from undersaturated 80% Sn–15% Bi–3% In–1% Zn–1% Sb solder melts at 450 ºC and $\omega = 24.0$ rad s^{-1} with those calculated using equation (6.30)

Time (s)	b_t ($\times10^{-7}$ m s^{-1})	$(b_0 + b_t)/2$ ($\times10^{-7}$ m s^{-1})	x_{under} ($\times10^{-6}$ m)	x_{exp} ($\times 10^{-6}$ m)	x_{over} ($\times10^{-6}$ m)
300	3.12	3.44	0.80	0.8 ± 0.1	0.87
600	2.59	3.18	0.94	1.0 ± 0.2	1.16
1200	1.79	3.02	1.00	1.5 ± 0.2	1.68
1800	1.23	2.50	1.20	1.8 ± 0.2	2.43

Another example of calculations is the case of the undersaturated 87.5% Sn–7.5% Bi–3% In–1% Zn–1% Sb alloy melt at 350ºC, in which $k = 4.5\times10^{-5}$ m s^{-1} at $\omega = 24.0$ rad s^{-1}, $c_s = 3.75$ kg m^{-3} (0.053 % Co in the soldering alloy [146]), $b_0 = 9.52\times10^{-8}$ m s^{-1}; ρ_{int}, φ and s/v are as before. The experimental value x_{300} of the $CoSn_2$ layer thickness at this temperature and a reaction time of 300 s is 0.6×10^{-6} m. By assuming $x_{300} = x_{max}$, one obtains from equation (6.30) $k_1 = x_{max}\,(b_0 + b_{300})/2 = 5.4\times10^{-14}$ m^2 s^{-1}. Comparison of calculated and experimental values of the $CoSn_2$ layer thickness is provided in Table 6.16.

Table 6.16. Comparison of experimental thicknesses of the $CoSn_2$ layer grown from undersaturated solder melts at 350ºC and $\omega = 24.0$ rad s^{-1} with those calculated using equation (6.30)

Soldering alloy	Time (s)	b_t ($\times10^{-8}$ m s^{-1})	$(b_0 + b_t)/2$ ($\times10^{-8}$ m s^{-1})	x_{under} ($\times10^{-6}$ m)	x_{exp} ($\times10^{-6}$ m)	x_{over} ($\times10^{-6}$ m)
87.5% Sn	600	7.27	8.40	0.64	0.7 ± 0.1	0.74
	1200	5.55	7.54	0.72	0.8 ± 0.2	0.97
	1800	4.24	6.88	0.78	1.1 ± 0.3	1.27
80% Sn	600	6.44	6.90	0.54	0.6 ± 0.1	0.62
	1200	5.64	6.50	0.60	0.8 ± 0.2	0.81
	1800	4.33	5.84	0.66	1.0 ± 0.3	1.05

Also included in the table are the results for an 80% Sn–15% Bi–3% In–1% Zn–1% Sb alloy, obtained using the following quantities: $k = 4.4\times10^{-5}$ m s^{-1} at $\omega = 24.0$ rad s^{-1}, $c_s = 2.96$ kg m^{-3} (0.041 % Co in the soldering alloy [146]), $b_0 = 7.35\times10^{-8}$ m s^{-1}, $x_{exp} = 0.5\times10^{-6}$ m at $t = 300$ s, $k_1 = 3.5\times10^{-14}$ m^2 s^{-1}. Again, the agreement of calculated and experimental values of the layer thickness is seen to be quite satisfactory for both alloys.

6.6: Basic kinetic dependences in solid-gas systems

As the kinetics of interfacial interaction of solids with gases have been considered in numerous books and original papers (see, for example, Refs [17, 18, 22, 23, 27, 28, 85-87]), consideration will here be restricted to a few remarks regarding the shape of the layer thickness-time dependence. First, the most probable dependence in the case of formation of non-volatile chemical compounds between solid *A* and gas *B* will be analysed, assuming that *B* is insoluble in *A* at a given temperature. Then, the effect of evaporation on the layer-growth

kinetics will be established. Finally, soft oxidation of chemical compounds will briefly be considered.

6.6.1: Compound layer thickness-time relationships

Although there are no essential difference in the mechanism of formation of the solid layers of chemical compounds at the interface of either two solid substances, or a solid and a liquid, or a solid and a gas, nevertheless in the latter case the layer thickness-time dependences observed experimentally are more diverse and complicated than in the first two cases because the growth kinetics of compound layers in the solid-gas systems are usually investigated by thermogravimetry over a comparatively wide time range. Under such conditions, significant changes in the layer-growth mechanism may take place, and this are reflected on the shape of experimental kinetic dependences. Therefore, the number of equations proposed for the mathematical description of those dependences is considerably greater than in the case of systems formed, for example, by two solids. Of these, different forms of linear, parabolic, paralinear, cubic and logarithmic laws are employed most frequently.

According to U.R. Evans [18], logarithmic equations (direct, reverse and asymptotic) are low-temperature laws. The reverse logarithmic law is valid if the layer-growth process is controlled by the electric potential gradient. This is probably the case with thin films of ionic compounds [22]. The asymptotic and direct logarithmic laws are due to the transport of matter through pores whose number varies in the course of interaction between a solid and a gas. In such a case, the growth process may happen to be more dependent upon the presence of macroscopic defects in a growing layer than upon its microscopic mechanism.

In the case of a single non-volatile chemical compound layer, some initial region of the layer thickness-time dependence is close to linear, followed by the gradual transition to a parabola. Such dependences are almost always observed in the oxidation, nitridation or sulphidation of metals, if temperature is not too high and the process is investigated by sufficiently sensitive experimental techniques. For example, B.S. Lee and R.A. Rapp [153] found the kinetics of gaseous sulphidation of molybdenum to be linear-parabolic at a temperature as high as 750 ºC, with the linear growth period extending at least to 2h (Fig. 6.24).

The higher the temperature, the narrower the time range of linear growth was. Above 800 ºC, the linear growth region was too narrow and therefore hardly observable. Note that the linear-to-parabolic transition took place at the MoS_2 layer thickness in the vicinity of 0.5 μm, which value is close to those for intermetallics and silicides. Growth of the MoS_2 layer is due to diffusion of sulphur ions or atoms across its bulk, followed by their subsequent interaction with the molybdenum atoms at the Mo–MoS_2 interface. Therefore, inert markers are found after the reaction at the interface between MoS_2 and the gaseous phase [153].

It seems relevant to remind once again that in the case of formation of a single-phase compound layer, the reverse (parabolic-to-linear) transition is impossible. From a physico-chemical viewpoint, it is only possible during the simultaneous occurrence of two or more

compound layers, as is indeed observed experimentally [27]. Parabolic-to-linear growth kinetics are thus indicative of the formation of multiple layers of oxides, nitrides, sulphides, *etc*., even though some of them may be hardly identifiable due to their extremely small thickness.

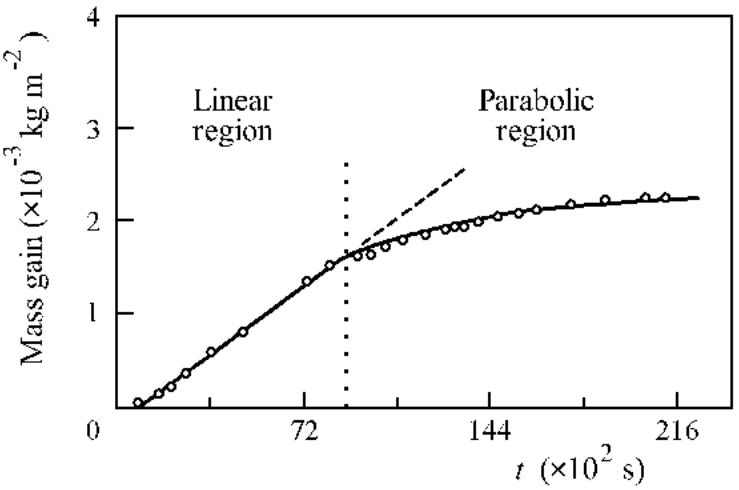

Fig. 6.24. Sulphidation kinetics of molybdenum from the gaseous phase at 750 ºC and a sulphur vapour pressure of 4 Pa (0.03 mm Hg) [153]. Growth of the MoS_2 layer is initially linear and then parabolic.

If two layers A_pB_q and A_rB_s are formed (see Fig. 3.1), the kinetic dependence is more complicated and can scarcely be described by any single analytical function. One of its most probable variants is shown schematically in Fig. 6.25. Both layers are assumed to form from the very beginning of interaction of solid A with gas B. Their growth kinetics are described by the system of differential equations (3.27).

In general, an initial region of the dependence of the mass of each of the two layers as well as their total mass upon time must be linear (region I in Fig. 6.25). It is the region of chemical control, with fast diffusion of both species across the bulks of both layers and slow chemical interaction at the layer interfaces. At longer times and an appropriate ratio of the chemical and diffusional constants, the layer, for example A_pB_q, may happen to grow over some period of time in the diffusion controlled regime with regard to both components, while the A_rB_s layer in the reaction controlled regime with regard to component B (see Chapter 3). In such a case, the thickness and hence the mass of the A_pB_q layer tends with increasing time to a limiting value determined by equation (3.41), whereas the thickness (mass) of the A_rB_s layer increases linearly. The summation of the masses of both layers yields a dependence which in region II is close to parabolic, while in region III to linear. This is *paralinear* growth kinetics.

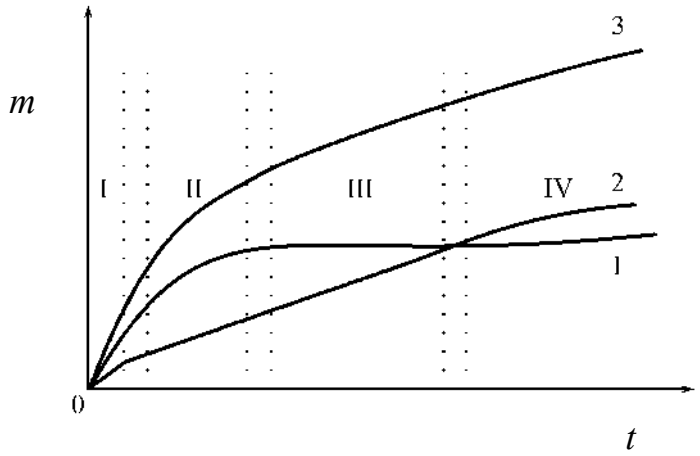

Fig. 6.25. Schematic diagram to illustrate one of possible kinetic relationships in the case of formation of two compound layers at the interface between solid *A* and gas *B*. 1, mass of the A_pB_q layer; 2, mass of the A_rB_s layer; 3, total mass gain of a solid specimen.

During further isothermal holding, a time will come for the A_rB_s layer to grow in the diffusion controlled regime with regard to component *B*. As a result, the A_pB_q layer loses a source of *B* atoms and therefore its growth must have slowed down considerably. However, this effect is in fact not so profound and practically unobservable since a significant reduction in the growth rate of the A_rB_s layer due to a change of the growth regime causes the A_pB_q layer to grow more rapidly, thereby compensating its decrease due to the former reason. Therefore, the A_pB_q layer thickness will start to increase, instead of being constant. Region IV thus corresponds to the so-called *postlinear* (or, more precisely, *postparalinear*) growth period [27] that is likely to be described by the system of differential equations (3.43).

It should be noted that at this stage the rate of increase of the total mass of the layers would be less than that which could be expected on the basis of a parabolic law. Therefore, if the kinetic data are formally treated using a power law, its exponent must in all likelihood be greater than 2. The cubic law may presumably hold in this region of growth of compound layers, though experimental values of the exponent are rarely observed to be constant and equal to 3. Most frequently, its value varies in the range 2.0-3.5 [18].

In such a case, it seems reasonable to treat the kinetic data using equations (3.43) and (3.50). However, thermogravimetric measurements alone, providing no information regarding the number of growing compound layers, their composition, thickness and structure, are insufficient for this purpose. It is necessary to use a few additional independent methods of investigation (metallography, X-ray diffraction, electron microscopy, electron probe microanalysis, Rutherford backscattering spectroscopy, *etc*.) in order to determine the phase identity and the thickness (or mass) of each of the layers formed.

Clearly, the duration of those growth stages in a particular solid-gas system may differ considerably. It results in a complicated kinetic curve, with its slope changing a few times due

to the change in the number of growing compound layers and in their growth regimes (see Chapter 3).

Since the solid phase under investigation may be not only an elementary substance but also a material of rather complicated chemical composition, interpretation of experimental results is in many cases a not so easy task which not always can be solved unambiguously. Further complications arise from layer cracking due to stress and other reasons. After reaching a certain thickness, compound layers often cracks along the whole interface or at local areas, providing direct access to the gas attack. Then, subsequent healing of cracks occurs until the cracking thickness is attained again. The cracking process is repeated again and again, thus being a continuous one over the surface of the solid phase as a function of time. Note that the sudden release of stress by the layer fracture may even cause an occasional vibration of the microbalance spring during thermogravimetric measurements, as was observed during the sulphidation of molybdenum [153]. Difficulties in interpreting the experimentally observed kinetic dependences are significantly aggravated, if volatile chemical compounds are formed in the course of interaction of solids with gases.

6.6.2: Influence of evaporation on the growth rate of a chemical compound layer

The process of evaporation of the volatile compound A_pB_q is described by equations similar to (6.15) and (6.16):

$$\frac{\mathrm{d}x_{\mathrm{evap}}}{\mathrm{d}t} = kc_{\mathrm{s}}V_{A_pB_q}\exp\left(-\frac{kSt}{v}\right) \tag{6.35}$$

and

$$x_{\mathrm{evap}} = \frac{V_{A_pB_q}c_{\mathrm{s}}v}{S}\left[1-\exp\left(-\frac{kSt}{v}\right)\right], \tag{6.36}$$

where x_{evap} is the thickness of the evaporated portion of the A_pB_q layer, m; t is the time, s; k is the evaporation-rate constant, m s^{-1}; c_{s} is the concentration of the A_pB_q compound in the diffusion boundary layer at the surface of a solid, mol m^{-3}; $V_{A_pB_q}$ is the molar volume of the A_pB_q compound, m^3 mol^{-1}; v is the volume of the gaseous phase, m^3; S is the surface area of the solid specimen, m^2.

In deriving equations (6.35) and (6.36) the A_pB_q compound was assumed to evaporate without decomposition. In such a case, growth kinetics of the A_pB_q compound layer between solid A and gas B are described by equation (6.19) in which $b = kc_{\mathrm{s}}V_{A_pB_q}$.

For solid-gas systems, in most cases the condition $\exp(-kSt/v) \approx 1$ is satisfied. Indeed, one of the following two variants is usually realised in experiments.

(1) Large volume of a gas is used. Hence, during the reaction time the chemical composition of the gaseous phase does not change significantly.

(2) Investigations are carried out in a flowing gas or under vacuum. Therefore, the reaction product is continuously removed away from the reaction site.

If so, the rate of evaporation of the growing A_pB_q layer is constant and equal to b. Consequently, the kinetics of layer formation are described by equation (6.22). It should be noted that a simpler equation, analogous to (6.24) but differing by the meaning of the coefficients, was first derived by I.N. Frantsevich *et al*. [154] in the framework of the electrochemical approach. Then, it was re-discovered a few times by other researchers, probably independently of each other.

In general, the volatile A_pB_q compound formed during the interaction of substances A and B is partitioned between the solid and gaseous phases, *i.e*. some its portion forms a solid layer adherent to the surface of substance A, whereas another portion evaporates into the gaseous phase. If $k_0 > b$ (or more generally $k_{0B1} + k_{0A2} > b$, see equation (6.31)), then the solid layer A_pB_q forms and grows at the A–B interface from the very beginning of interaction between solid A and gas B.

This happens when the sum of the rates of chemical transformations at the layer interfaces with initial substances exceeds its evaporation rate. In such a case, the A_pB_q layer adherent to the surface of substance A reaches a highest possible thickness determined by equation (6.26) and then grows no longer. Note that certain regions of the layer mass-time dependence may be either linear (at $k_0 << k_1/x$) or parabolic (at $k_0 >> b$ and $k_1/x >> b$).

When the thickness of the A_pB_q layer has reached its highest value x_{max}, the stationary state is established in which the mass loss of the solid phase due to evaporation is just compensated by the mass gain due to partial chemical reactions proceeding at the layer interfaces with initial substances A and B. Subsequently, the mass of the A_pB_q layer adherent to phase A remains constant, whereas the mass of its evaporated portion increases linearly. As a result, the mass of a solid specimen (substance A plus the A_pB_q layer) first increases, goes through a maximum, then begins to decrease and at t_0 proves equal to its initial value (Fig. 6.26). Thereafter, mass loss takes place instead of mass gain.

Such a dependence is frequently observed experimentally in the oxidation of transition metals forming volatile oxides and also of their alloys, carbides, nitrides, borides, silicides and other chemical compounds [27, 85, 87, 154-157]. An example based on the experimental results of E.A. Gulbransen and K.F. Andrew [157] is provided in Fig. 6.27.

At temperatures up to about 1150 ºC there were time periods of the mass gain of tungsten wires, whereas at a temperature of 1200 ºC or higher no mass gain was observed from the very beginning of their experiments since the volatile oxide WO_3 formed in the course of oxidation entirely evaporated into the gaseous phase. The boiling point of this compound is 1670 ºC [67]. It is known to volatilise appreciably at a temperature of 800 ºC.

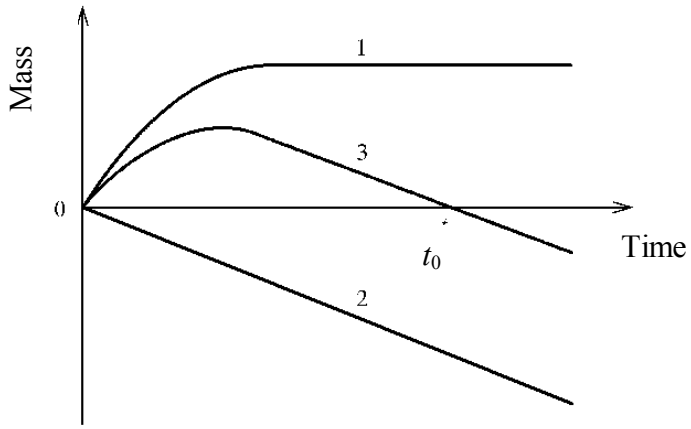

Fig. 6.26. Typical kinetic dependence in the case of formation of a volatile chemical compound evaporating at a constant rate. 1, mass of the solid A_pB_q layer adherent to phase A; 2, mass of the evaporated portion of the A_pB_q layer; 3, change of the total mass of a solid specimen relative to its initial value.

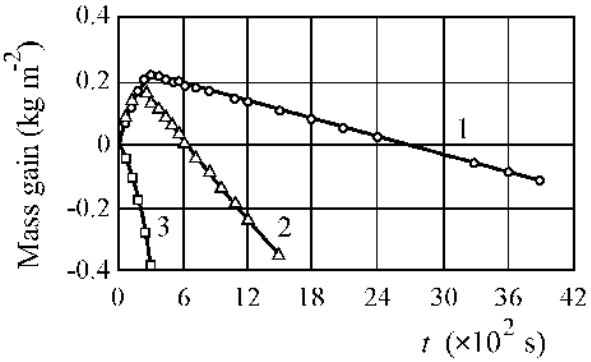

Fig. 6.27. Oxidation kinetics of tungsten wires at an oxygen pressure of 1.0×10^4 Pa (0.1 atm) [157]. Temperature: 1, 1100 ºC; 2, 1150; 3, 1200.

With technetium, no mass gain is observed at temperatures as low as 300 ºC [158]. The mass loss of its sheets strictly follows a linear relation. The reaction product is Tc_2O_7 (boiling point 311 ºC [67]).

The effect of decreasing pressure on the rate of oxidation of tungsten wires is similar to that of increasing temperature, as illustrated in Fig. 6.28. As no correction for the change in the surface area of the wires during the reaction have introduced, mass loss plots in Figs 6.27 and 6.28 are seen to be somewhat curved, instead of being straight lines.

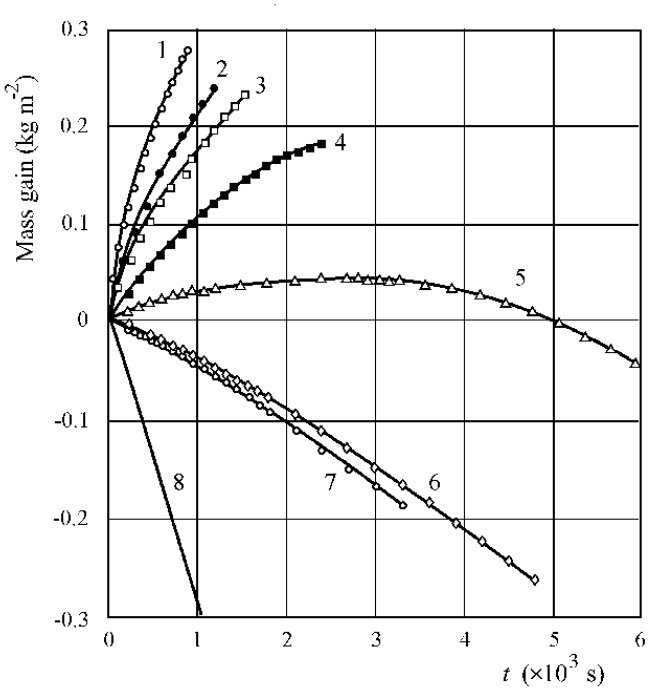

Fig. 6.28. Effect of oxygen pressure on the oxidation kinetics of tungsten at a temperature of 1050 ºC [157]. Pressure: 1, 1.0×10^4 Pa (0.1 atm); 2, 5.12×10^3 Pa (0.0512 atm); 3, 2.63×10^3 Pa (0.0263 atm); 4, 1.12×10^3 Pa (0.0112 atm); 5, 0.66×10^3 Pa (0.0066 atm); 6, 0.33×10^3 Pa (0.0033 atm); 7, 0.131×10^3 Pa (0.00131 atm); 8, volatility of WO_3 in vacuum.

Evidently, at a time t_0 when the mass of a solid specimen again becomes equal to its initial value, the condition $x_{max} = x_{evap}$ is satisfied (see Fig. 6.26). Since $x_{evap} = bt$, equation (6.26) yields

$$t_0 = \frac{k_1(k_0 - b)}{k_0 b^2} \quad . \tag{6.37}$$

At $t > t_0$, the process of interaction between initial substances A and B actually consists only in the transport of substance A, combined into the A_pB_q compound, into the gaseous phase. The amount of component B in the solid and gaseous phases remains constant. If the state (free or combined) in which substance A is present in the gaseous phase is neglected, the final result is seen to be such, as if A simply evaporates at a constant rate.

If at a given temperature and pressure $k_0 < b$ (or more generally $k_{0B1} + k_{0A2} < b$, see equations (6.22) and (6.23)), the A_pB_q compound is not formed as a solid layer between substances A and B. In this case, the rate of evaporation of the A_pB_q layer exceeds the rate of its formation at the A–B interface. Therefore, the reaction product is entirely removed away

from the solid surface into the gaseous phase. In the case under consideration, the rate of evaporation is limited by the rate of interfacial chemical interaction. Its value is clearly less than the evaporation rate b of a specimen prepared from the same A_pB_q compound.

It is necessary to differentiate between the two cases just considered, namely, when $k_0 > b$ and when $k_0 < b$. In the former case, the A_pB_q layer of constant thickness is present at the A–B interface, whereas in the latter the surface of substance A remains bare during the whole course of the reaction.

It is worth noting that in the case of formation of volatile chemical compounds the effect of temperature on the layer growth are often established by comparing the rate constants obtained from kinetic dependences at a constant observation time. Obviously, the results would be dependent upon whether measurements are made on ascending or descending portions of those dependences.

From curve 3 in Fig. 5.34, it must be clear that if measurements are carried out on its ascending portion, then the treatment of the experimental data using the Arrhenius relation yields positive values of the activation energy, though different at varying observation times. By contrast, if measurements are carried out on its descending portion, negative values of the activation energy will be obtained. It only means that the growth rate of the solid A_pB_q layer between the A and B phases increases with raising temperature at a lower rate than its evaporation rate.

The activation energy thus found reflects the overall effect of temperature on a few parameters characterising the process of interaction of those phases (see equation (6.19)). Not only is the temperature dependence of each of them characterised by its own activation energy, but it may happen to be quite different from temperature dependences of other parameters. Whether these were calculated from the ascending or descending portion of any experimental kinetic relationship, both sets of activation energies prove, therefore, to be of little practical value.

It seems to be much more relevant to establish the temperature dependence of each parameter (chemical and diffusional constants, the evaporation-rate constant, *etc*.) separately. The availability of such data would make it possible to adequately describe the process of growth of a chemical compound layer under conditions of its simultaneous evaporation.

It is important to mention another essential circumstance. The duration of experiments in solid-gas systems is usually long. Therefore, it is just these experiments in which the appearance of departure points on thermogravimetric curves, caused by the transition from the reaction to diffusion controlled regime of growth of chemical compound layers (see Chapter 3), might be revealed. This concerns the case where there are no noticeable changes in the system under investigation (the number of the layers, their phase identity, chemical composition and structure remain unchanged), and nevertheless the dependence of the total mass of solid substances upon time gradually changes, displaying noticeable deviation points.

The occurrence of two such points may be expected, if two compound layers grow simultaneously. If there are three or more compound layers, the kinetic dependence should in addition change considerably when some of those layers disappear after the others have reached their critical thickness with regard to components *A* and *B* (see Chapter 4). To avoid misleading conclusions, these peculiarities of multiple-layer formation must be taken into account in interpreting the experimental data on solid-gas interactions.

6.6.3: Partial oxidation of chemical compounds

If the initial solid substance is a chemical compound (an intermetallic, a silicide, *etc*.), then its oxidation can proceed via two different mechanisms, depending upon experimental conditions. Two oxides are formed in the severe oxidation (combustion) usually resulting in the disintegration of the initially compact solid phase. In the partial (soft) oxidation, the chemical compound undergoes a partial decomposition producing another chemical compound of the same class and an oxide.

Therefore, two solid layers occur at the interface between initial substances. One of these is an oxide layer, while the other is the layer of a chemical compound of the same *A*–*B* multiphase binary system, enriched in the non-oxidising element. In the course of partial oxidation, both layers remain more or less compact and adherent to the surface of an initial solid phase.

Consider the process of oxidation of Zr_2Al_3 as a typical example. The $ZrAl_2$ and ZrO_2 layers occur during its oxidation [159]. The overall chemical reaction of their formation is

$$2Zr_2Al_3 + O_2 = 3ZrAl_2 + ZrO_2. \qquad (6.38)$$

However, this equation provides no information about a real mechanism of layer growth. Indeed, reaction (6.38) cannot proceed any more immediately after the occurrence of the $ZrAl_2$ and ZrO_2 layers of appreciable thickness because these separate the reactants Zr_2Al_3 and oxygen from each other. Instead, partial chemical reactions will subsequently take place at appropriate interfaces [160].

Two molecules of Zr_2Al_3 decompose at interface 1 (Fig. 6.29) in accordance with the reaction

$$2Zr_2Al_3 = 3ZrAl_2 + Zr_{dif}, \qquad (6.39)$$

yielding three molecules of $ZrAl_2$ and releasing one zirconium atom. This released zirconium atom diffuses across the $ZrAl_2$ layer and then reacts at interface 2 with the oxygen atoms (or ions) to form more ZrO_2:

$$Zr_{dif} + 2O_{dif} = ZrO_2. \qquad (6.40)$$

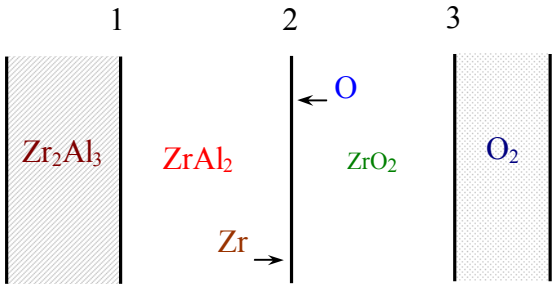

Fig. 6.29. Schematic diagram to illustrate the process of partial oxidation of the Zr_2Al_3 intermetallic compound.

An oxygen vacancy occurred at interface 2 moves on native sites of the ZrO_2 lattice to interface 3 where it is filled with an oxygen atom from the oxygen phase. Zirconium atoms are transported by the same mechanism through the $ZrAl_2$ layer. Continuous repeating of the elementary reaction-diffusion acts just described results in the growth of both compound layers.

Note that reaction (6.39) represents the phase transformation of Zr_2Al_3 into $ZrAl_2$ under the influence of reaction diffusion of the zirconium atoms from interface 1 to interface 2. It can proceed at any temperature whenever this reaction-diffusion process takes place.

The proposed mechanism of growth of the $ZrAl_2$ and ZrO_2 layers appears to be more likely than an alternative one [159] involving the simultaneous diffusion of oxygen and aluminium atoms. Indeed, the self-diffusion coefficient of oxygen in ZrO_2 is higher than that of zirconium [161]. Therefore, the diffusion coefficient of aluminium in this phase can hardly be expected to be sufficiently high to ensure a considerable flux of the aluminium atoms across its bulk. Probably, the same applies to the transport of oxygen atoms in the $ZrAl_2$ lattice.

For these reasons, the growth mechanism of the $ZrAl_2$ and ZrO_2 layers, involving diffusion of foreign atoms across their bulks, seems to be much less likely. Of course, there are also other conceivable mechanisms. To decide which one of those is operative, marker experiments, though not so easy to carry out with such brittle phases, are strongly desired.

As the Zr–Al–O system is ternary, the $ZrAl_2$ phase can form either a continuous coherent layer between Zr_2Al_3 and ZrO_2 or separate grains in the Zr_2Al_3 matrix near the Zr_2Al_3–ZrO_2 interface. Anyway, after successive oxidation of the same Zr_2Al_3 specimen the newly formed portions of the $ZrAl_2$ and ZrO_2 layers are likely to be revealed by metallographic examination ($ZrAl_2$ at interface 1 and ZrO_2 at interface 2).

Note that the chemical reactions similar to (6.38)-(6.40) take place in sintering of powder mixtures consisting of an intermetallic compound and an elementary substance [162, 163]. For example, I.F. Martynova *et al*. [163] found the Fe_2Ti and $TiNi_3$ layers to grow at the interface between FeTi and nickel (Fig. 6.30a).

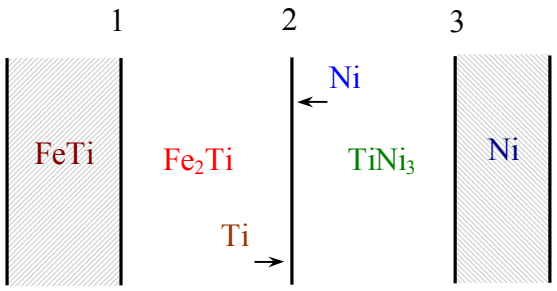

(a)

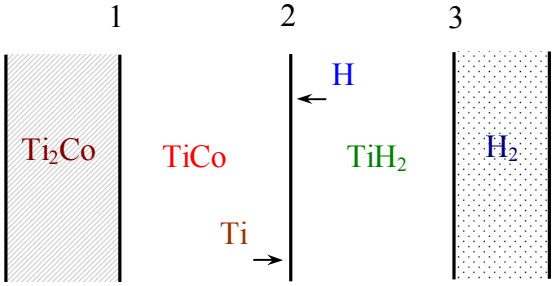

(b)

Fig. 6.30. Schematic diagrams to illustrate the process of formation of (a) the Fe_2Ti and $TiNi_3$ layers at the interface of FeTi with nickel and (b) the TiCo and TiH_2 layers at the interface of Ti_2Co with hydrogen.

The mechanism of their formation probably includes the decomposition of FeTi at interface 1

$$2FeTi = Fe_2Ti + Ti_{dif} \qquad (6.41)$$

and the subsequent reaction of the released titanium atoms (after their diffusion across the Fe_2Ti layer to interface 2) with the nickel atoms diffusing across the $TiNi_3$ layer

$$Ti_{dif} + 3Ni_{dif} = TiNi_3. \quad (6.42)$$

When investigating the process of destructive hydrogenation of Ti–*X* (*X* = Co, Cu and Ni) intermetallics, V.V. Skorokhod *et al*. [164, 165], T.I. Bratanich *et al*. [166-168] and O.V. Kucheriavyi *et al*. [169, 170] found that all the phases available on an appropriate binary phase diagram Ti–*X* are formed sequentially. The mechanism of their formation appears to be analogous to that of the Fe_2Ti and $TiNi_3$ layers occurring between FeTi and nickel. For example, formation of the TiCo and TiH_2 layers at the interface of Ti_2Co and hydrogen is due to partial chemical reactions (Fig. 6.30b)

$$Ti_2Co = TiCo + Ti_{dif} \quad (6.43)$$

and

$$Ti_{dif} + 2H_{dif} = TiH_2, \quad (6.44)$$

taking place at interfaces 1 and 2, respectively.

After the initial Ti_2Co phase is entirely consumed, further interaction of TiCo with hydrogen yields the layers of $TiCo_2$ and TiH_2 according to reactions

$$2TiCo = TiCo_2 + Ti_{dif} \quad (6.45)$$

and

$$Ti_{dif} + 2H_{dif} = TiH_2. \quad (6.46)$$

Thus, the sequence of formation of the Ti–Co intermetallic compounds (including the initial Ti_2Co one) is $Ti_2Co \rightarrow TiCo \rightarrow TiCo_2$, with only two layers (an intermetallic and TiH_2) occurring simultaneously in each intermetallic-hydrogen reaction couple. Similar sequences are observed in hydrogenising of Ti_2Cu and Ti_2Ni.

It is worth noting that the course of the process of partial oxidation is strongly dependent upon whether an initial chemical compound is taken alone or deposited on a substrate consisting of an oxidising element, as illustrated with the nickel silicide NiSi in Fig. 6.31. If alone, the NiSi compound is partially oxidised by oxygen, giving Ni_2Si and SiO_2 (see Fig. 6.31a).

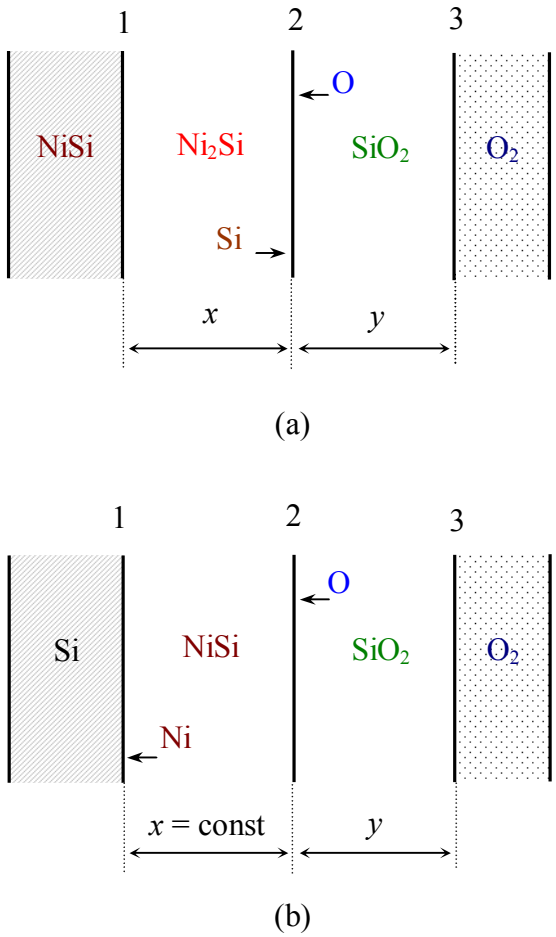

Fig. 6.31. Schematic diagram to illustrate the process of partial oxidation of the NiSi silicide. (a) free, (b) on a silicon substrate.

The reactions of their formation appear to be

$$2NiSi = Ni_2Si + Si_{dif} \qquad (6.47)$$

and

$$Si_{dif} + 2O_{dif} = SiO_2. \qquad (6.48)$$

These take place at interfaces 1 and 2, respectively. In this case, both compound layers grow simultaneously at the expense of the NiSi phase whose thickness steadily decreases with passing time.

By contrast, if a layer of the NiSi compound is deposited on a silicon substrate, then its thickness does not change at all during oxidation, as established by F.M. d'Heurle [171]. It means that the following partial chemical reactions take place (see Fig. 6.31b):

$$NiSi + 2O_{dif} = SiO_2 + Ni_{dif} \quad (6.49)$$

and

$$Ni_{dif} + Si_{substrate} = NiSi. \quad (6.50)$$

The former reaction proceeds at interface 2, while the latter at interface 1 after the backward diffusion of the released nickel atoms. The number of NiSi molecules entering into reaction (6.49) is seen to be equal to that occurring as a result of reaction (6.50). Thus, the disappearance of a NiSi molecule at one of the NiSi interfaces is compensated by its formation at the other.

Therefore, the thickness of the NiSi layer remains unchanged, whereas that of the SiO_2 layer increases with passing time. The net reaction is actually the oxidation of silicon from the substrate to form SiO_2. The NiSi layer of constant thickness simply moves as a whole deeper into the substrate bulk, without the loss of its integrity. Similar behaviour is likely to be observed in the course of interaction of intermetallics with other gases.

This example shows once again how important it is to consider the entire system in question on the whole, not dividing it into a number of individual parts which are supposed to be in local equilibrium with each other, as is often assumed. The latter approach is in most cases like the step-by-step approach to an absurd final result, even though each of those steps may seem rather substantiated.

According to the studies of M.A. Nicolet [172] and F.M. d'Heurle *et al*. [173], oxidation of transition-metal silicides, like that of silicon, obeys a linear-parabolic relation. Note that if the diffusion of oxygen atoms across the SiO_2 layer is the rate-determining step, the parabolic regions of oxidation of silicon and silicides should be characterised by the same growth-rate constant.

If not, then either the experiments were carried out under considerably differing conditions or the structure of the SiO_2 layer was different with various silicides. On the contrary, the linear-rate constant must clearly depend upon the chemical composition of silicides, as indeed observed experimentally [172, 173].

6.7: Formation of a compound layer in solid-liquid and solid-gas reactions: short conclusions

1. If the chemical compound is formed under conditions of simultaneous dissolution in the liquid phase or evaporation into the gaseous phase, then its layer does not occur at the *A–B* interface until the rate of dissolution or evaporation becomes equal to the sum of the rates of

chemical transformations (chemical reactions as such) taking place at the layer interfaces with initial substances *A* and *B*.

2. If the rate of layer formation is limited by the rate of diffusion of the atoms of reacting substances across its bulk, it is impossible to prevent the occurrence of this layer between *A* and *B* by any reasonable increasing the dissolution or evaporation rate. What is only possible is a considerable reduction of its thickness.

3. If the chemical compound layer dissolves or evaporates under isothermal conditions at a constant rate, its thickness reaches with passing time a certain highest value and then remains almost unchanged. Subsequently, the layer of constant thickness moves as a whole into the bulk of phase *A* until this phase is consumed completely.

4. At a considerable solubility of solid *A* in liquid *B*, formal search for the so-called layer-growth laws by means of mathematical treatment of the experimental data using linear, parabolic, logarithmic or other dependences does not seem to be reasonable. Each of the "laws" thus obtained holds only under particular (in most cases, unspecified) dissolution conditions. It is therefore sufficient to slightly change those conditions, and the "law" will also change. The same applies to the case of formation of the layer of a volatile chemical compound.

5. At finite values of the surface area of a solid and the volume of a liquid, the dissolution rate of the solid in the liquid phase decreases with passing time from its highest value to zero (when the saturation concentration is reached). The greater the surface area of the solid and the less the volume of the liquid, the quicker the saturation of the liquid by the dissolving substance is attained. With increasing degree of saturation, the influence of dissolution on the growth kinetics of a chemical compound layer gradually weakens and hence the layer thickness-time dependence asymptotically approaches that which would be observed in the case of a saturated solution of *A* in *B*.

6. Partial (soft) oxidation of a chemical compound is likely to result in the formation of the layers of two other compounds, one of which is an oxide and another is the other chemical compound of a given binary system, enriched in a non-oxidising element.

References

1. E.A. Moelwyn-Hughes. *Physical chemistry*. 2nd ed.- Oxford: Pergamon Press, 1961.
2. G.M. Barrow. *Physical chemistry*. 2nd ed.- New York: McGraw-Hill, 1961.
3. *Kurs fizicheskoy khimii* / Edited by Ya.I. Gerasimov.- Moskwa: Khimiya, 1966.- V.2.
4. *Fizicheskaya khimiya* / Edited by K.S. Krasnov.- Moskwa: Vysshaya Shkola, 1982.
5. *Fizicheskaya khimiya/* Edited by B.P. Nikolskiy.- Leningrad: Khimiya, 1987.
6. K.J. Laidler. *Physical chemistry*. 4th ed.- Orlando: Houghton Mifflin Harcourt (HMH), 2003.
7. C.N. Hinshelwood. The *kinetics of chemical change in gaseous systems*.- 3rd ed.- Oxford: Clarendon Press, 1933.
8. N.N. Semenov. *Tsepnye reaktsii*. - Moskwa-Leningrad: Goskhimizdat, 1934.
9. E.A. Moelwyn-Hughes. *The kinetics of reactions in solution*.- Oxford: Clarendon Press, 1933.
10. N.M. Emanuel, D.G. Knorre. *Kurs khimicheskoy kinetiki*.- Moskwa: Vysshaya Shkola, 1969.
11. E.N. Eremin. *Osnovy khimicheskoy kinetiki*. 2e izd.- Moskwa: Vysshaya Shkola, 1976.
12. K.J. Laidler. *Chemical kinetics*. 3rd ed.- New Jersey: Prentice Hall, 1987.
13. M.J. Pilling, P.W. Seakins. *Reaction kinetics*.- Oxford: Oxford University Press, 1997.
14. J.E. House. *Principles of chemical kinetics*. – Amsterdam: Elsevier, 2007.
15. R.H. Parker. *An introduction to chemical metallurgy*. 2nd ed.- Oxford: Pergamon Press, 1978.
16. V.I. Dybkov. S*olid state reaction kinetics*.- Kyiv: IPMS Publications, 2013.
17. V.I. Arkharov. *Okisleniye metallov pri vysokikh temperaturakh*.- Sverdlovsk: Metallurgizdat, 1945.
18. U.R. Evans. *The corrosion and oxidation of metals: Scientific principles and practical applications*.- London: Edward Arnold, 1960.
19. B.Ya. Pines. *Ocherki po metallofizike*.- Khar'kov: Izd-vo Khar'kovskogo Universiteta, 1961.
20. V.Z. Bugakov. *Diffuziya v metallakh i splavakh*. - Leningrad-Moskwa: Gostekhteoretizdat, 1949.
21. W. Seith. *Diffusion in Metallen*.- Berlin: Springer, 1955.
22. K. Hauffe. *Reaktionen in und an festen Stoffen*.- Berlin: Springer, 1955.
23. W. Jost. *Diffusion in solids, liquids, gases*.- New York: Academic Press, 1960.
24. Y. Adda, J. Philibert. *La diffusion dans les solides*.- Paris: Presses Universitaires, 1966. - V. I, II.

25. J.A. Hedvall. *Solid state chemistry*.- Amsterdam: Elsevier, 1966.
26. J.R. Manning. *Diffusion kinetics for atoms in crystals*.- Princeton-Toronto: D. Van Nostrand, 1968.
27. P.Kofstad. *High-temperature oxidation of metals*.- New York: Wiley, 1968.
28. P. Kofstad. *Nonstoichiometry, diffusion and electrical conductivity in binary metal oxides*.- New York: Wiley-Interscience, 1972.
29. N.A. Kolobov, M.M. Samokhvalov. *Diffuziya i okisleniye poluprovodnikov*.- Moskwa: Metallurgiya, 1975.
30. B.S. Bokstein. *Diffuziya v metallakh*.- Moskwa: Metallurgiya, 1978.
32. S. Mroveć. *Defects and diffusion in solids*.- Amsterdam: Elsevier, 1980.
33. H. Schmalzried. *Chemical kinetics of solids*.- Weinheim: Verlag Chemie, 1995.
34. H. Mehrer. *Diffusion in solids*: *Fundamentals*, *methods*, *materials*, *diffusion-controlled processes*. 2nd ed.- Berlin-Heidelberg: Springer, 2010.
35. A.M. Gusak, T.V. Zaporozhets, Yu. O. Lyashenko, S.V. Kornienko, M.O. Pasichnyy, A.S. Shirinyan. *Diffusion-controlled solid state reactions*: *In alloys, thin films, and nanosystems*.- Veinheim: Wiley-VCH, 2010.
36. D. Gupta. *Diffusion processes in advanced technological materials*.- Norwich: William Andrew, 2011.
37. W. Sprengel, T. Horikoshi, H. Nakajima. Single-phase interdiffusion in intermetallic compound CoTi // Scripta Mater.- 1996.- V. 34, No. 3.- P. 449-453.
38. M. Salamon, S. Dorfman, D. Fuks, G. Inden, H. Mehrer. Interdiffusion and diffusion of Al in iron aluminides // Defect Diffusion Forum.- 2001.- V. 194-199.- P. 353-358.
39. Y. Nose, H. Numakura, M. Koiwa, T. Ikeda, H. Nakajima. Tracer and chemical diffusion in Pt_3Fe // Defect Diffusion Forum.- 2001.- V. 194-199.- P. 559-364.
40. A.D. Smigelskas, E.O. Kirkendall. Zinc diffusion in alpha brass // Trans. AIME.- 1947.- V. 171.- P. 130-142.
41. H. Nakajima. The discovery and acceptance of the Kirkendall effect: The result of a short research career // J. Metals (JOM).- 1997.- V. 49, No. 6.- P. 15-19.
42. L.S. Darken. Diffusion, mobility and their interrelation through free energy in binary metallic systems // Trans. AIME. – 1948.- V. 175.- P. 184-201.
43. A.G. Guy. *Introduction to materials science*.- New York: McGraw-Hill, 1971.
44. N.B. Hannay. *Solid-state chemistry*.- New Jersey: Prentice-hall, 1969.
45. *Non-stoichiometric compounds* / Edited by L. Mandelcorn.- New York: Academic Press, 1964.
46. S.V. Divinski, St. Frank, U. Södervall, Chr. Herzig. Tracer measurements of Ni selfdiffusion and atomistic calculations of diffusion mechanisms in NiAl // Defect and Diffusion Forum.- 2001.- V. 194-199.- P. 487-492.
47. I. Stloukal, J. Čermak. Diffusion of zinc in two-phase Mg-Al alloy // Defect and Diffusion Forum.- 2007.- V. 263.- P. 189-194.

48. C. Wagner. The evaluation of data obtained with diffusion couples of binary single-phase and multiphase systems // Acta Metall.- 1969.- V. 17, No. 2.- P. 99-107.
49. T.Y. Tan, U. Gösele. Diffusion mechanisms and superlattice disordering in GaAs // Mater. Sci. Eng.: B.- 1988.- V. 1, No. 1.- P. 47-65.
50. I. Harrison. Impurity-induced disordering in III-V multi-quantum wells and superlattices // J. Mater. Sci.: Mater. Electron.- 1993.- V. 4, No. 1.- P. 1-28.
51. B. Schröder, V. Leute. Solid state reactions and transport properties in the quasi-binary system AgJ/RbJ // J. Phys. Chem. Solids.- 1980.- V. 41, No. 8.- P. 827-835.
52. E.A. Vasil'kovskaya, V.V. Gorskiy. Kinetika rosta promezhutochnykh faz v sisteme RbI-AgI // Izv. Akad. Nauk SSSR. Neorgan. Mater.- 1980.- V. 16, No. 7.- P. 1210-1212.
53. V.N. Chebotin, E.A. Vasil'kovskaya. Opredeleniye individual'nykh koeffitsientov diffuzii ionov Rb^+ i I^- v polikristallicheskom $RbAg_4I_5$ // Elektrokhim.- 1981.- V. 17, No. 12.- P. 1910-1912.
54. V.I. Smirnov. *Kurs vysshey matematiki*.- Moskwa: Nauka, 1967.- V.2.
55. L.S. Pontryagin. *Obyknovennye differentsial'nye uravneniya*.- Moskwa: Nauka, 1982.
56. U. Gösele, K.N. Tu. Growth kinetics of planar binary diffusion couples: "Thin film case" versus "Bulk cases" // J. Appl. Phys.- 1982.- V. 53, No. 1.- P. 3252-3260.
57. U. Gösele. Thin-film compound formation: Kinetics and effects of volume changes / In: *Alloying* (Eds. J.L. Walter, M.R. Jackson, Ch.T. Sims). - Metals Park (Ohio): ASM International, 1988.- P. 489-519.
58. B. Blanpain, J.W. Mayer, J.C. Liu, K.N. Tu. Kinetic description of the transition from a one-phase to a two-phase growth regime in Al/Pd lateral diffusion couples // J. Appl. Phys.- 1990.- V. 68, No. 7.- P. 3259-3267.
59. G. Ottaviani, M. Costato. Compound formation in metal-semiconductor interactions // J. Crystal Growth.- 1978.- V. 45.- P. 365-375.
60. K.N. Tu, G. Ottaviani, R.D. Thompson, J.W. Mayer. Thermal stability and growth kinetics of Co_2Si and CoSi in thin-film reactions // J. Appl. Phys.- 1982.- V. 53, No. 6.- P. 4406-4410.
61. M. Hansen. *Constitution of binary alloys*. 2nd ed.- New York: McGraw-Hill, 1958.
62. A.E. Vol. *Stroeniye i svoistva dvoynikh metallicheskikh sistem*.- Moskwa: Fizmatgiz, 1959.- V.1, 1962.- V.2.
63. L.F. Mondolfo. *Aluminium alloys: Structure and properties*.- London: Butterworths, 1976.
64. E.M. Tanguep Njiokep, M. Salomon, H. Mehrer. Growth of intermetallic phases in the Al-Mg system // Defect Diffusion Forum.- 2001.- V. 194-199.- P. 1581-1586.
65. N.N. Matyushenko. *Kristallicheskie struktury dvoynykh soedineniy*.- Moskwa: Metallurgiya, 1969.
66. V.I. Perel'man. *Kratkiy spravochnik khimika*.- Moskwa-Leningrad: Khimiya, 1964.
67. V.A. Rabinovich, Z.Ya. Khavin. *Kratkiy khimicheskiy spravochnik*.- Leningrad: Khimiya, 1991.

68. R.P. Elliott. *Constitution of binary alloys: First supplement*.- New York: McGraw-Hill, 1965.
69. F.A. Shunk. *Constitution of binary alloys: Second supplement*.- New York: McGraw-Hill, 1969.
70. A.E. Vol, I.K. Kagan. *Stroeniye i svoystva dvoynykh metallicheskikh sistem*.- Moskwa: Nauka, 1976.- V.3, 4.
71. *Binary alloy phase diagrams* / Edited by T.B. Massalski, H. Okamoto, P.R. Subramanian and L. Kacprzak.- ASM international, Ohio: 1990.- V.1-3.
72. *Diagrammy sostoyaniya dvoynikh metallicheskikh sistem* / Edited by N.P. Lyakishev. - Moskwa: Mashinostroenie, 1996.- V.1; 1997.- V.2; 1999.- V.3, Part 1; 2000.- V.3, Part 2.
73. E.G. Colgan. A review of thin-film aluminide formation // Mater. Sci. Reports.- 1990.- V. 5, No. 1.- P. 3-44.
74. Yu.E. Ugaste, P.A. Kyarsna. Kinetika formirovaniya diffusionnoy zony pri vzaimodeystvii medi s kadmiem // Fiz. Khim. Obrab. Mater.- 1996.- No. 6.- P. 88-91.
75. R. Pretorius. Prediction of silicide formation and stability using heats of formation // Thin Solid Films.- 1996.- V. 290-291.- P. 477-484.
76. V.I. Zmiy, A.S. Seryugina. Issledovaniye diffuzii v sisteme Mo-Si // Izv. Akad. Nauk SSSR. Neorgan. Mater.- 1971.- V. 7, No. 10.- P. 1730-1734.
77. P.C. Tortorici, M.A. Dayananda. Growth of silicides and interdiffusion in the Mo-Si system // Metall. Mater. Trans.: A.- 1999.- V. 30, No. 3.- P. 545-550.
78. V.V. Bogdanov, A.M. Gusak, L.N. Paritskaya, M.V. Yarmolenko. Osobennosti diffuzionnogo rosta faz v obraztsakh tsilindricheskoy formy // Metallofiz.- 1990.- V. 12, No. 3.- P. 60-66.
79. M.V.Yarmolenko, A.M.Gusak, F.A.Kotenev, I.F.Ladikova-Roeva. Osobennosti fazoobrazovaniya pri bystrom nagreve // Fiz. Khim. Obrab. Mater.- 1991.- No. 4.- P. 122-126.
80. T.C. Chou, L. Link. Solid-state interdiffusion in Ni-Mo diffusion couples at high temperatures // Scripta Mater.- 1996.- V. 34, No. 5.- P. 831-838.
81. E.K. Ohriner, E.P. George. Growth of intermetallic layers in the iridium-molybdenum system // J. Alloys Comp.- 1991.- V. 177, No. 2.- P. 219-227.
82. F.M. d'Heurle, P. Gas. Kinetics of formation of silicides: A review // J. Mater. Res.- 1986.- V. 1, No. 1.- P. 205-211.
83. *Thin films - Interdiffusion and reactions* / Edited by J.M. Poate, K.N. Tu and J.W. Mayer.- New York: Wiley, 1978.
84. S.P. Murarka. *Silicides for VLSI applications*.- New York: Academic Press, 1983.
85. I.I. Kornilov, V.V. Glazova. *Vzaimodeistviye tugoplavkikh metallov perekhodnykh grupp s kislorodom*.- Moskwa: Nauka, 1967.
86. *Oxydation des metaux* / Edited by J. Benard.- Paris: Gauthier-Villars, 1962.- V.I; 1964.- V.II.

87. R.F. Voitovich, E.I. Golovko. *Vysokotemperaturnoye okislenie metallov i splavov*.- Kiev: Naukova Dumka, 1980.
88. G. Hillmann, W. Hofmann. Diffusionmessungen im System Kupfer-Zirkonium // Z. Metallkunde.- 1965.- V. 56, No. 5.- P. 279-286.
89. K. Bhanumurthy, G.B. Kale, S.K. Khera. Diffusion reaction in the zirconium-copper system // Metall. Trans.: A.- 1992.- V. 23, No. 4.- P. 1373-1375.
90. O. Taguchi, Y. Iijima, K. Hirano. Reaction diffusion in the Cu-Ti system // J. Japan Inst. Metals - 1990.- V. 54, No. 6.- P. 619-627.
91. S.L. Markovski, M.C.L.P. Pleumeekers, A.A. Kodentsov, F.J.J. van Loo. Phase relations in the Pt-Ga-Sb system at 500°C // J. Alloys Comp.- 1998.- V. 268.- P. 188-192.
92. K.P.Gurov, B.A.Kartashkin, Yu.E.Ugaste. *Vzaimnaya diffuziya v mnogofaznykh metallicheskikh sistemakh*.- Moskwa: Nauka, 1981.
93. F.M. d'Heurle. Nucleation of a new phase from the interaction of two adjacent phases: Some silicides // J. Mater. Res.- 1988.- V. 3, No. 1.- P. 167-195.
94. *Chemistry of the solid state /* Edited by W.E. Garner. - London: Butterworths, 1955.
95. F.J.J. van Loo. Diffusion in the titanium-aluminium system. - Thesis, Eindhoven University of Technology, 1971.
96. S. Wöhlert, R. Bormann. Phase selection governed by different growth velocities in the early stages of the Ti/Al phase reaction // J. Appl. Phys.- 1999.- V. 85, No. 2.- P. 825-832.
97. R.J. Tarento, G. Blaise. Studies of the first steps of thin film interdiffusion in the Al-Ni system // Acta Metall.- 1989.- V. 37, No. 9.- P. 2305-2312.
98. S.L. Markovski, M.J.H. van Dal, M.J.L. Verbeek, A.A. Kodentsov, F.J.J. van Loo. Microstructology of solid-state reactions // J. Phase Equil.- 1999.-V. 20, No. 4.- P. 373-388.
99. K. Ishida, T. Nishizawa, M.E. Schlesinger. The Co-Si (cobalt-silicon) system // J. Phase Equil.- 1991.- V. 12, No. 5.- P. 578-586.
100. G.J. van Gurp, C. Langereis. Cobalt silicides layers on Si.1. Structure and growth // J. Appl. Phys.- 1975.- V. 46, No. 10.- P. 4301-4307.
101. S.S. Lau, J.W. Mayer, K.N. Tu. Interactions in the Co/Si thin-film system: 1. Kinetics // J. Appl. Phys.- 1978.- V. 49, No. 7.- P. 4005-4010.
102. S.L. Markovski, M.C.L.P. Pleumeekers, A.A. Kodentsov, F.J.J. van Loo. Phase relations in the Pt-Ga-Sb system at 500°C // J. Alloys Comp.- 1998.- V. 268.- P. 188-192.
103. T.G. Finstad. A Xe marker study of the transformation of Ni_2Si to NiSi in thin films // Phys. Status Solidi: (a).- 1983.- V. 63, No. 1.- P. 223-228.
104. F.M. d'Heurle, C.S. Petersson, J.E.E. Baglin, S.J. La Placa, C.Y. Wong. Formation of thin films of NiSi: Metastable structure, diffusion mechanisms in intermetallic compounds // J. Appl. Phys.-1984.- V. 55, No. 12.- P. 4208-4218.
105. M.R. Jackson, R.L. Mehan, A.M. Davis, E.L. Hall. Solid state SiC/Ni alloy reaction // Metall. Trans.: A.- 1983.- V. 14, No. 3.- P. 355-364.
106. J.H. Gülpen, A.A. Kodentsov, F.J.J. van Loo. The growth of silicide in Ni-Si and Ni-SiC diffusion couples.- Mater.Sci.Forum.- 1994.- V.155-156.- P.651-564.

107. J.S. Chen, E. Kolawa, M.-A. Nicolet, R.P. Ruiz, L. Baud, C. Jaussaud, R. Madar. Reaction of Ta thin film with single crystalline (001) ß-SiC // J.Appl.Phys.- 1994.- V.76, No.4.- P.2169-2175.
108. L. Baud, C. Jaussaud, R. Madar, C. Bernard, J.S. Chen, M.-A. Nicolet. Interfacial reactions of W thin film on single-crystal (001) ß-SiC // Mater. Sci. Eng.: B.- 1995.- V.29.- P.126-130.
109. J. Brandstötter, W. Lengauer. Multiphase reaction diffusion in transition metal-boron systems // J. Alloys Comp.- 1997.- V. 262-263.- P. 390-396.
110. W.J. Tomlinson, A.Easterlow. Kinetics and microstructure of oxidation of CoO to Co_3O_4 at 700-800^oC // J. Phys. Chem.Solids.- 1985.- V. 46, No. 1.- P. 151-153.
111. J.A. van Beek, S.A. Stolk, F.J.J. van Loo. Multiphase diffusion in the systems Fe-Sn and Ni-Sn // Z. Metallkunde.- 1982.- V. 73, No. 7.- P. 439-444.
112. W.L. Neijmeijer, B.H. Kolster. Microstructure and kinetics of the formation of Nb_3Sn from reaction between Nb_6Sn_5 and Nb // Z. Metallkunde.- 1990.- V. 81, No. 5.- P. 314-321.
113. D.W. Susnitzky, S.R. Summerfelt, C.B. Carter. Reaction couples of ceramic thin films prepared by CVD // Ultramicroscopy.- 1989.- V. 30, No. 1-2.- P. 249-255.
114. A. Shchukarev. Raspredeleniye veshchestv mezhdu dvumya nesmeshivayush-chimisya rastvoritelyami // Zhurn. Russk. Fiz.-Khim. Obshchestva.- 1896.- V. 28, No. 6.- P. 604-614.
115. W. Nernst. Theorie der Reaktiongeschwindigkeit in heterogenen Systemen // Z. physik. Chemie.- 1904.- V. 47, No. 1.- P. 52-55.
116. V.G. Levich. *Fiziko-khimicheskaya gidrodinamika*.- Moskwa: Fizmatgiz, 1959.
117. Yu.V. Pleskov, V.Yu. Filinovskiy. *Vrashchayushchiysya diskoviy elektrod*.- Moskwa: Nauka, 1972.
118. V.I. Nikitin. *Fiziko-khimicheskiye yavleniya pri vozdeystvii zhidkikh metallov na tverdiye*. - Moskwa: Atomizdat, 1967.
119. L.L. Bircumshaw, A.C. Riddiford. Transport control in heterogeneous reactions // Quarterly Reviews (London).- 1952.- V. 6.- P. 157-185.
120. *Fizicheskaya khimiya neorganicheskikh materialov* / Edited by V.N. Yeremenko.- Kiev: Naukova Dumka, 1988.- V.3.
121. T.F. Kassner. Rate of solution of rotating Ta disks in liquid tin // J. Electrochem. Soc.- 1967.- V. 114, No. 7.- P. 689-694.
122. V.I. Dybkov. *Vzaimodeystviye nekotorykh perekhodnykh metallov V, VI, VIII grupp s zhidkim alyuminiem*.- Dissert. kand. khim.nauk, Kievskiy universitet, 1974.
123. H.B. Dwight. *Tables of integrals and other mathematical data*.- New York: Macmillan, 1961.
124. N.S. Piskunov. *Differentsial'noye i integral'noye ischisleniya*.- Moskwa: Nauka, 1965.- V.2.
125. V.R. Ryabov. *Svarka plavleniem alyuminiya so stal'yu*.- Kiev: Naukova Dumka, 1969.
126. S.V. Lashko, N.F. Lashko. *Payka metallov*.- Moskwa: Mashinostroeniye, 1988.

127. E. Kamke. *Differential Gleichungen, Lösungsmethoden und Lösungen*: 1. *Gewöhnlich Differential Gleichungen*.- Leipzig: Springer, 1959.
128. A.K. Marishkin. K raschetu skorosti rastvoreniya intermetallida Fe_2Al_5 pri modelirovanii processa svarki plavleniem // Avtomat. Svarka.- 1974.- No. 12.- P. 61.
129. V.I. Zhalybin, Yu.G. Volovich, G.D. Danchenko, B.P. Vishnevskiy, A.P. Baranov. Kinetika rastvoreniya titana v nerzhaveyushchey stali // Izv. Akad. Nauk SSSR: Metally.- 1979.- No. 6.- P. 89-92.
130. T. Heumann, S. Dittrich. Űber die Kinetik der Reaktion von festem und flüssigem Aluminium mit Eisen // Z. Metallkunde.- 1959.- V. 50, No. 10.- P. 617-625.
131. V.N. Yeremenko, Ya.V. Natanzon, V.I. Dybkov. The effect of dissolution on the growth of the Fe_2Al_5 interlayer in the solid iron-liquid aluminium system // J. Mater. Sci.- 1981.- V. 16, No. 7.- P. 1748-1756.
132. V.N. Yeremenko, Ya.V. Natanzon, V.P. Titov. Kinetika rastvoreniya i koeffitsienty diffuzii zheleza, kobalta i nikelya v zhidkom alyuminii // Fiz.-Khim. Mekhan. Mater.- 1978.- No. 6.- P. 3-10.
133. *Ternary alloys*: *A comprehensive compendium of evaluated constitutional data and phase diagrams* / Edited by G. Petzow and G. Effenberg.- Weinheim: VCH, 1991.- V.5.
134. V.I. Dybkov. Fazoutvorennya na mezhi rozdilu zalizonikeleviy splav–aluminiy // Poroshk. Metallurg.- 1999.- No. 11-12.- P. 67-74.
135. V.I. Dybkov. Interaction of iron-nickel alloys with liquid aluminium: Part 2. Formation of intermetallics // J. Mater. Sci.- 2000.- V. 35, No. 7.- P. 1729-1736.
136. K. Barmak, V.I. Dybkov. Interaction of iron–chromium alloys containing 10 and 25 mass% chromium with liquid aluminium: Part I. Dissolution kinetics // J. Mater. Sci.- 2003.- V. 38, No. 7.- P. 3249-3255.
137. K. Barmak, V.I. Dybkov. Interaction of iron–chromium alloys containing 10 and 25 mass% chromium with liquid aluminium: Part II. Formation of intermetallic compounds // J. Mater. Sci.- 2004.- V. 39, No. 13.- P. 4219-4230.
138. F.J.J. van Loo. Multiphase diffusion in binary and ternary solid-state systems // Prog. Solid St. Chem.- 1990.- V. 20.- P. 47-99.
139. J.E. Morrel, Cheng Jin, A. Engström, J. Ågren. Three types of boundaries in multiphase diffusion couples // Scripta Mater.- 1996.- V. 34, No. 11.- P. 1661-1666.
140. *Lead-Free Electronic Solders* / Edited by K.N. Subramanian.- Berlin-Heidelberg: Springer, 2007.
141. K.N. Tu. *Solder joint technology*: *Materials, properties and reliability*.- Berlin-Heidelberg: Springer, 2010.
142. V.I. Dybkov, K. Barmak, W. Lengauer, P.Gas. Interfacial interaction of solid nickel with liquid bismuth and Bi-base alloys // J. Alloys Comp.- 2005.- V. 389, No. 1-2.- P. 61-74.
143. K. Barmak, D.C. Berry, V.R. Sidorko, A.V. Samelyuk, V.I. Dybkov. Interfacial interaction of nickel with liquid Pb-free Sn-Bi-In-Zn-Sb soldering alloys / Proceedings of

Materials Science and Technology Conference MS&T-2007: Processing and Product Manufacturing: Lead-Free Solders, 16-20 September 2007, Detroit, USA.- P. 525-535.
144. V.I. Dybkov. Effect of dissolution on the Ni_3Sn_4 growth kinetics at the interface of Ni and lLiquid Sn-base solders // Solid State Phenomena.- 2008.- V. 138.- P. 153-158.
145. V.I. Dybkov, V.G. Khoruzha, V.R. Sidorko, K.A. Meleshevich, A.V. Samelyuk, D.C. Berry, K. Barmak. Interfacial interaction of solid nickel with liquid Pb-free Sn–Bi–In–Zn–Sb soldering alloys // J. Alloys Comp.- 2008.- V. 460, No. 1-2.- P. 337-352.
146. K. Barmak, D.C. Berry, V.G. Khoruzha, V.R. Sidorko, K.A. Meleshevich, A.V. Samelyuk, V.I. Dybkov. Dissolution kinetics and diffusion of cobalt in Pb-free Sn-Bi-In-Zn-Sb soldering alloys / Proceedings of Materials Science and Technology Conference MS&T-2008: Pb-Free, Pb-Bearing Joining and Packaging Materials and Processes for Microelectronics, October 5-9, 2008, Pittsburgh, PA, USA.- P. 262-273.
147. V.I. Dybkov. The growth kinetics of intermetallic layers at the interface of a solid metal and a liquid solder // J. Metals (JOM). - 2009.- V. 61, No. 1.- P. 76-79.
148. G.A. Pribytkov, V.I. Itin. Kinetika rastvoreniya nikelya i stannidov nikelya v zhidkom olove // Izv. Vuzov: Fizika.- 1975.- No. 9.- P. 100-105.
149. V.I. Dybkov, O.V. Duchenko. Growth kinetics of compound layers at the nickel-bismuth interface // J. Alloys Compounds.- 1996.- V. 234, No. 2.- P. 295-300.
150. V.P. Glagoleva, G.S. Zhdanov. Struktura sverkhprovodnikov: Rentgeno-graficheskoe opredelenie struktury Bi_3Ni // Zhurn. Eksp. Teoret. Fiz.- 1954.- V. 26, No. 3.- P. 337-344.
151. Chao-hong Wang, Sinn-wen Chen. Cruciform pattern formation in Sn/Co couples // J. Mater. Res.- 2007.- V. 22.- P. 3404-3409.
152. E.E. Havinga, H. Damsma, P. Hokkeling. Compounds and Pseudo-Binary Alloys with the $CuAl_2$(C16)- Type Structure: I. Preparation and X-Ray Results // J. Less-Common Metals.- 1972.- V. 27.- P. 169-186.
153. B.S. Lee, R.A. Rapp. Gaseous sulfidation of pure molybdenum at 700-950 ºC // J. Electrochem. Soc.-1984.- V. 131, No. 12.- P. 2998-3006.
154. I.N. Frantsevich, R.F. Voitovich, V.A. Lavrenko. *Vysokotemperaturnoye okisleniye metallov i splavov*.- Kiev: Gostekhizdat UkrSSR, 1963.
155. R.F.Voitovich. *Okislenie karbidov i nitridov*.- Kiev: Naukova Dumka, 1981.
156. V.A. Lavrenko, V.L. Tikush. *Khimicheskoye vzaimodeystviye materialov s razrezhennymi atomarnymi i molekulyarnymi gazami*.- Kiev: Naukova Dumka, 1992.
157. E.A. Gulbransen, K.F. Andrew. Kinetics of the oxidation of pure tungsten from 500ºC to 1300ºC // J. Electrochem. Soc.- 1960.- V. 107, No. 7.- P. 619-628.
158. V.I. Spitsin, K.G. Bukov, A.M. Emelyanenko, L.N. Fedotov, T.K. Titova. Vysokotemperaturnoye okisleniye metallicheskogo tekhnetsiya // Zhurn. Neorg. Khimii.- 1988.- V. 33, No. 10.- P. 2449-2452.
159. M. Paljevič. Selective oxidation of Zr_2Al_3 // J. Alloys Compounds.- 1993.- V. 191, No. 1.- P. 27-29.

160. V.I. Dybkov. Comment on the paper "Selective oxidation of Zr_2Al_3" by M. Paljevič // J. Alloys Comp.- 1994.- V. 215, No. 1-2.- P. L1.
161. R.F. Voitovich. *Okislenie tsirkoniya i ego splavov*.- Kiev: Naukova Dumka, 1989.
162. V.V. Skorokhod, Yu.M. Solonin, I.V. Uvarova. *Khimicheskiye, diffuzionnye i reologicheskiye processy v tehnologii poroshkovykh materialov*.- Kiev: Naukova Dumka, 1990.
163. I.F. Martynova, S.M. Solonin, V.V. Skorokhod, T.I. Bratanich. Rentgenograficheskoye izucheniye vzaimodeystviya mezhdu intermetallidom i svyazkoy pri spekanii kompozita TiFe-Ni // Poroshk. Metallurg.- 1990.- No. 10.- P. 92-95.
164. V.V. Skorokhod, T.I. Bratanich, O.V. Kucheriavyi, L.I. Kopylova, M.V. Karpets, N.A. Krapivka. Osobennosti reaktsii vzaimodeystviya intermelallida Ti_2Cu s vodorodom / Abstr. V Intern. Conf. „Materials and coatings under extreme conditions".- Zhukovka, Crimea, Ukraine, 2008.- P. 120.
165. V.V. Skorokhod, T.I. Bratanich, O.V. Kucheriavyi. Processy mekhanicheskoy i khimicheskoy destruktsii pri vzaimodeystvii hidridoobrazuyushchikh intermetallidov s vodorodom / Abstr. VI Intern. Conf. „Materials and coatings under extreme conditions".- Ponizovka, Crimea, Ukraine, 2010.- P. 52.
166. T.I. Bratanich, V.V. Skorokhod, O.V. Kucheriavyi, L.I. Kopylova, M.O. Krapivka. Osoblyvosti vzaemodii intermetalidiv Ti_2Ni ta TiNi z vodnem ta syntez nanostrukturnykh compozytiv na ikh osnovi. I: Fazovi peretvorennya Ti_2Ni v protsesakh hidruvanyya // Struct. Materialoved.- 2010.- No. 1.- P. 25-29.
167. T.I. Bratanich, V.V. Skorokhod, O.V. Kucheriavyi, A.V. Kotko. Osoblyvosti vzaemodii intermetalidiv Ti_2Ni ta TiNi z vodnem ta syntez nanostrukturnykh compozytiv na ikh osnovi. II: Doslidzhennya shvydkosti DH Ti_2Ni ta TiNi i syntez nanostrukturnykh compozytiv na ikh osnovi // Struct. Materialoved.- 2010.- No. 2.- P. 44-50.
168. T.I. Bratanich, V.V. Skorokhod, O.V. Kucheriavyi, L.I. Kopylova, N.A. Krapivka. Phase transformations in Ti_2Cu during destructive hydrogenation // Intern. J. Hydrogen Energy.- 2011.- V. 36, No. 1.- P. 1312-1315.
169. O.V. Kucheriavyi, T.I. Bratanich, V.V. Skorokhod, L.I. Kopylova, M.O. Krapivka. Strukturno-fazoviy mekhanizm i shvydkist vzaemodii intermetalidiv TiCu, Ti_3Cu_4, Ti_2Cu_3 z vodnem. 1: Reaktsii utvorennya ta rozkladannya hidrydiv intermetalidiv // Poroshk. Metallurg.- 2012.- No. 3-4.- P. 131-140.
170. O.V. Kucheriavyi, T.I. Bratanich, V.V. Skorokhod, L.I. Kopylova, A.V. Kotko. Strukturno-fazoviy mekhanizm i shvydkist vzaemodii intermetalidiv TiCu, Ti_3Cu_4, Ti_2Cu_3 z vodnem. 2: Destruktyvne hidruvanyya intermetalidiv // Poroshk. Metallurg.- 2012.- No. 5-6.- P. 105-111.
171. F.M. d'Heurle. Thermal formation of SiO_2 over NiSi, $NiSi_2$ and$CoSi_2$ via silicide decomposition // Thin Solid Films.- 1983.- V. 105.- P. 285-292.
172. M.-A. Nicolet. Oxidation of silicides: Summary // Mater. Res. Soc. Symp. Proc.- 1985.- V. 40.- P. 317-322.

173. F.M. d'Heurle, A. Cros, R.D. Frampton, E.A. Irene. Thermal oxidation of silicides on silicon // Philos. Mag.: B.- 1987.- V. 55, No. 2.- P. 291-308.

Subject index

Collaborators

Even though only the head is needed to put forward a theory, any experimental work almost always demands more than two hands and therefore can hardly be carried out properly without skilled collaborators. The help of V.R. Sidorko, V.G. Khoruzha, L.V. Goncharuk, A.V. Samelyuk, V.V. Berezutsky, S.V. Bykova, L.A. Duma, I.G. Kondratenko, K.A. Meleshevich, E.S. Rabotina, D.M. Pashko and V.M. Petukh with preliminary work, maintenance of equipment and carrying out experiments is acknowledged with sincere gratitude.

L.A. Duma

V.R. Sidorko

V.M. Petukh

A.V. Samelyuk

V.V. Berezutsky

E.S. Rabotina

L.V. Goncharuk

V.G. Khoruzha

Producers

This book is a result of consolidated efforts of the workers of Dybkov Production Group, Unlimited.

W, M, GM

W = wife, M = mother,
GM = grandmother

S = son,
DL = daughter-in-law

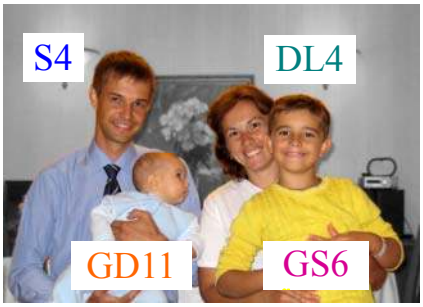

GS = grandson

GD = granddaughter

(Executive Producer)

<необмежена продюсерська група **ДИБКОВ – DYBKOV** production group, unlimited>

Наукове видання

В. І. Дибков
V.I. Dybkov

Хімічна кінетика
Chemical kinetics

(англійською мовою)

Авторський оригінал

Electronic version

Надруковано в Україні
Printed in Ukraine